THE EFFECTS OF MAGNETIC FIELDS ON OSCILLATIONS IN THE SOLAR ATMOSPHERE

David J. Evans

A Thesis Submitted for the Degree of PhD
at the
University of St Andrews

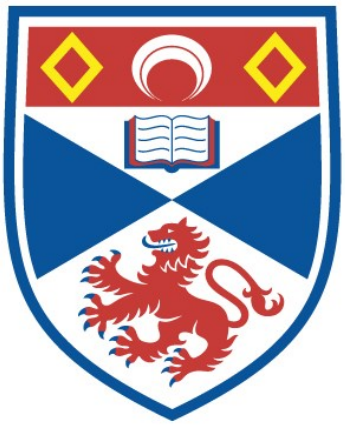

1990

The Effects of Magnetic Fields on Oscillations in the Solar Atmosphere

David J. Evans

A thesis submitted for the degree of Doctor of Philosophy at the University of St. Andrews

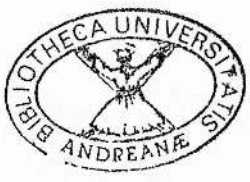

ProQuest LLC.
789 East Eisenhower Parkway
P.O. Box 1346
Ann Arbor, MI 48106 – 1346

Abstract.

A study has been made of wave propagation in two regions of the solar atmosphere in which magnetic forces are significant. Sunspot observations indicate a rich variety of characteristic modes of oscillation roughly divided into three categories: three minute umbral oscillations, five minute umbral oscillations and penumbral waves. Outside of intense magnetic flux concentrations the oscillation spectrum is dominated by the five minute period. These waves are trapped in a cavity whose upper boundary may be affected by the magnetism of the chromosphere.

A sunspot has been modelled by a uniform cylindrical flux tube. The allowable modes of oscillation are found to vary as the atmospheric parameters change with depth. Umbral three minute oscillations are interpreted as *slow body modes*. The umbral five minute oscillations arise through a complicated interaction with acoustic waves outside the sunspot. This drives *fast body modes* as well as waves simply passing through the flux tube. The former may propagate upwards and become *fast surface waves*. Fast and *slow surface waves* may explain some of the oscillations of the penumbra.

The magnetic structure of the chromosphere has been modelled as an isothermal atmosphere permeated by a uniform and horizontal magnetic field. A dispersion relation for the trapped waves below such an atmosphere has been derived and both asymptotic and numerical solutions found. The effect of a uniform magnetic field is to increase the frequency of the trapped modes. A physical explanation for these changes in frequency has been put forward. Observational evidence may indicate that such effects are indeed seen. This model has been further generalised to take some account of the variation in canopy height which has been observed.

Copyright

I, David John Evans, hereby certify that this thesis has been composed by myself, that it is a record of my own work, and that it has not been accepted in partial or complete fulfilment of any other degree or professional qualification.

Signature of Candidate _____

Date 18th January 1990

I hereby certify that the candidate has fulfilled the conditions of the Resolution and Regulations appropriate to the Degree of Ph.D.

Signature of Supervisor _____

Date 18 January 1990

I was admitted to the Faculty of Science of the University of St. Andrews under Ordinance General No. 12 on 1st October 1986 and as a candidate for the degree of Ph.D. on 1st October 1987.

Signature of Candidate _____

Date 18th January 1990.

Acknowledgements.

The task of a PhD supervisor is to take a rough hewn and intellectually naive graduate and produce a streamlined and effective researcher. A thankless task at the best of times due to the uncertain nature of research. However, it is true to say that I have learned a vast amount in the last three years and for this I will be eternally grateful to my supervisor, Bernie Roberts. To have done this in such a courteous and hospitable manner is an achievement in itself. Add to this the generous welcome that Bernie and Margaret have always given me and I really could ask for nothing more.

Eric Priest and Alan Hood have given tirelessly of their time and wisdom concerning some of the more mysterious secrets of mathematics, physics and FORTRAN! They and many other members of the Mathematics and Physics departments have shown me much hospitality and good humour which has made my time here quite pleasurable. A special mention should be made of the late Professor Newby Curle whose charm and wisdom will be sorely missed by staff and students alike.

On a more practical note I would like to thank the University of St. Andrews for financial support through the Guthrie Research Studentship and also additional funding for travel. Without such generosity none of this would be possible.

Finally I must mention all my friends and colleagues both inside the University and out in the wider world. They have made my time here so enjoyable that I shall be very sorry to leave. I only hope that they have sampled some of that pleasure also.

Contents

1. Introduction

1.1 Motivation

All elastic materials in the Universe support oscillations of one form or another. The nature of these oscillations are interesting in themselves, but their study can also provide vital clues to the make-up of the environment in which they occur. Waves are the most natural way to transmit energy from regions of high activity to the more quiescent parts of the medium. They are inevitable whenever there is a rapid disturbance to any region of elastic materials. Thus in order to understand the energy flow in a system it is vital to understand how its wave motions behave. The aim here is to increase our understanding of the way in which the magnetic fields of the solar atmosphere affect oscillatory motions there. This will help us to exploit the diagnostic potential of the waves in determining atmospheric structure, and it will enable us to examine the energy transport due to the various modes.

The effects of magnetic fields on bulk motions, as described by magnetohydrodynamics (MHD), are significant when the magnetic forces are comparable with the fluid stresses. This is commonly measured by the "plasma beta" which is defined by the ratio of fluid to magnetic pressure:

$$\beta = \frac{\gamma}{2}\frac{p}{B^2/2\mu}, \qquad (1.1)$$

where γ is the adiabatic index, p (N m^{-2}) is the fluid pressure, B is the magnetic field strength measured in Tesla and μ is the permeability of free space ($4\pi \times 10^{-7}$ henry m^{-1}). Usually β is defined as simply the ratio of plasma pressure to magnetic pressure, i.e. with the $\gamma/2$ factor removed from equation (1.1). When studying wave motion however, it is more convenient to use the ratio of sound and Alfvén speed which results in the definition given (see section 1.2.3).

In the layers of the Sun that are readily visible, β is small (i.e. magnetic forces are important) in two particular regions. In the photosphere and below, the magnetic fields are

dominated by the motions of the fluid. The effect of this is to concentrate the magnetic flux into small "flux-tubes" where the plasma beta is around one or less (e.g. Spruit and Roberts, 1983). The most obvious example of such a flux concentration is a sunspot.

The top of the convection zone is covered by a pattern of small convective granules with diameters around 1000-2000 km. Superimposed on this is a larger scale convection pattern consisting of supergranules with diameters around 30,000 km and they last for around 1 or 2 days. The flow wells up in the centre, moves across the cell at around 0.3-0.4 km s-1, and then falls down the sides. Due to the frozen-in flux condition of the plasma, this flow tends to concentrate magnetic flux into small tubes along the intergranular boundaries (e.g. Galloway and Weiss, 1981). The dynamic pressure of this flow can produce flux-tubes with strengths of around a few hundred Gauss. The observations indicate that the intense flux-tubes have strengths around 0.1-0.2 T (1-2 kG) and sizes below 300 km. Such conditions can be created from the moderate flux-tubes brought together by supergranular flow, through a convective instability which has the effect of evacuating the tube and hence strengthening the magnetic field (Webb and Roberts, 1978).

At the photosphere, the external gas pressure becomes comparable with the magnetic pressure. Also at this level, the pressure scale height reaches its minimum of around 100 km. Thus, in rising by only 500 km from the photosphere, the ambient gas pressure will fall to an almost negligible amount. In such a situation the magnetic pressure will cause the intense photospheric flux-tubes to rapidly fan out and fill the near vacuum in the chromosphere. The field lines at the edge of the intense flux-tubes will, in this way, outline not only the supergranular sides but also their tops (see Figure 1.1). The overall effect is to create a near horizontal layer of magnetic flux in which motions are dominated by the field. This is commonly referred to as the magnetic canopy.

Giovanelli and Jones (1982) have made a detailed observational study of the chromospheric field. Observations at various heights show sharp, fine-scale magnetic elements in the photosphere but a far more diffuse pattern only a few hundred kilometres higher up. The height of the canopy field, measured relative to the photosphere, varies between 150 km close to sunspots, to 1000 km in magnetically weak regions. On average, it is around 450 km but depends on the strength of magnetic activity. Thus, it can be

expected that the average canopy height will fall at the maximum of solar activity.

These, then, are the two regions of the solar atmosphere where magnetic effects on the dynamics of the fluid are important. Spruit and Roberts (1983) review the structuring of the solar atmosphere due to the magnetic field in more detail. Within this scenario there are three principal forces able to drive oscillations. Firstly, fluid pressure is of great importance in supporting the basic acoustic modes in the photosphere and below. This is also the regime in which gravity makes it presence most keenly felt. Finally, the photospheric flux-tubes and chromospheric canopy fields outlined above, submit to strong magnetic forces.

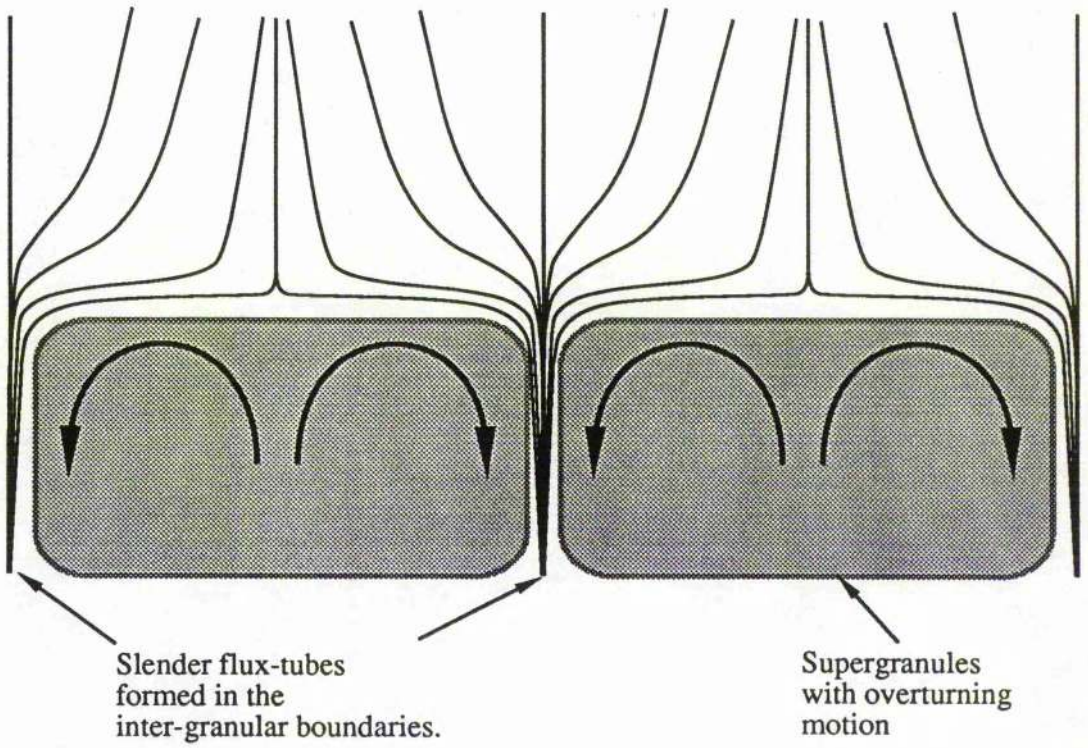

Figure 1.1 Supergranules (shaded) concentrate magnetic flux into the intergranular lanes. These concentrations become intense flux-tubes by the action of convective collapse. Just above the photosphere the ambient pressure drops rapidly and so the flux-tubes expand out to fill the available space. This has the effect of forming a chromospheric canopy field which is roughly horizontal.

To analyse all these effects concurrently is immensely difficult and so most of the work presented here has to make certain simplifying assumptions. For the same reason, the

oscillations in the magnetic regions discussed above are not well understood. This work will investigate the nature of oscillations in a sunspot, flux-tube or active region, and also the way in which a magnetic chromosphere can influence the propagation of acoustic waves in the body of the photosphere and below.

1.2 Sunspot Oscillations

1.2.1 Sunspot Structure

Sunspots appear as dark patches on the solar disc when viewed in visible light. Their diameters are typically 3×10^4 km and they are usually found in groups referred to as active regions. They appear dark because their temperatures are about 4000 K compared to a mean photospheric temperature of around 6000 K. Careful spectral analysis shows significant Zeeman splitting of magnetically sensitive lines within the dark umbra. These indicate magnetic field strengths in a sunspot of up to 0.3 T (3000 G). Sunspots are the largest of a hierarchy of magnetic flux-tubes starting from small elements with sizes below current telescopic resolution, and ranging through pores (about 500 km in diameter), having field strengths of approximately 0.15 T (1500 G).

Sunspots are distinguished from other magnetic elements by having a penumbra surrounding the darker umbra. The penumbra delineates the region where the magnetic field is fanning out. It lies on top of the photosphere (i.e. the level where the optical depth, as viewed from the vicinity of the Earth, for the continuum is 1) and has a filamentary structure of light and dark bands when viewed in the Hα spectral line. These appear to delineate regions of concentration and evacuation the cause of which is uncertain. Magnetic fields in the outer penumbra are around 0.02 T (200 G) in strength, and are almost horizontal.

The shape of a sunspot may be envisaged as being like that of a trumpet horn, facing upwards, and floating in the solar atmosphere. The structure below the photosphere is not well known. The orthodox view is that the flux-tube extends below the surface with roughly vertical sides (e.g. Meyer, Schmidt and Weiss,1977). Such a structure is subject to a fluting instability (e.g. Parker, 1974) which tends to break it up into smaller elements. Meyer et al (1977) showed that where the magnetic field has fanned out, the reduced density

inside the sunspot stabilises this disintegration via buoyancy. When the inclination of the side of the sunspot to the vertical falls below a critical value, buoyancy is no longer able to restrain the fluting instability. Consequently, it is quite possible that below the photosphere, a sunspot consists of a cluster of smaller, stable flux-tubes. This idea was first formulated by Parker (1979a). It is hoped that a study of the oscillations exhibited by a sunspot may indicate which of these hypotheses is nearest the truth.

1.2.2 Sunspot Oscillations

Beckers and Tallant (1969) were the first to record oscillatory behaviour in spectral lines formed within a sunspot. Since that time there have been many observations of oscillations in different parts of sunspots. Moore and Rabin (1985) give a useful review of this and other dynamical phenomena in sunspots.

The strongest and most commonly observed oscillation is the "three minute" umbral oscillation. These are seen at various levels, from the photosphere to the chromosphere, within the umbra. Periods observed are around three minutes but can range from 100 s to 200 s (frequency from 5 to 10 mHz). The velocity amplitude is between 0.1 kms^{-1} and 10 kms^{-1}, depending on the height of formation of the spectral line used. Interestingly, these oscillations exist within cells of coherence having diameters between 2000 km and 10000 km. In the chromosphere, the power spectrum for this range of frequencies shows several quite sharp peaks while the photospheric spectrum is more diffuse.

At photospheric levels, there is also a weak oscillation with period around 5 minutes. This is not commonly observed due to its low amplitude (< 0.1 km s^{-1}) but there seems little doubt that it is generally there. Though this oscillation is also seen within umbrae, it is unlikely to be confused with the three minute oscillations because there is no power in the five minute band above the photosphere. In fact, the difference in behaviour of the two oscillations with varying umbral depth is an important distinguishing feature. Again, there exist several peaks, in this case around 3 mHz.

Three and five minute oscillations will be the main concern here. However, where appropriate, the oscillations of the penumbra will also be discussed. The first penumbral oscillations to be observed were "running penumbral waves" (Giovanelli, 1972; Zirin and

Stein, 1972). They consist of bands of vertical velocity fluctuations which propagate outwards from the umbra-penumbra boundary. Periods generally range from three to six minutes, while propagation speeds are around 10-25 kms^{-1}. More recently, detailed observations (e.g. Lites, 1988) of the penumbra have revealed oscillations which are not of the same form as running penumbral waves. These appear as power peaks at frequencies around 3 mHz and sometimes as low as 0.7 mHz.

1.2.3 Magnetohydrodynamic Waves

Clearly then, a sunspot supports a wide range of oscillations. This has prompted some interesting theoretical work in an attempt to explain the various observations. Before discussing this theoretical work on umbral oscillations, it may be useful to briefly summarise the basic nature of magnetohydrodynamic waves. This will be done by simply examining the modes of oscillation supported by a uniform fluid, permeated by a constant magnetic field. The fluid is assumed to be compressible and of infinite conductivity, while small variations are taken to be adiabatic. Thus the equations that describe its motion are (e.g. Priest, 1982):

$$\rho\frac{D\mathbf{v}}{Dt} = -\nabla p + \mathbf{j}\times\mathbf{B}\,, \tag{1.2}$$

$$\frac{D\rho}{Dt} + \rho\nabla.\mathbf{v} = 0\,, \tag{1.3}$$

$$\frac{D}{Dt}\left(\frac{p}{\rho^{\gamma}}\right) = 0\,, \tag{1.4}$$

$$\frac{\partial\mathbf{B}}{\partial t} = \nabla\times(\mathbf{v}\times\mathbf{B})\,, \tag{1.5}$$

$$\mathbf{j} = \frac{1}{\mu}\nabla\times\mathbf{B}\,, \tag{1.6}$$

$$\nabla.\mathbf{B} = 0. \tag{1.7}$$

Here, ρ is the density and p the pressure of the fluid, $\mathbf{v}$ is the Eulerian velocity field, $\mathbf{j}$ is the current density and $\mathbf{B}$ is the magnetic field, while μ is the permeability of free space.

The basic (static) state is taken to be:

$$p = p_0 \, , \; \rho = \rho_0 \, , \; \mathbf{v} = \mathbf{0} \, , \; \mathbf{B_0} = B_0 \mathbf{e}_z \tag{1.8}$$

in Cartesian coordinates, x, y, z. Subscripted variables are constant and $\mathbf{e}_z$ is the unit vector in the z-direction. The perturbations about this basic state are assumed to be small so that a linear analysis is valid. Perturbations are assumed to take the form

$$\mathbf{v} = \bar{\mathbf{v}} \exp(i\,\omega t - i\,\mathbf{k}.\mathbf{r}) \, , \tag{1.9}$$

$\mathbf{r}$ being the position vector, $\mathbf{k}$ the wave-vector, ω the angular frequency and barred quantities are constants. Then, the following dispersion relation may be derived (e.g. Roberts, 1985):

$$(\omega^2 - k_z^2 v_A^2)(\omega^4 - [c_s^2 + v_A^2]\, k^2 \omega^2 + k^2 k_z^2 c_s^2 v_A^2) = 0 \, . \tag{1.10}$$

Here $k=|\mathbf{k}|$ is the amplitude of the wave-vector and k_z is its z-component, $c_s=(\gamma p_0/\rho_0)^{1/2}$ is the sound speed and $v_A=(B_0^2/\mu\rho_0)^{1/2}$ is the Alfvén speed. These two speeds are characteristic of the medium. In the absence of a magnetic field, v_A is zero and equation (1.10) reduces to the dispersion relation for acoustic waves (and the degenerate solution $\omega^2=0$).

There are three modes of interest. The most obvious from equation (1.10) is the solution

$$\omega^2 = k_z^2 v_A^2 \, , \tag{1.11}$$

which is known as the *Alfvén* wave. It is easy to show that motions involved in the propagation of this wave are incompressible and always transverse to the direction of the magnetic field. The fluid and magnetic pressure perturbations (i.e., p and $\mathbf{B}.\mathbf{B}_0/\mu$) are both identically zero, while the magnetic tension ($2\mathbf{B}.\mathbf{B}_0/\mu R_{curv}$, R_{curv} being the radius of

curvature of the field line) is parallel to the velocity. Both magnetic tension and velocity perturbations are perpendicular to the wave-vector.

The work described in the following chapters is mostly concerned with compressible oscillations. Hence, there will be little discussion of Alfvén waves. The more important modes here are the *slow* and *fast magnetoacoustic* waves, given by the remaining two roots of equation (1.10). These modes are compressible and are essentially propagated by magnetic and fluid pressure. Their dispersion relations are illustrated in Figure 1.2. This is a polar plot of the phase speed ω/k against the angle θ between the wave-vector $\mathbf{k}$ and the magnetic field $\mathbf{B}_0$. It is obvious why the modes are so called. An important point to notice is that the propagation for the fast mode is broadly isotropic whilst the slow mode is highly anisotropic, being "guided" along the magnetic field lines.

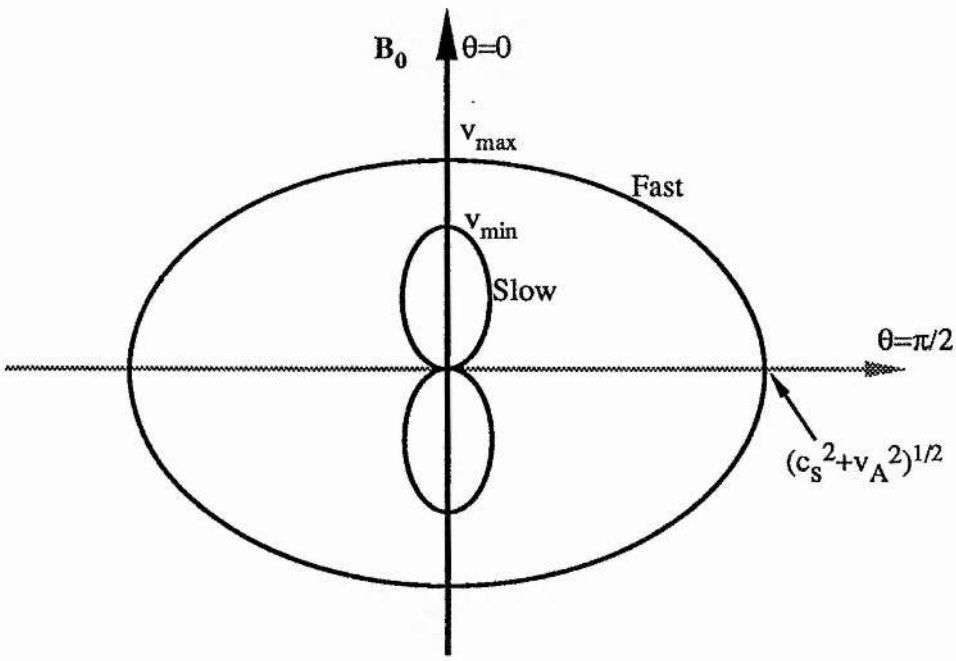

Figure 1.2 Polar plots of the fast and slow magnetoacoustic waves, given by equation (1.10), showing the variation in the phase speed ω/k as a function of θ measured from the direction of $\mathbf{B}_0$. $v_{max}=\max\{c_s, v_A\}$ and $v_{min}=\min\{c_s, v_A\}$. Note that the slow mode is highly anisotropic, being "guided" by the magnetic field lines.

The fundamental difference between the fast and slow modes lies in the phase relationship of the fluid and magnetic pressures. For the fast mode, both fluid and magnetic

pressures act in phase and so combine their effects to produce a faster propagation speed across the magnetic field (there cannot be a magnetic pressure perturbation along the magnetic field). In contrast, the slow mode's magnetic pressure perturbation is exactly 180° out of phase with the fluid pressure. Consequently, they tend to cancel out in the direction transverse to the magnetic field, and so there is very little propagation except along the field lines.

The precise behaviour of the fast and slow magnetoacoustic modes varies depending on the strength of the magnetic field, as measured by $\beta=c_s^2/v_A^2$ (this is the same definition as given in equation 1.1). Another way of looking at this is to say that the nature of the modes is determined by the ordering of the various characteristic speeds. Outside of the chromosphere and corona and the upper regions of magnetic elements, v_A is negligible in comparison to c_s. However, the opposite is true inside these magnetically dominated regions. The upper reaches of a sunspot have quite low values of β (around 0.1 in the upper umbral chromosphere). The value of β increases with depth, reaching 1 at about the photosphere and growing further with depth in the convection zone. Thus the wave modes within a sunspot may vary with depth.

Mode	Large β	Small β
Slow	$\omega^2/k^2 \approx v_A^2 \cos^2\theta$	$\omega^2/k^2 \approx c_s^2 \cos^2\theta$
Fast	$\omega^2/k^2 \approx c_s^2 + v_A^2 \sin^2\theta$	$\omega^2/k^2 \approx v_A^2 + c_s^2 \sin^2\theta$

Table 1.1. Magnetoacoustic dispersion relations for large and small β plasmas. The angle between the magnetic field and the wave-vector is θ.

In order to have some idea of the dependence of magnetoacoustic modes on the strength of the magnetic field, it is instructive to study the behaviour of the solutions to equation (1.10) in the limits of small and large β. The approximate dispersion relations are given in Table 1.1, in which θ is the angle between the magnetic field and the wave vector. From

this it can be seen that for small magnetic fields the slow mode is degenerate (i.e. $\omega^2 \rightarrow 0$ as $v_A \rightarrow 0$), while for strong fields it behaves like an acoustic mode channelled by the lines of magnetic flux. The fast mode, however, remains much the same for all field strengths, simply interchanging the dominant transmission force between magnetic and fluid pressure for strong and weak fields, respectively. In the absence of magnetism, the slow mode "vanishes" and the fast mode becomes the familiar acoustic mode.

Finally, it is of interest to examine the behaviour of the transverse and longitudinal components of the velocity. Without loss of generality, it may be assumed that the y-component of the wavevector is zero. Denoting fast and slow modes by subscripted f and s respectively, it can be shown that for a strong field

$$\left(\frac{v_z}{v_x}\right)_f \approx \frac{\beta}{2}\sin 2\theta\,, \quad \left(\frac{v_z}{v_x}\right)_s \approx \frac{-1}{\beta \sin\theta\ cos\theta} \tag{1.12}$$

and for a weak field

$$\left(\frac{v_z}{v_x}\right)_f \approx \frac{1}{\tan\theta}\,, \quad \left(\frac{v_z}{v_x}\right)_s \approx -\tan\theta\,. \tag{1.13}$$

Thus, it is clear that for a low β plasma, the slow mode motions are predominantly field-aligned, the reverse being true for the fast mode. Also, with a weak magnetic field the fast mode motions are those of an acoustic wave.

1.2.4 Theoretical Interpretations of Sunspot Oscillations

In a gravitationally stratified atmosphere, the temperature gradient is crucial in determining whether adiabatic fluid perturbations are convectively stable or not. A simple "parcel" argument (e.g. Priest, 1982) can be used to show that if the temperature gradient exceeds the adiabatic temperature gradient, then the atmosphere will be unstable to convection. In spherical coordinates the adiabatic temperature gradient is given by

$$\frac{dT}{dr} = -\left(\frac{\gamma - 1}{\gamma}\right)\frac{g m_{av}}{k_B}, \tag{1.14}$$

where g is the acceleration due to gravity, m_{av} is the mean particle mass and k_B is Boltzmann's constant. A temperature gradient that is steeper than the adiabatic value is called *superadiabatic*.

Due to the efficiency with which fluid motions transport heat, in the convection zone the temperature gradient remains very close to the adiabatic value, except in the surface layers. When the temperature has become low enough, the electrons and protons of the plasma recombine to form a significant population of hydrogen atoms. This has the effect of dramatically decreasing the amount of photon scatter due to free electrons and hence radiation can freely escape from this level. Consequently, there is very little heating of the neutral hydrogen by radiation from below so that the temperature falls more rapidly with height. This causes a superadiabatic layer to form in the 2000 km below the photosphere, though its effects are only significant in the top 200-400 km (e.g. Moore, 1973; his Figure 1).

It is clear that due to advection of flux lines in an ideal MHD fluid a vertical magnetic field threading through a plasma will inhibit the overturning motion associated with convection. In this way, a strong enough field will cause an oscillatory motion, rather than instability. If there is strong radiative heat transport and a superadiabatic temperature gradient, it is possible for this oscillation to grow in amplitude from one cycle to the next. At maximum compression (rarefaction) and depth (height), an oscillating fluid parcel will gain (lose) heat from the surroundings and, because it must maintain lateral pressure balance, decrease (increase) in density. Buoyancy forces will then ensure that the fluid parcel returns to its equilibrium position with increased kinetic energy, hence causing a growth in oscillation amplitude. Such a motion is referred to as being *overstable*.

In the course of investigating energy transport by convective motions in a sunspot, Danielson and Savage (1968) concluded that, because hydromagnetic calculations did not allow instabilities it was necessary to invoke overstability. Their calculations indicate that the periods of these overstable oscillations could vary from 1 minute up to 1 hour, depending on the imposed vertical wavelength, taken by Danielson and Savage to be twice the local pressure scale height. Hence, the periods of interest, i.e. the 3 and 5 minute umbral oscillations, are easily within these bounds. Danielson and Savage speculate about the amount of energy that could be carried by waves generated by overstable convection but find

it to be quite low in comparison with the "missing energy flux" of a sunspot (i.e. the difference between the energy radiated by a sunspot umbra and that radiated by an equivalent area of the quiet photosphere).

Following on from this work, Moore (1973) specifically suggested that the umbral flashes observed by Beckers and Tallant (1969) and the running penumbral waves reported by Zirin and Stein (1972) and Giovanelli (1972) were both driven by overstable convection in the subphotospheric umbra. He employed the Boussinesq approximation (i.e. density perturbations are assumed to be negligible except in the gravitational potential) within a layer of fluid, stratified by gravity and permeated by a vertical magnetic field, in order to calculate likely periods of oscillation that might be driven in the subphotosphere of a sunspot umbra. Rigid wall boundary conditions (vertical component of velocity equal to zero) are employed at the top and bottom of a layer of arbitrary thickness. This calculation then gives the frequencies and growth rates of trapped overstable modes. Only the fundamental modes are considered and layers with thicknesses of 350 km and 700 km, centred on the peak of the superadiabatic temperature gradient, are discussed. These yield periods of approximately 140s and 270s, respectively. The growth rates of the 140s mode also match the coherence times of the umbral flashes, while 270s is around the correct period for running penumbral waves.

Mullan and Yun (1973) extended Moore's analysis by studying the depth dependence of the frequency of overstable oscillations in the umbral atmosphere and including the effects of resistivity. They found that above the level 250 km below the temperature minimum, joule dissipation is sufficient to overcome the growth of overstable motions. Below this level overstability is able to occur and the periods range from 100 s upwards. This may explain the lower limit of observed umbral oscillations but there is no obvious reason why particular frequencies should be observed where others are not. To match the observations, Mullan and Yun conclude that the source of the oscillations should lie between 250 km and 650 km below the temperature minimum.

Uchida and Sakurai (1975) proposed that the source of umbral oscillations is convective overstability in the photosphere, but that this drives a resonant cavity in the umbral atmosphere. Their model umbra consists of two isothermal layers, one to represent

the photosphere/chromosphere and the upper layer to represent the corona. This is permeated by a uniform vertical field, which is reasonable for the lower layer and is justified in the coronal layer by arguing that this upper layer only serves to reflect waves propagating up from below. Also, it is assumed that waves cannot penetrate below the level of forcing due to overstability, because the magnetic field lines are too heavily loaded with fluid. This is a weakness because it need not cause a reflection, the kinetic energy of the wave still being able to propagate unhindered. Further assumptions are made in their analysis. The vertical component of velocity is assumed to be negligible in comparison with the horizontal ones. This will have the effect of removing the slow mode in regions of low β. The plasma is assumed to be dominated by the magnetic field and this is clearly not valid in the lower levels of the model. This is justified by saying that only the Alfvén wave is of interest and so the effects of compression are negligible. In the real solar atmosphere, the effects of compression are likely to be of great importance, however.

The radial component of the velocity is taken to be zero at the assumed sunspot radius, hence causing the radial wavenumber to take on a discrete set of values. The horizontal velocity is taken to be zero at the level of overstable forcing while the horizontal component of the field is zero at the interface between the two layers. In this way a resonant cavity is formed having a fundamental period of 160 s and harmonics with period 75 s,50 s, 30 s, etc. These results indicate the possibility of a genuine cavity existing, but the assumptions made with regard to the effects of compressibility, and to the boundary conditions on the cavity, are quite severe. It is necessary to have a non-isothermal atmosphere in order to get genuine reflections.

In the course of investigating the effects of cooling by overstable waves in a sunspot, Roberts (1976) found that periods for the oscillations were of the order of 200-400 s. In view of the predominance of periods in the three minute range this was further investigated by using different parameters in order to produce the desired results. This can be done with numbers which are still well within the realms of physical acceptability for typical sunspot structures. Thus it seems that overstability can easily produce the desired frequencies of oscillation. However this calculation again relied on the Boussinesq approximation while employing quite large length-scales.

In order to try and relax some of the assumptions made by Uchida and Sakurai, and to avoid Boussinesq approximations, Antia and Chitre (1978) performed a boundary value calculation by numerical methods. This included thermal conductivity, a polytropic atmosphere (i.e. a linear temperature profile) and full compressibility so that more relevant modes should be excited. Boundary conditions are then applied at two heights in order to form the cavity. The calculations give frequencies and growth rates for the modes, which are themselves overstable.

Two series of modes are found to exist, fast and slow with high and low frequencies respectively (the modes are identified by studying the phase relationships between the various perturbed quantities). Periods are between 50 s and 110 s for the fast modes and 235 - 285 s for slow modes, depending on the precise boundary conditions used. In the absence of the magnetic field the fast modes become acoustic waves while the slow modes become convective or buoyancy modes. This fits with the classification of fast and slow magnetoacoustic modes given in section 1.2.3. Antia and Chitre conclude that the fast modes give best agreement with the observations of umbral flashes. The parameters used for their umbral model would place this cavity in the sub-photospheric region. The main questions arising from this work is the validity of applying the boundary conditions at two arbitrary heights in order to form the cavity. It is more acceptable to simply require the energy density to remain finite at great height and depth. The system can then settle into a cavity resonance of its own choosing rather than it being imposed from outside. Also, it is of interest to know what the effect of an umbral chromosphere would be.

Scheuer and Thomas (1981) and Thomas and Scheuer (1982) adopted the viewpoint that the umbral oscillations are a resonant response of the umbra to overstable convection, forcing from below. They performed more detailed calculations than previous work in order to test this hypothesis. They used a three layer model atmosphere consisting of two isothermal layers representing the corona and the photosphere/chromosphere, with a polytropic convection zone. Rigid tube boundary conditions were employed. This gives a series of modes with discrete radial wavenumbers but only the fundamental mode is considered. The atmosphere was driven at the photosphere by purely vertical or purely horizontal motions. The vertical boundary conditions have the effect of ensuring that the

energy density of the perturbations asymptote to zero at large height and depth. The frequency of forcing was varied and the level of response noted so that the frequencies of maximum response can be derived. These are the "resonant" frequencies, though due to some leakage the resonances are not perfect.

Their results give resonant frequencies in rough agreement with the frequencies of umbral oscillations. The form of kinetic energy shows a concentration around the photosphere and below, though there is a small remnant in the chromosphere also. They denote the node as being a "fast magnetoatmospheric" wave though this should be regarded with some care since it need not have the characteristics of a fast magnetoacoustic wave at all heights (Thomas, 1984). Their results would seem to support those of Antia and Chitre (1978). Boundary value calculations, with the boundaries extended until no further change in mode frequencies is apparent, give results in good agreement with the resonant transmission results.

The second paper (Thomas and Scheuer, 1982) uses a far more detailed model umbra to calculate eigenmodes. Here, the lower boundary is moved to tune the cavity to the periods of the observations. The results are insensitive to the coronal structure but, depending on the magnetic field strength and the temperature gradient in the convection zone, the required height of the lower boundary can vary from 70 km above the photosphere to 270 km below. Because of the somewhat arbitrary nature of the lower boundary level, the results for the more detailed model umbra are less convincing than for the calculations done in the earlier paper. However, it does serve to indicate how sensitive such calculations are to atmospheric structure. This is in contrast to the lack of dependence on coronal structure. This is essentially due to the strong reflection created by the rapid temperature increase at the transition region.

The results of this model, together with the similar work of Uchida and Sakurai, and of Antia and Chitre, indicate that 3 minute umbral oscillations are caused by a sub-photospheric "fast" mode resonance driven by overstable convection in the same region. An alternative view, suggesting a chromospheric resonance, has been put forward in recent years and this will be discussed in the following paragraphs.

With the aim of testing models of sunspot atmospheres, Zhugzhda, Locans and Staude

(1983) investigated the modes of oscillation that should be supported. This work followed an earlier paper (Zhugzhda and Locans, 1981) suggesting that there may exist a chromospheric resonant cavity which could be used for "sunspot seismology". Three sunspot models, due to Staude (1981), are used. The main variation between them is the extent of the chromosphere (roughly the distance between the temperature minimum and the transition region) which has values of 1400 km, 1050 km and 700 km.

The analysis is based on an analytic solution of the wave equations which is valid for constant magnetic field and temperature, amongst other things. These solutions also require the plasma β to be small so that they are strictly only valid in the chromosphere and above. The atmosphere is divided into many layers, in each of which the above assumptions are made. The atmosphere is then driven from below in order to find the peaks of transmission, as in Scheuer and Thomas (1981). The three model atmospheres give fundamental resonances with periods of 183 s, 161 s, 145 s in order of decreasing chromospheric extent. Since the chromospheric structure has a significant effect on the frequency of oscillation, it is argued that the cavity must be essentially chromospheric. This cavity is not perfect as there is some leakage of the slow modes. The waves, which may be regarded as acoustic waves guided along the magnetic field lines, are reflected by the rapidly increasing sound and Alfvén speeds around the transition region at a maximum of the cut-off frequency (see section 1.3.1) $\omega_{ac}=\gamma g/2c_s$ at the temperature minimum (i.e. sound waves cannot propagate with frequencies below ω_{ac}). Clearly then, the resonant frequency is highly dependent on the atmospheric structure. Each model also shows a resonance with a period of 173 s which is interpreted as being due to a photospheric cavity of the kind Scheuer and Thomas (1981) investigated.

In a subsequent paper (Zhugzhda, Staude and Locans, 1984) the authors repeated their calculations for a series of umbral models, obtaining similar results to those of the first paper. Comparison of the predicted periods with observations enables the "better" models to be selected. They also note that observations of chromospheric lines indicate vertical phase speeds much less than the Alfvén speed, i.e. slow mode propagation, which would tend to support the chromospheric cavity hypothesis.

Gurman and Leibacher (1984) have pursued a similar line of investigation. They

consider slow modes to be acoustic modes channelled along the magnetic field-lines, again only valid in the chromosphere. Several model atmospheres have been used, including one to represent the quiet Sun. This model is driven for a range of frequencies in order to find the maxima of transmission as in Scheuer and Thomas (1981) and Zhugzhda et al (1983). Results support those of Zhugzhda et al. They conclude that higher harmonics, which have periods outside the normal 3 minute band, are not observed in sunspots due to the unspecified source rather than the cavity. Several cavities seem to exist and the interactions between these should be studied further.

In a series of papers, Zhugzhda and Dzhalilov (1982, 1984a, b) develop a theory describing the transformation of magneto-atmospheric modes in a gravitationally stratified, isothermal, magnetic atmosphere. This work is based on an analytic solution, in terms of Meijer functions, for the equation describing magnetoacoustic waves under the given assumptions. In regions where β is small or large, the usual modes appropriate to those limits can be identified asymptotically. In the region where $\beta \approx 1$, these modes interact and cause mode transformations to occur. These ideas have been used to extend the theory of umbral oscillations in Zhugzhda (1984) and Zhugzhda, Locans and Staude (1987).

The scheme developed on the basis of this work consists of three separate resonant cavities which may interact with each other. The first is the photospheric/chromospheric cavity which is essentially that of Zhugzhda et al (1983) and Gurman and Leibacher (1984). Here, however, the reflection due to the cut-off frequency at the temperature minimum is supplemented by that due to the increasing temperature above the photosphere. This hybrid cavity gives resonances around the 3 minute band, as before.

Below the photosphere there is postulated the existence of two further cavities: a magnetically modified acoustic cavity and a subphotospheric slow mode cavity. The first of these is essentially the p-mode cavity of the quiet Sun (see section 1.3 on Helioseismology) with some account taken for the vertical magnetic field. The effects of the magnetism will be limited to the upper region where $\beta < 1$ and will not have a drastic effect due to the large extent of the cavity (depth of 10^4 km - 10^5 km) compared with that of the magnetic layers. Thus, this cavity is taken to explain the 5 minute oscillations observed in the umbral photosphere. It is also suggested that this is the fast mode cavity investigated by Thomas

and Scheuer (1982) except that their boundary conditions do not allow the correct frequencies.

The slow mode cavity of the subphotosphere acts separately from the fast mode subphotospheric cavity. It is essentially an overstable convective mode with a fundamental period of around 30 minutes. This is quite similar to the values of lifetimes for umbral dots (Moore and Rabin, 1985) so this cavity is postulated as an explanation for them.

In summary then, there are two competing theories as to the true nature of umbral 3 minute oscillations: a fast mode photospheric resonance (Scheuer and Thomas, 1981), and an essentially chromospheric, slow mode resonance (Zhugzhda, Locans and Staude, 1983). As yet, a completely satisfactory consensus has not emerged. The model of Scheuer and Thomas (1981) used a rough model of the umbral atmosphere so that chromospheric resonance would not be expected. While Scheuer and Thomas (1982) employs a more detailed model, the numerical approach used is not entirely convincing. The imposition of a lower reflecting boundary at arbitrary heights in order to generate the appropriate periods is slightly contrived and not fully justified. At the same time, all the work of Zhugzhda and co-workers relies on solutions which are valid only for a low β plasma and predominantly field aligned propagation. The models based on the theory of wave transformation suffer from the fact that these calculations are performed for isothermal atmospheres and so should be used with care. The conclusions of these models are not necessarily incorrect but there remain important questions over them.

In all of the work described above, the emphasis has been on the creation of cavities in stratified atmospheres. While this is an important approach, the lateral structuring of the magnetic field has all but been ignored. Structuring can significantly affect the nature of wave propagation (e.g. Edwin and Roberts, 1983) so that its neglect could be quite serious. Roberts (1981a) and Abdelatif (1988) have both briefly discussed the modes of oscillation that are likely to arise in a magnetically structured environment such as may be associated with a sunspot. However, this discussion could be pursued much further in light of recent observations and this is the approached that will be adopted here. To include the effects of both gravitational stratification and magnetic structuring is very difficult. Hence, the effects of gravity will be ignored in preference for the influence of the magnetic field. The results

will then be interpreted in the context of the physics of a sunspot.

Running penumbral wave models can be separated into two classes, though the distinction between them is sometimes hazy. The first is *surface waves*, which are waves propagating parallel to an interface such that their amplitude decays roughly exponentially on both sides of the interface (e.g. water waves on the surface of the sea). Secondly there are trapped wave models. These are more like the cavities discussed above and consist of modes propagating in a cavity formed by reflecting boundaries either side, and parallel to, the interface.

Compressible surface waves on a single magnetic interface were first dealt with by Wentzel (1979) and more fully by Roberts (1981a). For the case of one side of the interface being field free while the other side is permeated by a uniform magnetic field which is parallel to the interface, there will always be a *slow surface wave* with longitudinal (i.e. along the field lines) phase speed less than the *tube speed* c_T and the sound speed of the field free medium, c_{se}. The tube speed is defined by

$$c_T = \left(\frac{c_s^2 v_A^2}{c_s^2 + v_A^2} \right)^{\frac{1}{2}},$$

and is a third characteristic speed in magnetically structured media. In addition, if the field-free medium is hotter than the magnetic region, then a second *fast surface wave* may propagate, having longitudinal phase speed greater than c_s, the sound speed in the magnetic region, and less than both of c_{se} and v_A. It has been suggested that gravity modified waves of this sort may be the cause of the running penumbral waves (Small and Roberts, 1984; Miles and Roberts, 1989b).

Nye and Thomas (1974) examined the trapping of gravity modified magnetoacoustic waves in the penumbral atmosphere. For the case of constant pressure scale height and sound and Alfvén speeds, the modes of interest are denoted "plus" and "minus" modes. In the limit of g tending to zero, these become fast and slow magnetoacoustic waves respectively.

Using a diagnostic diagram for a three layer model penumbra, they show that the plus modes are trapped by the Alfvén speed increasing with height and the sound speed increasing with depth. The minus modes are not trapped because their vertical phase speed in the lower atmosphere is less than the Alfvén speed which all but vanishes at great depth. These arguments are supported by a crude W.K.B. analysis for the plus mode cavity. Hence, they propose that the running penumbral waves are vertically trapped plus modes.

In a subsequent paper, Nye and Thomas (1976b) pursue this idea with a particular model atmosphere in which analytic solutions are possible. This consists of modelling the penumbra by a uniform horizontal field in an isothermal, gravitationally stratified atmosphere. Below this is a polytropic field-free medium. The energy density of perturbations is required to be integrable over the entire atmosphere and the vertical velocity and total Lagrangian pressure perturbation at the interface between the two regions are necessarily continuous. This forms a cavity for gravitationally modified fast magnetoacoustic modes because the Alfvén speed increases exponentially with height and the sound speed increases monotonically with depth. As might be expected, the results show a series of harmonics. There is also a minus mode present, having longitudinal phase speed less than the Alfvén speed at the interface. This is a gravitationally modified slow surface mode.

Using the observations of running penumbral waves, Nye and Thomas argue that the fundamental (lowest frequency) plus mode is the most likely candidate. In terms of the calculations to be presented in chapter 3, which are based on this model, this mode is a magnetically modified f-mode, as can be seen from the eigenmode plots of Nye and Thomas (1976b); their Figure 4. It could be the case that such oscillations are seen in the penumbra due to the effects of the penumbral field on the p- and f-modes (see section 1.3). This would be in addition to the surface waves propagating out from the umbra. Recent observations (Lites, 1988) would seem to support this view. These points will be discussed further in later chapters.

As discussed earlier, Zhugzhda et al (1987) postulate the existence of a sub-photospheric acoustic wave cavity, essentially the p-mode cavity (see section 1.3)

modified in the upper layers by the vertical magnetic field. This is put forward as the cause of the photospheric five minute oscillation observed in the umbra. For the same reasons, they also postulate that the driving mechanism may be the same as that of the p-mode cavity of the quiet Sun. This being the case, it will be difficult to distinguish between the acoustic cavity in the umbra and the p-mode cavity outside. In reality they will become one and the same, the sunspot simply acting as an inhomogeneity within the overall cavity. This is essentially the view put forward by Thomas (1981).

It is generally agreed that the 5 minute oscillation in the photospheric umbra is the passive response of the sunspot to the excitation by p-modes outside. There are many questions as to the exact nature of this interaction however. Abdelatif, Lites and Thomas (1986) argue that there is a resonant transmission effect whereby certain frequencies are preferentially transmitted into the umbra over others. Also there appears to be a shift towards shorter wavenumber since the phase speed of a wave propagating into the spot will increase from the sound speed to the fast mode speed. These effects can be demonstrated using simple slab and tube models of a sunspot as in Abdelatif and Thomas (1987). More recently, there have been observations of the absorption of p-mode energy by sunspots (Braun, Duvall and Labonte, 1987, 1988). These indicate that up to 50% of p-mode energy can be absorbed by sunspots. Some attempts to explain this by resonant absorption in the sunspot side have not been able to match the observations (Hollweg, 1988). Clearly though, the lateral structuring of the magnetic field is important in discussion the interaction of the p-modes with sunspots.

1.2.5 Sunspot Model

From the above discussion, it can be seen that the complexity of sunspot structure makes the interpretation of the oscillations therein very difficult. The structure is complicated by gravitational stratification and by sharp lateral magnetic field variations. A considerable amount of work has been done considering the effects of gravity as outlined in the previous section. Almost always though, it has been expedient to ignore the true effects of the lateral magnetic structure. When they have been included, there has been no consideration of the external medium; the sunspot boundary has been assumed to be a perfect

reflecting boundary. It is important to know when this is valid. Some waves may be trapped within the flux-tube while others may propagate in and out through the magnetic interface. In the latter case it is important to know about the characteristic reflection and transmission coefficients.

The gravitational and thermal stratification mean that the characteristics of a flux-tube modelling a sunspot will vary with height. This may have important consequences if modes can change from being trapped in the tube at one height to being able to escape higher up.

The existence of the magnetic interface also raises the possibility of surface waves. As pointed out earlier, surface waves may be important in explaining penumbral waves. Running penumbral waves originate from the inner umbra and propagate along the magnetic interface as it fans out into the chromosphere. This implies that their source may be surface waves of the tube structure below the photosphere. Thus, it is important to be clear about possible surface modes that may exist at different levels in the sunspot.

The philosophy here will be to examine the modes of oscillation of a cylindrical magnetic flux-tube in a field free environment. The temperature of the fluid inside and outside will be taken to be constant though they need not be the same value. The various parameters defining the equilibrium will be chosen to mimic those in a sunspot at several different levels.

Such a model has been studied before (e.g. Edwin and Roberts, 1983) but the application to sunspots has not been fully exploited. Abdelatif and Thomas (1987) and Abdelatif (1988) have looked at the ideas outlined above but a detailed study of the observations with the flux-tube model in mind remains to be done. Hopefully this will shed some light on the problem of identifying the complex nature of sunspot oscillations.

1.3 Effects of a Magnetic Canopy on p- and f-mode Oscillations.

1.3.1 Trapped Modes in the Solar Convection Zone

Thirty years ago, it was discovered that the surface of the Sun oscillates in a very regular way. Oscillations with a period of around five minutes and amplitudes up to 1 m s^{-1} were detected on all parts of the solar disc (Leighton, 1960; Evans and Michard, 1962;

Leighton, Noyes and Simon, 1962). Several theories were put forward to explain these motions. Ulrich (1970) and shortly after Leibacher and Stein (1971) proposed that the observations were the particular signature of a resonant cavity residing in the solar interior. Their results predicted a very characteristic, parabolic pattern of dispersion curves in a plot of frequency against horizontal wavenumber. Deubner (1975) was able to make sufficiently high quality observations to show that this characteristic pattern was indeed present in the solar five minute oscillations, hence confirming the trapped mode theory.

Ignoring the effects of magnetic fields in the solar interior, the formation of the five minute cavity can be understood by considering the propagation of acoustic waves. The essential physical conditions are that the solar interior has a temperature, and hence sound speed, steadily increasing from the temperature minimum at the surface towards the core. If there is a sudden disturbance in the fluid some distance below the solar surface, acoustic waves will propagate away in all directions. A wavefront propagating downward at some non-zero angle to the vertical will be swung round to propagate horizontally and then to move upwards, due to the difference in phase speed between each end of the wavefront (see Figure 1.3). Thus waves originally propagating downwards will be refracted upwards.

Because of the refraction of the atmosphere, all waves will eventually propagate upwards, their direction becoming more nearly vertical as they approach the photosphere. At the temperature minimum, the density falls off with height at a greater rate than at any other point in the Sun. If the density scale-height (i.e. the height required for a drop in density by a factor e) is much less than the vertical wavelength of a sound wave propagating vertically upwards, the photosphere will effectively be a sudden density discontinuity. This will cause the wave to be reflected back downwards again. Equivalently, a stratified medium is only able to support propagating waves above the *cut-off* frequency. High frequency oscillations will propagate normally, but due to the relatively low inertia of the layers above the driver (i.e. in the direction of decreasing density), the atmosphere can respond rapidly to low frequency disturbances and so the fluid simply moves as a whole. The acoustic cut-off frequency for a gravitationally stratified, isothermal atmosphere is $\omega_{ac}=\gamma g/2c_s$ (Lamb, 1908) which clearly has a maximum value at the temperature minimum. Thus, waves with frequencies below this maximum value are reflected at some level around

the photosphere or below.

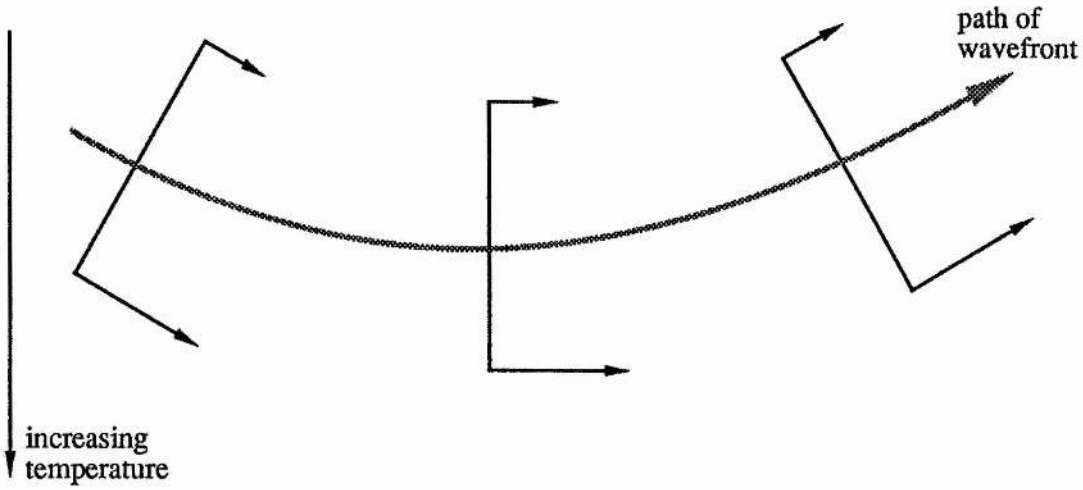

Figure 1.3 Motion of an acoustic wavefront propagating in a medium with sound speed increasing downwards. The length of the arrows on wavefronts indicates the magnitude of the sound speed at that point.

This means that for a plane parallel atmosphere there is a vertical cavity formed by the reflecting regions outlined above. This means that only those waves which traverse the cavity and return to their original position with no change in phase do not suffer constructive interference. Hence there is a mode structure in the vertical (or radial) direction which is parametrised by the *radial order* n. In the spherical case, it is also necessary to have constructive interference after traversing one complete circumference. This introduces two further mode numbers: *spherical harmonic degree l*, essentially a measure of the overall horizontal wavenumber, and *azimuthal order* m, the number of nodes along the direction of the azimuthal axis. This is entirely analogous to the simple, quantum mechanical description of the hydrogen atom which has the same energy level classification.

The interference of waves propagating around the cavity will cause a standing wave pattern such that the energy density outside the cavity decays to zero. An analysis of the problem in spherical polar coordinates (r, θ, ϕ) allows a solution for the radial displacement ξ' of the form (e.g. Deubner and Gough, 1984)

$$\xi' = \xi(r)\, P_l^m(\cos\theta)\, e^{im\phi}\, e^{i\omega t}, \tag{1.15}$$

where P_l^m is the associated Legendre function. The degree l takes values 0, 1, 2... while the azimuthal order m = 0, ±1, ±2, ...±l. The function $\xi(r)$ is then determined by an ordinary differential equation in r, subject to suitable boundary conditions. Solution of this gives the eigenmodes and eigenfrequencies for the particular model. If the model of solar structure is spherically symmetric, the eigenmodes and eigenfrequencies are independent of m, or, in other words, the eigenmodes are $(2l+1)$-fold degenerate. For such a case, the radial equation for adiabatic oscillations, ignoring the perturbation to the gravitational potential, is given by (e.g. Deubner and Gough, 1984)

$$\Psi'' + \kappa^2 \Psi = 0\,, \tag{1.16}$$

where

$$\Psi = \rho_0^{1/2}\, c_s^2\, \mathrm{div}\,\xi\,, \quad \kappa^2 = \frac{\omega^2 - \omega_c^2}{c_s^2} + \frac{l(l+1)}{r^2}\left(\frac{N^2}{\omega^2} - 1\right)$$
$$\omega_c^2 = \frac{c_s^2}{4H^2}(1 - 2H')\,, \quad H = \frac{\rho_0}{\rho_0'}, \quad N^2 = g\left(\frac{1}{H} - \frac{g}{c_s^2}\right), \tag{1.17}$$

ω_c^2 is the generalised acoustic cut-off frequency, H is the density scale-height, N is the buoyancy (Brunt-Väisälä) frequency and $'$ denotes differentiation with respect to r. When positive, N^2 is the square of the natural frequency for oscillations driven by buoyancy, but if N^2 is negative then it represents the squared growth rate for convective instability. The condition for marginal stability of a gravitationally stratified atmosphere, discussed in section 1.2.4 (equ. 1.14), is equivalent to N^2=0.

The equivalent problem for a plane parallel stratified atmosphere gives very similar results except that there is no "quantisation" due to the spherical geometry. If k is the horizontal wavenumber in a model which is rotationally symmetric about the direction of gravity, then

$$\kappa^2 = \frac{\omega^2 - \omega_c^2}{c_s^2} + k^2\left(\frac{N^2}{\omega^2} - 1\right). \tag{1.18}$$

By comparison of (1.17) and (1.18) it is clear that modes on the solar surface are equivalent to modes in the plane parallel case with horizontal wavenumber

$$k = \frac{\sqrt{l(l+1)}}{R_{sun}}, \tag{1.19}$$

where R_{sun} is the Sun's radius at the photosphere. For modes with horizontal wavelengths comparable to R_{sun} (i.e. small k, l) the plane approximation is not good but it works well for large values of l.

It is useful, at this point, to examine the behaviour of a plane parallel atmosphere with a linear temperature profile approximating the convection zone. With z directed vertically downwards, a marginally stable atmosphere ($N^2 \equiv 0$) requires that the temperature be given by

$$T_0 = \left(\frac{\gamma - 1}{\gamma}\right) \frac{m_{av}\, g}{k_B} z, \tag{1.20}$$

where m_{av} is the mean particle mass and k_B is Boltzmann's constant. Assuming hydrostatic balance against a uniform gravitational field and that the gas is ideal, it is easy to show that

$$c_s^2 = (\gamma - 1)gz, \quad H = (\gamma - 1)z, \quad \omega_c^2 = \frac{g(2\gamma - 1)}{4(\gamma - 1)z},$$

so that equation (1.18) reduces to

$$\kappa^2 = -k^2 + \frac{\omega^2}{(\gamma - 1)gz} + \frac{1 - 2\gamma}{4(\gamma - 1)^2 z^2}. \tag{1.21}$$

In order to solve equation (1.16) for this model with evanescent boundary conditions for the energy density as $z \to 0$ and ∞, it is possible to use W.K.B. (Wentzel Kramers and Brillouin) theory (e.g. Bender and Orszag, 1978). The zeros, or turning points, of κ^2 are given by

$$z = \frac{\omega^2}{2(\gamma-1)gk^2}\left(1 \pm \left[1 + \frac{g^2k^2(1-2\gamma)}{\omega^4}\right]^{\frac{1}{2}}\right), \qquad (1.22)$$

and these are denoted z_1 and z_2 such that $z_1 < z_2$. W.K.B. theory then states that the eigenfrequencies are given by the following formula, involving the Bohr-Sommerfeld integral (see Bender and Orszag, 1978):

$$\int_{z_1}^{z_2} \kappa \, dz = (n - \frac{1}{2})\,\pi\,, \quad n = 1, 2, 3\ldots \qquad (1.23)$$

This result is asymptotically correct in the limit $n \to 0$. Performing this integral (see Appendix 1 at the end of this chapter) then yields the dispersion relation

$$\frac{\omega^2}{gk} = \left(1 - \gamma + \sqrt{2\gamma - 1}\ \right) + 2(\gamma - 1)n\,. \qquad (1.24)$$

This result is only approximate but it shows very clearly the characteristic parabolic dependence of ω on k which was confirmed observationally by Deubner (1975).These dispersion curves are illustrated in Figure 1.4.

Previously, this calculation has been performed by assuming that $\omega_c=0$ and taking the upper turning point at z=0. This leads to a simpler calculation with result:

$$\frac{\omega^2}{gk} = (1 - \gamma) + 2(\gamma - 1)n. \qquad (1.25)$$

Though equations (1.24) and (1.25) have the same qualitative form the simple calculation is less accurate for small n (the exact result is $\omega^2/gk = 1 + 2(\gamma-1)n$ as will be shown in Chapter 3). This is because low frequency modes are reflected by the acoustic cut-off at a lower level than for high frequencies. Assuming the upper turning point is at z=0 is thus less accurate for low frequency, i.e. low n, modes. The solution presented here gives an

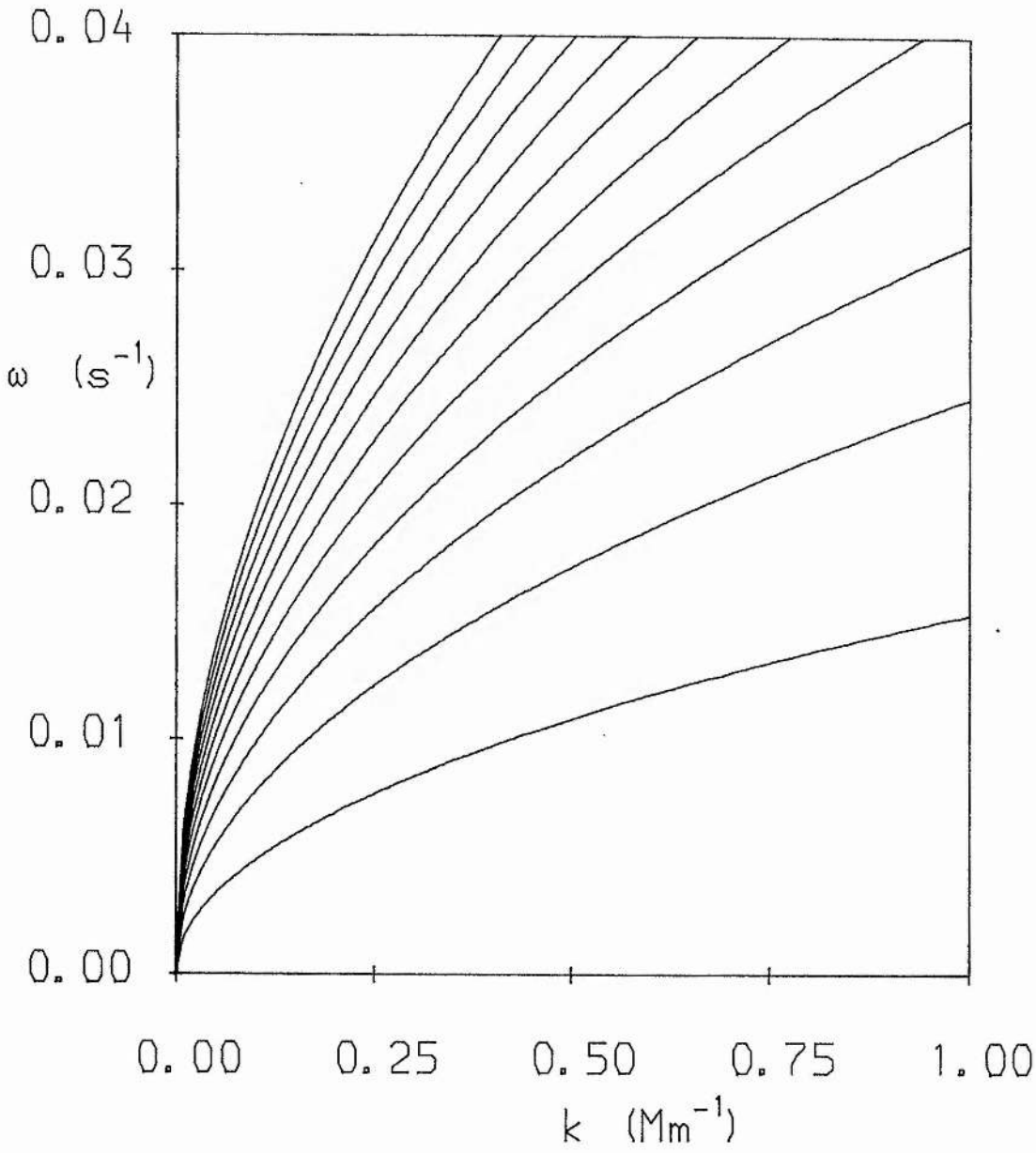

Figure 1.4 An illustration of the of the dispersion relations (1.24) for p-modes in a simple model chromosphere. The value of γ used here is 5/3 and the modes with n=1, 2,...10 plus the f-mode are shown here. The f-mode is the lowest frequency solution and the frequency of the p-modes increases with n. The characteristic shape of these curves has been observationally confirmed, originally by Deubner (1975) and many times since.

improved, yet still straightforward, derivation.

The sequence of modes given by equation (1.24) are essentially acoustic waves trapped in the manner outlined above. For this reason they are denoted *p-modes*, indicating the importance of fluid pressure. When the model atmosphere is not marginally stable (buoyancy frequency non-zero), there is a second sequence of lower frequency modes, supported by buoyancy forces. For an unstable atmosphere these are simply convective modes which do not propagate but in the opposite case they are gravity waves and hence denoted *g-modes*.

The Brunt-Väisälä or buoyancy frequency, defined in equation (1.17), is the natural frequency of oscillation for adiabatic motions. If these motions are not adiabatic then the energy transfer will lessen the density deficit which drives the oscillation, hence decreasing the frequency. In this sense the Brunt-Väisälä frequency is the maximum allowed for buoyancy oscillations (Leibacher and Stein, 1981). The natural frequency for oscillations is also reduced by the fluid being partially ionised. In this case the fluctuations in internal energy are partly absorbed by changes in the amount of ionisation. This has the effect of reducing the buoyant restoring force.

Because of variations in the temperature gradient, radiative opacities, ionisation, etc, the value of N^2 will vary through the interior of the Sun. In particular, the dependence of N^2 on g, the acceleration due to gravity, means that $N^2 \rightarrow 0$ with proximity to the solar centre. By definition, $N^2 \leq 0$ throughout the convection zone. A buoyancy oscillation below the convection zone will thus be unable to propagate out to the surface or in to the centre and is hence trapped in a cavity of its own making. This low frequency cavity gives rise to the solar g-modes. Unfortunately, because they are trapped so far below the surface, their detection is immensely difficult and reported observations remain controversial.

Finally, there is a third important mode; it lies between the p- and g-modes in character and frequency. This mode is referred to as the fundamental or *f-mode* and is analogous to a surface wave on deep water, having the dispersion relation $\omega^2 = gk$. The primary characteristic of the f-mode is that the fluid motions associated with it are incompressible. It does not propagate vertically but is channelled horizontally, having its energy concentrated around the photosphere. The f-mode is also distinctive in that its dispersion relation is

entirely independent of the temperature structure of the atmosphere. This point will be discussed further in Chapter 3 where it will be demonstrated that chromospheric magnetic fields influence the f-mode, hence yielding an important test of the theory.

1.3.2 Helioseismology

P- and f-modes have been thoroughly investigated in the past few years and are an interesting phenomenon in themselves. Their greatest value, however, lies in the detailed dependency of p-mode frequencies on the internal structure of the Sun. Modes with varying horizontal wavenumber reside in cavities of differing depth, and so a collection of frequencies of many modes contains information on the internal solar structure at all levels. Locally, a p-mode can be thought of as an acoustic wave with dispersion relation

$$\omega^2 = c_s^2 \left(k_{hor}^2 + k_{vert}^2 \right) , \qquad (1.26)$$

where k_{hor} and k_{vert} are horizontal and vertical components of the wavevector, respectively. The lower turning point of the cavity occurs when the wave is propagating horizontally, i.e. $k_{vert} = 0$. Thus it can be seen that increasing values of l, or k_{hor}, require decreasing values of sound speed at the lower turning point, i.e. the cavity depth decreases. Hence low l modes sample almost all the solar interior while high l modes are only dependent on the structure of the surface layers.

The study of oscillations on the surface of the Sun for the purpose of inferring internal structure, *Helioseismology*, is one of only two methods currently available for probing below the solar surface. The second method is the observation of neutrinos emanating from the nuclear reactions in the solar core. However, the results from this work indicate that the observed flux is somewhat below that predicted by standard solar models (Davis, Evans and Cleveland, 1978). Thus, an alternative method is vital to determine what is wrong with the standard theory.

The ideal method for inferring data on the internal variation of sound speed with depth would be to devise a way of inverting the frequency data directly. This has been done approximately using an asymptotic version of the p-mode dispersion relations and very

reasonable results have been obtained (Christensen-Dalsgaard et al, 1985). Naturally the asymptotic results will contain errors, so it is desirable to devise a more accurate inversion process. It is not at all certain that this will in fact be feasible due to the possibility that the problem is ill-posed and/or oversensitive to small changes in the raw data, so the alternative of investigating various models of solar structure is very important.

The obvious models to start with are those derived from standard stellar evolution theory and calibrated for the surface abundance of elements and the luminosity of the Sun. This internal structure is then used to frame the eigenmode problem which is solved numerically to find the characteristic frequencies of oscillation. In general, these "standard model" calculations assume that the oscillations are linear and adiabatic, that the Sun is spherically symmetric, and that the effects of magnetism and convection are negligible (Christensen-Dalsgaard, 1986).

The calculations of the standard model have predicted frequencies quite close to the observed values. Nevertheless, there are errors which exceed the observational accuracy. The character of the error would suggest that they are not due to a marked difference in the elemental abundances used in the standard model (Christensen-Dalsgaard and Gough, 1980) but rather, are the result of some physical effect, or effects, which have been neglected. The possible candidates for such an effect are quite numerous, typical examples being variation in the equation of state of the solar plasma, non-adiabaticity of the oscillation, particularly in the surface layers, weakly interacting massive particles in the solar core, convection and turbulence, etc. Some of the more recent models (Christensen-Dalsgaard, Däppen and Lebreton, 1988) indicate that after employing a sophisticated equation of state, the remaining errors increase with increasing l. Since high l modes exist in a cavity near the surface, it must be the case that this is where the problems lie. Indeed, the physics of motion in the superadiabatic layer is poorly understood due to the influence of partial ionisation, the transition from optically thick to optically thin radiation and from high to low β plasma.

In the work to be described here, attention will be focussed on the effect of magnetic fields in the surface layers of the Sun on the p- and f-modes. These magnetic fields may produce the same form of frequency shift as is required to explain the error in the standard model. A second reason for being interested in magnetic effects is the recent evidence of

variations in p-mode frequencies over the solar cycle. This was first noticed by Woodard and Noyes, (1985) and similar results for low l modes have been given by Fossat et al (1986), Gelly et al (1986), Henning and Scherrer (1986), Isaak et al (1986) and Pallé, Régulo and Roca Cortes (1989). For intermediate values of l, Duvall et al (1988) have recently reported frequency decreases of up to 0.5 μHz for the same part of the solar cycle. No results for high l modes are available as yet. The most prominent global variation in the solar cycle is that of the magnetic field. Thus it is important to understand how magnetic fields can influence p-modes.

There are three regions in which magnetic effects have been examined: strong fields around the base of the convection zone; fibril fields below the photosphere; and chromospheric canopy fields. Of these, most attention has been given to the first two. Roberts and Campbell (1986) and Campbell and Roberts (1986) have investigated the effect that a magnetic field at the base of the convection zone can have on the frequencies of low degree p-modes. High degree modes will be unaffected since their lower turning point is above the base of the convection zone. They suggest that changes in the strength of the field over the solar cycle could explain the frequency change observed by Woodard and Noyes (1985). The detailed calculations suggest that a peak field strength of 5-100 T (5×10^5-10^6 G) at the base of the convection zone would be necessary. This figure is large in the context of dynamo theory but is not unrealistic in view of the gas pressure at that depth.

Vorontsov (1986), Gough and Thompson (1986a) and Thompson (1988) have examined the effect that a toroidal magnetic field just below the convection zone should have on the splitting of the azimuthal degeneracy of modes in a spherically symmetric star. They find that frequencies should indeed be split but that there is also a periodic dependence of the frequency shift on frequency. Vorontsov finds no evidence for this in the data of Libbrecht and Zirin (1985) but Thompson (1988) claims to see the predicted effect in the frequencies published by Duvall et al (1988). Here the required field strength is again of the order 50 T(5×10^5 G). It should be noted however that Gough and Thompson (1986a) find that this magnetic field configuration cannot explain frequency splitting data given by Duvall, Harvey and Pomerantz (1986).

Belvedere (1986) has examined the effects of toroidal magnetic fields also. His work

has been applied to stars of the Sun's spectral neighbourhood (spectral types F5-K0). He concludes that effects for field strengths of the order 5 T (5×10^4 G) should be observable in the Sun's case.

Analysis of the data of Duvall et al (1986) has been carried out by Dziembowski and Goode (1986) who conclude that the observations cannot be explained simply on the basis of rotation. They also postulate fields at the base of the convection zone having a strength of around 100 T (10^6 G). They point out that this could have a large impact on dynamo theory. Gough and Thompson (1986b) believe the observations indicate there is some perturbation that is restricted to small latitudes like those in which sunspots are found. One possibility for such an effect is the fibril field residing in the convection zone.

Fibril fields and their interaction with acoustic waves have been investigated by Bogdan and Zweibel (1985), Zweibel and Bogdan (1986), Bogdan and Cattaneo (1989) and Zweibel and Däppen (1989). The first two of these papers examines a statistical ensemble of scatterers (i.e. the flux-tubes) and the average effect this will have on acoustic wave frequencies. They find that frequency changes of the order of 0.1%-0.3% are possible, the direction of the change depending on the detailed properties of the flux-tubes. The effect of a fibril field is stronger than that of a diffuse field and, furthermore, if it is localised in the Sun then there could be a strong contribution to splitting of degenerate modes. Bogdan and Cattaneo (1989) have developed an alternative method for tackling the problem in order to overcome questions concerning the validity of the averaging, while Zweibel and Däppen (1989) are attempting to take stratification fully into account.

As discussed earlier, apart from the intense flux-tubes making up the fibril field below the photosphere and toroidal fields at the base of the convection zone, the final region in which magnetic effects are important is the canopy field in the chromosphere. It has already been pointed out that the differences between observed frequencies and those predicted by standard solar models, suggest that a significant part of the error lies in the surface physics. A significant part of this physics is the magnetic field. Therefore, Campbell and Roberts (1989) have investigated the effect that such a field would have on the dispersion curves for p- and f-modes.

Since the effects of a canopy field will be restricted to modes trapped near the surface

(i.e. high l modes), it is only necessary to examine the behaviour of waves with short horizontal wavelength. Consequently, it is justifiable to consider the problem in plane geometry. The model of Campbell and Roberts consists of a simple convection zone with a stably stratified, linear temperature profile. This is truncated towards the top and an isothermal atmosphere permeated by a magnetic field is added. The field is chosen to decrease exponentially in strength, thus giving a constant, Alfvén speed. This will underestimate the influence of the magnetic atmosphere since the Alfvén speed in the solar chromosphere in fact rises quite rapidly before reaching a fairly constant value in the corona.

The calculations show that frequency shifts for a given horizontal wavenumber, can be up to the order of 10 μHz for the high l modes ($l \approx 1000$). For most modes the effect of the field is to reduce frequencies. The f-mode, however, shows an increase in frequency while the n=1 p-mode shows an increase for small l and the reverse for large l. Field strengths used in these computations are around 3 mT (30 G) at the base of the canopy.

The work presented in chapter 3 generalises and extends this model. The major change is to the chromosphere in which the magnetic field is now taken to be uniform. The analysis utilises an exact solution originally due to Adam (1975) and Nye and Thomas (1976). This model is unrealistic in the sense that the Alfvén speed increases exponentially without bound. In reality the Alfvén speed profile will lie somewhere between the two models. Therefore it is a useful model to examine since between them the two modes provide be upper and lower "bounds" to the effects that may occur in reality. Finally, in order to assess the effect of a variable canopy height, a further generalisation is introduced in chapter 4. Both these models are solved analytically in the long wavelength limit and numerically in the general case.

1.4 Outline of Remaining Chapters

The discussion of oscillations in a sunspot is presented in Chapter 2 (see also Evans and Roberts, 1990a). First, the basic model is developed and an investigation of the modes present for various sets of relevant parameters described. This is followed by a discussion of the observational data on sunspot oscillations in the light of the model. Some discussion

of the interaction of acoustic waves with a magnetic interface is also included.

Chapter 3 develops the basic model for analysing the effect of a chromospheric magnetic field on p- and f-mode dispersion curves. This is also discussed in Evans and Roberts (1990b). A complicated dispersion relation is derived and this is solved analytically in the limit of small horizontal wavenumber, and numerically for the more general case. These results are then expounded and discussed and the various effects explained. A detailed comparison with the results of Campbell and Roberts (1989) is made.

The model developed in Chapter 3 does not allow the examination of what may happen if the height of the canopy varies. In order to discuss this problem, a more general three layer model is described in Chapter 4. This contains an extra field-free, isothermal layer between the two layers of the previous model. The consequences of varying the canopy height are then assessed.

Finally, the results of this work are summarised and general conclusions are drawn in Chapter 5.

Appendix 1

It is possible to write κ in the form

$$\kappa^2 = \frac{k^2}{z^2}(z - z_1)(z_2 - z).$$

Then the integral of equation (1.23) becomes

$$I = \int_{z_1}^{z_2} \frac{\sqrt{(z - z_1)(z_2 - z)}}{z}\, dz,$$

where

$$z_1 + z_2 = \frac{\omega^2}{(\gamma - 1)gk^2}, \quad z_1 z_2 = \frac{2\gamma - 1}{4(\gamma - 1)^2 k^2}.$$

The integral may be calculated as follows:

$$I = \int_{z_1}^{z_2} \frac{-z^2 + (z_1 + z_2)z - z_1 z_2}{z\sqrt{-z^2 + (z_1 + z_2)z - z_1 z_2}}\, dz$$

$$= \frac{1}{2}\int_{z_1}^{z_2} \frac{-2z + (z_1 + z_2)}{\sqrt{-z^2 + (z_1 + z_2) - z_1 z_2}}\, dz + \left(\frac{z_1 + z_2}{2}\right)\int_{z_1}^{z_2} \frac{dz}{\sqrt{-z^2 + (z_1 + z_2) - z_1 z_2}}$$

$$- z_1 z_2 \int_{z_1}^{z_2} \frac{dz}{z\sqrt{-z^2 + (z_1 + z_2)z - z_1 z_2}}$$

$$= 0 + \left(\frac{z_1 + z_2}{2}\right)\int_{-\frac{\pi}{2}}^{\frac{\pi}{2}} d\theta - z_1 z_2 \int_{\frac{1}{z_2}}^{\frac{1}{z_1}} \frac{dt}{\sqrt{-1 + (z_1 + z_2)t - z_1 z_2 t^2}},$$

where

$$t = \frac{1}{z}, \quad z - \left(\frac{z_1 + z_2}{2}\right) = \left(\frac{z_2 - z_1}{2}\right)\sin\theta.$$

Thus

$$I = \frac{\pi(z_1 + z_2)}{2} - \sqrt{z_1 z_2}\int_{-\frac{\pi}{2}}^{\frac{\pi}{2}} d\alpha,$$

where

$$z_1 z_2 t - \left(\frac{z_1 + z_2}{2}\right) = \left(\frac{z_2 - z_1}{2}\right)\sin\alpha.$$

Finally

$$I = \pi\left(\left(\frac{z_1 + z_2}{2}\right) - \sqrt{z_1 z_2}\right) = \pi\left(\frac{\omega^2}{2(\gamma - 1)gk^2} - \frac{\sqrt{2\gamma - 1}}{2(\gamma - 1)k}\right)$$

and equation (1.24) then follows.

2. Sunspot Oscillations

2.1 Basic Model

2.1.1 The Dispersion Relation

Below the temperature minimum of the photosphere, i.e. below the level where the penumbrae of sunspots reside, it is justifiable to consider photospheric flux-tubes and sunspots as being vertical cylinders with, at least to a first approximation, straight sides (Meyer et al., 1977). Insofar as the direct effects of gravity are to be neglected in this study of sunspot oscillations, it therefore suffices to consider the simple situation of a cylindrical flux tube in a uniform, field-free medium. Inside the flux tube the medium will be taken to be uniform, though with different parameters to the external fluid. This configuration is sketched in Figure 2.1. The analysis then consists of examining the nature of linear oscillations about this equilibrium. Some solutions are radially evanescent outside the tube and for the most part these will be the focus of attention. However, with the interaction of p-modes and sunspots in mind, there will also be some discussion of waves which are radially propagating outside the tube.

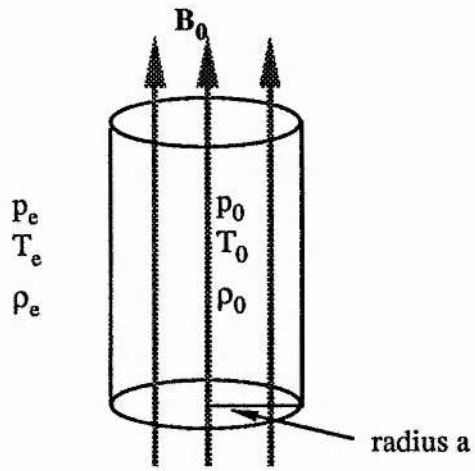

Figure 2.1. Equilibrium configuration for flux tube model of a sunspot.

Consider, then, a cylindrical magnetic flux tube of radius a, embedded in a uniform

field-free atmosphere. In a cylindrical coordinate system (r,θ,z) with an axially symmetric magnetic field $B_0(r)\mathbf{e}_z$, uniform within the tube and aligned along the z-axis, magnetostatic pressure balance requires that the sum of the gas pressure p_0 and the magnetic pressure $B_0^2/2\mu$ inside the tube be equal to the external confining pressure p_e, i.e.

$$p_0 + \frac{B_0^2}{2\mu} = p_e. \tag{2.1}$$

Linear, adiabatic perturbations about the equilibrium are described by the equations of ideal magnetohydrodynamics (see section 1.2.3) which yield (e.g. Roberts, 1986)

$$\frac{\partial p_T}{\partial t} = \rho_0 v_A^2 \frac{\partial v_z}{\partial z} - \rho_0 \left(c_s^2 + v_A^2 \right) \operatorname{div} \mathbf{v} \ , \tag{2.2}$$

$$\rho_0 \left(\frac{\partial^2}{\partial t^2} - v_A^2 \frac{\partial^2}{\partial z^2} \right) v_r + \frac{\partial^2 p_T}{\partial r \, \partial t} = 0 \ , \tag{2.3}$$

$$\rho_0 \left(\frac{\partial^2}{\partial t^2} - v_A^2 \frac{\partial^2}{\partial z^2} \right) v_\theta + \frac{1}{r} \frac{\partial^2 p_T}{\partial \theta \, \partial t} = 0 \ , \tag{2.4}$$

$$\frac{\partial^2 v_z}{\partial t^2} - c_s^2 \frac{\partial}{\partial z} \left(\operatorname{div} \mathbf{v} \right) = 0. \tag{2.5}$$

These equations apply to the more general case where the equilibrium model varies continuously as a function of r alone. In this more general case, equation (2.1) is simply replaced by

$$\frac{d}{dr} \left(p + \frac{B_0^2}{2\mu} \right) = 0. \tag{2.6}$$

The terms introduced here include the perturbation in total pressure p_T, made up of the gas pressure perturbation p and the magnetic pressure perturbation p_m ($= \mathbf{B_0}.\mathbf{B}/\mu$, for perturbed field **B**): $p_T = p + p_m$. The velocity is $\mathbf{v} = (v_r, v_\theta, v_z)$, and the sound and Alfven speeds are $c_S(r) = (\gamma p_0/\rho_0)^{1/2}$ and $v_A(r) = (B_0^2/\mu\rho_0)^{1/2}$, respectively, for a gas of density $\rho_0(r)$,

pressure $p_0(r)$, magnetic field $B_0(r)e_z$ and magnetic permeability μ.

Fourier decomposition of the perturbations in the form

$$v_r = v_r(r)\, e^{i(\omega t + n\theta - kz)}$$

etc, where ω and k are the angular frequency and vertical wavenumber respectively, for a mode with azimuthal order n, leads to (e.g. Roberts, 1986)

$$\frac{d}{dr}\left(\frac{\rho_0(k^2v_A^2-\omega^2)}{m_0^2+n^2/r^2}\frac{1}{r}\frac{d}{dr}(r\,v_r)\right)-\rho_0(k^2v_A^2-\omega^2)v_r=0\,, \qquad (2.7)$$

$$\rho_0(k^2v_A^2-\omega^2)\frac{1}{r}\frac{d}{dr}\left(\frac{1}{\rho_0(k^2v_A^2-\omega^2)}r\frac{dp_T}{dr}\right)-(m_0^2+n^2/r^2)\,p_T=0\,, \qquad (2.8)$$

where

$$m_0^2=\frac{(k^2c_s^2-\omega^2)(k^2v_A^2-\omega^2)}{(c_s^2+v_A^2)(k^2c_T^2-\omega^2)}, \qquad c_T^2=\frac{c_s^2v_A^2}{c_s^2+v_A^2}.$$

The characteristic speed c_T is the *tube speed* and is strongly associated with slow magnetoacoustic modes in the presence of magnetically structured media, while $-m_0^2$ is essentially the square of the radial wavenumber of the oscillation.

For the case of a uniform medium, Equation (2.8) reduces to Bessel's equation with general solution

$$p_T=\begin{cases} A_1 I_n(m_0r)+A_2 K_n(m_0r)\,, & m_0^2>0\,, \\ A_3 J_n(n_0r)+A_4 Y_n(n_0r)\,, & n_0^2=-m_0^2>0\,, \end{cases} \qquad (2.9)$$

for arbitrary constants A_1 to A_4. J_n and Y_n are Bessel functions of the first and second kind and I_n and K_n are modified Bessel functions of the first and second kind. The Bessel functions correspond to oscillatory solutions in r and the modified Bessel functions to

non-oscillatory solutions in r. The nature of the oscillation, whether it is radially propagating or evanescent, depends on the sign of m_0^2. The waves are radially propagating when m_0^2 is negative and radially evanescent when m_0^2 is positive.

Within the flux tube, where the field is uniform, p_T must be bounded so that

$$p_T = \begin{cases} A_1 I_n(m_0 r), & m_0^2 > 0, \\ A_3 J_n(n_0 r), & m_0^2 < 0, \end{cases} \qquad (r < a) \qquad (2.10)$$

since K_n and Y_n are unbounded at the origin. Also, p_T must remain bounded as $r \to \infty$ so that outside the tube (where the magnetic field is zero)

$$p_T = \begin{cases} A_{e2} K_n(m_e r), & m_e^2 > 0, \\ A_{e3} J_n(n_e r) + A_{e4} Y_n(n_e r), & m_e^2 < 0, \end{cases} \qquad (r > a) \qquad (2.11)$$

where

$$m_e^2 = \frac{k^2 c_{se}^2 - \omega^2}{c_{se}^2}, \qquad n_e^2 = -m_e^2,$$

and $c_{se} = (\gamma p_e/\rho_e)^{1/2}$ is the sound speed in the environment of the tube (where the gas density and pressure are ρ_e and p_e, respectively).

The main interest here is the distinctive umbral oscillations which have no analogue in the quiet photosphere around a sunspot. Added to this, when considering the interaction of p-modes and sunspots in the context of umbral five minute oscillations, it will be necessary to examine the effect of modes which are propagating outside the spot. However, to begin with, the solutions to be examined will be those that correspond to modes trapped within the body of the sunspot, given by assuming that the oscillations are radially evanescent outside the tube. This corresponds to the case $m_e^2 > 0$, i.e.

$$\frac{\omega^2}{k^2} < c_{se}^2 .$$

The case of modes which propagate outside the tube has been discussed by Roberts and Webb (1979), Spruit (1982) and Cally (1986). A further discussion of this topic is given in section 2.2.2.

Across the boundary of the tube it is clearly necessary, from physical considerations, that the radial velocity, v_r, be continuous. From equations (2.2)-(2.5) it may easily be shown that (see Appendix 2)

$$\rho_0 (k^2 v_A^2 - \omega^2) v_r = -i \omega \frac{dp_T}{dr} . \qquad (2.12)$$

Integrating this equation across the boundary of the flux tube shows that if v_r is continuous then p_T must also be continuous. Application of the two continuity conditions at r = a to the solutions (2.9) and (2.10) yields the dispersion relations (Wilson 1980; Spruit 1982; Edwin and Roberts 1983):

$$\rho_0(k^2 v_A^2 - \omega^2) m_e \frac{K_n'(m_e a)}{K_n(m_e a)} + \rho_e \omega^2 m_0 \frac{I_n'(m_0 a)}{I_n(m_0 a)} = 0 , \qquad (m_0^2, m_e^2 > 0) \qquad (2.13)$$

$$\rho_0(k^2 v_A^2 - \omega^2) m_e \frac{K_n'(m_e a)}{K_n(m_e a)} + \rho_e \omega^2 n_0 \frac{J_n'(n_0 a)}{J_n(n_0 a)} = 0, \qquad (m_0^2 < 0, m_e^2 > 0) \qquad (2.14)$$

where the dash denotes the derivative of the functions with respect to their argument. For the case n=0, (2.13) was derived by Roberts and Webb (1978).

Following Roberts (1981b, c), solutions with $m_0^2 > 0$, i.e. modes that are both internally and externally evanescent in r, are termed *surface modes* , whilst those with $m_0^2<0$, corresponding to internally propagating in r, are *body modes* ; both surface and body modes exhibit motions which are essentially confined to the tube (since $m_e > 0$). This is illustrated in Figure 2.2.

In section 1.2.3. it was shown that the ratio of longitudinal (i.e., field aligned) and

transverse components of velocity is a feature which distinguishes the fast and slow magnetoacoustic modes from one another. Having found the dispersion relation it is now possible to calculate the ratio of velocities in the radial and vertical directions for the modes of a flux tube. Each of the variables (v_r, p_T etc) are proportional to a Bessel function or its derivative. The coefficient of the Bessel function represents the "amplitude" of the particular variable concerned. Denoting this by $||$, it is easy to show that (see Appendix 2)

$$\frac{|v_z|}{|v_r|} = k\, c_s^2 \left(\frac{(\omega^2 - k^2 v_A^2)}{(\omega^2 - k^2 c_s^2)(\omega^2 - k^2 c_T^2)(c_s^2 + v_A^2)} \right)^{1/2} . \qquad (2.15)$$

This will be referred to later.

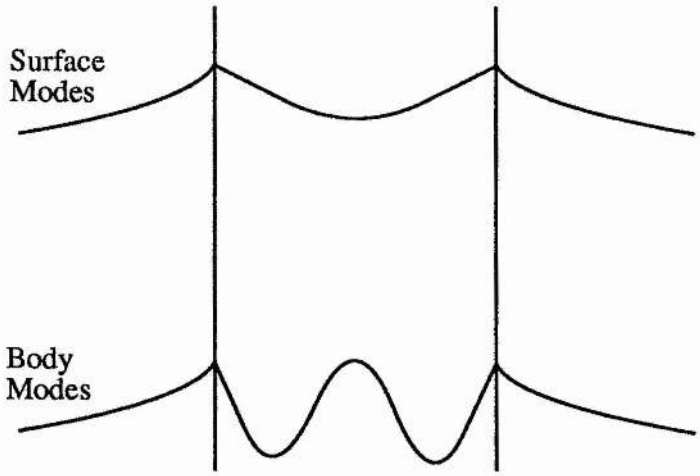

Figure 2.2. Classification of oscillatory modes of a flux tube. Modes which are radially evanescent within the tube are called *surface modes* while modes which are oscillatory as a function of r are called *body modes*.

2.1.2 The Parameter Regimes

Before solving the dispersion relations (2.13) and (2.14), it is necessary to carefully consider the values of the various characteristic speeds to use since these determine the allowable solutions. Figure 2.3 presents a sketch of the sound and Alfvén speeds in a model umbra (after Spruit, 1981) in which it is clear that high up in the sunspot the Alfvén speed is

dominant, while deep down the reverse is true. Due to the inhibition of convection inside the sunspot, the temperature is lower than outside. Hence, the external sound speed exceeds c_s. With depth the difference in the two sound speeds will become less pronounced as the effects of radiative transfer become important.

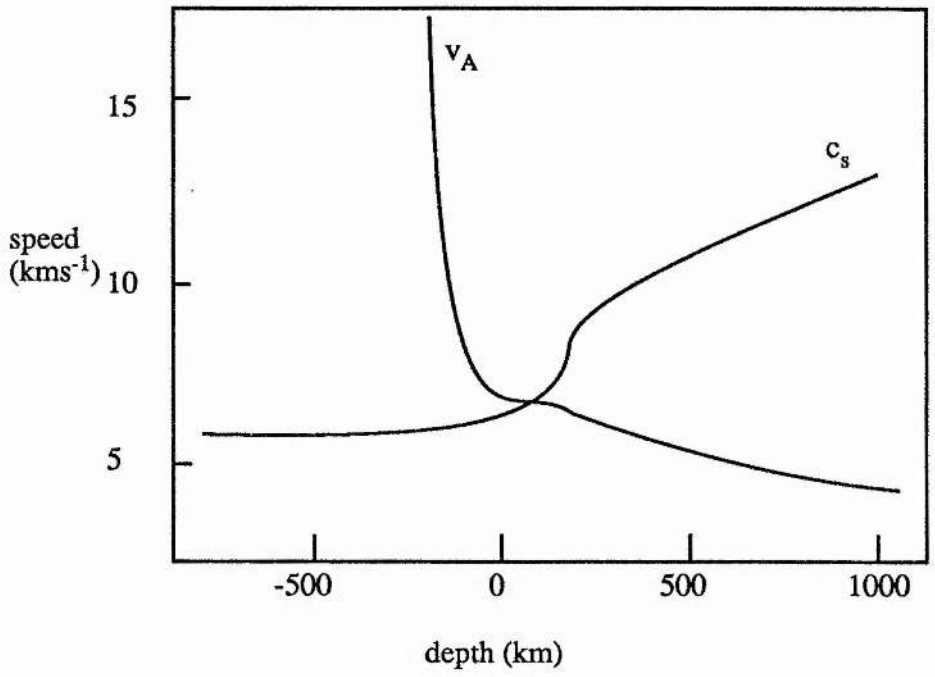

Figure 2.3. Sketch of the behaviour of the sound and Alfvén speeds in a model sunspot umbra, as a function of depth (after Spruit, 1981). Depth is measured downwards, and is taken to be zero at the photosphere (optical depth, $\tau = 1$).

In order to determine the classification of the oscillation modes, it is necessary to know the signs of m_0^2, which is a function of the frequency ω and the vertical wavenumber k. The effect is to divide the ω-k plane into regions in which different types of modes are allowed. These regions are bounded by the lines given by the phase speed ω/k being equal to one of the characteristic speeds c_T, c_s, and v_A; modes with $\omega/k > c_{se}$ are not evanescent outside the tube. Thus the crucial point is to know the ordering of these speeds. From the discussion of the previous paragraph it can be seen that there are three parameter regimes to consider (c_T is always less than v_A or c_s) :

$$c_T < v_A < c_s < c_{se}, \qquad c_T < c_s < v_A < c_{se}, \qquad c_T < c_s < c_{se} < v_A.$$

Since m_0^2 is symmetric in v_A and c_s, the relative sizes of these two speeds has no qualitative effect on the modes which are allowed. This is analogous to the usual magnetoacoustic modes in a uniform medium (see section 1.2.3). Thus it is only necessary to consider two cases:

$$\text{(i) } v_A < c_s < c_{se},$$

$$\text{(ii) } c_s < c_{se} < v_A.$$

For the actual parameter values, the prototype sunspot model of Pizzo (1986) has been used as a guide (see his Figures 5, 6 and 10). The values are taken at approximately 100 km below and 150 km above the level where $\tau_c=1$ in the centre of the umbra to represent cases (i) and (ii), respectively. The numbers are given (to 2 significant figures) in Table 2.1 and the derived characteristic speeds are shown in Table 2.2. Also, the value of another characteristic speed, c_k, defined as

$$c_k = \left(\frac{\rho_0}{\rho_e + \rho_0} \right)^{1/2} v_A .$$

is given in Table 2.2. The importance of this speed will be brought out in the next section.

	T_0(K)	T_e(K)	B_0(T)	ρ_0(kgm^{-3})	ρ_e(kgm^{-3})	p_0(Nm^{-2})	p_e(Nm^{-2})
(i)	7000	8800	0.22	1.3×10^{-3}	1.4×10^{-3}	6.0×10^{4}	7.9×10^{4}
(ii)	3900	10250	0.2	2.0×10^{-4}	3.2×10^{-4}	5.0×10^{3}	2.1×10^{4}

Table 2.1. Model parameters for a sunspot at (i) a depth 100km below the $\tau_c = 1$ level in the umbra, and (ii) 150km above the $\tau_c = 1$ level; after Pizzo (1986).

	c_k	c_T	c_s	v_A	c_{se}
(i)	3.7	4.5	8.6	5.3	9.7
(ii)	7.8	5.7	6.4	12.6	10.5

Table 2.2. Characteristic speeds (in kms^{-1}) at the levels (i) and (ii) given in Table 2.1. The speed c_k is defined in the text.

2.1.3 Solutions to the Dispersion Relations

The dispersion relations (2.13) and (2.14) have been solved numerically for the two cases given in Tables 2.1 and 2.2. Figure 2.4 indicates schematically the regions for which modes exist for the two cases, and also gives their classification as defined in section 2.1.1. The terms fast and slow refer to the phase speed being less than, or greater than, $\inf\{c_s, v_A\}$, in a similar fashion to the case of a uniform medium. The difference between the two cases is that fast body modes, which are permitted to propagate below the $\tau_c = 1$ level (case i), become fast surface modes above (case ii). A comprehensive discussion of the allowed modes for various other cases is given in Abdelatif (1988).

Figures 2.5 and 2.6 show the calculated modes for cases (i) and (ii), respectively. For the surface modes, curves for n = 0, 1 and 2 have been plotted. Higher azimuthal order modes differ little from the n = 2 case. The body modes are shown for n = 0 and 1. There are an infinite number of modes for each value of n, analogous to standing waves on a string fixed at two points. Here, only the first three solutions have been shown. Higher order ($n \geq 2$) modes, not shown here, follow a similar pattern. For the slow body modes, higher harmonics have lower phase speeds with the reverse being true for the fast body modes. For n=0 there is also a solution $\omega/k = v_A$. This is the incompressible Alfvén wave since, on substituting this dispersion relation into the original equations (2.2)-(2.5), it can be shown that $p_T, v_z \equiv 0$ and

$$v_r = -\frac{in}{r}\int v_\theta \, dr \,. \qquad (2.16)$$

Since n=0 here, the velocity is purely azimuthal. This mode is not relevant to umbral

oscillations since it would not result in vertical Doppler shifts in the umbra, its motions being entirely in the horizontal plane.

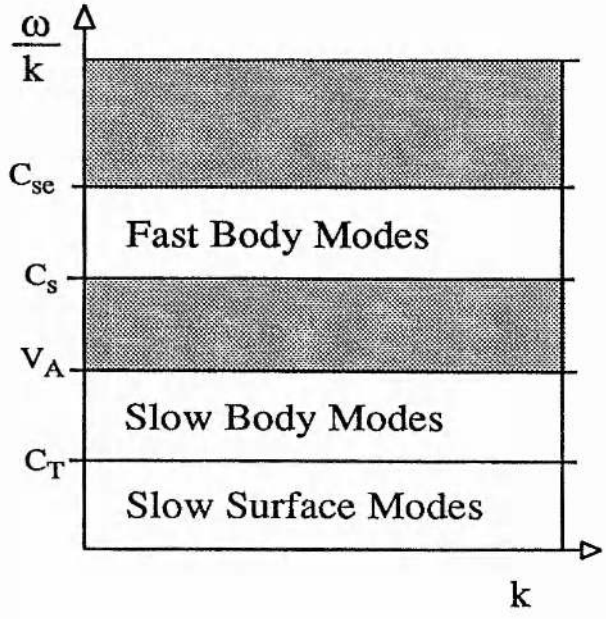

(i)

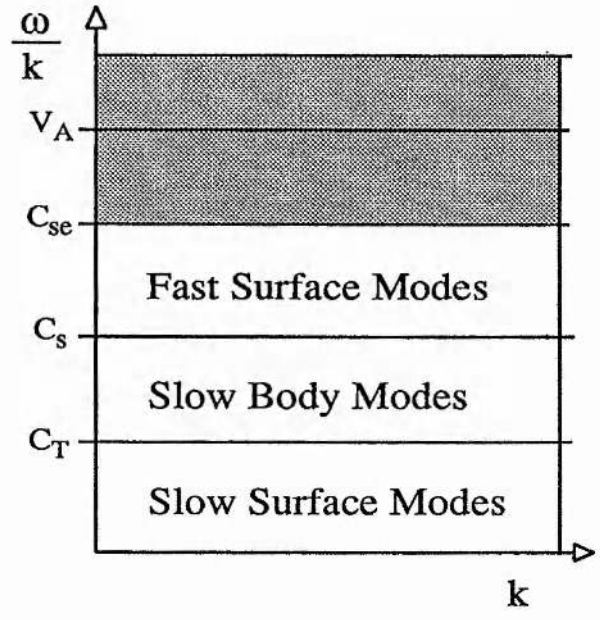

(ii)

Figure 2.4. The phase-speed-against-k plane is divided up by the characteristic speeds, as shown here for cases (i) and (ii). Regions which are shaded allow no modes with $m_e^2>0$.

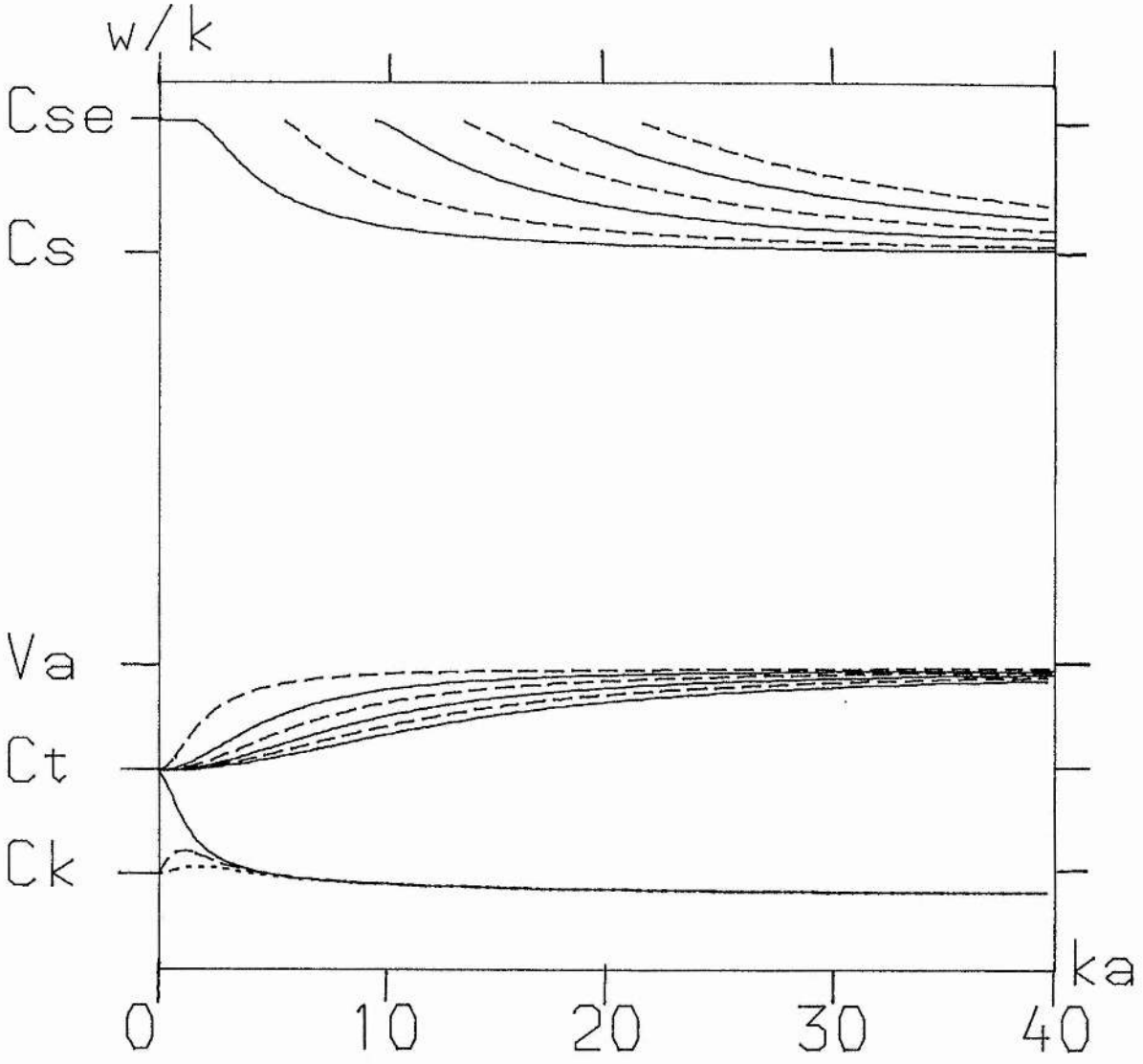

Figure 2.5. Solutions of the dispersion relation for case (i). Solid lines represent n=0 modes, dashed lines n=1, and dotted lines, n=2. The slow surface modes (phase speed<c_T) show virtually identical behaviour for ka large. For the body modes, only the first three solutions have been plotted. For a given value of ka, the lowest harmonics are those with highest phase speed for slow body modes (c_T<phase speed<v_A), and lowest phase speed for the fast body modes (c_s<phase speed<c_{se}). Only the fundamental, n=0, fast body mode can propagate for all ka. Characteristic speeds are c_k=3.7 kms^{-1}, c_T=4.5 kms^{-1}, v_A=5.3 kms^{-1}, c_s=8.6 kms^{-1}, c_{se}=9.7 kms^{-1}.

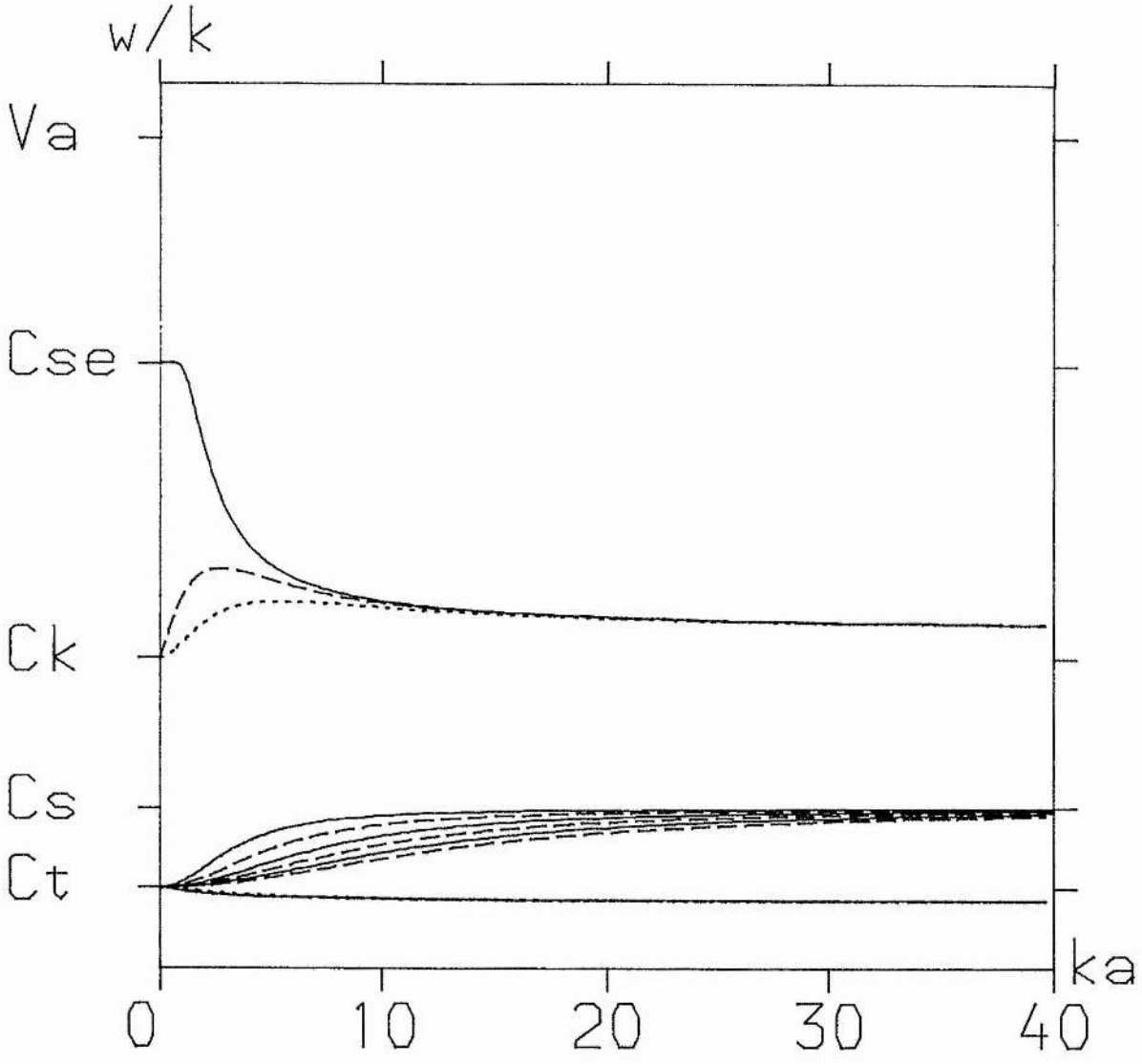

Figure 2.6. Solutions of the dispersion relation for case (ii). Note that the fast body modes of case (i) have given way to fast surface modes (c_s<phase speed<c_{se}). Here the characteristic speeds are: c_T=5.7 kms^{-1}, c_s=6.4 kms^{-1}, c_k=7.8 kms^{-1}, c_{se}=10.5 kms^{-1}, v_A=12.6 kms^{-1} . All the slow surface modes (n=0, 1, 2,...), with phase speed below c_T are virtually identical. Note that the fastest slow body mode here has n=0. This is in contrast to case (i) in which the fastest mode has n=1.

The behaviour of surface modes for small ka and n>0 is largely governed by the value of c_k. If $c_k<c_T$ then the slow surface modes with n>0 have phase speed $\approx c_k$ for small ka whilst for n=0 the phase speed $\approx c_T$. Otherwise, all the slow surface modes satisfy $\omega/k \rightarrow c_T$ as $ka \rightarrow 0$. In Figure 2.6 the slow surface modes for n = 0, 1 and 2 are almost identical. In case (ii) the speed c_k still plays an important role, being the limiting phase speed for the fast surface modes with n>0. Generally there will always be a c_k mode for each n>0. The speed c_k may lie anywhere in the ordering of the characteristic speeds. These modes can sometimes cross from body mode regions to surface mode regions or vice-versa and in this sense are sometimes hybrid modes. However the exact value of c_k does not significantly alter the pattern of modes illustrated in Figures 2.5 and 2.6, merely shifting the positions of the phase speed curves for small ka. Examples of c_k modes for other sets of parameters can be found in Edwin and Roberts (1983) and Abdelatif (1988).

The fast body modes of case (i) are all much the same except the n=0 mode with lowest phase speed. This latter mode asymptotes to c_{se} for small ka, but all the other modes exhibit a cut-off wavenumber, below which they are unable to propagate as fast body modes. The phase speed of these modes increases with harmonic number for given n, and with n for a given harmonic.

The dispersion relations (2.13) and (2.14) may also be solved asymptotically in the limit of long vertical wavelength ($ka \rightarrow 0$). These solutions shed some light on the numerical solutions already given, and so are listed here for completeness. Most have been derived before except for the generalisations to high (n>1) azimuthal orders.

Case (i).

Slow Surface Modes.

n=0:

$$\frac{\omega^2}{k^2} \sim c_T^2 \left(1 + \frac{1}{4} \left(\frac{\rho_e}{\rho_0} \right) \frac{c_s^2 - c_T^2}{c_s^2 + v_A^2} k^2 a^2 \ln (k^2 a^2) \right) \qquad (2.17)$$

(Roberts and Webb, 1978, 1979).

n=1:

$$\frac{\omega^2}{k^2} \sim c_k^2 \left(1 - \left(\frac{\rho_e}{\rho_e + \rho_0} \right) \left(\frac{c_{se}^2 - c_k^2}{c_{se}^2} \right) k^2 a^2 \ln (ka) \right) \tag{2.18}$$

(Edwin and Roberts, 1983).

n≥2:

$$\frac{\omega^2}{k^2} \sim c_k^2 \left(1 + \frac{k^2 a^2}{4n} \varepsilon \right) \quad , \tag{2.19}$$

where

$$\varepsilon = \frac{n(v_A^2 - c_k^2) - (n+2)\left(\frac{\rho_e}{\rho_0}\right) c_k^2}{(n+1) v_A^2} \cdot \frac{(1 - c_k^2/c_s^2)(1 - c_k^2/v_A^2)}{1 - c_k^2/c_T^2} + \frac{n\left(\frac{\rho_e}{\rho_0}\right) c_k^2 - (n-2)(v_A^2 - c_k^2)}{(n-1) v_A^2} (1 - c_k^2/c_{se}^2).$$

Slow Body Modes.

n=0:

$$\frac{\omega^2}{k^2} \sim c_T^2 \left(1 + \frac{c_T^2}{c_s^2 + v_A^2} \frac{k^2 a^2}{(j_{0,i}')^2} \right), \tag{2.20}$$

where $j_{0,i}'$ is the ith zero of J_0' , $j_{0,1}' \neq 0$ (Roberts and Webb, 1979) .

n≥1:

$$\frac{\omega^2}{k^2} \sim c_T^2 \left(1 + \frac{c_T^2}{c_s^2 + v_A^2} \frac{k^2 a^2}{\nu^2} \right), \tag{2.21}$$

where ν is given by

$$\nu \frac{J_n'(\nu)}{J_n(\nu)} = n \frac{\rho_0}{\rho_e} \left(\frac{v_A^2}{c_T^2} - 1 \right). \tag{2.22}$$

Fast Body Mode.

n=0:

$$\frac{\omega^2}{k^2} \sim c_{se}^2 \left(1 - \frac{1}{k^2 a^2} \exp \left[- \frac{\rho_0}{\rho_e} \frac{(c_s^2 + v_A^2)(c_{se}^2 - c_T^2)}{c_{se}^2 (c_{se}^2 - c_s^2)} \frac{1}{k^2 a^2} \right] \right). \tag{2.23}$$

Case (ii).

Slow Surface Modes.

n=0: as (2.17).

n≥1:

$$\frac{\omega^2}{k^2} \sim c_T^2 \left(1 - \frac{c_T^2}{c_s^2 + v_A^2} \frac{k^2 a^2}{\mu^2} \right), \tag{2.24}$$

where μ is given by (Edwin and Roberts, 1983)

$$\mu \frac{I_n'(\mu)}{I_n(\mu)} = n \frac{\rho_0}{\rho_e} \left(\frac{v_A^2}{c_T^2} - 1 \right). \tag{2.25}$$

Fast Surface Modes.

n=0: as (2.23).

n≥1: as (2.18), (2.19).

Slow Body Modes.

As (2.20), (2.21).

All these relations can be easily derived, given the asymptotic expansions for I_n, J_n and K_n (Abramowitz and Stegun, 1965). One difference that is worth noting between cases (i) and (ii) is the ordering of the slow body modes. Comparing Figures 2.5 and 2.6, it can be seen that in case (i) it is a mode with n=1 which has the greatest phase speed while in case (ii) the n=0 mode takes this place. Comparison of the two cases reveals that in (i) there appears to be an additional n=1 mode taking the place of the fastest mode.

For a given value of n, it is convenient to define the fundamental mode to be that with no nodes in the radial part of the eigenfunction for p_T. Then the mth harmonic is the mode with m radial nodes. With these definitions, an examination of the eigenfunctions shows that in case (i) the n=1 slow body mode with highest phase speed is a fundamental mode, and the phase speed of the other modes decreases monotonically with increasing harmonic

number. However, in case (ii) the mode with highest phase speed and n=1 is the first harmonic. In other words, the fundamental mode is missing in case (ii). In contrast, the n=0 mode is always without a fundamental. The modes with n>1 behave like the n=1 modes. For a given harmonic, the phase speed decreases monotonically with n. This result can also be seen from the asymptotic formula (2.21).

From the equation (2.22) for ν, it can be seen that, because the ratio $J_n'(\nu)/J_n(\nu)$ ranges over all of $(-\infty,\infty)$between consecutive zeros of J_n, there must be an infinite number of roots for ν, and hence an infinite number of slow body modes. The interest, however, centres on the behaviour of the left hand side of (2.22) between $\nu=0$ and the first zero, $j_{n,1}$, of J_n. First, it should be noted that for $n\geq 1$,

$$f_n(x) \equiv x\frac{J_n'(x)}{J_n(x)} = x\frac{J_{n-1}(x)}{J_n(x)} - n\ . \tag{2.26}$$

Hence

$$f_n(x) \sim n - \frac{x^2}{2n\,(2n+2)} + O(x^4), \tag{2.27}$$

in the limit $x\to 0$. Thus, f_n decreases from n for small, positive x. It is a general result (Abramowitz and Stegun, 1965) that

$$j_{n-1,1} < j_{n,1}. \tag{2.28}$$

Therefore, f_n encounters the first zero of J_{n-1} before the first zero of J_n, and

$$f_n(j_{n-1,1}) = -n. \tag{2.29}$$

Subsequently, f_n must tend to $-\infty$, as $x \to j_{n,1}$ from below. Thus, on the interval $(0, j_{n,1})$ the function f_n ranges continuously from n and approaching $-\infty$ (see Figure 2.7).

Any local maxima x_{max} in this interval must satisfy $f_n'(x_{max})=0$. But

$$f_n'(x) = -x\left(\frac{J_{n-1}(x)}{J_n(x)}\right)^2 + 2n\left(\frac{J_{n-1}(x)}{J_n(x)}\right) - x, \tag{2.30}$$

so that $f_n'(x)=0$ implies

$$x\frac{J_{n-1}(x)}{J_n(x)}-n=\pm\sqrt{n^2-x^2}\ . \tag{2.31}$$

The left hand side of this equation is simply $f_n(x)$ so that at any maximum

$$f_n(x_{max})=\pm\sqrt{n^2-x^2}\ . \tag{2.32}$$

From this, it can be deduced that in the interval $(0, j_{n,1})$ the function $f_n(x)$ takes on all values of x between n and $-\infty$, and $f_n(x)\leq n$.

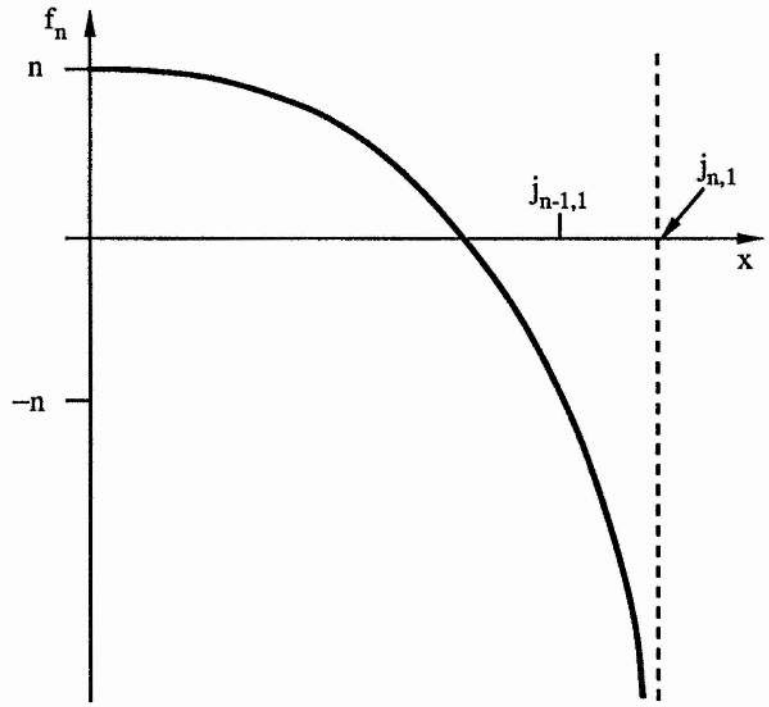

Figure 2.7. Sketch of the function $f_n(x)$ for $0<x<j_{n,1}$ where $j_{n,1}$ is the first zero of J_n.

Returning to equation (2.22), it is now easy to see that the first root for v will lie in the interval $(0,j_{n,1})$, if and only if

$$\frac{\rho_0}{\rho_e}\left(\frac{v_A^2}{c_T^2}-1\right)\leq 1. \tag{2.33}$$

Such a root corresponds to the fundamental slow body modes for n≥1 and (2.33) is the condition for them to exist. This argument does not apply for n=0 and in this case the fundamental is always absent. The condition (2.33) is satisfied in case (i) but not in case (ii). Hence, the fundamental modes for n≥1 are present in Figure 2.5 but not in 2.6.

An approximation often employed for the body modes (e.g. Scheuer and Thomas, 1981) is to use a "rigid tube" boundary condition, corresponding to taking $v_r=0$ at r=a. This results in the following dispersion relation which is much simpler than those given in equations (2.13) and (2.14):

$$a^2 \frac{(\omega^2 - k^2 c_s^2)(\omega^2 - k^2 v_A^2)}{(c_s^2 + v_A^2)(\omega^2 - k^2 c_T^2)} = (j_{n,m}')^2. \qquad (2.34)$$

For the most part this approximation is reasonable in estimating the dispersion relations. However, it cannot cope with the fundamental body modes in the case of n=0. Equation (2.34) gives the results $\omega/k=v_A$, c_s for the lowest harmonic, n=0, slow and fast body modes, respectively, in case (i). This is very inaccurate, especially for small k. Unfortunately, in the models of sunspot oscillations discussed in Chapter 1, those that do take the lateral structure into account employ the rigid tube approximation and usually only consider the modes with n=0, exactly those for which the approximation is worst.

The reason for the break down in the case of the fast body mode is that such oscillations have relatively strong motions outside the tube and so the assumption of a rigid tube can distort the problem significantly. This can be seen in Figure 2.8 where the longitudinal velocity component, v_z, for a slow and a fast body mode are displayed. The edge of the plot is outside the tube but is clearly distorted for the fast mode but virtually undisturbed for the slow mode. The modes chosen for this plot are the n = 0, first harmonics with ka=10.

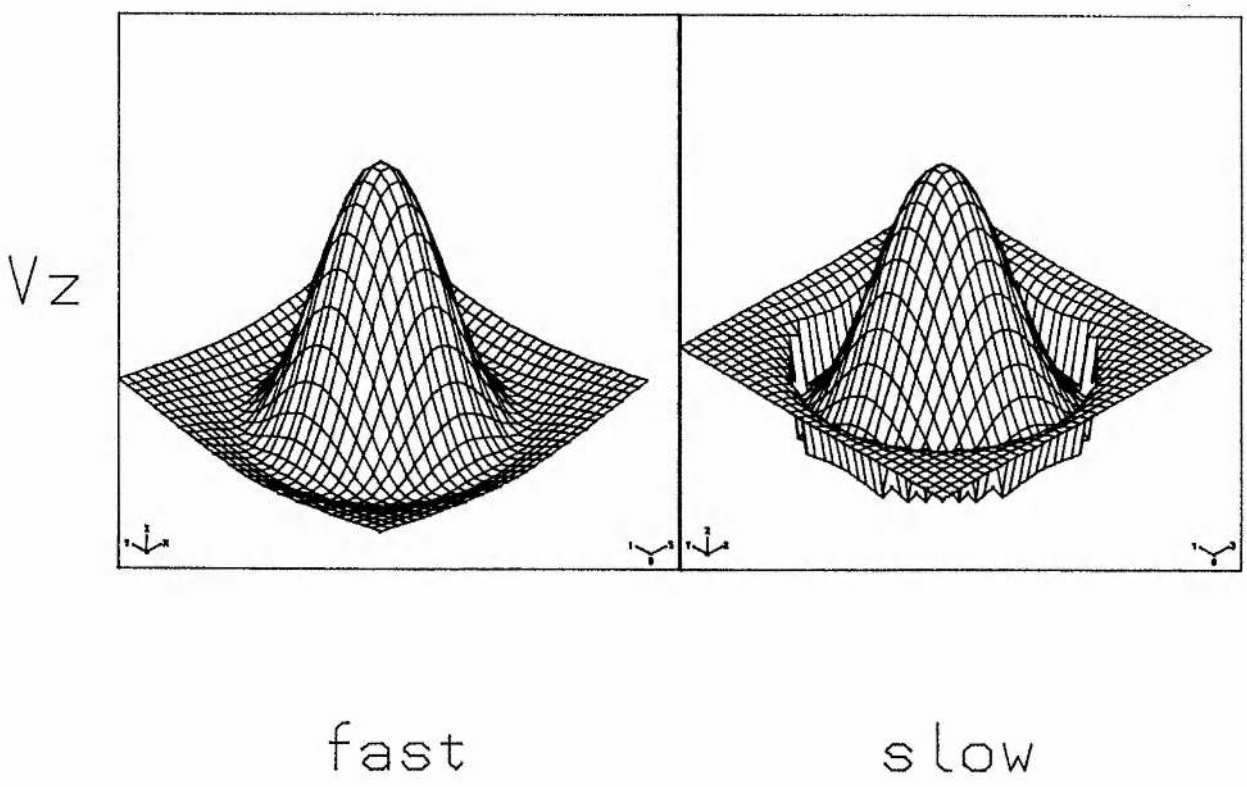

Figure 2.8. Plots of the longitudinal motion v_z for fast and slow body modes in case (i). The side of the square has length 2.5a. Note that the environment is more disturbed for the fast wave than for the slow. Here ka = 10 and n = 0. These are both first harmonics since for the slow wave the fundamental mode does not appear in Figure 2.4 so that direct comparison would not be possible (see text).

2.2 Applications

2.2.1 Three-minute Oscillations

Much work has been done on the observation and interpretation of the three minute oscillations. Moore and Rabin (1985) give an excellent review of the observations, whilst Lites and Thomas (1985), Lites (1986a,b), Gurman (1987), Balthasar et al. (1987) and Thomas et al. (1987) are a selection of more recent work. In order to clarify the discussion, the term "three minute oscillations" will be taken to mean the umbral oscillations with periods in the range 110-200 s and which are detected over a variety of heights from the umbral photosphere to the transition region. These modes were first seen in their more extreme form as "umbral flashes" by Beckers and Tallant (1969). Since then there have been many observations of oscillations and flashes with periods in the range of interest, and at several different levels in the umbra. They are only detected inside the umbrae of stable spots, there being a noticeable absence of power in these ranges for young, developing or unstable spots (Lites and Thomas, 1985). No correlation between sunspot structure and period has been established.

Oscillations with periods in the range 110-200s are observed at various heights in a sunspot, though with differing degrees of clarity (Thomas et al., 1987). Power spectra of the Doppler velocity indicate the existence of up to approximately five peaks whose exact position varies from spot to spot and with height in the umbra but are always in the range for three minute oscillations. Amplitudes are approximately 0.1 kms^{-1} in the photosphere (Abdelatif, Lites and Thomas, 1986) and 5-11 kms^{-1} in the chromosphere (Beckers and Tallant, 1969; Lites, 1986b). This range of amplitudes is not surprising due to the density stratification caused by gravity implying that a wave with constant energy would have a much smaller amplitude in the deeper parts of the spot. Unfortunately, a consequence of this is that three minute oscillations are difficult to detect at photospheric levels. Evidence for the existence of photospheric three minute oscillations is given by Beckers and Schultz (1972), Rice and Gaizauskas (1973), Thomas et al. (1984), Lites and Thomas (1985), and Abdelatif, Lites and Thomas (1986). There is a wealth of observational evidence for three minute oscillations above the photosphere. It is reasonable, though not certain, that these

oscillations are manifestations of the same phenomenon at different heights. Support for this hypothesis is given by the coherence analysis of Lites and Thomas (1985) and Thomas et al. (1987). Henceforth, it will be implicitly assumed that the three minute oscillations extend coherently from the photosphere to the transition region.

Before discussing the nature of umbral oscillations, it is worth considering the structure of the sunspot itself. As discussed in section 1.2.1, it is uncertain whether sunspots consist of a single tube-like column of magnetic flux or a collection of smaller flux-tubes held together by some external force. For a single tube, the model presented in the previous section has an obvious application. In the flux tube bundle though, it is necessary to envisage the effect that closely packed tubes may have on each other and what sort of pattern of oscillation may exist across the umbra. This point should be borne in mind throughout the ensuing discussion.

In offering an interpretation of these oscillations with the simple tube model presented here, attention will be focussed on the body modes. The observations of Giovanelli (1972) and Lites (1986a) indicate peaks and troughs of vertical velocity amplitude across the umbra. This is consistent with the theoretical nature of body modes. A similar effect is shown in Figure 5 of Beckers and Schultz (1972). There is general agreement (Beckers and Schultz, 1972; Giovanelli, 1972; Lites, White and Packman, 1982; Lites, 1986) that there appear to be cells of coherence in umbrae whose size is 2"-4" (≈2000 km). Within such cells there may be vigorous motion with a characteristic frequency in the three minute range, while outside there is a more quiescent behaviour.

The nature of body and surface modes is quite distinct as regards patterns of velocity across the tube. Body modes show significant amplitude across the interior of the tube, with the number of nodes increasing with azimuthal order and harmonic number. By contrast, surface modes attain a maximum in amplitude at the edge of the tube. Clearly, the observations indicate that surface modes of a single, large tube are inappropriate to oscillations in the central part of the umbra. If there is a fragmented sunspot structure, surface modes would be expected to produce a pattern of rings of high velocity amplitude, outlining the flux-tubes making up the sunspot. The evidence again contradicts this view (Figure 2 of Giovanelli, 1972; Figure 4 of Lites, 1986a reproduced on the next page).

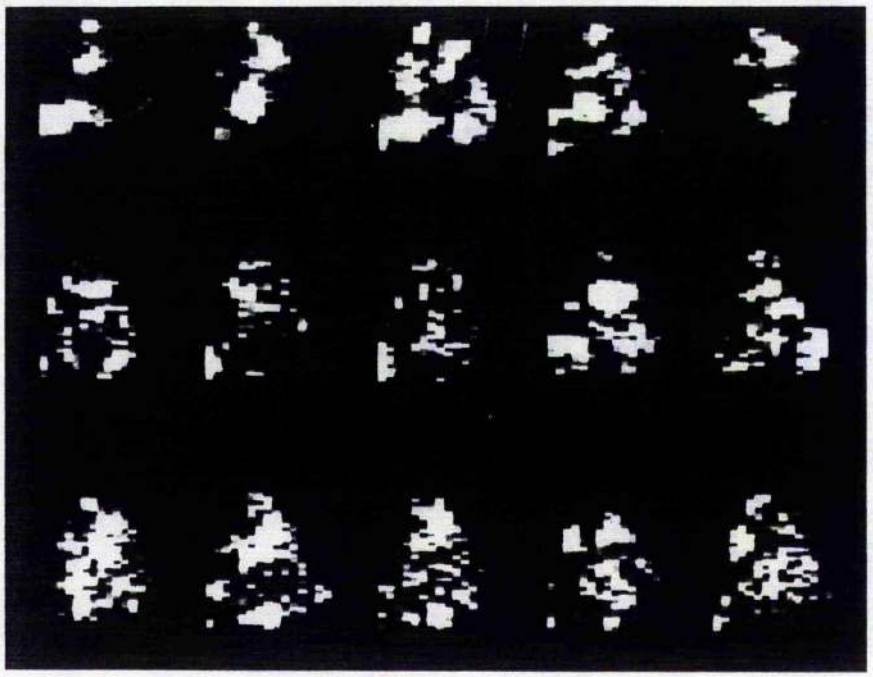

FeI AMPLITUDE

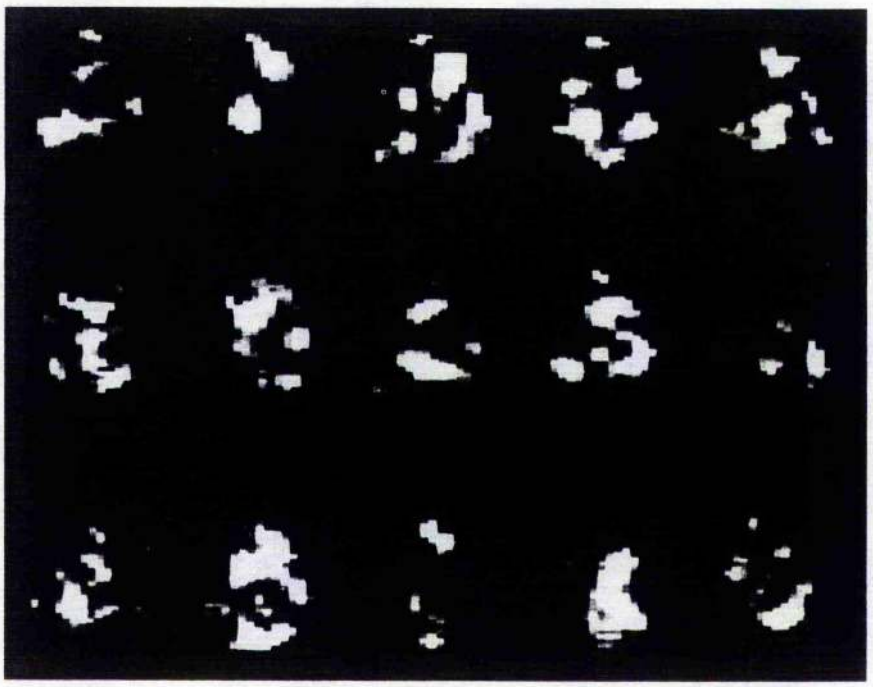

CaII AMPLITUDE

G. 4.—Each image shows the rms oscillatory amplitude as a function of position within the umbra of data set 5 (Paper II) at a given frequency. Upper images he rms amplitudes for Doppler shifts of the Fe I λ5434 line; the lower images show them for core intensity fluctuations in the λ8498 line. The frequency of ation progresses from 5.3 mHz in the upper right to 8 mHz in the lower left in increments of 0.195 mHz. Images thus span the range of frequencies in the 3 e band. The intensity scale of each umbral image has been adjusted so that it spans the full range of gray levels. Note the Fe I and Ca II images correspond quite t the lower frequencies (*top two rows:* lowest 10 frequencies).

Thus, it seems that an explanation for umbral oscillations must rely on body modes. Whether this should be in the context of the single tube or fragmented umbral models will be discussed later.

In the parameter regime appropriate to photospheric layers (case i: $v_A<c_s<c_{se}$) there exist both fast and slow body modes, whereas in the higher layers (case ii: $c_s<c_{se}<v_A$) only the slow body modes occur. Since *three minute oscillations* are observed at both these levels it seems reasonable to identify them with *slow body* modes.

However, Abdelatif(1988) has suggested that three minute oscillations are *fast* body modes, on the basis that fast body modes cannot propagate into the chromosphere (since they are absent in case ii) and three minute oscillations are observed to be evanescent at this level. The observations also show that five minute oscillations are not detected at levels above the photosphere in the umbra. Thus, the three minute oscillations are the more persistent of the two observed in the umbra. It would seem that the most obvious way to match this behaviour with the model presented here is to assume that three minute oscillations are slow body modes. In any case, since the evanescence in the chromosphere is due to the cut-off frequencies introduced by gravity this is an effect not included in our model.

A significant distinguishing feature between slow and fast modes, is the orientation of the fluid velocities (see section 1.2.3), slow modes being channelled along the field lines and fast modes propagating more or less isotropically. It is very difficult to determine observationally the ratio of the velocity amplitudes parallel and transverse to the magnetic field in the umbra but the general belief is that motions in the chromosphere are predominantly aligned with the field (e.g. Uexküll, Kneer and Mattig, 1983). In the photosphere this may not be so pronounced since the field is less dominant there. The observations of Beckers and Tallant (1969) show umbral flashes and small "clouds" of material which have proper motions closely following the field lines. Assuming that umbral flashes are large amplitude extensions of three minute oscillations, it is reasonable to assume that the chromospheric oscillations are mainly aligned with the magnetic field.

Now, from equation (2.15) it can be seen that motions are predominantly field aligned (i.e. $v_z \gg v_r$) for $\omega^2 \approx k^2 c_T^2$ or $\omega^2 \approx k^2 c_s^2$ (provided v_A is not close to c_T or c_s). When $v_A>c_s$, the slow body mode region is bounded by c_T and c_s and so $|v_z|/|v_r|$ will be large.

Consequently, above the photosphere the motions involved in the slow body modes are predominantly field aligned, matching the observational description given above. Hence, it seems likely that the three minute oscillations are indeed slow modes. This conclusion was also reached by Uexküll, Kneer and Mattig (1983) following an analysis of vertical propagation speeds for three minute umbral oscillations.

There are two main candidates for the excitation of three minute oscillations: forcing by overstable oscillations in the superadiabatic layers below the photosphere as originally put forward by Danielson and Savage (1968) and followed up by Moore (1973), Mullan and Yun (1973) and Thomas and Scheuer (1982), and broad-band, turbulent "white noise", as suggested by Zhugzhda et al. (1983, 1984, 1985) and Gurman and Leibacher (1984). To these could be added driving by external p-modes, and buffeting by external convective cells on various scales (granules, supergranules, etc.).

The p-modes seem unlikely to act as the driving mechanism for three minute oscillations, since a predominance of periods around five minutes would then be expected. Observations at chromospheric levels show strong oscillations at three minutes but virtually nothing in the five-minute band. Umbra No 3, a sunspot still in the process of formation observed by Lites and Thomas (1985), showed no significant power in the three minute band but did exhibit strong five minute oscillations. This would again suggest that three minute oscillations are not driven by the p-modes since they should then be present in all three umbrae. It seems much more likely that the p-modes would drive umbral five minute oscillations.

In order to assess the periods that may be generated by granules, supergranules, etc., it may be assumed that at the subphotospheric levels, $v_A \approx 5 kms^{-1}$ and $c_T \approx 4 kms^{-1}$. Then, the two cases of tube radius a=2000 km and a=10000 km, representing extremes in tube size, may be examined in detail. Use of the dispersion relations (2.13) and (2.14), as displayed in Figure 2.5, then allows an investigation of prospective driving mechanisms. Figure 2.5, in particular, allows an assessment of the range of allowable phase speeds for the first few harmonics of the slow body modes, depending on the value of ka. The results are given in Table 2.3. The model would suggest several peaks, corresponding to the various modes, within the range of periods given.

λ	10^4km	10^3km	500km
τ(a=2000 km)	2380-2500s	200-250s	100-120s
τ(a=10^4 km)	2080-2500s	200-210s	100-104s

Table 2.3 The range of periods τ ($\equiv 2\pi/\omega$) predicted by the solutions of dispersion relations (2.13) and (2.14) displayed in Figure 2.5, for various imposed vertical lengthscales λ ($\equiv 2\pi/k$). λ is taken to be 10^4km to represent supergranulation, 10^3 km for granulation and 500 km for overstable convection. The periods τ are calculated for tubes of radius a=2000 km and a=10,000 km.

A scale of $\lambda = 10^4$km has been taken as representative of supergranular buffeting. Clearly this does not produce the desired periods. Thus, supergranules may be ruled out as a driving source for three minute oscillations, leaving granules impacting on the side of the spot or overstable convection within the spot as possibilities.

Slow modes propagate predominantly along the magnetic field, so it is unlikely that an external generation mechanism would produce them with any significant power in the umbra. Also, Lites and Thomas (1985) and Abdelatif, Lites and Thomas (1986) find that the umbral oscillations are strongest near the centre. Thus, any external mechanism is unlikely to drive the umbral three minute oscillation.

Moore (1973), following Danielson and Savage (1968) and Savage (1969), studied the problem of overstable oscillatory convection in the superadiabatic layers below the surface. In this work he chose a typical length-scale of 350 km ,corresponding to a typical wavelength of 700 km. The superadiabatic layer is strong enough to create significant overstability only over the top few hundred kilometres; see ,for example, Parker (1979b, p.265). Thus, it is quite conceivable that the required length-scale for the observed periods is present in overstable oscillations. In the course of studying overstability in sunspots, Roberts (1976) concluded that periods of around 150 s were quite reasonable.

Recently, Hurlburt et al. (1989) have investigated in some detail the behaviour of

convection in the presence of a vertical magnetic field. The nature of the solutions they obtain is similar to the pattern of oscillation observed in sunspot umbrae. Weiss et al. (1989) have looked at a more realistic umbral atmosphere though with umbral dots (Moore and Rabin, 1985) as the primary application. In general though, this work indicates that overstable convection is a very reasonable source of oscillations in a sunspot umbra. Thus, it can be concluded that umbral, three minute oscillations are slow body modes driven by internal, overstable convection. With a=2000 km and a vertical wavelength=700 km, the slow body modes illustrated in Figure 2.5 would give six power peaks in the range 130-150 s; this agrees well with observations. With a=10,000 km, the range in period becomes 130-140 s. Hence the smaller value of radius a (i.e. corresponding to a fragmented sunspot) seems more favourable.

Several authors (Giovanelli 1972; Phillis 1975; Lites 1986a) have noticed a dependency of the oscillation period on position within an umbra. There appear to be cells of coherence, roughly 3 arcseconds (≈2000 km) in diameter, across the sunspot. Giovanelli (1972) indicates that different points in an umbra have their own characteristic frequencies. Figure 1 of Beckers and Schultz (1972) indicates that the period of oscillation increases with distance from the centre of the umbra. Lites (1986a) looks at different patches of umbra separately and finds that each has a distinct power spectrum. Furthermore, he finds that the period of power peaks in a patch tend to drift in time or switch from one value to another.

Returning to the two possible models for a sunspot, a single large tube or a flux tube bundle, illustrated in Figure 2.9, it is not possible, simply on the basis of the periods produced in Table 2.3 to choose between the two suggestions, though the flux tube bundle seems slightly more favourable. The observations indicating a localised nature of the three minute oscillations would seem to favour the flux tube bundle hypothesis, since it is difficult to see how a single large tube could support modes in which period varies with position in the manner outlined by Lites (1986a).

A flux tube bundle model can easily match the observed local nature of umbral oscillations. It is quite natural to expect each tube to have its own characteristic frequencies, etc. The observations of Lites (1986a) indicate a broad similarity in the power spectra for the different patches, but it is clear that there are distinctions. This is to be expected for separate

tubes that are broadly similar. Weak correlation between tubes could occur due to some 'leakage' from one tube to another at lower levels in the spot where slow modes are less confined by the field. Also, it is reasonable to expect that the patches Lites used for the observations would not coincide with the hypothesised small flux-tubes. Consequently, the spectrum of a given patch may be a composite derived from two or more flux-tubes. Then, the simple fact of one tube's oscillation growing while another's decayed would appear as if the patch covering both tubes *switched* from one mode to another.

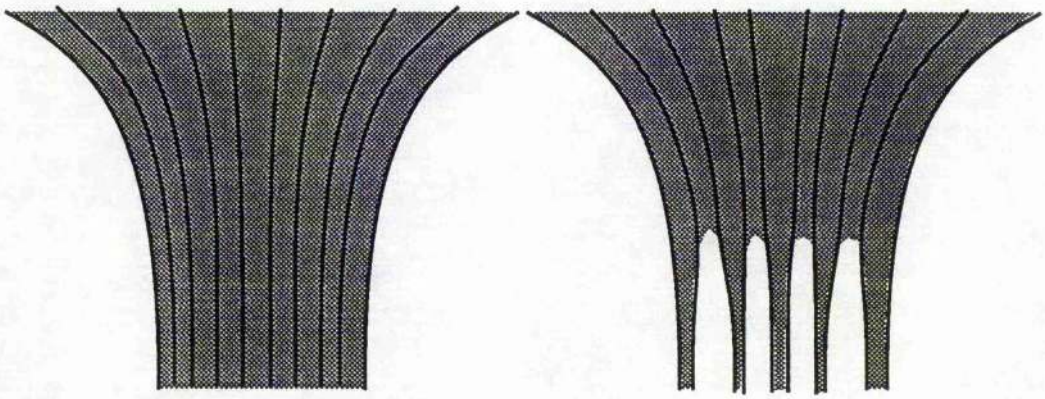

Figure 2.9. Sketch of the two suggested sunspot structures. The conventional single tube model is shown in (a) and the fragmented structure suggested by Parker (1979a) in (b).

Recently, Garcia de la Rosa (1987) has observed the development and breakup of sunspots, indicating that pore-sized elements retain their identity throughout. It would be of considerable interest if such observations could be repeated with an examination of the oscillations in each pore throughout the breakup. The bundle hypothesis suggests that a thin tube approximation may be used, as in the work of Hollweg and Roberts (1981). With various assumed magnetic geometries, Hollweg and Roberts were able to generate the appropriate periods.

In summary, then, it has been argued that overstable convection in the subphotospheric regions is the predominant source of slow waves with periods in the range 110-200s. These waves may propagate at all levels in the spot. The observed variation of periods across an umbra favours a sunspot structure that is fragmented into individual tubes, as put forward by

Parker (1979a).

2.2.2 Five Minute Umbral Oscillations and the Absorption of p-modes by Sunspots

Oscillations with periods around five minutes are detected in photospheric spectral lines formed in the umbral photosphere of sunspots (Soltau, Schroter and Wohl, 1976; Giovanelli, Livingston and Harvey, 1978; Thomas, Cram and Nye ,1982, 1984; Abdelatif, Lites and Thomas, 1986; Balthasar, Kuveler and Wiehr, 1987). As with three minute oscillations, they may exhibit a cellular pattern. Five minute umbral oscillations are lower in amplitude than those found in the quiet Sun (Abdelatif et al., 1986; Balthasar et al., 1987). There is no indication that these five minute oscillations exhibit the same characteristic dispersion curves as for the p-modes of the quiet Sun. As mentioned earlier, Lites and Thomas (1985) examined three umbrae, one of which was still in the process of formation, and found that whereas only the two well formed spots exhibited three minute oscillations, all three showed signs of five minute oscillations. Thus, whatever drives five minute oscillations in a sunspot it cannot be strongly influenced by the stability or youth of the spot. It seems likely, as Thomas (1981) has suggested, that the p-modes of the quiet Sun are responsible for driving five minute oscillations in sunspots.

Power spectra indicate several peaks around the 300 s period for depths which roughly correspond to case (i) of the model described in the earlier sections of this chapter. Spectral lines whose height of formation corresponds to case (ii) show little, or no power in the five minute band. Abdelatif et al. (1986) conclude that the peaks indicate a filtering of frequencies due to the sunspot structure. They also detect a shift towards lower horizontal wavenumbers in going from the quiet Sun to an umbra. This arises due to an increase in horizontal phase speed from acoustic to fast magnetoacoustic.

To discuss the interaction of external acoustic waves with the flux tube, it is necessary to examine solutions (2.11) with $m_e^2<0$. To represent an incident acoustic wave and its reflection, the appropriate form of the solution outside the tube is

$$p_T = H_n^{(1)}(n_e r) + C_e H_n^{(2)}(n_e r), \qquad r > a, \tag{2.35}$$

where $H_n^{(1)}$, $H_n^{(2)}$ are Hankel functions of the first and second kind representing incoming and outgoing acoustic waves respectively. As before, matching solution (2.35) to the solution $p_T = A_0 J_n(n_0 r)$ for r<a allows A_0 and C_e to be determined. The expression (2.35) represents an incoming wave of unit amplitude and an outgoing wave with amplitude C_e. The values of A_0 and C_e then determine the reflection and transmission properties of the tube for the steady state represented by (2.35). In this way acoustic waves outside the flux tube generate an oscillatory pattern within the tube which is qualitatively the same as that for fast body modes.

The condition for waves outside the tube to propage is simply $n_e^2>0$. The expressions n_0, n_e play the same role as would the horizontal wave number for a plane geometry. From continuity arguments, it is clear that the frequency and vertical wavenumber is identical for the exterior and interior solutions and hence there is a relationship between n_0 and n_e. This simply reflects the fact that there will be a change in horizontal wavenumber between the inside and outside of the tube. For a given value of frequency ω and external horizontal wavenumber n_e, it is easy to show that

$$n_0^2 = \frac{\left(\omega^2\left[1-\frac{c_s^2}{c_{se}^2}\right]+c_s^2 n_e^2\right)\left(\omega^2\left[1-\frac{v_A^2}{c_{se}^2}\right]+v_A^2 n_e^2\right)}{\left(c_s^2+v_A^2\right)\left(\omega^2\left[1-\frac{c_T^2}{c_{se}^2}\right]+c_T^2 n_e^2\right)}. \qquad (2.36)$$

The values of the external horizontal wavenumber n_e and the frequency ω will be determined by the p-mode dispersion relations for the exterior of the sunspot.

For the parameter values of case (i), that is $c_{se}>c_s>v_A>c_T$, the squared internal horizontal wavenumber n_0^2, regarded as a function of n_e^2 with ω fixed, has the form

$$f(x) = \frac{(a+x)(b+x)}{c+x},$$

with x taking the place of n_e^2 and a, b, c>0. Furthermore c>a and c>b. A simple sketch shows that f>0 and is monotonically increasing for x>0.

Applying this to n_0^2, it is easy to see that, for waves that are propagating outside the flux tube ($n_e^2>0$), only disturbances with

$$n_0^2 \geq n_{0\,min}^2$$

will be generated. Here

$$n_{0\,min}^2 = \frac{\omega^2 \left(1 - \frac{c_s^2}{c_{se}^2}\right)\left(1 - \frac{v_A^2}{c_{se}^2}\right)}{c_s^2 \left(1 + \frac{v_A^2}{c_s^2}\right)\left(1 - \frac{c_T^2}{c_{se}^2}\right)} . \qquad (2.37)$$

Disturbances with $n_0^2<n_{0\,min}^2$ are fast body modes, confined to the interior of the tube.

Below the photosphere, v_A^2/c_{se}^2, c_T^2/c_{se}^2 and v_A^2/c_s^2 are small (see Figure 2.2) so that $n_{0\,min}^2$ is approximately

$$n_{0\,min}^2 \approx \frac{\omega^2 (c_{se}^2 - c_s^2)}{c_s^2 c_{se}^2} . \qquad (2.38)$$

As mentioned earlier, the temperature outside a sunspot is larger than the internal temperature so $c_s^2<c_{se}^2$. Also, both sound speeds increase with depth. The influence of the magnetic field relative to the fluid pressure decreases with depth. Thus, the inhibiting effect of the magnetic field on convection also decreases with depth. Together with the effects of radiative heat transfer, it is expected that the internal and external temperatures, and hence the internal and external sound speeds, of the sunspot will become more nearly equal in the lower levels. Therefore, in the deeper regions of a sunspot, where magnetic effects are small, $n_{0\,min}^2$ will decrease with depth.

Suppose that interaction between a flux tube and p-modes at some particular depth generates a wave within the sunspot having a value of n_0^2 marginally above $n_{0\,min}^2$ at that level. Some of this wave energy will propagate up the flux tube maintaining the same values of frequency ω and horizontal wavenumber n_0. At some higher level, $n_{0\,min}^2$ will have increased in value and thus may be greater than n_0^2 for the wave under consideration. In

which case the wave is completely reflected at the tube boundary where $n_0^2 < n_0^2{}_{min}$. In other words, the wave becomes a fast body mode. Hence p-modes can generate internal tube waves which can become fast body modes as they propagate upwards. Five minute umbral oscillations are thus a mixture of fast body modes and p-modes passing through the sunspot.

As already pointed out, a distinguishing feature between the two cases of the model is that the fast body modes of case (i) are replaced by fast surface modes in case (ii). This naturally raises the question of what happens to the fast body modes as conditions change from case (i) to case (ii). Defining a critical wavenumber k_c to be the wavenumber where a fast body mode dispersion curve intersects the line $\omega/k = c_{se}$, it follows from the dispersion relation (2.14) that

$$\frac{\rho_0}{\rho_e} k_c^2 \left(v_A^2 - c_{se}^2 \right) n = k_c^2 c_{se}^2 \, \overline{n_0} \, a \, \frac{J_n'(\overline{n_0} a)}{J_n (\overline{n_0} a)}, \tag{2.39}$$

where

$$\overline{n_0}^2 = \frac{k_c^2 (c_{se}^2 - c_s^2)(c_{se}^2 - v_A^2)}{(c_s^2 + v_A^2)(c_{se}^2 - c_T^2)}$$

is n_0^2 evaluated for $\omega = k_c c_{se}$. For $n = 0$ equation (2.39) reduces to

$$k_c a = \left(\frac{(c_{se}^2 - c_T^2)(c_s^2 + v_A^2)}{(c_{se}^2 - c_s^2)(c_{se}^2 - v_A^2)} \right)^{1/2} j_{0,s}', \tag{2.40}$$

where $j_{0,s}'$ is the sth zero of J_0' (Note: $J_0' = J_1$, $j_{0,1}' = j_{1,1} = 3.8317$, $j_{0,2}' = 7.0156$, $j_{0,3}' = 10.1735$, etc.)

The transition between cases (i) and (ii) occurs when v_A exceeds c_{se}. Therefore, it is of interest to understand the behaviour of the fast body modes as v_A approaches c_{se} from below. From equation (2.40) it can be seen that as $v_A \rightarrow c_{se}$ the critical (or cut-off) values k_c all tend to infinity: the fast body mode dispersion curves of Figure 2.5are "squeezed"

between c_{se} and v_A. The one exception to this is the fundamental, n=0 mode which exists for all vertical wavenumbers k.

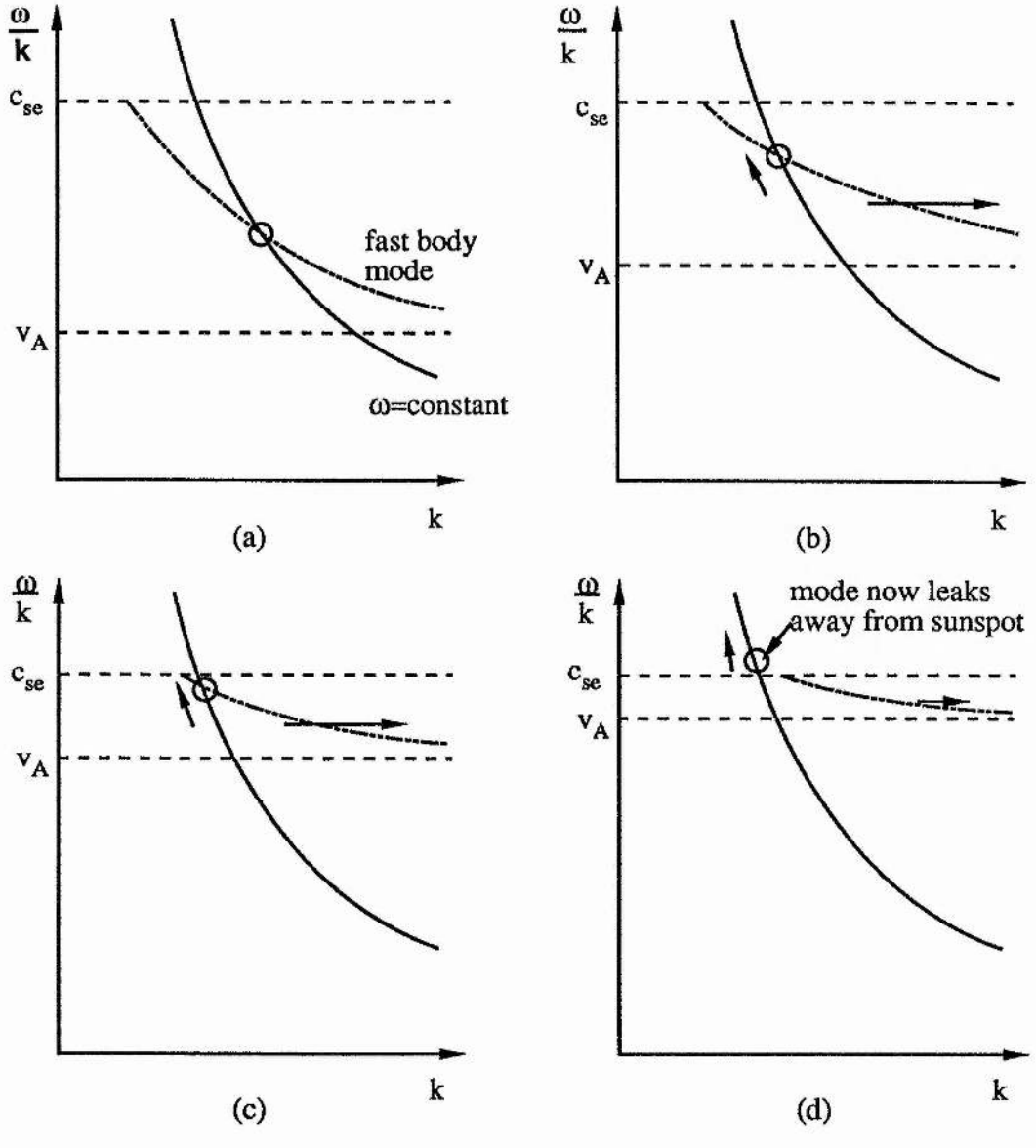

Figure 2.10. A schematic illustration of the effects of increasing v_A towards c_{se} on a particular fast body mode (marked by the circle). As v_A increases, i.e. moving from (a) to (d), the dispersion curve moves to the right. Thus it intersects the curve ω=constant at increasing phase speeds. Eventually it crosses the line $\omega/k=c_{se}$ into the region of external propagation ($m_e^2<0$) at which point the fast body mode leaks away.

At a given height in the sunspot, suppose a fast body mode oscillates with frequency ω

and vertical wavenumber k. As it propagates up the sunspot, the frequency will remain constant while k will change in response to changing physical conditions. This behaviour can be represented on the dispersion curve diagram, Figure 2.5, as the hyperbola $c=\omega/k$, where ω is a constant and c is the vertical phase speed. The mode under discussion is then given by the intersection of this hyperbola with the relevant dispersion curve. This is illustrated in Figure 2.10.

For simplicity, it is convenient to assume c_{se} is constant while v_A increases. This will not affect the final conclusion since the crucial feature is the "squeezing out" of the fast body modes. As v_A increases, the dispersion curves move toward larger values of k. The mode with fixed ω must remain on the hyperbola and will simply "slide along" according to where the dispersion curve intersects. From Figures 2.10b, c it can be seen that the effect of increasing v_A is to move the mode in question closer to the line $\omega/k= c_{se}$. Ultimately it will cross this line (Figure 2.10d) and hence become a mode which propagates laterally outside the sunspot, having $m_e^2<0$. In other words, the fast body mode will leak away from the sunspot. Observationally, they would be difficult to detect since the waves would have the same frequency of around 3.3 mHz that the p-modes in the surrounding active region have. There should be some evidence of scattering, however, due to inevitable differences in horizontal wavenumber between p-modes and leaking fast body modes which would show up in dispersion curves.

Recently, Braun, Duvall and Labonte (1987, 1988) have discovered that a sunspot can absorb up to half of the energy available in p-modes that strike its edges. They examined the pattern of five minute oscillations surrounding a sunspot and decomposed this into radially propagating waves approaching and receding from the spot. Their procedure is the observational equivalent of the Hankel function representation in equation (2.35). This results in two ω-k diagrams, one for in-going and one for out-going waves. Braun et al. find a reduction in power for the reflected waves in comparison to the in-going ones. The authors also present a more quantitative analysis by masking out the regions between the p-mode ridges and calculating absorption coefficients for the remaining modes. It is found that the absorption increases with horizontal wavenumber until reaching a steady value of approximately 50% at $k\approx0.5$ Mm^{-1} as can be seen from their Figure 2 reproduced overleaf.

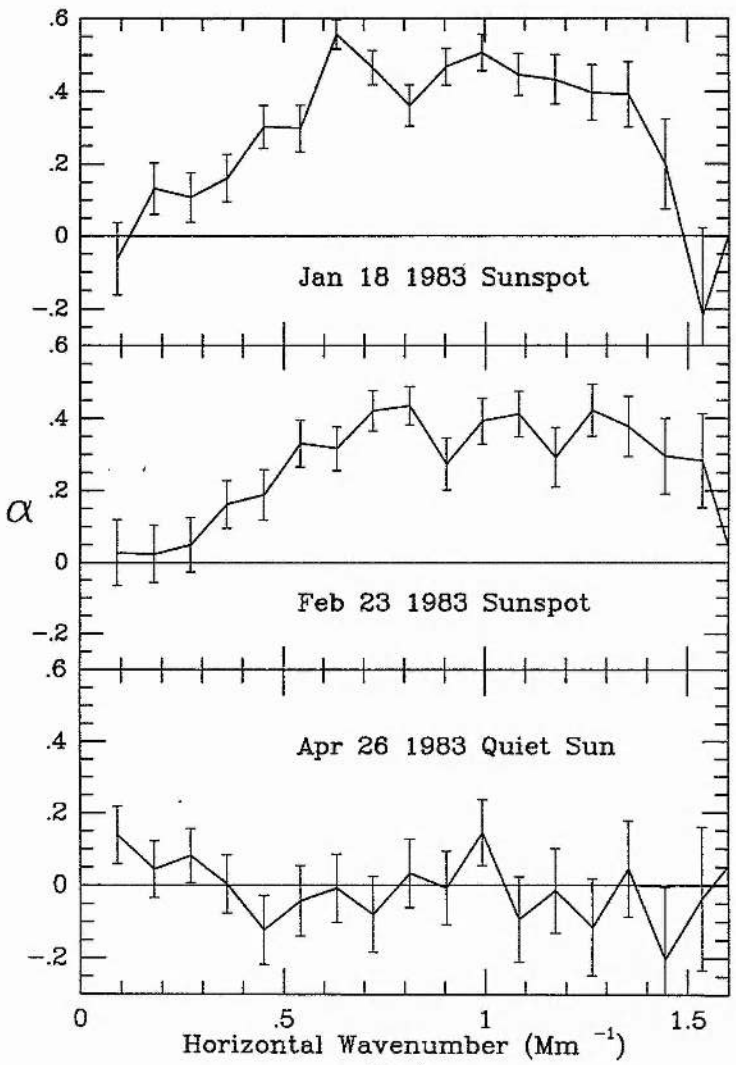

FIG. 2a

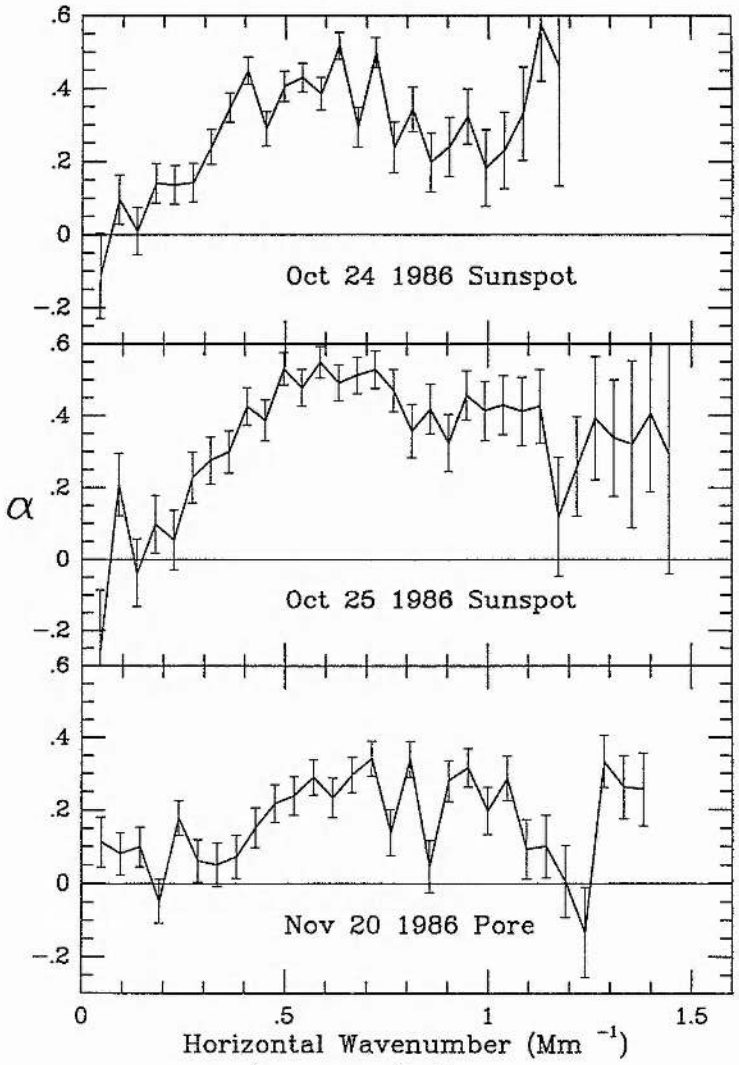

FIG. 2b

FIG. 2.—(*a*) The absorption coefficient α (defined in text) vs. horizontal wavenumber for the 1983 data. (*b*) Same as (*a*) for the 1986 data. In all cases α is shown up to the horizontal wavenumber where *p*-mode power can still be discerned from the background noise. In this and all subsequent plots the errors in the observed absorption were calculated from the statistical properties of the power spectra and a standard treatment of error propagation.

In other words, apart from very long wavelengths, about half the energy available in p-modes is consumed by the sunspot in some manner. They calculate that there is an energy flux of about 10^7 erg cm^{-2} s^{-1} going into a sunspot. Further investigations by Braun et al. (private communication) have shown even larger absorption coefficients in the neighbourhood of strong active regions.

If this absorption depends significantly on subphotospheric sunspot structure then detailed study may provide a probe for the hidden layers of sunspots. Braun et al. (1988) discuss some possible explanations for the absorption of p-modes. Hollweg (1988) has investigated the possibility that these waves are dissipated by resonance absorption in the boundary of the sunspot, and finds that while the effect is not insignificant it falls a long way short of the magnitude of absorption that is actually observed. The work of Bogdan and Zweibel (1987) on the scattering of acoustic waves by fibril fields is also of possible relevance. However, their calculations are difficult to apply directly to a sunspot because they assume small filling factors. Nonetheless, Braun et al. conclude that it is unlikely that such scattering could generate an apparent absorption of the order of 50%.

The process by which fast body modes in a sunspot are driven by p-modes interacting with the spot, as developed here, offers another possible explanation since one result of this process is to take energy from p-modes and trap it within the sunspot. To investigate this possibility, it is necessary to know how much acoustic wave energy is absorbed by a magnetic interface. A general discussion of such a process has been given by Rae and Roberts (1983). Their equation (21) gives the energy flux of an incident wave which is transmitted and reflected at the magnetic interface. From this it is possible to derive the absorption coefficient, i.e. the ratio of transmitted energy to incident energy. Employing the same notation as for the sunspot calculation above, it may be shown that the fraction of energy absorbed by a wave incident on a magnetic interface is A^2, given by

$$A^2 = \frac{4X}{(1+X)^2} \tag{2.41}$$

where

$$X = \frac{\rho_0}{\rho_e}\frac{n_e}{n_0}\left(\frac{n_e^2 v_A^2}{\omega^2} + \left[1 - \frac{v_A^2}{c_{se}^2}\right]\right).$$

The absorption coefficient A^2 is plotted in Figure 2.11 for the parameters of case (i) and with ω=0.01 s^{-1} and 0.03 s^{-1}, a frequency band including the 5 minute oscillations. Evidently A^2 shows the same behaviour for small horizontal wavenumber n_e as observed by Braun et al. For n_e>0.5 Mm^{-1}, however, there must be some mechanism moderating the absorption. Since n_e and k are related by

$$n_e^2 = \frac{\omega^2}{c_{se}^2} - k^2,$$

it follows that for small n_e, k is large and so the wave propagates in a largely vertical direction. Such waves will rapidly reach the height where they may be trapped within the sunspot and so, nearly all the the absorbed p-mode energy in this case is lost from the quiet Sun (see Figure 2.12a). On the other hand, as n_e increases, the incident wave propagates more and more nearly horizontal. This means that much of the wave energy will reach the opposite boundary of the sunspot and re-emerge relatively unscathed (Figure 2.12b). This will have the desired effect of moderating the absorption.

This is only a sketch of how such a mechanism may work. Since it requires both structuring of the magnetic field for the initial absorption, and gravitational stratification for the trapping at greater heights, it will be difficult to model this in a fully consistent stratified model, though it may be possible to perform a numerical simulation of the process.

2.2.3 Penumbral Waves

Giovanelli (1972, 1974) and Zirin and Stein (1972) first observed oscillations in the penumbra of a sunspot. In movies of a spot viewed in the wings of the Hα spectral line, dark rings around part of the umbra were seen to propagate outwards. They have amplitudes of approximately 1kms^{-1} at the umbral-penumbral boundary and have phase speeds in the range 10-30 kms^{-1}. Periods observed show quite a range of values. Thomas, Cram and Nye (1984) report periods around 200-300 s, whilst Lites (1988) finds frequencies as low as 0.7 mHz (periods as high as 1400 s). Several authors have reported a relationship between umbral oscillations and penumbral waves (Giovanelli 1972, Lites, White and Packman 1982; Lites 1988) which may be interpreted as being due to their having a common

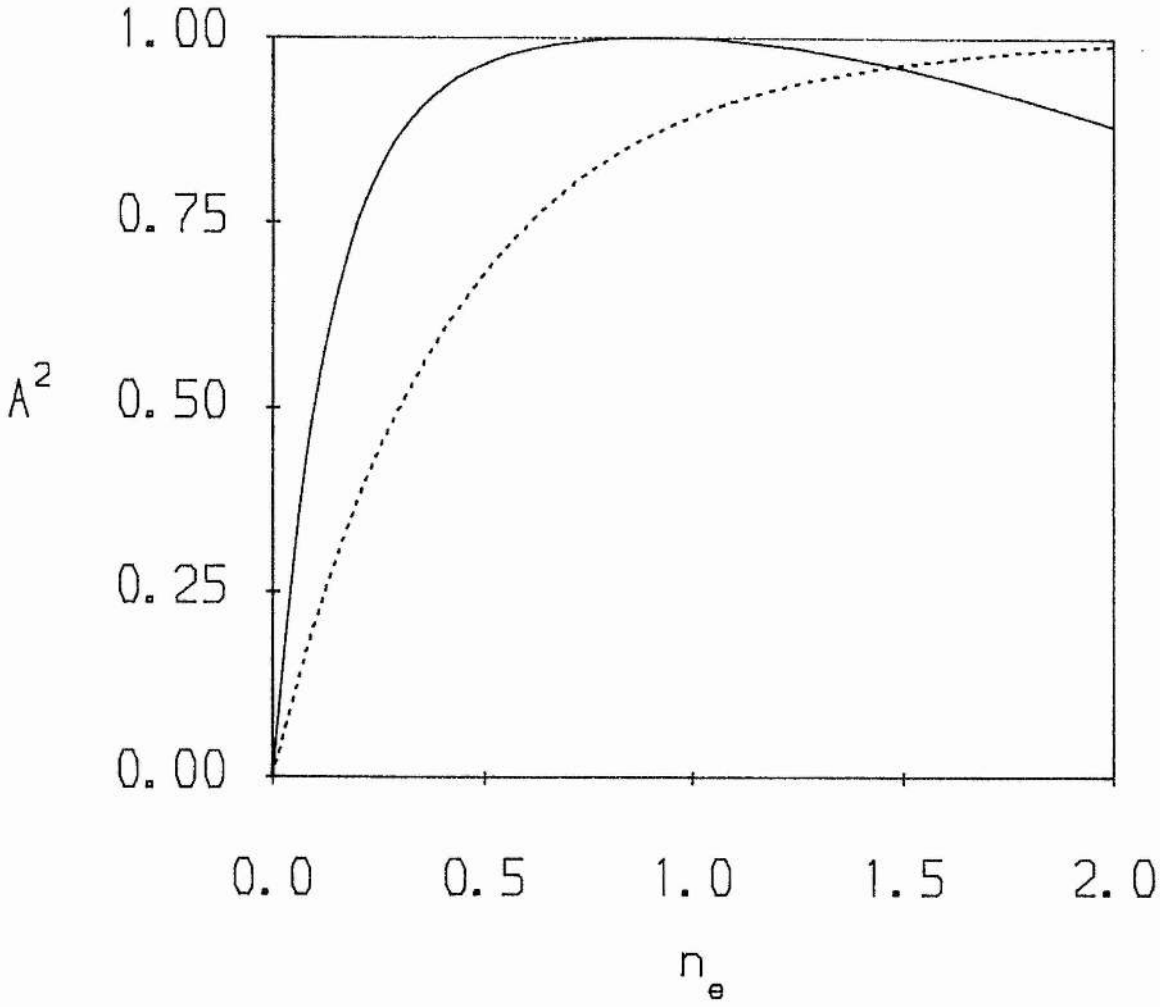

Figure 2.11. Plot of the absorption coefficient for acoustic waves encountering a magnetic interface as a function of the horizontal wavenumber in the field-free region. The parameters used here are the same as for case (i): $v_A<c_s<c_{se}$. The solid line is for $\omega=0.01$ s^{-1} and the dotted line is for $\omega=0.03$ s^{-1}, corresponding to cyclic frequencies ($\omega/2\pi$) of 1.59 mHz and 4.77 mHz respectively. Note the increase in absorption for small n_e, much as observed by Braun, Duvall and Labonte (1988).

source (Moore 1973). Recent observations by Lites (1988) of penumbral waves are particularly detailed. He reports frequencies of ≈3.5 mHz (period≈286 s) and ≈2 mHz (period≈500 s) in the upper photosphere, but only ≈3.5 mHz higher up in the penumbral chromosphere. Also, he states that motions in the high photosphere are predominantly aligned with the field; previously the motion was thought to be transverse. The alignment of the motions in the penumbral chromosphere remains uncertain. The 3.5 mHz waves in the chromospheric penumbra do not show the characteristic pattern of p-modes, despite the close similarity of the frequencies. In the outer penumbra, the power spectrum and nature of the oscillations indicate a simple response to the p-modes of the quiet Sun. These are essentially p-modes modified by the effects of a chromospheric field. This topic will be examined in the next chapter.

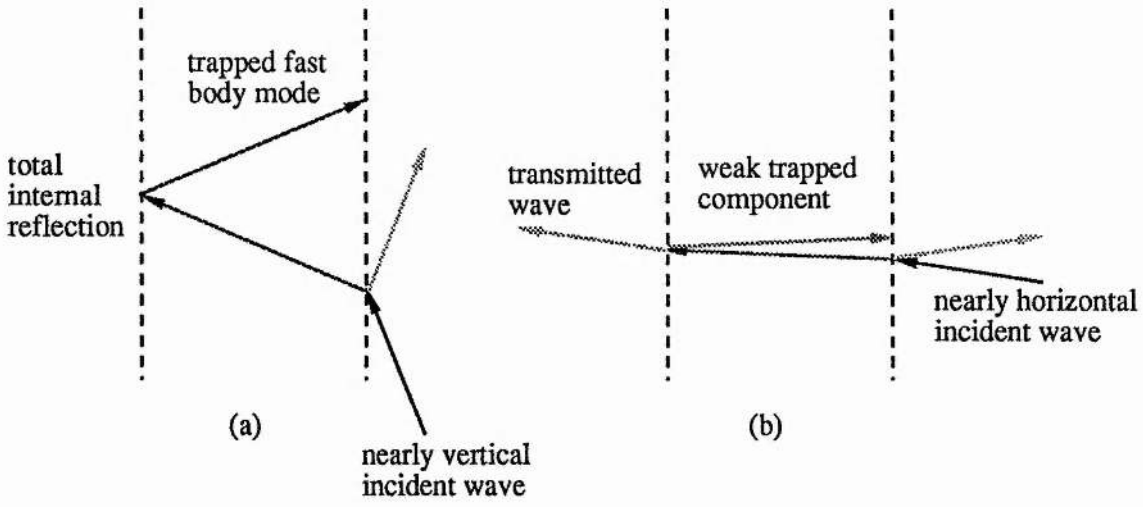

Figure 2.12. An illustration of the difference in behaviour between nearly vertical (a) and nearly horizontal waves (b) incident on a sunspot. In (a) all the wave energy transmitted into the sunspot is trapped due to rapid upward propagation. In (b) a significant amount of the wave energy transmitted into the sunspot leaks out the other side.

Clearly, a flux tube model does not represent the penumbra. However, it is possible that penumbral oscillations emanate from the lower parts of the sunspot and so have their origin as some kind of tube wave, in which case it is probable that the observed oscillations are surface modes, confined to the edge of the tube and only becoming visible when these

edges fan out. The surface modes would be guided along the curving magnetic interface. In case (ii) of the flux tube model, as appropriate to the upper levels where the spot begins to fan out, two surface modes are possible, the slow and the fast waves. The motions associated with slow surface waves are predominantly field aligned. This is in accord with the observations of Lites (1988) who indicates that the penumbral oscillations are field-aligned in the photosphere near the umbra. This is not necessarily the case in the penumbral chromosphere. In other words, field-aligned motions are restricted to the photospheric parts of the penumbra. The lack of detection of the 2 mHz frequency in the penumbral chromosphere reported by Lites (1988), could indicate a correlation between this lower frequency and the field aligned motions. Consequently, it seems natural to identify these 2 mHz oscillations as slow surface modes and the 3.5 mHz waves as fast surface modes.

This identification is also supported by an examination of the variation in amplitude of the surface modes, with distance from the interface. Miles and Roberts (1989a), following on from Roberts (1981a), have recently discussed magnetoacoustic surface modes at an interface between a magnetic and a non-magnetic region. They find that there exist two surface waves, fast and slow, but that only for certain orderings of the characteristic speeds are both permitted. When both fast and slow surface waves are present Miles and Roberts (1989a) find that the penetration depth (i.e. the distance from the interface at which the wave amplitude is reduced by a factor e) for the fast surface mode is greater than that for the slow surface mode. A similar result can be seen here by examining the penetration depth, $1/m_0$, inside the tube of the flux tube model for $\omega^2 \approx k^2 c_T^2$ (slow) and $\omega^2 \approx k^2 c_{se}^2$ (fast). This could explain, within the present interpretation, why Lites (1988) does not find frequencies around 2 mHz in the upper penumbral chromosphere, this being further from the magnetic interface than the penumbral photosphere. The chromospheric oscillations in the penumbra will originate from nearer the centre of the umbra than the photospheric ones. Thus, since the slow surface mode has a smaller penetration depth than the fast surface mode, it is expected that there will be a significant reduction in the strength of the slow mode in comparison with the fast, around the central regions of the tube.

This naturally raises the question of how the surface modes are driven. Despite the

low phase speed of the slow surface modes, it is only necessary to have a wavelength of the order of 1000 km to generate such long periods as seen by Lites (1988). Thus it is quite conceivable that the slow surface waves are generated by granules outside the spot impacting against the sides. On the other hand, many observations (Lites, 1984; Thomas, Cram and Nye, 1984; Giovanelli, 1972; Zirin and Stein, 1972; Musman, Nye and Thomas, 1976) indicate that the running penumbral waves have periods in the range 200-300 s and that there are some correlations between the penumbral waves and umbral three minute oscillations. From this, Moore, (1973) concluded that there exists a common source, namely overstable convection, in which case, adopting the same mechanism as employed to drive the slow body modes means imposing a vertical wavelength of approximately 700 km. The results of Figure 2.5 then indicate that periods of around 200 s result. Thus the slow surface modes could be driven by granular buffeting or overstable convection, with overstable convection being preferred in light of the reported correlation between the umbral and penumbral oscillations.

In the lower levels of a sunspot, modelled by case (i), there are no fast surface modes. However, in the previous section it was shown that fast body modes could be driven by the interaction between p-modes and sunspots. As these body modes propagate vertically upwards they approach the level where $v_A=c_{se}$. At this level, only the fundamental, n=0 fast body mode remains, the other fast body modes having been "squeezed out", as discussed in the previous section. As v_A approaches c_{se} from below, the dispersion curve for the n=0, fundamental fast body mode, reduces to $\omega/k=v_A=c_{se}$, and so $n_0^2\rightarrow 0$. Thus, the eigenfunction for p_T in this degenerate case is simply a constant. For case (ii), a similar fate awaits the n=0 fast surface mode as v_A approaches c_{se} from above. In this sense then, the fast surface mode and the fundamental fast body mode for n=0, are simply manifestations of the same thing in the two cases of $v_A>c_{se}$ and $v_A<c_{se}$. Thus, the fast body mode in the lower reaches of the sunspot will become the fast surface mode higher up. With the fast body mode in the lower reaches of the spot being driven by the p-modes, this particular mode offers a natural explanation of the 5 minute penumbral oscillation that has the markedly different character to the quiet Sun 5 minute modes, as reported by Lites (1988).

Is there sufficient energy in the p-modes to drive the penumbral waves? Giovanelli et

al. (1978) estimate an energy flux in running penumbral waves of very much less than 3×10^6 erg cm^{-2} s^{-1}. Assuming this energy to be radiated over the entire spot with a radius of 10^4 km gives a total energy flux for running penumbral waves over the whole spot of very much less than $3\times10^6.\pi.(10^9)^2$ erg $s^{-1}\approx10^{25}$ erg s^{-1}. On the basis of stochastic excitation by turbulent convection, Libbrecht (1988) estimates a total energy flux in p-modes of $\approx10^{30}$ erg s^{-1}. Distributed uniformly over the surface of the Sun implies an energy flux into a sunspot of at most 5×10^{25} erg s^{-1}. Thus it would seem that there is sufficient energy available in p-modes to generate running penumbral waves. These figures also compare well with the report in Braun, Duvall and Labonte (1988) that the energy flux into a sunspot from p-modes is approximately 10^7 ergs cm^{-2} s^{-1}.

2.3 Summary

The basic sunspot configuration has been modelled by an isolated magnetic flux tube within a uniform, field-free medium. The tube supports several different modes of oscillation, which are isolated to the flux tube in the sense that their amplitudes decay roughly exponentially outside the tube. The waves are denoted fast and slow modes according to the magnitude of their vertical phase speeds in comparison with $\inf\{v_A, c_s\}$, and body and surface modes according to whether they are oscillatory or evanescent within the tube (Roberts, 1981b).

For a sunspot, the ordering of the characteristic speeds, important for determining which oscillation modes are permitted, changes with height. In particular, the Alfvén speed increases with height. This has the effect of separating out two regions depending on the ordering of v_A and c_{se}, the external sound speed. Low down in a spot, $v_A < c_{se}$ and fast and slow body modes as well as slow surface modes are permitted. Higher in the spot, where $v_A > c_{se}$, the slow surface and body modes are still permitted but the fast body modes give way to fast surface modes.

In the context of this model, the three minute umbral oscillations are interpreted as slow body modes driven by overstable convection arising in the superadiabatic layer just below the photosphere. This would roughly agree with the chromospheric, slow mode resonator of

Zhugzhda and co-workers (see section 1.2.4), except that they do not invoke overstability as the driving mechanism. However, this does not necessarily rule out the "fast" wave photospheric resonator of Scheuer and Thomas (1981), since the distinction between fast and slow modes is somewhat blurred in the presence of gravitational stratification.

P-modes in the neighbourhood of a sunspot will drive fast magnetoacoustic oscillations within the umbra. If this occurs at a depth where the influence of the magnetic field is small, then it has been shown that these oscillations could drive fast body modes higher up. Thus, five minute oscillations in the umbra may be a mixture of fast body modes trapped within the spot and p-modes propagating through the spot. As the critical level where $v_A=c_{se}$ is approached, many of these fast body modes may leak energy away to the surrounding atmosphere. Finally, the fundamental, n=0 fast body mode is able to propagate through the critical level and becomes a fast surface mode.

Penumbral waves seem likely to be some form of surface wave, launched from the sunspot below the level where its field fans out. These could be either fast or slow surface waves. The fast surface wave has as its ultimate source the five minute oscillations in the quiet Sun. This could explain the presence of a five minute penumbral oscillation whose nature seems distinct from the p-modes. Running penumbral waves generally seem to have different periods. These could be due to slow surface waves driven by overstable convection or granular buffeting on the side of the sunspot.

These results are summarised schematically in Figure 2.13.

Appendix 2.

The governing equations are those of ideal, adiabatic, perfectly conducting MHD:

$$\rho \frac{Dv}{Dt} = -\nabla + \mathbf{j} \times \mathbf{B}, \qquad \text{(A2.1)}$$

$$\mathbf{j} = \frac{1}{\mu} \nabla \times \mathbf{B}, \quad \text{div } \mathbf{B} = 0,$$

$$\frac{D\rho}{Dt} + \rho \nabla . v = 0, \qquad \text{(A2.2)}$$

$$\frac{\partial \mathbf{B}}{\partial t} = \text{curl}\,(\mathbf{v} \times \mathbf{B}), \tag{A2.3}$$

$$\frac{D}{Dt}\left(\frac{p}{\rho^{\gamma}}\right) = 0. \tag{A2.4}$$

With a cylindrical coordinate system, it is assumed here that the equilibrium is axially and vertically (i.e. along the z-axis) symmetric, varying only with radius r, and that the magnetic field is aligned with the z-axis. Then (A2.1) reduces to

$$\frac{d}{dr}\left(p_0 + \frac{B_0^2}{2\mu}\right) = 0, \tag{A2.5}$$

the subscript 0 denoting equilibrium quantities.

A linear analysis of the perturbations about the equilibrium gives the equations (2.2)-(2.5). Fourier analysis of these four equations can be performed by writing

$$v_r = v_r(r)\, e^{i\,(\omega t + n\theta - kz)}$$

and similarly for all other variables. This gives

$$i\,k\rho_0\, c_s^2\, v_z - \frac{i\,n\rho_0}{r}(c_s^2 + v_A^2)v_\theta - \frac{\rho_0}{r}(c_s^2 + v_A^2)\frac{d}{dr}(r\,v_r) - i\,\omega p_T = 0, \tag{A2.6}$$

$$\rho_0\,(\omega^2 - k^2 v_A^2)v_\theta + \frac{n\omega}{r}\,p_T = 0, \tag{A2.7}$$

$$(k^2 c_s^2 - \omega^2)v_z - \frac{nk}{r}c_s^2\,v_\theta + \frac{i\,kc_s^2}{r}\frac{d}{dr}(r\,v_r) = 0, \tag{A2.8}$$

$$i\,\omega\frac{dp_T}{dr} + \rho_0\,(k^2 v_A^2 - \omega^2)\,v_r = 0. \tag{A2.9}$$

Eliminating v_θ and v_z from (A2.6)-(A2.8) then gives

$$\rho_0 (k^2 v_A^2 - \omega^2)\left[(c_s^2 + v_A^2)(k^2 c_T^2 - \omega^2)\right]\frac{1}{r}\frac{d}{dr}(r\, v_r) +$$
$$\left[(k^2 c_s^2 - \omega^2)(k^2 v_A^2 - \omega^2) + \frac{n^2}{r^2}(c_s^2 + v_A^2)(k^2 c_T^2 - \omega^2)\right] i\,\omega p_T = 0. \qquad \text{(A2.10)}$$

The equations (2.6) and (2.7) for v_r and p_T can then be derived from (A2.9) and (A2.10).

In a uniform medium, the equation for p_T reduces to

$$r^2 \frac{d^2 p_T}{dr^2} + r\frac{dp_T}{dr} - (m_0^2 r^2 + n^2)\, p_T = 0, \qquad \text{(A2.11)}$$

For $m_0^2>0$ this is the modified Bessel equation and for $m_0^2>0$ it is simply the Bessel equation, hence the solution (2.8). In terms of p_T, v_r and v_z are given by (A2.7) and (A2.9). A similar expression for v_θ may be derived from (A2.6)-(A2.8):

$$\rho_0(c_s^2 + v_A^2)(\omega^2 - k^2 c_T^2)\, v_z - \omega\, k\, c_s^2\, p_T = o. \qquad \text{(A2.12)}$$

Assuming m_0^2, $m_e^2>0$, continuity of p_T at r=a implies

$$A_1\, I_n(m_0 a) = A_{e2}\, K_n(m_e a). \qquad \text{(A2.13)}$$

Using (A2.9), continuity of v_r at r=a requires that

$$-A_1 \frac{i\,\omega}{\rho_0(k^2 v_A^2 - \omega^2)} m_0\, I_n'(m_0 a) = A_{e2}\frac{i}{\rho_e \omega} m_e\, K_n'(m_e a). \qquad \text{(A2.14)}$$

Eliminating A_1 and A_{e2} between (A2.13) and (A2.14) then gives the dispersion relation (2.13). Equation (2.14) is derived in the same manner using the appropriate solution inside the tube for $m_0^2<0$.

Writing p_T as $f(m_0 r)$ inside the flux tube, where f is the appropriate Bessel function or sum of Bessel functions, (A2.9) and (A2.12) can be combined to show that

$$\frac{v_z}{v_r} = -k\, c_s^2 \left(\frac{(\omega^2 - k^2 v_A^2)}{(c_s^2 + v_A^2)(\omega^2 - k^2 c_T^2)(\omega^2 - k^2 c_s^2)} \right)^{\frac{1}{2}} \frac{f(m_0 r)}{f'(m_0 r)} . \qquad \text{(A2.15)}$$

The functions f and f´ simply describe the oscillatory nature of the solution, so in terms of simple amplitudes, the only important expression is

$$k\, c_s^2 \left(\frac{(\omega^2 - k^2 v_A^2)}{(c_s^2 + v_A^2)(\omega^2 - k^2 c_T^2)(\omega^2 - k^2 c_s^2)} \right)^{\frac{1}{2}}$$

as given in equation (2.15).

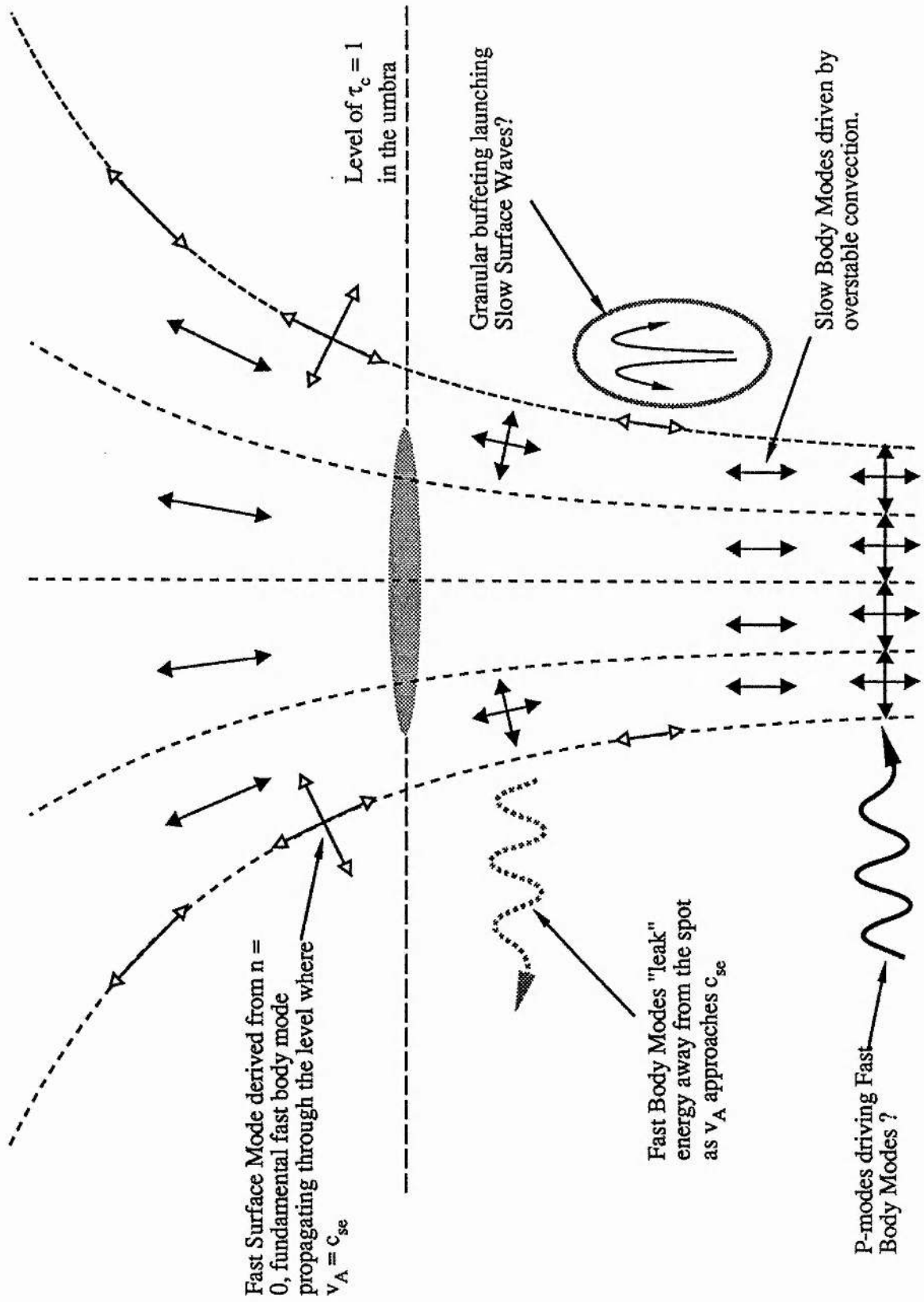

Figure 2.13. Summary of the modes of oscillation of a Sunspot. See section 2.3 for full description

3. The Effect of Chromospheric Canopy Fields on p-modes.

3.1 Introduction

Since the confirmation by Deubner (1975) of the theoretical interpretation of solar "five-minute oscillations", or p-modes, there have been many attempts to produce a definitive solar model which reproduces all the observed frequencies to within the limits of observational uncertainties. The quality of the observations is exceedingly high, with accuracies of up to 1 part in 10,000, making the task of the theorist all the more demanding. Thus far, no single model can reproduce all observed frequencies to the required accuracy, despite the inclusion of many and various effects, ranging from fundamental particles in the solar core to sophisticated versions of the equation of state.

Magnetic effects have, on the whole, been ignored. At first sight this seems reasonable since the dynamics of the convection zone, where the p-mode cavity resides, is dominated by the fluid pressure. It is perhaps only in the photosphere and above that the magnetic field is expected to have an appreciable influence, and here the solar p-modes are generally evanescent. However Bogdan and Zweibel (1985), Zweibel and Bogdan (1986), Bogdan (1989), and Bogdan and Cattaneo (1989) have examined the effect of photospheric fibril fields on p-mode frequencies and find changes in frequency which are significant in comparison to observational accuracy. At higher levels in the solar atmosphere, where the magnetic field dominates the gas pressure, fibril fields fan out and form an overlying "canopy" field (Giovanelli, 1980). It is the effect of such a chromospheric field that will be discussed here, continuing the investigation begun in Campbell and Roberts (1989).

Since p-modes are evanescent in the vicinity of these canopy fields it might be expected that the effect of the magnetic field would be slight. However, the general structure of the atmosphere above the photosphere is important in determining the rate of evanescence, i.e. the rapidity with which the eigenmodes decay with height. In extreme cases this would mean that the upper boundary was effectively a rigid wall (infinite rate of evanescence or decay) or a completely free boundary (zero rate of evanescence), such as the open end of an

organ pipe. Thus the form of the upper atmosphere determines the nature of the reflecting boundary and hence the fine structure of the eigenfrequencies. Since the magnetic field is a significant part of the solar atmosphere, it can be expected that its effects are important.

Recent sophisticated models of the solar interior (e.g. Christensen-Dalsgaard, Däppen and Lebreton, 1988) indicate that the discrepancies between observed and calculated values of the frequencies tend to be larger for high degree modes. These are the modes which are trapped near to the surface layers of the Sun. The implication is that at least one of the sources of error is located around the photosphere. Due to the rough balance between magnetic and gas forces, and the existence of a superadiabatic temperature profile, this is a difficult region to model. Here, a very simple model is used. This makes it easier to bring out the influence of the magnetic field and, to a lesser extent, the chromospheric temperature. The model and approach used is similiar to that of Campbell and Roberts (1989).

The convection zone is modelled as a fluid having a linear temperature profile, the gradient of which may be chosen such that stratification due to gravity is marginally stable to adiabatic convective motions. Above the temperature minimum the atmosphere is assumed to be isothermal and permeated by a uniform horizontal magnetic field. This is essentially the model used by Nye and Thomas (1976b) in their investigation of running penumbral waves (see Chapter 2). Here, however, the interest is on the frequencies of the p- and f-modes and how these are affected by the magnetic field, a topic not explored previously save for the work of Campbell and Roberts. For an isothermal atmosphere with a uniform magnetic field the Alfvén speed increases exponentially with height. This is in contrast to the model of Campbell and Roberts (1989) in which the Alfvén speed is taken to be uniform. In a sense, the two models represent extremes with the real profile in chromospheric Alfvén speed lying between the two. Both these models will be examined in the hope that they shed light on the physical processes involved and hence give some indication of the effects that are likely to be seen in the Sun.

3.2 The Model and Dispersion Relations

Surface effects on p-mode dispersion relations are likely to be significant for large l

since these are the modes trapped high up in the convection zone (see section 1.3.2). These modes have short horizontal wavelengths and this may be accurately modelled by employing a plane parallel atmosphere. The medium is stratified by gravity, taken to be acting in the positive z-direction. The temperature $T_0(z)$ in the medium is taken to vary linearly with depth in the "convection zone" ($z>0$) and to be constant in the "chromosphere" ($z<0$):

$$T_0(z) = \begin{cases} T_p\,(1 + z/z_0)\ , & z > 0\ , \\ T_c\ , & z < 0\ . \end{cases} \tag{3.1}$$

Here, T_p and T_c are constants representing the temperatures at the top of the convection zone (i.e. the photosphere) and the bottom of the chromosphere, respectively, and z_0 is the temperature scale height at the top of the convection zone.

The atmosphere is assumed to be made up of an ideal gas satisfying the equations of magnetostatic balance which, for a horizontal magnetic field aligned with the x-axis, are

$$\frac{d}{dz}\left(p_0 + \frac{B_0^2}{2\mu}\right) = \rho_0 g\ , \tag{3.2}$$

$$p_0 = R\rho_0 T_0\ , \tag{3.3}$$

where $p_0(z)$ and $\rho_0(z)$ are the gas pressure and density, B_0 is the magnetic field strength, assumed constant, g is the acceleration due to gravity and μ ($=4\pi\times10^{-7}$ henry m^{-1}) is the magnetic permeability. In the above R is equal to k_B/m_{av}, with k_B (Boltzmann's constant) $=1.381\times10^{-23}$ JK^{-1}, and m_{av} is the mean particle mass of the plasma; R is assumed to be constant. The uniform magnetic field B_0 is confined to the atmosphere ($z<0$).

Solving equations (3.2) and (3.3) gives

$$p_0(z) = \begin{cases} p_p\,(1 + z/z_0)^{m+1}\ , & z > 0\ , \\ \left(p_p - \dfrac{B_0^2}{2\mu}\right)\exp\left(\dfrac{z}{H_c}\right), & z < 0\ , \end{cases} \tag{3.4}$$

and

$$\rho_0(z) = \begin{cases} \frac{p_p}{RT_p}(1 + z/z_0)^m , & z > 0 , \\ \frac{1}{RT_c}\left(p_p - \frac{B_0^2}{2\mu}\right)\exp\left(\frac{z}{H_c}\right), & z < 0 . \end{cases} \tag{3.5}$$

Here,

$$H_c = \frac{RT_c}{g}, \quad m = \frac{gz_0}{RT_p} - 1$$

are the chromospheric density scale height and the polytropic index, respectively, while p_p is the gas pressure at the top of the convection zone.

The equations governing the motion are:

$$\frac{D\rho}{Dt} + \rho\nabla.\mathbf{u} = 0 \quad , \tag{3.6}$$

$$\rho\frac{D\mathbf{u}}{Dt} = -\nabla p + \mathbf{j} \times \mathbf{B} + \rho g \quad , \tag{3.7}$$

$$\frac{\partial \mathbf{B}}{\partial t} = \nabla \times (\mathbf{u} \times \mathbf{B}) \quad , \tag{3.8}$$

$$\frac{D}{Dt}\left(\frac{p}{\rho^\gamma}\right) = 0 \quad , \tag{3.9}$$

where

$$\nabla.\mathbf{B} = 0, \qquad \mathbf{j} = \frac{1}{\mu}\nabla \times \mathbf{B}.$$

The velocity field is taken to be two-dimensional: $\mathbf{u} = (u_x, 0, u_z)$ is the velocity field whose y-component is assumed to be 0, γ is the adiabatic index and D/Dt ($=\partial/\partial t + \mathbf{u}.\nabla$) denotes the convective derivative.

Since solar five-minute oscillations are of small amplitude when compared with local

sound speeds, etc., it is justifiable to use a simple linear analysis of the above equations. On expressing all perturbation quantities in the form $\mathbf{u} = (u_x(z), 0, u_z(z))\exp i(\omega t - kx)$, etc, the governing equation may be derived (Goedbloed 1971, Adam 1977, Roberts 1985):

$$\frac{d}{dz}\left(\frac{\rho_0(c_s^2+v_A^2)(\omega^2-k^2c_T^2)}{(\omega^2-k^2c_s^2)}\frac{du_z}{dz}\right)=\left(\frac{\rho_0 g^2k^2}{\omega^2-k^2c_s^2}-\rho_0(\omega^2-k^2v_A^2)-gk^2\frac{d}{dz}\left[\frac{\rho_0c_s^2}{\omega^2-k^2c_s^2}\right]\right)u_z, \tag{3.10}$$

where $c_s(z)=(\gamma p_0/\rho_0)^{1/2}$ is the local sound speed, $v_A(z)=B_0/(\mu\rho_0)^{1/2}$ is the local Alfvén speed and $c_T(z)=c_sv_A/(c_s^2+v_A^2)^{1/2}$ is the MHD cusp (or tube) speed. For the derivation of this equation see Appendix 3. Equation (3.10) holds for an arbitrary stratification in horizontal magnetic field and temperature satisfying equations (3.2) and (3.3).

In the convection zone ($z>0$) where $v_A=0$, it is convenient to use $\Delta=\text{div}\,\mathbf{u}$ as the dependent variable. Then it can be shown that (see Appendix 3)

$$\left(1-\frac{k^2c_s^2}{\omega^2}\right)\Delta=\frac{gk^2}{\omega^2}u_z+\frac{du_z}{dz}\quad, \tag{3.11}$$

and

$$(\omega^4-g^2k^2)\,u_z=g(k^2c_s^2-\gamma_p\omega^2)\Delta-\omega^2c_s^2\frac{d\Delta}{dz}\quad, \tag{3.12}$$

γ_p being the adiabatic index in the region $z>0$. Assuming $\omega^2 \neq gk$, the governing equation for Δ may then be derived (Lamb, 1932):

$$\frac{d^2\Delta}{dz^2}+\left(\frac{c_s^{2\prime}}{c_s^2}+\frac{\gamma_pg}{c_s^2}\right)\frac{d\Delta}{dz}+\left(\left[\frac{\omega^2-k^2c_s^2}{c_s^2}\right]-\frac{gk^2}{\omega^2}\left[\frac{c_s^{2\prime}}{c_s^2}-(\gamma_p-1)\frac{g}{c_s^2}\right]\right)\Delta=0, \tag{3.13}$$

the dashes denoting derivatives of equilibrium quantities with respect to depth z.

Lamb (1932) has shown that in the special case of a linear temperature profile this equation can be solved in terms of confluent hypergeometric functions. For the model used here,

$$\Delta = \exp(-k[z+z_0])\left(C_1 M(-a, m+2, 2k[z+z_0]) + C_2 U(-a, m+2, 2k[z+z_0])\right),$$

(3.14)

where

$$a = \frac{\omega^2}{2gk}\frac{m+1}{\gamma_p} + \left(m - \frac{m+1}{\gamma_p}\right)\frac{gk}{2\omega^2} - \frac{m}{2} - 1,$$

C_1, C_2 are arbitrary constants, and M and U are Kummer's functions (Abramowitz and Stegun, 1965; Chapter 13).

Since (Abramowitz and Stegun, 1965)

$$M(a, b, z) \sim \frac{\Gamma(b)}{\Gamma(a)} e^z z^{a-b}, \quad z \to \infty, \tag{3.15}$$

equations (3.12) and (3.14) show that unless $C_1 = 0$ the kinetic energy density, $\rho_0 u^2/2$, will be unbounded as $z \to \infty$. These solutions would represent a source of motion infinitely far down in the convection zone. The discussion here is concerned with modes which are trapped in the upper part of the convection zone, so that it is necessary to take $C_1=0$. Hence

$$\Delta = \exp(-k[z+z_0]) C_2 U(-a, m+2, 2k[z+z_0]) \quad , \qquad (z>0). \tag{3.16}$$

Then, using equation (3.12) and the result (Abramowitz and Stegun, 1965)

$$\frac{d}{dz}(U(a, b, z)) = -a\, U(a+1, b+1, z), \tag{3.17}$$

it follows that

$$(\omega^4 - g^2k^2) \exp(-k[z+z_0])\, u_z =$$

$$C_2 \left(\left[kc_s^2(\omega^2+gk) - \gamma_p g\omega^2\right] U(-a, m+2, 2k[z+z_0]) - 2a\omega^2 c_s^2 k\, U(-a+1, m+3, 2k[z+z_0])\right),$$

$$(z>0). \tag{3.18}$$

Turning now to the region $z < 0$, for an isothermal atmosphere with a uniform magnetic field equation (3.10) reduces to

$$\left(A_1 + A_2\exp(-A_3 z)\right)\frac{d^2u_z}{dz^2} + A_1A_3\frac{du_z}{dz} + \left(A_4 - k^2A_2\exp(-A_3 z)\right)u_z = 0, \tag{3.19}$$

where

$$A_1 = \omega^2 c_{sc}^2\ ,\quad A_2 = v_{Ac}^2(\omega^2 - k^2c_{sc}^2),\quad A_3 = \gamma_c g / c_{sc}^2 = 1/Hc,$$

$$A_4 = (\gamma_c - 1)k^2g^2 + \omega^2(\omega^2 - k^2c_{sc}^2)\ .$$

Here, c_{sc}^2 is the sound speed for $z<0$, v_{Ac}^2 is the Alfvén speed at the base of the chromosphere and γ_c is the adiabatic index in the chromosphere. The transformation (Adam, 1975; Nye and Thomas, 1976a)

$$\zeta = -\frac{A_1}{A_2}\exp(A_3 z)\ ,\qquad V = u_z\,\zeta^{-k/A_3}\ , \tag{3.20}$$

applied to equation (3.19), gives the hypergeometric equation

$$\zeta(1-\zeta)\frac{d^2V}{d\zeta^2} + \left(r - [p+q+1]\,\zeta\right)\frac{dV}{d\zeta} - pqV = 0, \tag{3.21}$$

where

$$p+q = \frac{2k}{A_3} + 1,\quad pq = \frac{k}{A_3}\left(\frac{k}{A_3} + 1\right) + \frac{A_4}{A_1A_3^2},\quad r = \frac{2k}{A_3} + 1\ .$$

The general solution of equation (3.21) in the vicinity of $\zeta=0$ is (Abramowitz and Stegun, 1965; Chapter 15)

$$V = \alpha_1 F(p, q, r, \zeta) + \alpha_2\,\zeta^{1-r}F(p-r+1, q-r+1, 2-r, \zeta)\ , \tag{3.22}$$

α_1, α_2 being arbitrary constants and F the hypergeometric function defined by the Gauss series (Abramowitz and Stegun, 1965)

$$F(p, q, r, \zeta) = 1 + \frac{pq}{r}\zeta + \frac{p(p+1).q(q+1)}{r(r+1)}\frac{\zeta^2}{2!} + \ldots \qquad (3.23)$$

In the chromosphere, the magnetic energy density of the perturbation is $E_B=(\mathbf{B_0}+\mathbf{B}).(\mathbf{B_0}+\mathbf{B})/2\mu-\mathbf{B_0}^2/2\mu$ which, to linear order, is $\mathbf{B_0}.\mathbf{B}/\mu$. Using equations (3.6)-(3.9), it can easily be shown that (see Appendix 3)

$$E_B = \frac{i}{\omega}\frac{B_0^2}{\mu}\frac{du_z}{dz} \ . \qquad (3.24)$$

Again, since the interest here is centred on trapped modes, both kinetic and magnetic energy densities must vanish in the limit $z\rightarrow -\infty$ ($\zeta\rightarrow 0$). From equation (3.22) it is found that

$$u_z = \alpha_1\left(-\frac{A_1}{A_2}\right)^{k/A_3} e^{kz}\, F\left(p, q, r, -\frac{A_1}{A_2}e^{A_3 z}\right) + \alpha_2\left(-\frac{A_1}{A_2}\right)^{-k/A_3} e^{-kz}\, F\left(p-r+1, q-r+1, 2-r, -\frac{A_1}{A_2}e^{A_3 z}\right). \qquad (3.25)$$

Then, using the result (Abramowitz and Stegun, 1965)

$$\frac{d}{dz}F(a, b, c, z) = \frac{ab}{c}F(a+1, b+1, c+1, z), \qquad (3.26)$$

and equation (3.23), it is easy to show that E_B will vanish as $z \rightarrow -\infty$ only if $\alpha_2=0$. Thus

$$u_z = \alpha_1\, e^{kz}\, F\left(p, q, r, -\frac{A_1}{A_2}e^{A_3 z}\right), \quad (z<0). \qquad (3.27)$$

It may easily be verified that this solution gives both magnetic and kinetic energy densities that

decline to zero as $z \to -\infty$.

The region of real space $(0, -\infty)$ covering the chromospheric part of the atmosphere is mapped by the transformation (3.20) into the region $(-\zeta_1, 0)$, or $(0, -\zeta_1)$ if $\zeta_1<0$, in ζ-space, where

$$\zeta_1 = \frac{\omega^2 c_{sc}^2}{v_{Ac}^2(\omega^2 - k^2 c_{sc}^2)} \ . \tag{3.28}$$

The hypergeometric equation (3.21) has three regular singular points at $\zeta=0, 1, \infty$. The boundary conditions relating to the decrease of total energy density as $z \to -\infty$ has the effect of removing the singular part of the solution (3.22) in the vicinity of $\zeta=0$. The analytic continuation of the remaining solution shows that there is a logarithmic singularity at $\zeta=1$ (Abramowitz and Stegun, 1965). This will only cause a problem if $-\zeta_1 \geq 1$, i.e. if

$$\frac{\omega^2 c_{sc}^2}{v_{Ac}^2(\omega^2 - k^2 c_{sc}^2)} \leq -1, \tag{3.29}$$

that is, if

$$c_{Tc}^2 \leq \omega^2/k^2 \leq c_{sc}^2 \ , \tag{3.30}$$

where

$$c_{Tc}^2 = \frac{c_{sc}^2 v_{Ac}^2}{c_{sc}^2 + v_{Ac}^2} \ .$$

This is the range of phase speed in which the solution for u_z is singular indicating that resonance is occurring and that resistive and viscous effects will become important. So long as the phase speed remains outside the range (3.30), there will be no problems and the solutions are everywhere bounded. The singularity at $\zeta=\infty$ corresponds to $\omega^2/k^2=c_{sc}^2$, and so is covered by (3.30) also.

Equations (3.18) and (3.27) are the solutions for u_z in the two regions of the atmosphere. At the interface between the magnetic and non-magnetic regions it is clear that

the vertical component of velocity, u_z, must be continuous. Then, integrating equation (3.10) across the interface yields a second condition, namely that

$$\frac{\rho_0 (c_s^2 + v_A^2)(\omega^2 - k^2 c_T^2)}{\omega^2 - k^2 c_s^2} \frac{du_z}{dz} + \left(\frac{gk^2 \rho_0 c_s^2}{\omega^2 - k^2 c_s^2} \right) u_z , \tag{3.31}$$

or equivalently

$$i\,\omega p_T + g\rho_0 u_z,$$

must also be continuous at the interface. The term p_T is the sum of the magnetic and gas pressure, i.e. $p_T = p + \mathbf{B}_0.\mathbf{B}/\mu$. Application of these two conditions to the solutions (3.18) and (3.27) then yields the dispersion relation

$$gk^2 + k\omega^2 - \frac{\gamma_p g \omega^2}{c_{sp}^2} - 2ak\omega^2 \frac{U(-a+1,\, m+3,\, 2kz_0)}{U(-a,\, m+2,\, 2kz_0)} =$$

$$\left(\frac{\rho_{0c}}{\rho_{0p}} \right) \frac{(\omega^2 - k^2 c_{sc}^2)(\omega^4 - g^2 k^2)}{gk^2 c_{sc}^2 + (c_{sc}^2 + v_{Ac}^2)(\omega^2 - k^2 c_{Tc}^2)\left(k - \frac{pq}{r} \frac{A_1 A_3}{A_2} \frac{F(p+1,\, q+1,\, r+1,\, -A_1/A_2)}{F(p,\, q,\, r,\, -A_1/A_2)} \right)} , \tag{3.32}$$

where ρ_{0p} and ρ_{0c} are the densities on the lower and upper side of the interface, respectively. A relation equivalent to equation (3.32) in the case of $\rho_{0p} = \rho_{0c}$ has been obtained by Nye and Thomas (1976b) in their investigations of running penumbral waves.

It is convenient to cast equation (3.32) in dimensionless form:

$$2aK\,\Omega^2 \frac{U(\,1-a,\, m+3,\, 2K\,)}{U(\,-a,\, m+2,\, 2K\,)} + (m+1)\,\Omega^2 - K(1+\Omega^2) =$$

$$\frac{\Lambda(\Lambda\,\Omega^2 - K)(1 - \Omega^4)}{\chi\left(\Lambda + \varphi\left(1 + \frac{1}{\beta} \right)\left(\Lambda\,\Omega^2 - \frac{K}{1+\beta} \right) \right)} , \tag{3.33}$$

where

$$K = kz_0\,, \quad \Omega^2 = \frac{\omega^2}{gk}, \quad \Lambda = \frac{m+1}{\gamma_p}\frac{c_{sp}^2}{c_{sc}^2}, \quad \beta = \frac{c_{sc}^2}{v_{Ac}^2}, \quad \chi = \frac{T_p}{T_c}\left(\frac{2\beta}{\gamma_c + 2\beta}\right),$$

and

$$\varphi = \left(1 - \beta\,\Omega^2 \frac{\left[1 + \frac{\gamma_c - 1}{\gamma_c}\frac{1}{\Omega^2} + \frac{\Omega^2}{\gamma_c}\right]}{\left[\frac{2K}{\gamma_c \Lambda} + 1\right]\left[\Omega^2 - \frac{K}{\Lambda}\right]} \frac{F(\,p+1,\, q+1,\, r+1,\, -A_1/A_2\,)}{F(\,p,\, q,\, r,\, -A_1/A_2\,)} \right).$$

Equation (3.33) is the basis of this investigation. It is a very general relation, covering not only the influence of a uniform magnetic atmosphere on p- and f-modes but also on g-modes and their unstable counterpart (convection). It additionally includes gravity modified magnetoacoustic surface waves (see, for example, Roberts 1981a; Miles and Roberts 1989a, b) in a stratified atmosphere. However, this discussion will concentrate on the p- and f-modes.

3.3 Asymptotic Solutions to the Dispersion Relation

3.3.1 Solutions in the limit $K \to 0$

Despite the complexity of the dispersion relation (3.33), it proves possible to extract analytic information about the oscillation modes in the limit of small kz_0, which in fact covers much of the wavenumber range that is of interest. These asymptotic solutions will be derived in the next section before going on to a numerical evaluation. First, it is useful to look at the solutions in the limit $K \to 0$.

Since $K = kz_0$, the limit $K \to 0$ can be regarded as the result of letting z_0 become small. From equation (3.1) defining the temperature structure, it can be seen that $-z_0$ is the point where T_0 would be zero were the linear temperature profile of the convection zone to extend up into the chromosphere. Thus, taking $z_0 = 0$ leaves the atmosphere as a simple polytrope with no chromosphere. This is just the example which was analysed with the WKB method in section 1.3.1. In order to find the solutions in this case, it is necessary to examine the

behaviour of the dispersion relation (3.33) as $K \to 0$.

It will be assumed that as $K \to 0$, $\Omega^2 \to \Omega_*^2$ and that $\Omega_*^2 \neq 0$. Solutions corresponding to $\Omega_*^2 = 0$ represent gravity modified surface waves. These modes are not relevant to the discussion here and so will be ignored. With these assumptions it is easy to show that as $K \to 0$

$$p + q \to 1, \quad pq \to 0, \quad r \to 1, \quad -\frac{A_1}{A_2} \to -\beta . \tag{3.34}$$

Thus

$$\varphi \to 1 - \beta \left(1 + \frac{\gamma_c - 1}{\gamma_c} \frac{1}{\Omega_*^2} + \frac{\Omega_*^2}{\gamma_c} \right) \frac{F(1, 2, 2, -\beta)}{F(0, 1, 1, -\beta)} \quad . \tag{3.35}$$

Using the special case of the hypergeometric function (Abramowitz and Stegun, 1965)

$$F(a, b; b; z) = (1-z)^{-a} \quad , \tag{3.36}$$

the right hand side of the dispersion relation (3.33) then reduces to

$$\frac{\gamma_c \beta \Lambda \Omega_*^2 (1 - \Omega_*^4)}{\chi (\beta [1 - \Omega_*^4] + \gamma_c \Omega_*^2)} . \tag{3.37}$$

The asymptotic behaviour of the confluent hypergeometric U-function is given by (Abramowitz and Stegun, 1965)

$$U(c, d, z) \sim \frac{\Gamma(d-1)}{\Gamma(c)} z^{1-d}, \quad z \to 0. \tag{3.38}$$

Thus, providing $(-a)$ does not tend to 1, 0, or any negative integer, the left hand side of (3.33) reduces to zero in the limit as $K \to 0$. The limiting form of the dispersion relation for this limit is simply

$$\frac{\gamma_c \beta \Lambda \Omega_*^2 (1-\Omega_*^4)}{\chi(\beta[1-\Omega_*^4]+\gamma_c \Omega_*^2)} = 0. \qquad (3.39)$$

The solutions to (3.39) are $\Omega_*^2=0, \pm 1$. If $\Omega_*^2=1$ then $a=-1$ which is disallowed in the derivation of (3.39). $\Omega_*^2=-1$ gives complex roots which are not of interest here. Finally, $\Omega_*^2=0$ will be ignored here, as stated above. Hence there are no interesting solutions for this case.

The only remaining cases to consider are the ones where $a \rightarrow -1, 0, 1, 2, 3...$ From the definition of a this simply gives the results

$$\frac{\Omega_*^2}{2}\frac{m+1}{\gamma_p}+\left(m-\frac{m+1}{\gamma_p}\right)\frac{1}{2\Omega_*^2}-\frac{m}{2}-1=n-1, \quad n=1, 2, 3... \qquad (3.40)$$

and

$$\frac{\Omega_*^2}{2}\frac{m+1}{\gamma_p}+\left(m-\frac{m+1}{\gamma_p}\right)\frac{1}{2\Omega_*^2}-\frac{m}{2}=0. \qquad (3.41)$$

Equation (3.40) gives the two series of solutions which are the p- and g-modes for this particular atmospheric model. For a marginally stable atmosphere, $m=1/(\gamma_p-1)$ and then (3.40) reduces to

$$\Omega_*^2 = 1 + 2(\gamma_p - 1)n, \qquad (3.42)$$

the result stated in section 1.3.1. These are the p-modes. The second series of solutions collapses to $\Omega_*^2=0$ as would be expected for g-modes in a marginally stable atmosphere. In more general circumstances, the g-modes satisfy $\Omega_*^2<0$ (convection) for an unstable atmosphere and $\Omega_*^2>0$ for a stable atmosphere.

Equation (3.41) yields the solutions

$$\Omega_*^2 = 1 \text{ and } \Omega_*^2 = -1 + \frac{\gamma_p m}{m+1}. \qquad (3.43)$$

The first of these is the f-mode.

All the solutions given by equations (3.40) and (3.41) must still give a non-contradictory statement for the limit of the dispersion relation. This will be demonstrated in the next section where the asymptotic corrections due to the magnetic field are derived. All these solutions, except the second in (3.43), are then seen to be genuine.

3.3.2 Asymptotic Corrections due to a Uniform Chromospheric Magnetic Field

It is desired to find the corrections to the p- and f-modes given by (3.40) and (3.41) for small K due to the chromosphere. It is thus necessary to expand the dispersion relation for small K. Using (Abramowitz and Stegun, 1965)

$$U(a, b, z) = \frac{\pi}{\sin \pi b}\left(\frac{M(a, b, z)}{\Gamma(1+a-b)\,\Gamma(b)} - z^{1-b}\,\frac{M(1+a-b, 2-b, z)}{\Gamma(a)\,\Gamma(2-b)}\right), \qquad (3.44)$$

it may be shown that

$$2aK\,\Omega^2\,\frac{U(1-a, m+3, 2K)}{U(-a, m+2, 2K)} =$$

$$\frac{a\,\Omega^2\,\dfrac{M(-a-m-1, -m-1, 2K)}{\Gamma(1-a)\,\Gamma(-m-1)} - a\,\Omega^2\,(2K)^{m+2}\,\dfrac{M(1-a, m+3, 2K)}{\Gamma(-a-m-1)\,\Gamma(m+3)}}{(2K)^{m+1}\,\dfrac{M(-a, m+2, 2K)}{\Gamma(-a-m-1)\,\Gamma(m+2)} - \dfrac{M(-a-m-1, -m, 2K)}{\Gamma(-a)\,\Gamma(-m)}}. \qquad (3.45)$$

Here it must be assumed that m is not an integer. From the physical point of view, m being an integer has no significance. Therefore it must be the case that the final results for integral m will be identical with those given here, but the derivation is more complicated.

Clearly the terms involving $\Gamma(1-a)$ and $\Gamma(-a)$ in (3.45) must be treated with care. This must be examined in three separate cases as follows.

Case (i) $a \to n-1$, $n = 2,3,4...$; p- and g-modes.

In this case it is convenient to assume

$$\Gamma(-a) \sim \theta_n (2K)^{-s}, \qquad K \to 0, \tag{3.46}$$

θ_n and s being constants yet to be determined. This corresponds to

$$a \sim (n-1) + \frac{(-1)^n}{\theta_n (n-1)!}(2K)^s \qquad \text{as } K \to 0, \tag{3.47}$$

and

$$\Omega^2 \sim \Omega_*^2 + \frac{(-1)^n}{\left(\frac{m+1}{\gamma_p} - \frac{1}{\Omega_*^4}\left[m - \frac{m+1}{\gamma_p}\right]\right)\theta_n (n-1)!}(2K)^s. \tag{3.48}$$

Assuming Ω_*^2 to be non-zero, it is found that as $K \to 0$,

$$\Gamma(1-a) \sim -a\,\theta_n (2K)^{-s}, \; pq \to 0, \; p+q \to 0, \; r \to 1, \; -A_1/A_2 \to -\beta.$$

If $s<m+1$, then the left-hand side of the dispersion relation (3.33) reduces to 0 in the limit $K \to 0$. In this case the only "solutions" are those found for the case where a did not tend to -1, 0 or a positive integer. If $s>m+1$, then the left-hand side of equation (3.33) reduces to $(m+1)\Omega_*^2$, and solutions to the dispersion relation in this case are $\Omega_*^2=0, -1 \pm \sqrt{2}$. Of these, only $\Omega_*^2 = -1+\sqrt{2}$ may be relevant. In this case

$$a = -\frac{m+1}{\gamma_p} + \frac{\sqrt{2}-1}{2}m - 1, \tag{3.49}$$

and in general this is not equal to the required $(n-1)$.

Thus, the only remaining possibility is that $s=m+1$. The right hand side of the dispersion relation reduces to the expression given in (3.39). Equating the limits of both sides then gives

$$(m+1)\Omega_*^2 + \frac{\Omega_*^2/\Gamma(-m-1)}{\frac{1}{\Gamma(-m)} - \frac{\theta_n}{\Gamma(-n-m)\Gamma(m+2)}} = \frac{\gamma_c \beta \Omega_*^2 (1-\Omega_*^4)}{\chi\,(\gamma_c \Omega_*^2 + \beta[1-\Omega_*^4])}, \quad n=2,3\ldots \tag{3.50}$$

which can be used to determine θ_n.

Case (ii) $a \to 0$ as $K \to 0$; p- and g-modes.

In this case it is convenient to assume that as $K \to 0$

$$a \sim \theta\,(2K)^s, \tag{3.51}$$

so that

$$\Gamma(-a) = -\frac{\Gamma(1-a)}{a} \sim \frac{-1}{\theta\,(2K)^s}\quad, \tag{3.52}$$

and

$$\Omega^2 \sim \Omega_*^2 + \frac{\theta\,(2K)^s}{\left(\dfrac{m+1}{\gamma_p} - \dfrac{1}{\Omega_*^4}\left[m - \dfrac{m+1}{\gamma_p}\right]\right)}. \tag{3.53}$$

Repeating the argument used above, again gives s=m+1, but this time

$$(m+1)\,\Omega_*^2 + \frac{\theta\,\Omega_*^2 / \Gamma(-m-1)}{\dfrac{1}{\Gamma(-m-1)\,\Gamma(m+2)} + \dfrac{\theta}{\Gamma(-m)}} = \frac{\gamma_c \beta\,\Lambda\,\Omega_*^2\,(1-\Omega_*^4)}{\chi\,(\gamma_c\,\Omega_*^2 + \beta[\,1-\Omega_*^4\,])}\quad, \tag{3.54}$$

which may be used to determine θ.

When these results are put together it turns out that the asymptotic solution for Ω^2 in case (ii) is simply the result of case (i) evaluated for n=1. The final expression, valid as $K \to 0$, is

$$\Omega^2 \sim \Omega_*^2 + \frac{2\,\Gamma(1+m+n)\,\gamma_c\,([\,1-\Omega_*^4\,] - 2\Omega_*^2)}{\left(\dfrac{m+1}{\gamma_p} - \left[m - \dfrac{m+1}{\gamma_p}\right]\dfrac{1}{\Omega_*^4}\right)(n-1)!\,\Gamma(m+2)\,\Gamma(m+1)\,(\gamma_c + 2\beta)\,(1-\Omega_*^4)}\,(2K)^{m+1}\quad, \tag{3.55}$$

with Ω_*^2 given by

$$\frac{m+1}{\gamma_p}\Omega_*^2+\left(m-\frac{m+1}{\gamma_p}\right)\frac{1}{\Omega_*^2}-(m+2)=2(n-1),\qquad n=1,\ 2,\ 3,\ldots. \tag{3.56}$$

Equations (3.55) and (3.56) give the asymptotic solutions to (3.33) for the p- and g-modes.

Case (iii) $a \to -1$ as $K \to 0$; f-mode.

The correction for the f-mode is distinctive, as might be expected in view of the characteristic differences between f- and p-modes. Since $a \to -1$ as $K \to 0$, the left hand side of (3.33) simply reduces to zero. For the second root of (3.43) the dispersion relation becomes the same as equation (3.39) in this limit implying that $\Omega_*^2=0, \pm 1$. This is clearly contradictory so that this root must be discarded. This just leaves the f-mode. Since for this mode $\Omega_*^2=1$, the right hand side of the dispersion relation also vanishes and it is necessary to find the leading order behaviour of the dispersion relation in the limit $K \to 0$.

Assuming that

$$\Omega^2 \sim 1 + r\,(2K)^s\,, \tag{3.57}$$

then it follows that

$$a \sim -1+\varepsilon, \tag{3.58}$$

$$\varepsilon=\left(\frac{m+1}{\gamma_p}-\frac{m}{2}\right)r\,(2K)^s.$$

Using the definition of the confluent hypergeometric M-function (Abramowitz and Stegun, 1965)

$$M(c,d,z)=1+\frac{c}{d}z+\frac{c(c+1)}{d(d+1)}\frac{z^2}{2!}+\ \ldots\ , \tag{3.59}$$

the left hand side of the dispersion relation can be expanded for small K as follows. Here

O(x) denotes terms of order x and o(x) denotes terms of smaller order than x.

$$M(-1-a-m, -m-1, 2K) \sim 1 + \frac{m}{m+1}(2K) + \frac{m-1}{m+1}\frac{(2K)^2}{2!} + O(K^3) + \frac{(2K)\varepsilon}{m+1} + o(K^{s+1}),$$

(3.60)

$$\Gamma(1-a) = -a\Gamma(-a), \quad \Gamma(-a) \sim 1 - \Gamma'(1)\varepsilon + o(K^s), \tag{3.61}$$

the dash denoting the derivative. Then

$$a\,\Omega^2 \frac{M(-1-a-m, -m-1, 2K)}{\Gamma(1-a)\,\Gamma(-m-1)} \sim$$

$$\frac{-1}{\Gamma(-m-1)}\left(1 + \frac{m}{m+1}(2K) + \frac{m-1}{m+1}\frac{(2K)^2}{2!} + O(K^3) + r(2K)^s + \Gamma'(1)\varepsilon + o(K^s)\right), \tag{3.62}$$

and

$$M(1-a, m+3, 2K) \sim 1 + \frac{2}{m+3}(2K) + \frac{2.3}{(m+3)(m+4)}\frac{(2K)^2}{2!} + O(K^3)$$

$$- \frac{(2K)\varepsilon}{m+3} + o(K^{s+1}), \tag{3.63}$$

$$\Gamma(-1-a-m) \sim \Gamma(-m) - \Gamma'(-m)\varepsilon + o(K^s). \tag{3.64}$$

Thus

$$a\,\Omega^2(2K)^{m+2} \frac{M(1-a, m+3, 2K)}{\Gamma(-1-a-m)\,\Gamma(m+3)} \sim$$

$$\frac{(2K)^{m+2}}{\Gamma(-m)\Gamma(m+3)}\left(-1 - \frac{2}{m+3}(2K) - \frac{2.3}{(m+3)(m+4)}\frac{(2K)^2}{2!} + O(K^3) + \left[1 - \frac{\Gamma'(-m)}{\Gamma(-m)}\right]\varepsilon - r(2K)^s + o(K^s)\right).$$

(3.65)

$$M(-a, m+2, 2K) \sim 1 - \frac{a}{m+2}(2K) + \frac{a(a-1)}{(m+2)(m+3)}\frac{(2K)^2}{2!} + O(K^3), \tag{3.66}$$

which implies that

$$\frac{(2K)^{m+1}M(-a,\, m+2,\, 2K)}{\Gamma(-1-a-m)\Gamma(m+2)} \sim$$

$$\frac{(2K)^{m+1}}{\Gamma(m+2)\Gamma(-m)}\left(1+\frac{2K}{m+2}+\frac{(2K)^2}{(m+2)(m+3)}+O(K^3)+\frac{\Gamma'(-m)}{\Gamma(-m)}\varepsilon+o(K^s)\right). \qquad (3.67)$$

Finally,

$$M(-1-a-m,\, -m,\, 2K) \sim 1+2K+\frac{(2K)^2}{2!}+O(K^3)+\frac{(2K)\varepsilon}{m}+o(K^{s+1}), \qquad (3.68)$$

and hence

$$\frac{M(-1-a-m,\, -m,\, 2K)}{\Gamma(-m)\Gamma(-a)} \sim \frac{1}{\Gamma(-m)}\left(1+(2K)+\frac{(2K)^2}{2!}+O(K^3)+\Gamma'(1)\varepsilon+o(K^s)\right). \qquad (3.69)$$

Taken together these results mean that the left hand side of the dispersion relation (3.33) reduces to

$$O(K^3)+o(K^s)-\frac{(2K)^{m+1}}{\Gamma(m+1)}+o(K^{m+1}), \qquad (3.70)$$

when $\Omega^2 \to 1$.

The leading order behaviour of the right hand side is much easier to determine. The numerator of the right hand side of (3.33) reduces to

$$-2\Lambda^2 r\,(2K)^s+O(K^{s+1}). \qquad (3.71)$$

Thus, fortunately, it is only necessary to determine the limit of the denominator as $K \to 0$.

Using (3.34)-(3.37) this can easily be determined and shows that the right hand side of (3.33) is asymptotically equal to

$$-\frac{2\Lambda\beta r}{\chi}(2K)^s + O(K^{s+1}). \tag{3.72}$$

Comparison of (3.70) and (3.72) indicates that s=m+1, as for the p-modes, and thus

$$\frac{1}{\Gamma(m+1)} = \frac{2\Lambda\beta r}{\chi}, \tag{3.73}$$

which determines r.

Finally, then, it follows that

$$\Omega^2 \sim 1 + \frac{\gamma_c}{(\gamma_c + 2\beta)\,\Gamma(m+2)}(2K)^{m+1}. \tag{3.74}$$

This is the f-mode.

Relations (3.55) and (3.74) give the corrections to Ω_*^2 due to a chromosphere permeated by a uniform, horizontal magnetic field. Similar results have been derived for the case of a magnetic chromosphere with a magnetic field declining in such a way that the Alfvén speed is uniform. In that case the dispersion relation is (Campbell and Roberts, 1989)

$$2aK\Omega^2\frac{U(1-a,\,m+3,\,2K)}{U(-a,\,m+2,\,2K)} + (m+1)\Omega^2 - (1+\Omega^2)K =$$

$$\frac{m+1}{\gamma_c}\left(\frac{\gamma_c}{2}+\beta\right)\frac{(\Omega^2 - K/\Lambda)(1-\Omega^4)}{\beta + (1+\beta)\left(\Omega^2 - \dfrac{K/\Lambda}{1+\beta}\right)\Phi}, \tag{3.75}$$

where

$$\Phi = -\frac{\Gamma\Lambda}{2K} + \left(\frac{\Gamma^2\Lambda^2}{4K^2} - \frac{\Lambda}{K}\frac{(\Gamma-1) + (\Omega^2 - \frac{1}{\beta}K/\Lambda)(1-\Omega^4)}{\left(1+\frac{1}{\beta}\right)\left(\Omega^2 - \dfrac{K/\Lambda}{1+\beta}\right)}\right)^{\frac{1}{2}}, \quad \Gamma = \frac{2\beta\gamma_c}{2\beta+\gamma_c}.$$

An analysis similar to that presented above yields asymptotic solutions in which the correction to Ω_*^2 is proportional to (K^{m+2}). Thus, the magnitude of the correction due to the uniform field is one order of K larger. It is also worth noting that while the corrections of (3.55) and (3.74) vanish in the limit of zero field, this is not the case in the equivalent results of Campbell and Roberts (1989). Their results on the p-mode frequencies are due to the combined effect of an isothermal atmosphere and a magnetic field. Put another way, the effect of a magnetic chromosphere with a uniform Alfvén speed can be mimicked by a change in the temperature of that region. This is not the case for the model presented here. The greater influence of the uniform magnetic field is not unexpected, however, since the field in the model of Campbell and Roberts (1989) decreases exponentially with height so that its strength is significant only very close to the interface between the two regions. These points will be discussed in more detail later.

3.4 Numerical Solutions

3.4.1 Numerical Method

Since it is expected that the effect of a chromospheric magnetic field will be greatest for modes with largest horizontal wavenumber (i.e. the modes trapped closest to the top of the convection zone) it is important to find solutions beyond the validity of the asymptotic formulae derived in the previous section. For this reason the dispersion relation (3.33) has been solved numerically by regarding it as a function of Ω for given values of K.

The most appropriate form of the dispersion relation for numerical solution is given by multiplying through by the denominators of (3.33) to give

$$\chi\left(\Lambda+\frac{\varphi}{K}\left[1+\frac{1}{\beta}\right]\left[\Lambda\Omega^2-\frac{K}{1+\beta}\right]\right)\times$$

$$\left(2aK\Omega^2U(1-a,\,m+3,\,2K)+U(-a,\,m+2,\,2K)\left[(m+1)\Omega^2-K(1+\Omega^2)\right]\right)$$

$$-\Lambda\,(\Lambda\Omega^2-K)(1-\Omega^4)\,U(-a,\,m+2,\,2K)=0. \qquad (3.76)$$

This avoids problems arising from zeros of these denominators. For a given value of K equation (3.76) can be solved by using standard methods with the values given by the asymptotic solutions of (3.55) and (3.74) as an initial guess.

The only complications in this method are the evaluation of the functions U and F. The confluent hypergeometric function U was evaluated using the routine available in the Vaxmath library and written by W. Fullerton. This is a very reliable routine except for when the parameter a is very close to an integer. This problem can be avoided since when a is exactly an integer the U-function is given by (Abramowitz and Stegun, 1965)

$$U(-n, \alpha+1, x) = (-1)^n \, n! \, L_n^{(\alpha)}(x), \tag{3.77}$$

where $L_n^{(\alpha)}$ are Laguerre polynomials. This expression is substituted when the Vaxmath routine fails.

In this investigation, the hypergeometric function has been evaluated by employing the integral formula (Abramowitz and Stegun, 1965)

$$F(p, q, r, \zeta) = \frac{\Gamma(r)}{\Gamma(q)\Gamma(r-q)} \int_0^1 t^{q-1}(1-t)^{r-q-1}(1-t\,z)^{-p}\,dt, \quad (c>b>0). \tag{3.78}$$

This integral can be evaluated numerically using standard routines. The method is reasonably reliable and fails only occasionally when the integrand has a singularity which is too extreme. If a great deal of calculation was necessary this method would be too slow but it was found to be quite adequate for the present purposes.

Finally, it is necessary to choose a suitable set of parameters that mimic the atmospheric structure as well as possible within the context of the model. The observations of Giovanelli and Jones (1982) indicate that, on average, the canopy field is around 500 km above the photosphere (i.e. the level where the optical depth for the continuum is 1). This places the canopy at around the temperature minimum. Consequently, the values of T_p, ρ_{0p}, p_p, etc are taken to be those at the temperature minimum. The precise values are taken from H.S.R.A. (Gingerich et al., 1971) and are listed in Table 3.1. In the numerical calculations

it is assumed that the atmosphere is marginally stable, so that $m=1/(\gamma_p-1)$. For illustrative purposes the values of the horizontal wavenumber k are related to the spherical harmonic degree l using the formula

$$k=\frac{\sqrt{l(l+1)}}{R_{sun}}, \tag{3.79}$$

as described in section 1.3.1.

3.4.2 The Effect of High Chromospheric Temperatures

The magnetic canopy of the solar chromosphere is associated with a sharp change in the magnetic field strength and it seems likely that the temperature may suffer a substantial change also. For this reason it is worth looking briefly at the effect on the mode frequencies that varying the chromospheric temperature T_c can have. To do this, the magnetism of the atmosphere will be ignored, though in reality, of course, it is the magnetism that causes the temperature changes. The frequencies of oscillation for zero field also need to be calculated in order to make comparisons with the magnetically modified frequencies. Setting the field to zero also affords a simpler picture of the mode structure and this permits a clearer physical description of the causes of frequency changes. Magnetic effects are discussed in the ensuing sections.

The dispersion relation for zero field can be obtained from equation (3.33) by taking the limit of zero field strength, i.e. $\beta\rightarrow\infty$. This gives

$$2aK\,\Omega^2\frac{U(1-a,m+3,2K)}{U(-a,m+2,2K)}+(m+1)\,\Omega^2-K(1+\Omega^2)=$$

$$\frac{\Lambda(\Lambda\Omega^2-K)(1-\Omega^4)}{\frac{T_p}{T_c}\Lambda\left(1+\frac{\gamma_c\Lambda\Omega^2}{2K}\left[-1+\left\{1-4\frac{K}{\gamma_c^2\Lambda}\left(\frac{[\gamma_c-1]+\Omega^2[\Omega^2-K/\Lambda]}{\Omega^2}\right)\right\}^{\frac{1}{2}}\right]\right)}, \tag{3.80}$$

in agreement with Campbell and Roberts (1989) when $T_p = T_c$ and $\gamma_p = \gamma_c$.

T_p	4170 K
p_p	86.82 kg m^{-1} s^{-2}
γ_p, γ_c	5/3
m	3/2
R	6425.97 m^2 s^{-2} K^{-1}
g	274.0 m s^{-2}
R_{sun}	6.96×10^8m
c_{sp}	6.6829 km s^{-1}
$v_{Ac}(B_0=10G)$	0.4967 km s^{-1}
$v_{Ac}(B_0=30G)$	1.5184 km s^{-1}
$v_{Ac}(B_0=100G)$	6.7335 km s^{-1}

Table 3.1 Parameters used for the basic atmospheric model. The value of m is given by assuming marginally stable, adiabatic stratification i.e., $m = 1/(\gamma_p - 1)$. The Alfvén speeds are calculated assuming that $T_c = T_p$.

Clearly, the term inside the square root of (3.80) must be positive. This corresponds to the solution in the chromosphere ($z<0$) being evanescent. If it is negative the waves propagate away to $-\infty$ and hence no cavity exists. Consequently, there exists a range of Ω^2 in which genuinely trapped modes are allowed. This is given by

$$\Omega^4 - \left(\frac{K}{\Lambda} + \frac{\gamma_c^2 \Lambda}{4K}\right)\Omega^2 + (\gamma_c - 1) \leq 0. \qquad (3.81)$$

This restriction is due to acoustic cut-off in the isothermal chromosphere and in the limit $k \to 0$ inequality (3.81) simply gives

$$\omega^2 \leq \omega_{ac}^2 = \left(\frac{\gamma_c g}{2 c_{sc}} \right)^2 . \tag{3.82}$$

Figure 3.1 illustrates the change in cyclic frequency ν ($=\omega/2\pi$) for several modes as a function of chromospheric temperature T_c. The base model is taken to be $T_c=T_p=4170$ K. Then, the frequency difference $\delta\nu=\nu(T_c)-\nu(4170K)$ is plotted as a function of T_c up to $T_c=50{,}000$ K for modes with radial orders n = 1, 3, 5 and degrees l = 50, 150, 250, 350. It is clear that the frequency of the modes decreases with increasing T_c, the magnitude of the effect increasing monotonically with both degree l and radial order n. The modes with highest order and degree are quite sensitive to changes in the chromospheric temperature, with frequency decreases of over 20 μHz. The curves stop at the point where the acoustic cut-off is reached. For n = 5, l = 350 this happens at a very low temperature so that none of the curve is visible in Figure 3.1.

The f-mode ($\Omega^2=1$) has not been included in Figure 3.1 since in the absence of a magnetic field its frequency is entirely unaffected by variations in chromospheric temperature or, for that matter, with variations in the temperature structure generally. This is because the f-mode is not actually a solution of (3.80) but arises from the case not examined in equation (3.12), namely $\omega^2=gk$. For this particular case the solution, after applying the appropriate boundary conditions concerning the kinetic energy density, is simply

$$\Delta \equiv 0, \quad u_z = C\, e^{-kz}, \tag{3.83}$$

where C is an arbitrary constant. The solution is entirely independent of the temperature structure of the atmosphere. Thus, in the absence of magnetic forces, and possibly other non-fluid perturbations, the f-mode will always have the same solution and dispersion relation. The only time this is not true is if the atmospheric structure implies that solution (3.83) would have unbounded kinetic energy for either of $z \to \pm\infty$, in which case the f-mode does not exist. This behaviour of the f-mode is quite distinctive and consequently of some

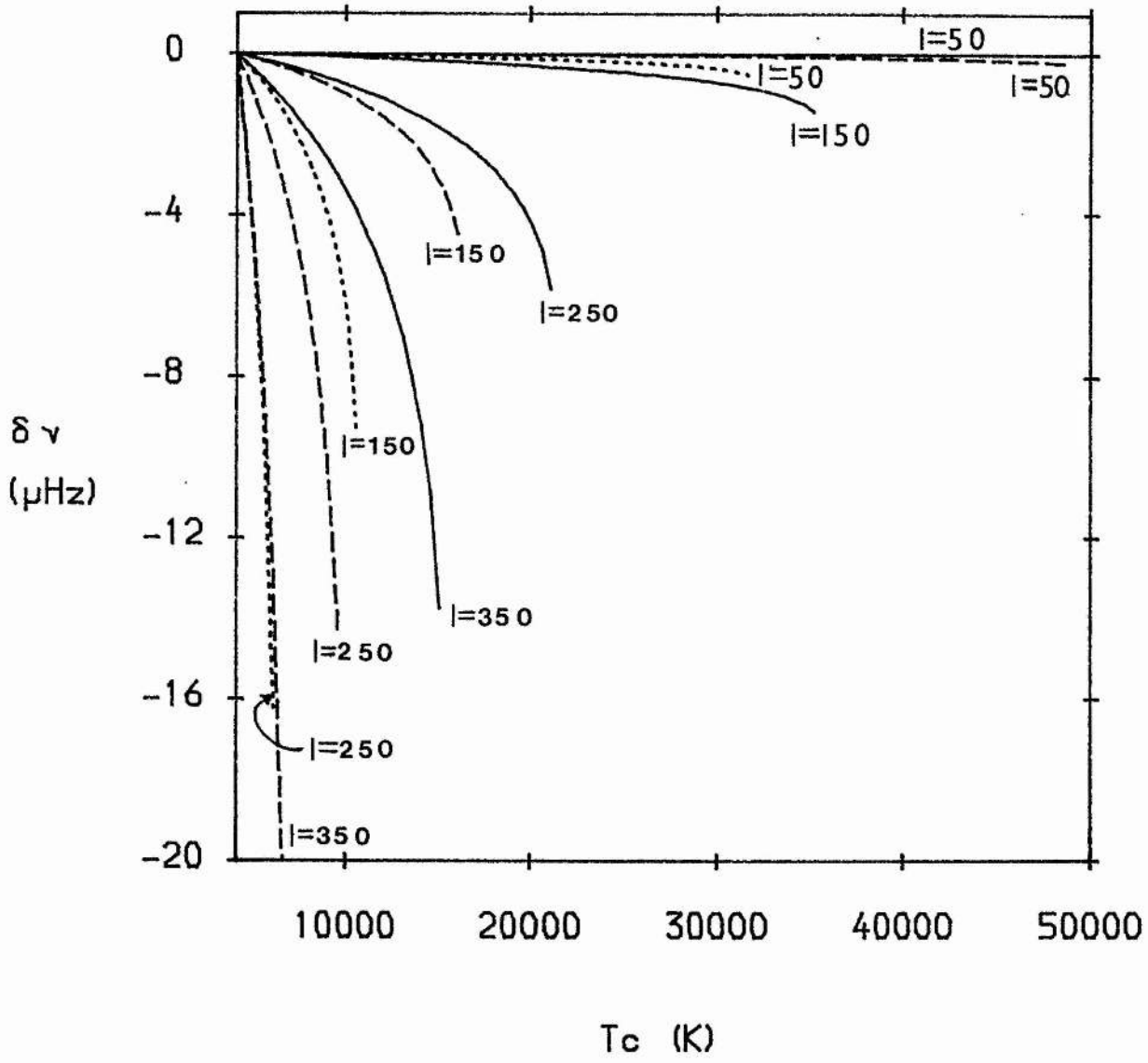

Figure 3.1 Frequency shift $\delta\nu = \nu(T_c) - \nu(T_p)$ as a function of chromospheric temperature T_c in the absence of a magnetic field. The parameters used are displayed in Table 3.1. Solid lines denote n=1, dashed lines n=3 and dotted lines n=5. For each n curves for l=50, 150, 250, 350, have been shown except for n=5 where the l=350 mode is absent.

significance.

3.4.3. The Effect of a Magnetic Field

In order to study the effects of introducing a magnetic field the model given in Table 3.1 has been used with a chromospheric temperature T_c=4170 K as a base from which to make comparison. As in the previous section the stratification of the convection zone is assumed to be marginally stable. Figures 3.2-3.7 show the variation of frequency with the strength of the magnetic field at the base of the chromosphere, up to a maximum of 0.01 T (100 G). The f-mode and p-modes with n=1, 2 have been illustrated here. The behaviour of modes with n>2 follows the pattern for n=1, 2. Both numerical and asymptotic solutions have been given and for small K (say, K≤0.1) the results are in good agreement . For ease of comparison, the equivalent results for the constant Alfvén speed model, computed from equation (3.75), have also been illustrated. The maximum possible field strength at the base of the magnetic region in these models occurs when the gas pressure in the upper region falls to zero, the magnetic field having completely evacuated the atmosphere; this occurs for B_0≈0.014 T (140 G).

Figures 3.8-3.10 show the variation of the frequency shift with degree l for the f-mode and the first two p-modes. The magnetic field is taken to be 0.003 T (30 G) in these plots. Figures 3.11 and 3.12 summarise the uniform field model by plotting the frequency shift, that is the frequency with the field present minus that with no field, against the mode frequency in the absence of the magnetic field for a representative set of modes. Figures 3.13 and 3.14 are the equivalents for the constant Alfvén speed model.

In Figure 3.10 it can be seen that the curves stop at around l=800. In the case of the constant Alfvén speed model this is due to the magnetoacoustic cut-off frequency discussed earlier. For the f-mode and the n=1 p-mode this cut-off occurs above l=1000 and so does not appear in Figures 3.8 and 3.9. The reason the curve for the constant B model stops is simply one of mathematical convenience. For l above the critical value where the curve stops, the parameters p and q of the hypergeometric function become complex conjugates hence making the numerical evaluation more difficult. It was felt that the little extra information to be gained by continuing computation into the complex regime does not justify

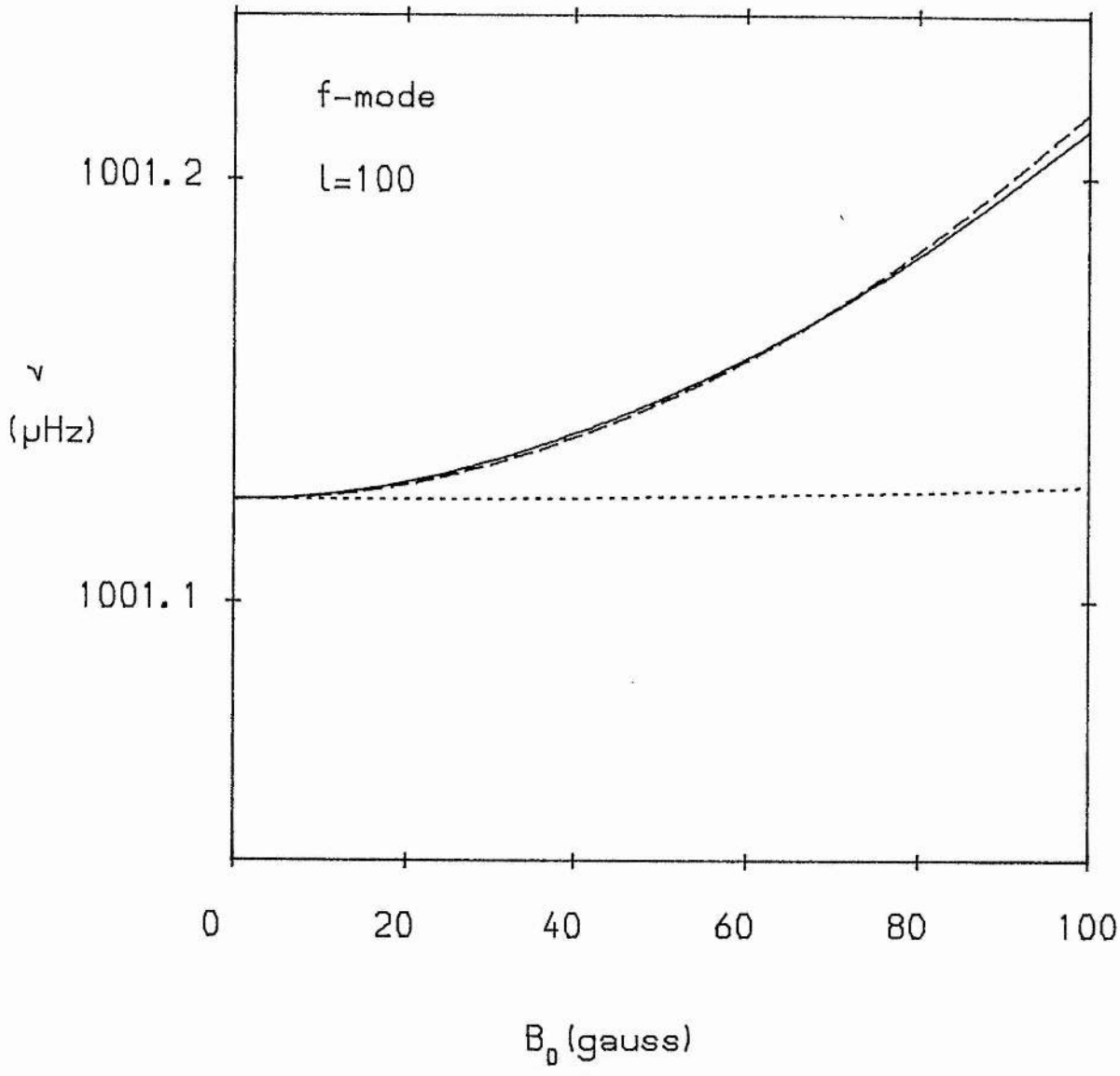

Figure 3.2 Variation of the frequency of the l=100 f-mode as a function of the field strength at the base of the chromosphere. The solid line is the numerical solution for the constant B model, the dotted line is for the constant Alfvén speed model and the dashed line shows the asymptotic solution (equation (3.74)) for the uniform field model. The chromospheric temperature is fixed at T_c=4170K, which is the value of the temperature at the top of the convection zone also. Atmospheric parameters are as in Table 3.1.

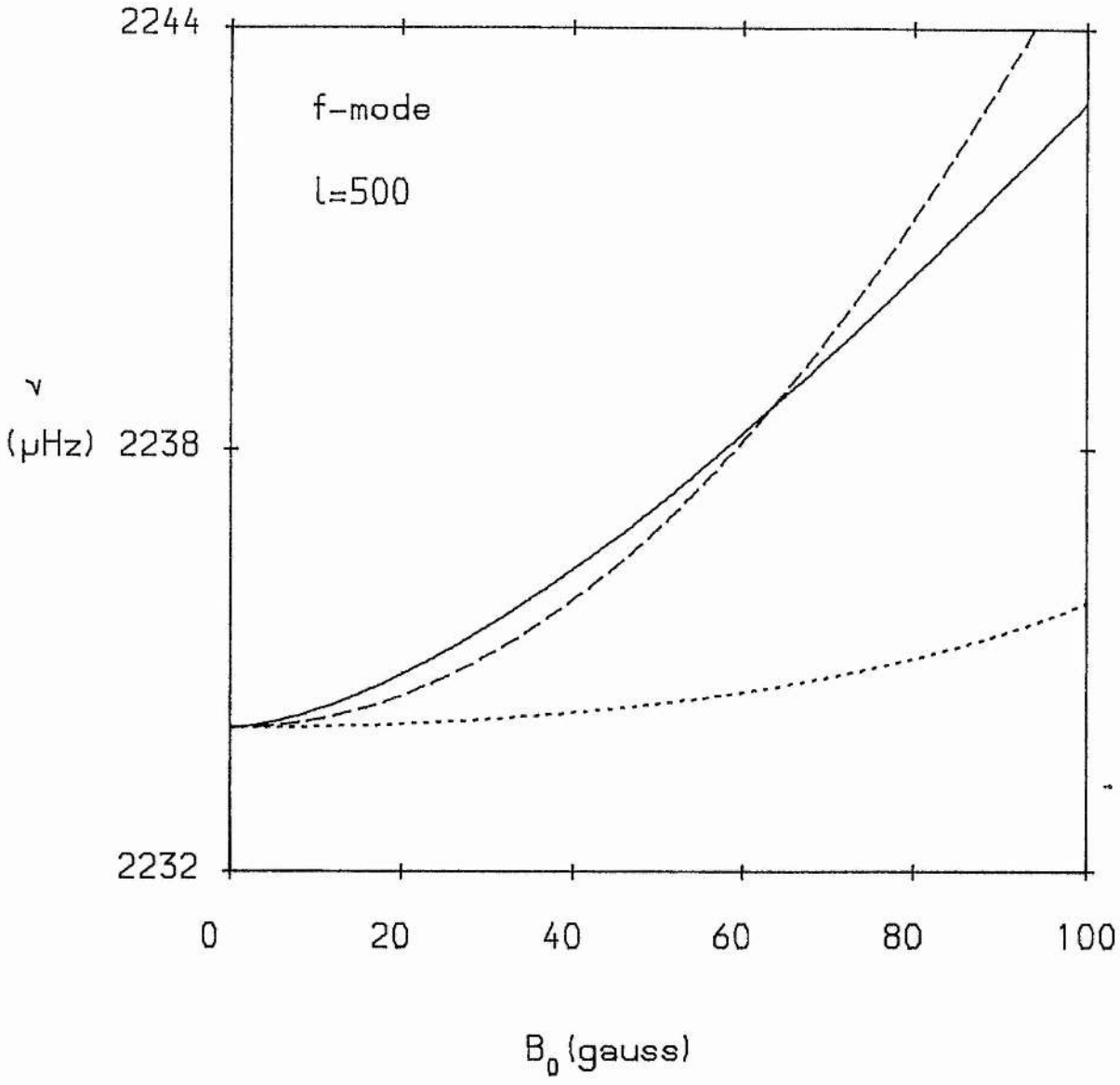

Figure 3.3 Increase in frequency of the f-mode as a function of chromospheric field strength, for degree l=500. Atmospheric parameters as in Table 3.1. Solid line is for constant B and dotted for constant Alfvén speed, while the dashed line gives the asymptotic solution for the uniform field model.

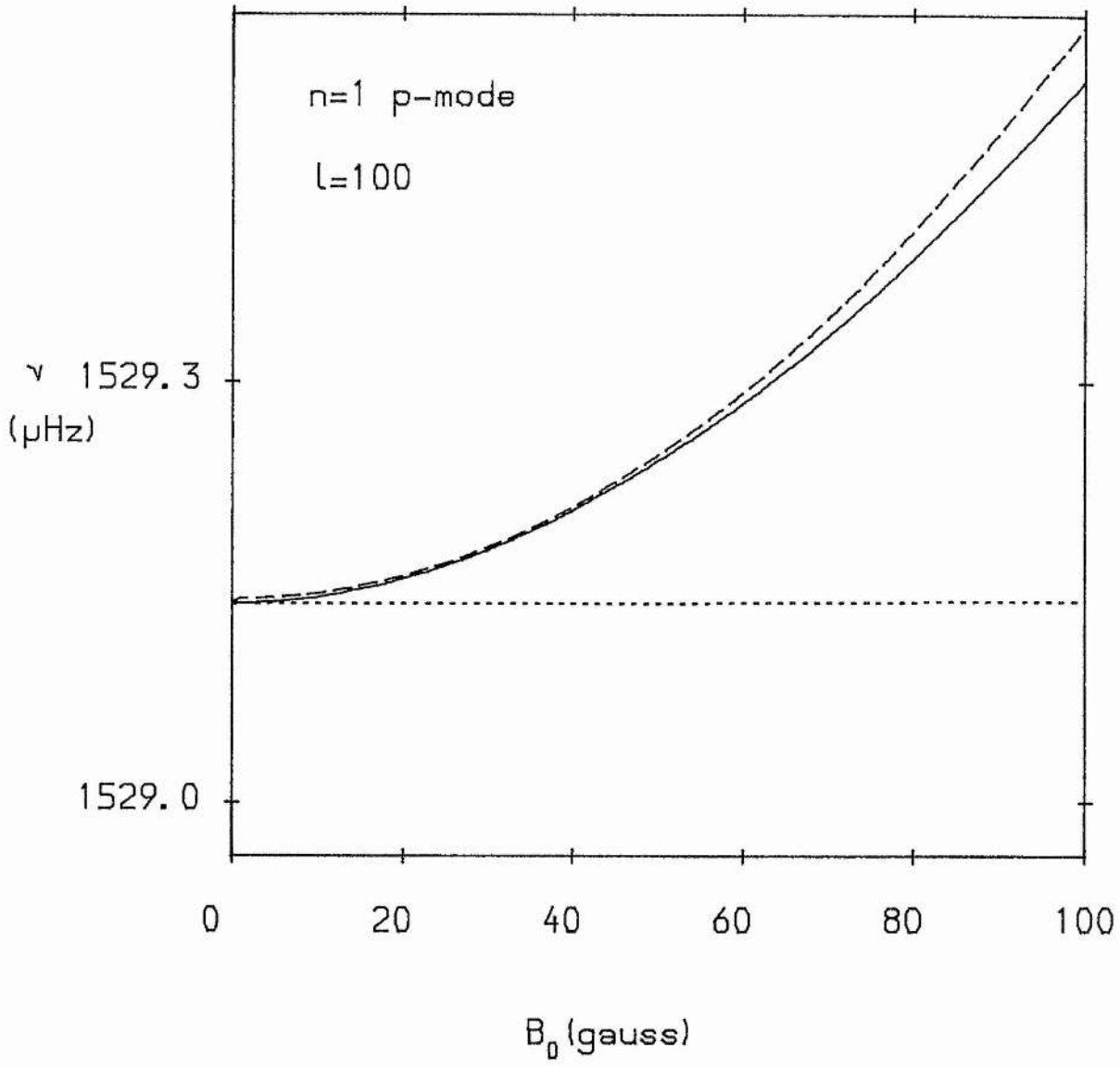

Figure 3.4 Increase in frequency of the n=1 p-mode as a function of chromospheric field strength, for degree l=100. Atmospheric parameters are as in Table 3.1 and linestyles are as in Figure 3.2.

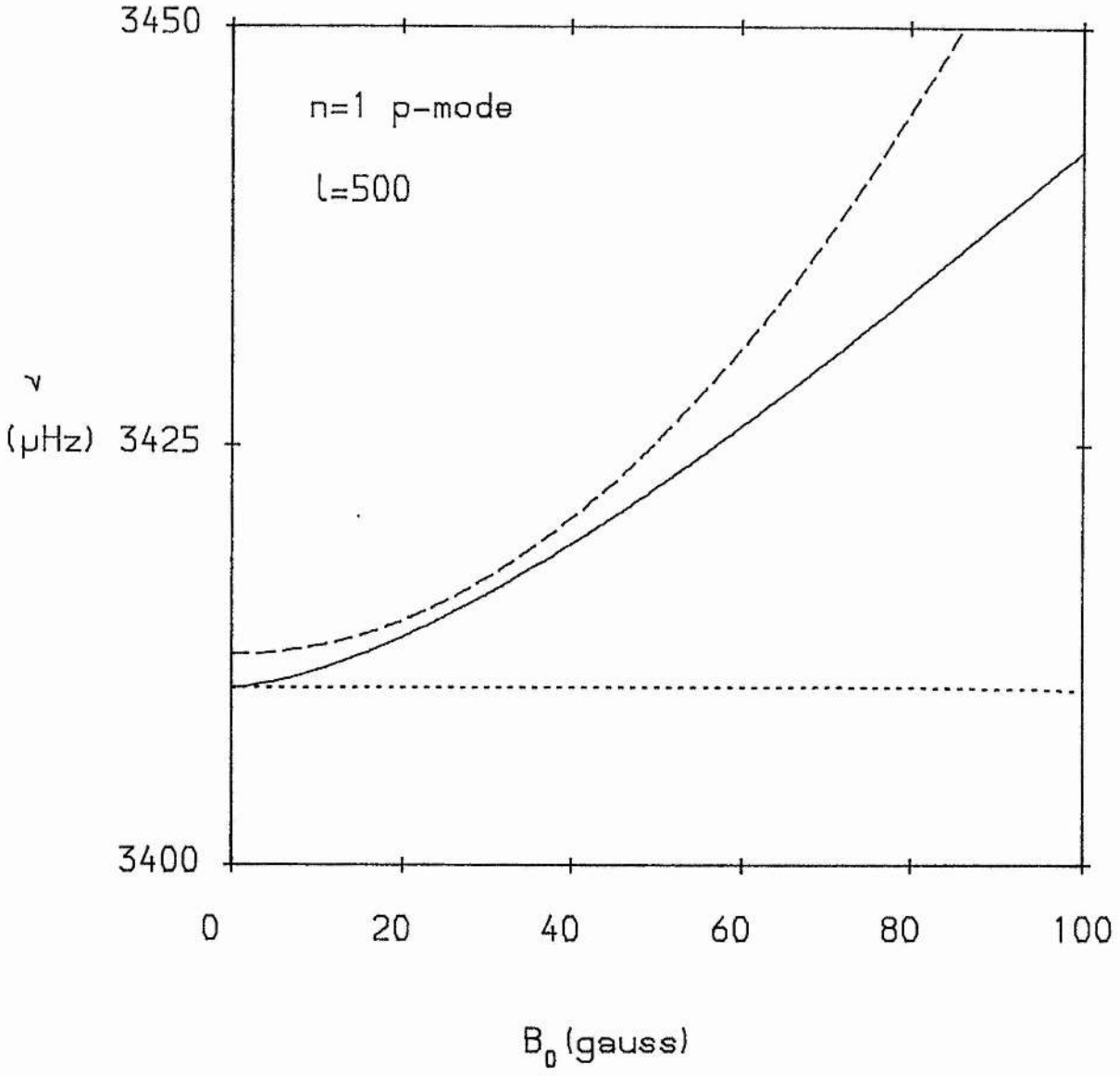

Figure 3.5 Increase in frequency of the n=1 p-mode as a function of chromospheric field strength, for degree l=500. Atmospheric parameters are as in Table 3.1 and linestyles are as in Figure 3.2.

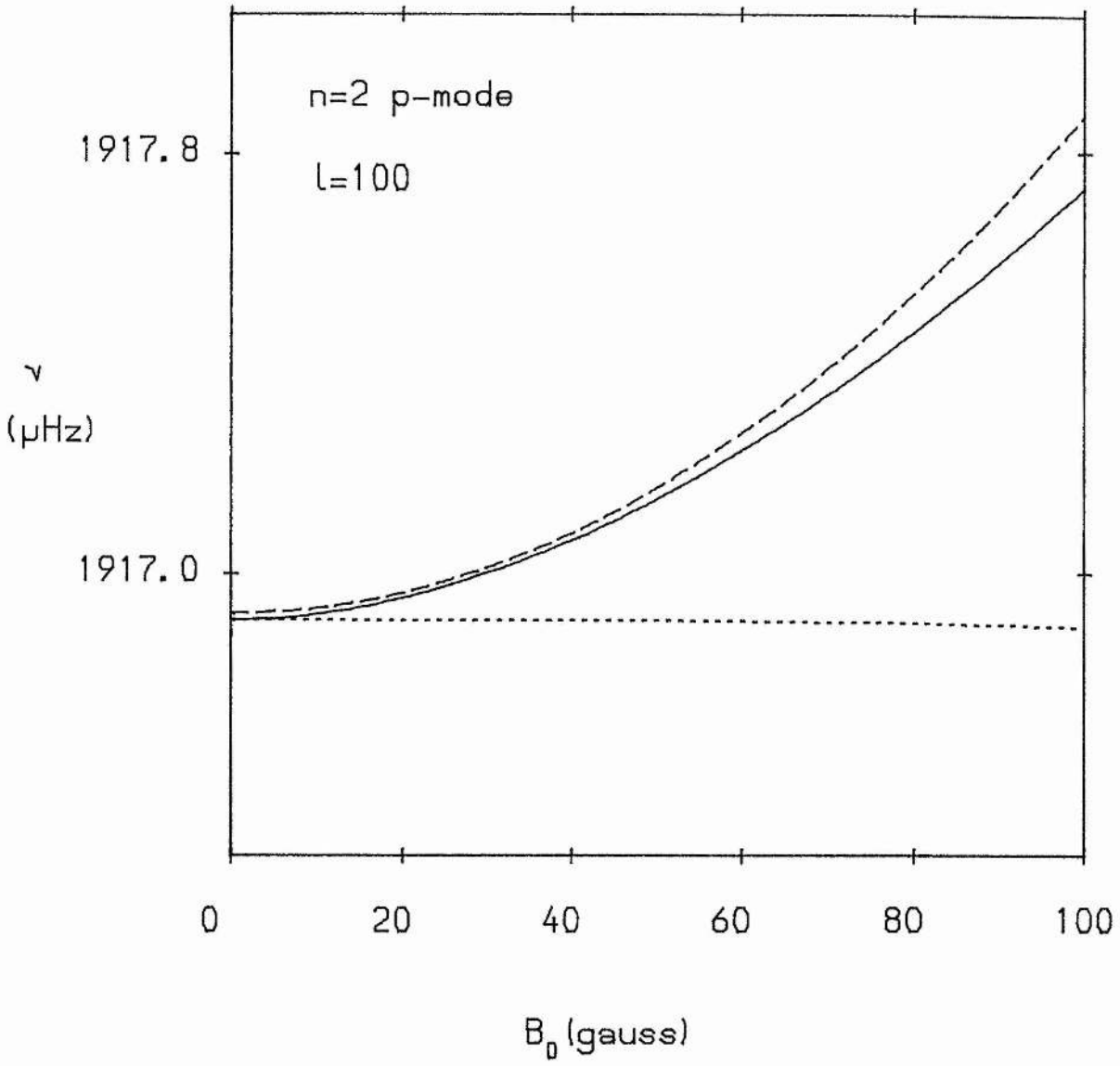

Figure 3.6 Increase in frequency of the n=2 p-mode as a function of chromospheric field strength, for degree l=100. Atmospheric parameters are as in Table 3.1 and linestyles are as in Figure 3.2.

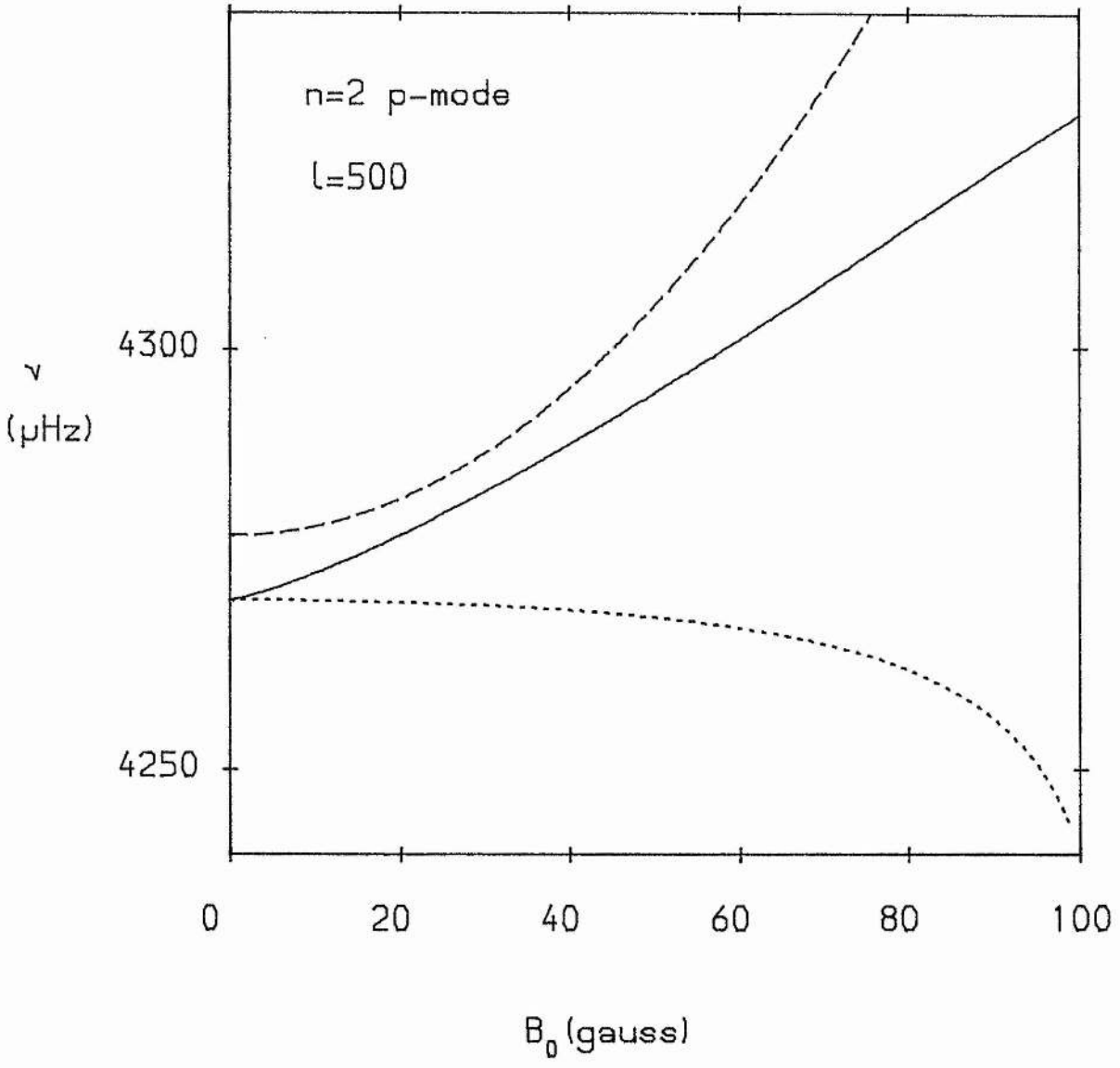

Figure 3.7 Increase in frequency of the n=2 p-mode as a function of chromospheric field strength, for degree l=500. Atmospheric parameters are as in Table 3.1 and linestyles as in Figure 3.2.

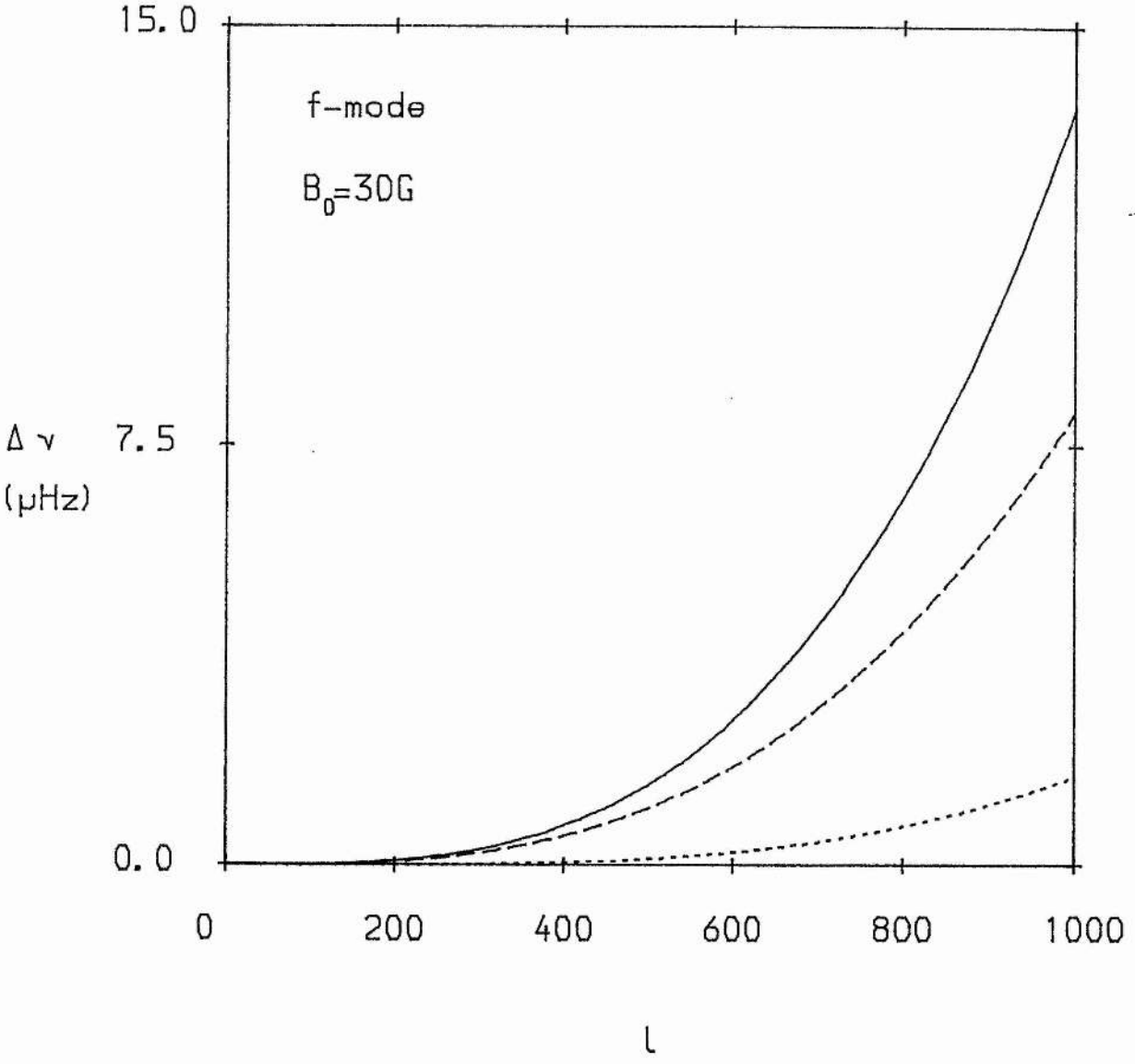

Figure 3.8 Variation of the frequency shift $\Delta\nu=\nu(B)-\nu(0)$ against degree l for the f-mode in a field of B_0=30 G and a chromosphere with T_c=4170 K. Atmospheric parameters are as in Table 3.1. The solid line represents the constant B model while the dotted line is for the constant Alfvén speed model and the dashed line is the asymptotic solution for the constant B model.

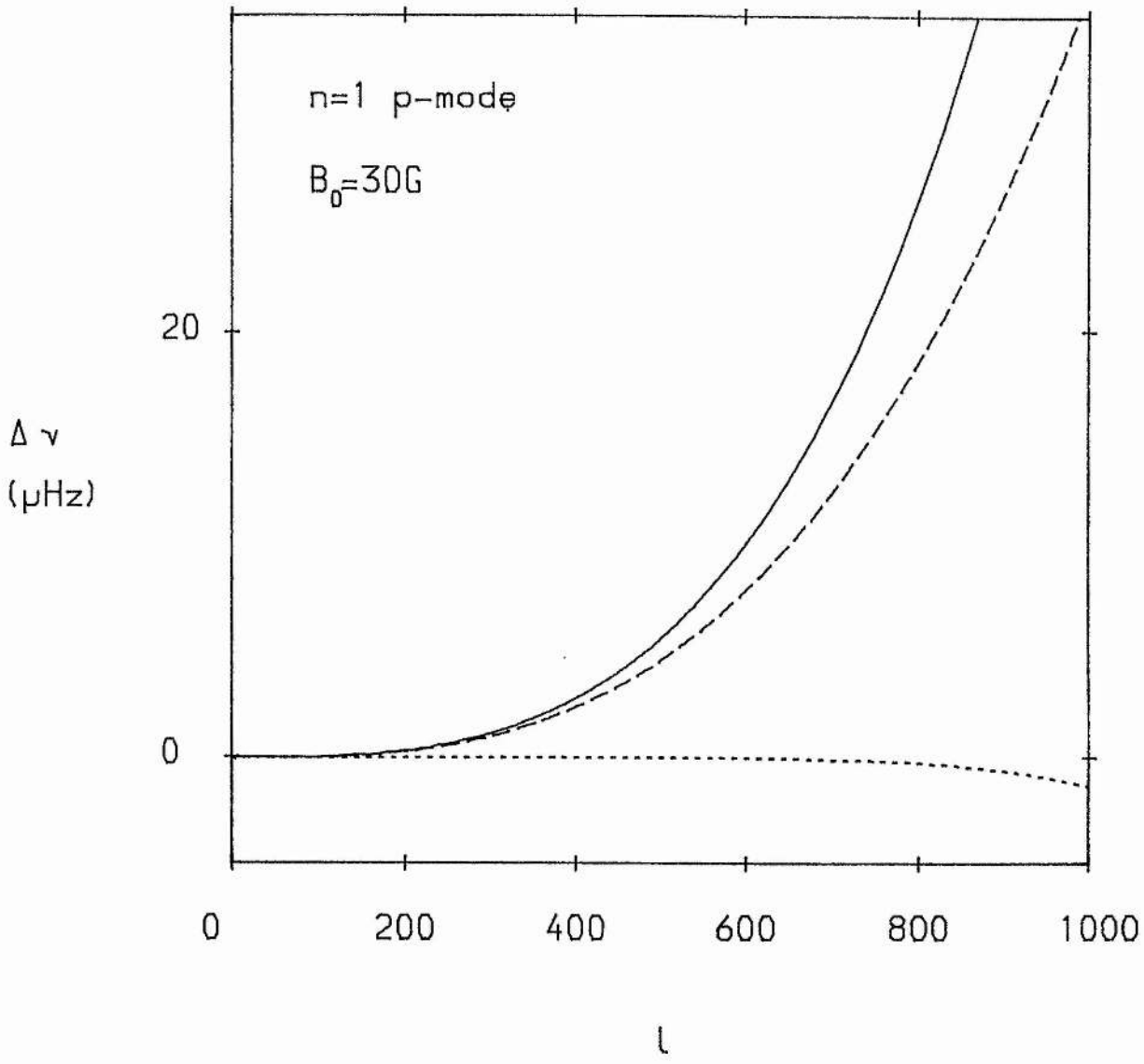

Figure 3.9 Variation of the frequency shift $\Delta\nu = \nu(B)-\nu(0)$ against degree l for the n=1 p-mode in a field of B_0=30 G and a chromosphere with T_c=4170 K. Atmospheric parameters are as in Table 3.1. Linestyles as in Figure 3.8.

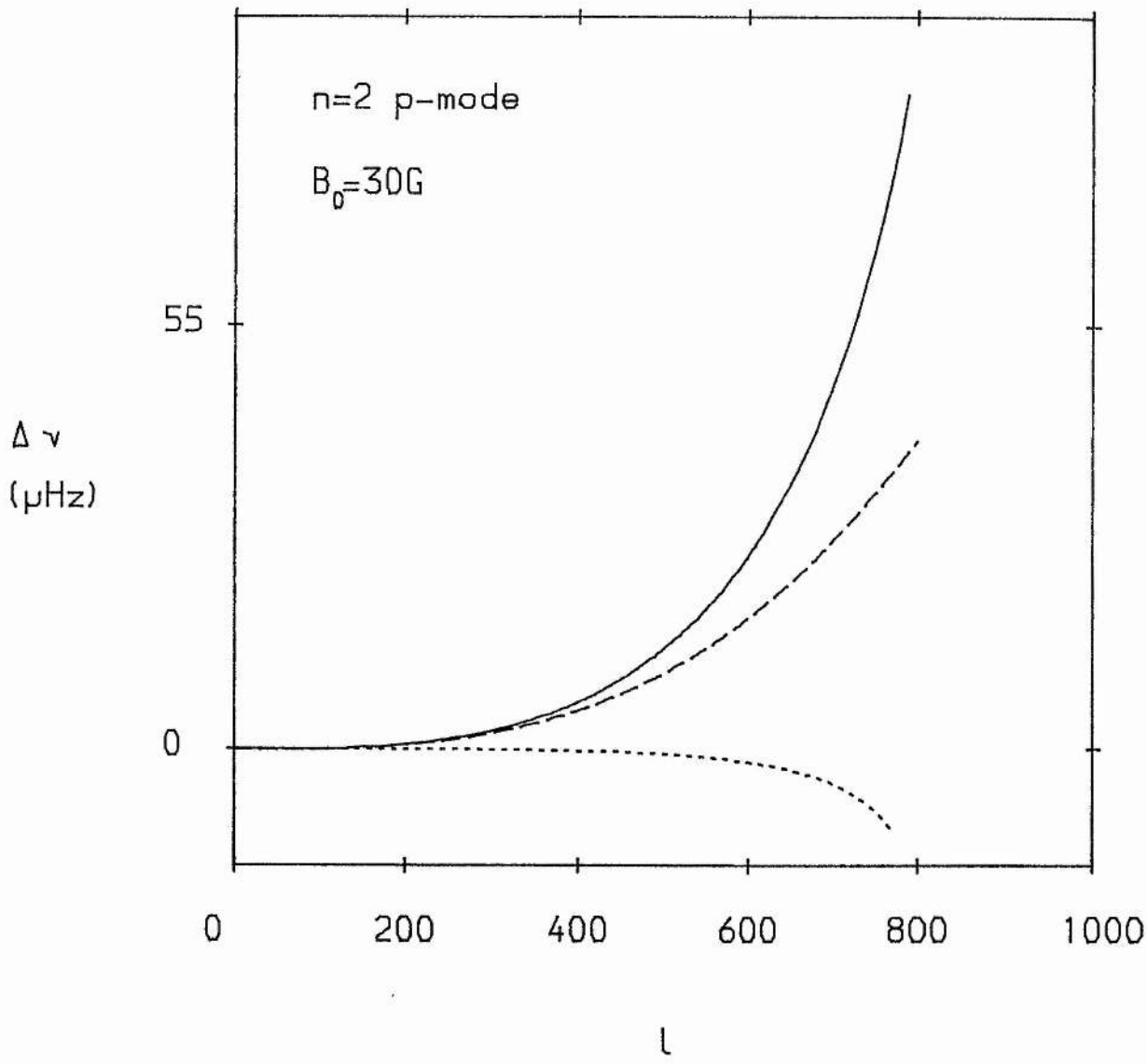

Figure 3.10 Variation of the frequency shift $\Delta\nu = \nu(B)-\nu(0)$ against degree l for the n=2 p-mode in a field of B_0=30 G and a chromosphere with T_c=4170 K. Atmospheric parameters are as in Table 3.1 and linestyles are as in Figure 3.8. The curves stop at around l=800 due to cut-off effects. For the constant Alfvén speed curve, this is the magnetoacoustic cut-off discussed in Campbell and Roberts (1989). For the constant B curve, the cut-off simply denotes the point where the arguments of the hypergeometric function become complex.

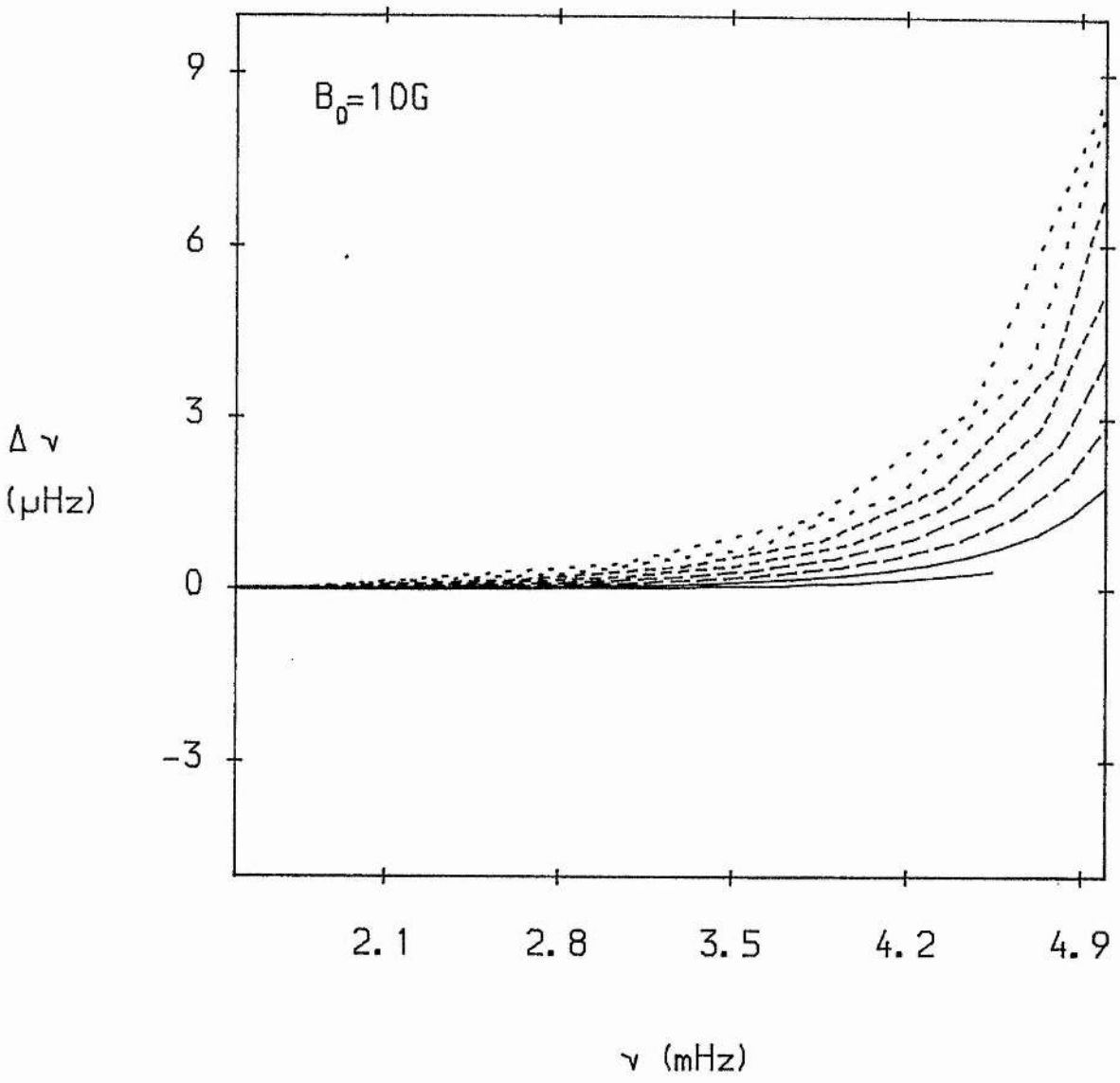

Figure 3.11 The frequency shift $\Delta\nu$ ($=\nu(B_0)-\nu(0)$) as a function of ν, for a uniform chromospheric magnetic field B_0=10 G and a temperature of 4170 K.Atmospheric parameters are as in Table 3.1 Curves shown are for l=50, 100....350, 400. Solid lines are for $0 < l \leq 100$, long dashed lines are for $100 < l \leq 200$, short dashed for $200 < l \leq 300$, and dotted for $300 < l \leq 400$.

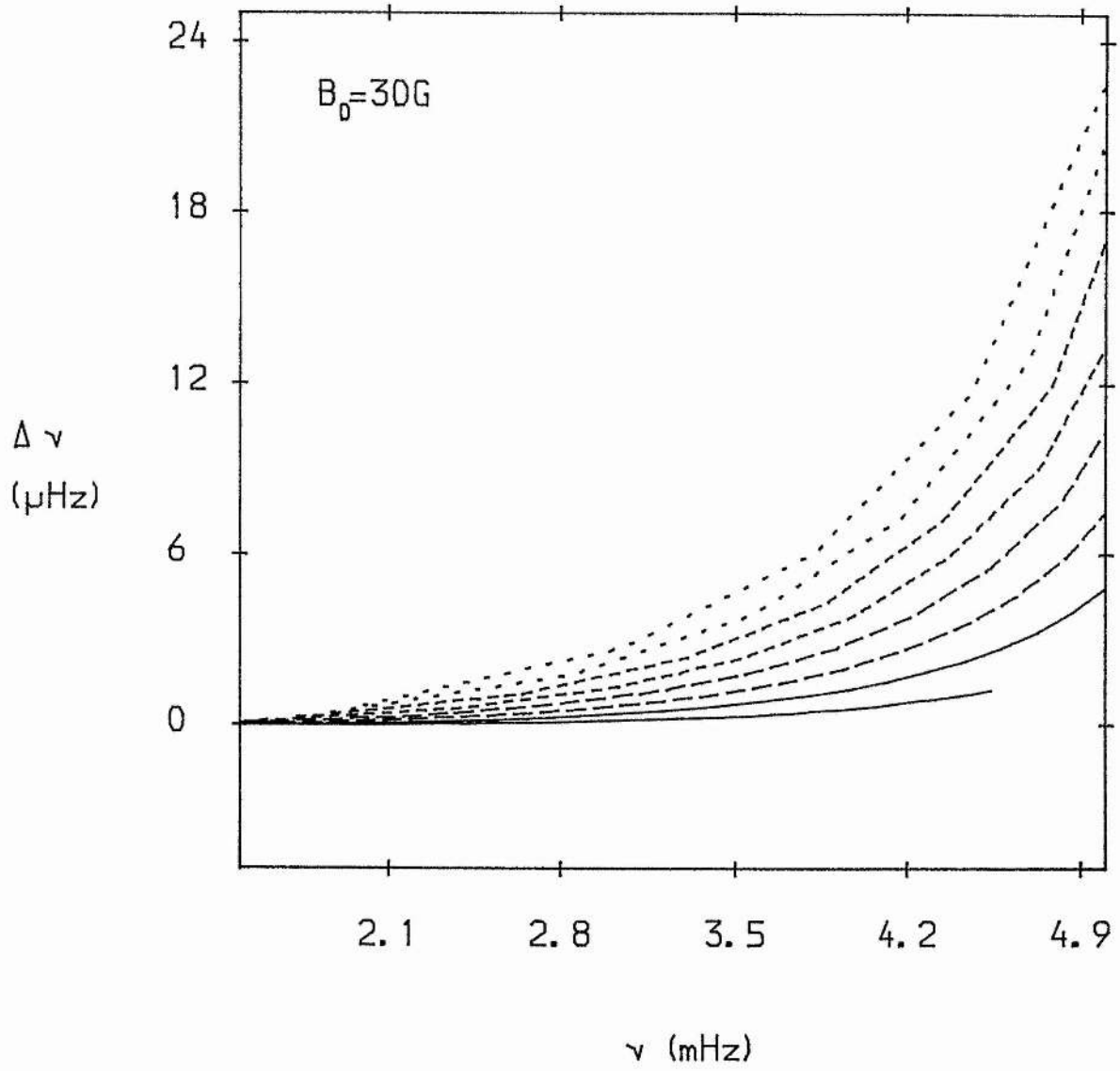

Figure 3.12 The frequency shift $\Delta\nu$ ($=\nu(B_0)-\nu(0)$) as a function of ν, for a uniform chromospheric magnetic field B_0=30 G, with other parameters as in Figure 3.11. Curves shown are for l=50, 100....350, 400. Solid lines are for $0 < l \leq 100$, long dashed lines are for $100 < l \leq 200$, short dashed for $200 < l \leq 300$, and dotted for $300 < l \leq 400$.

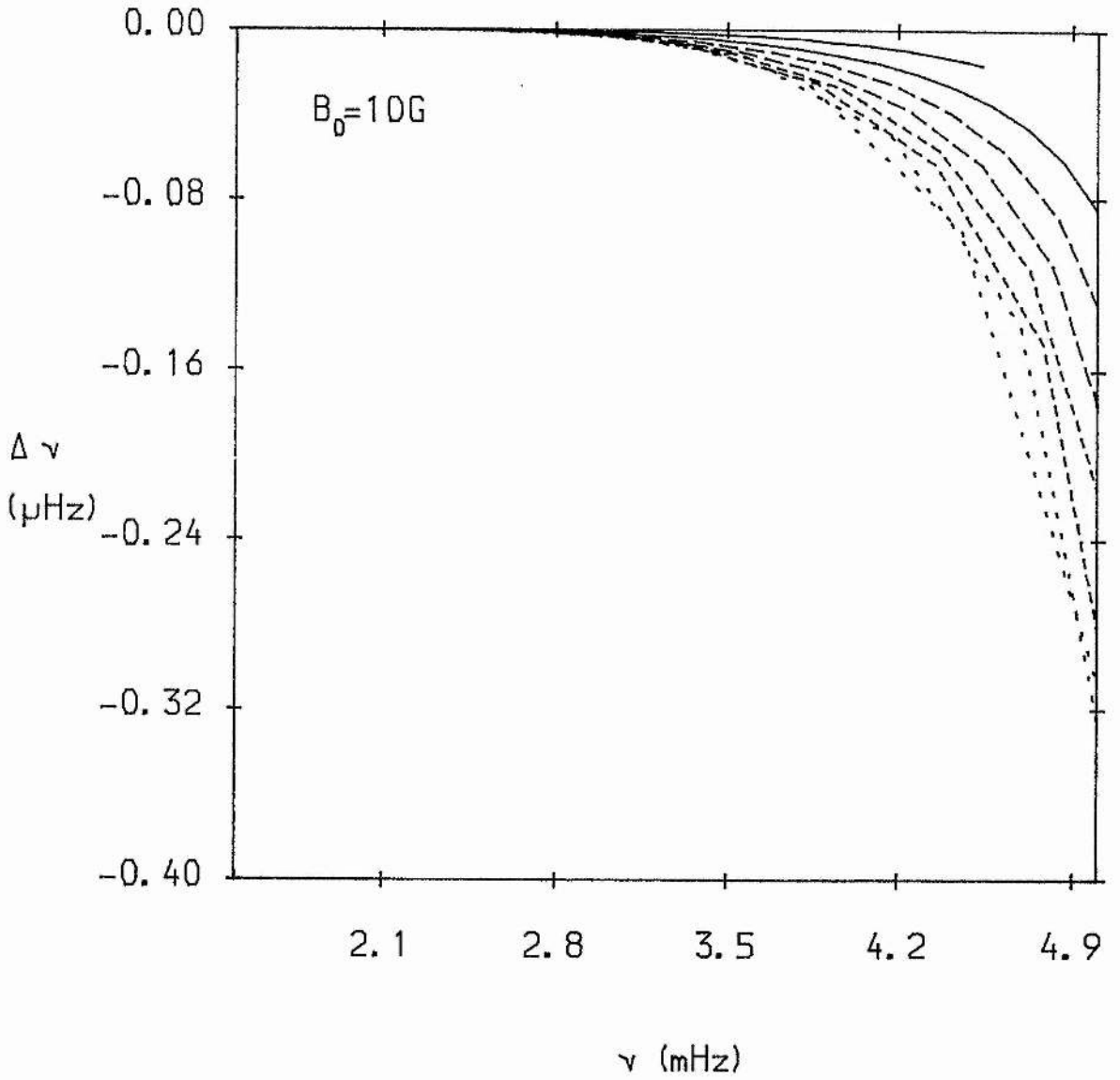

Figure 3.13 The equivalent of Figure 3.11 for the constant Alfvén speed model.

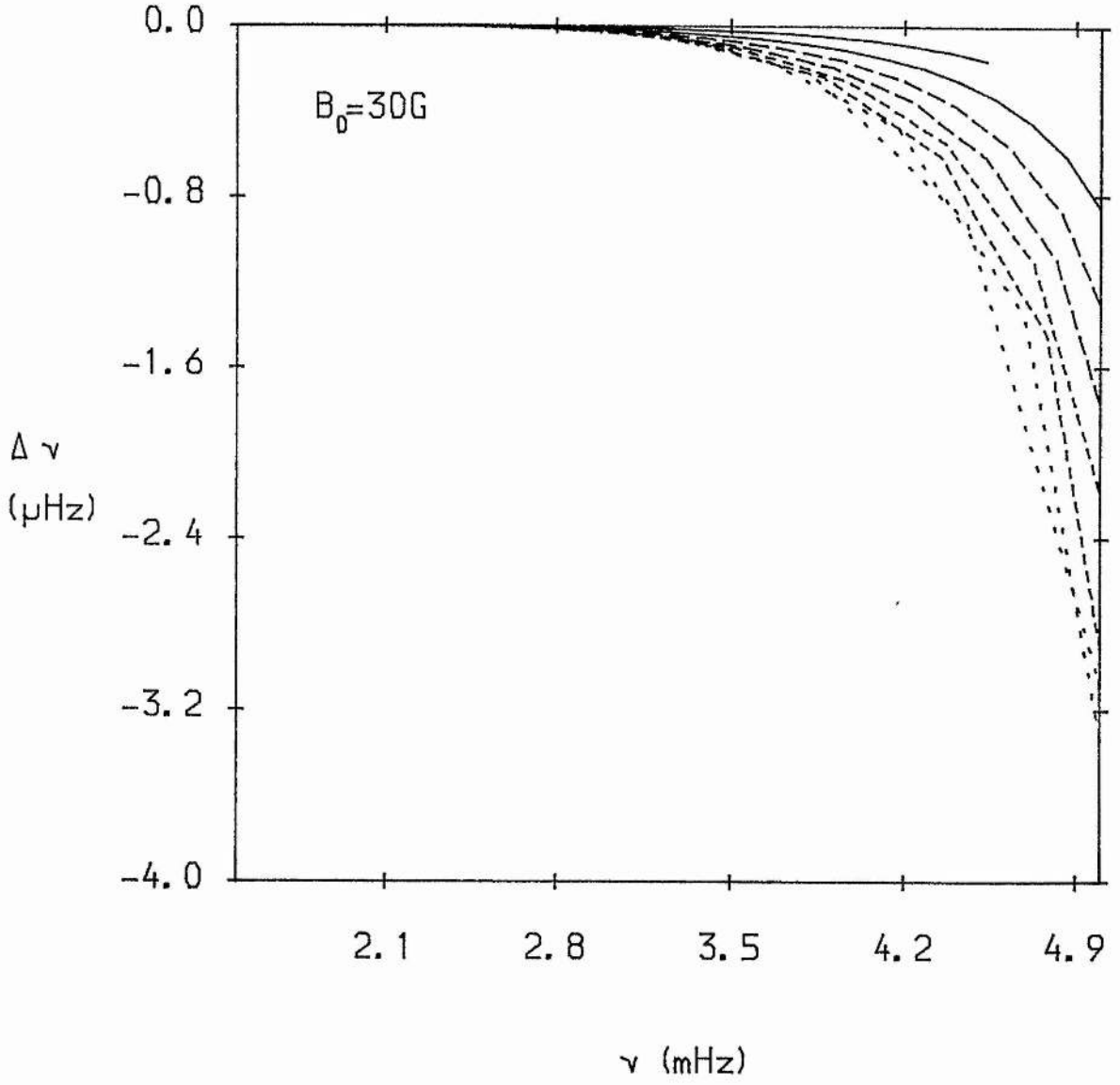

Figure 3.14 The equivalent of Figure 3.12 for the constant Alfvén speed model.

the effort required in performing such calculations. An examination of the expression for u_z, given in equation (3.27), in the limit of $z \to -\infty$ shows that, for *any* frequency, u_z will always become evanescent, eventually. Hence, it is not possible for any cut-off effect to exist in this model since this would require an oscillatory behaviour as $z \to -\infty$.

It is interesting to examine the values of Ω^2 for which p and q are complex (r is always real). From the definition of p and q,

$$p+q = 1+\frac{2K}{\gamma_c\Lambda}, \quad pq = \frac{K}{\gamma_c\Lambda}\left(\frac{K}{\gamma_c\Lambda}+1\right)+\frac{\gamma_c-1}{\gamma_c^2}\frac{K}{\Lambda\Omega^2}+\frac{K}{\gamma_c^2\Lambda}\left(\Omega^2-\frac{K}{\Lambda}\right), \qquad (3.84)$$

it can be shown that

$$p,\, q = \frac{K}{\gamma_c\Lambda}+\frac{1}{2}\pm\left(1-4\,\frac{K}{\gamma_c^2\Lambda}\left[\frac{(\gamma_c-1)+\Omega^2(\Omega^2-K/\Lambda)}{\Omega^2}\right]\right)^{\frac{1}{2}}. \qquad (3.85)$$

Thus, the condition for p, q to be real is that the expression within the square root be positive. This is exactly the condition required for genuinely trapped modes to exist in the field free model. Thus condition (3.81) must be satisfied in order to avoid p and q being complex. Since the purpose here is to compare frequencies for a magnetic chromosphere with those of a field free atmosphere, there is no point in looking at cases with no field free reference frequency, i.e. the cases for which p and q are complex.

The physical interpretation of this behaviour is quite simple. In the field free case, inequality (3.81) must be satisfied in order to stop acoustic waves being able to propagate out of the top of the cavity. When a magnetic field with a uniform Alfvén speed is added the frequency at which cavity leakage occurs is changed since waves are now of the fast magnetoacoustic type in the chromosphere. This introduces the magnetoacoustic cut-off discussed by Campbell and Roberts (1989). On the other hand, if a uniform magnetic field is added to the isothermal atmosphere, the Alfvén speed, and hence fast magnetoacoustic phase speed, increases exponentially with height. The effect of this is to create a reflection for waves of any frequency, due simply to the increasing phase speed. In other words,

there is no cut-off effect for this model. This is unlikely to be realistic since, even if the Alfvén speed does increase rapidly in the lower chromosphere, it will soon, within a few hundred kilometres, reach the roughly constant value of the corona. In this respect the present model is a poor representation of the real chromosphere.

The nature of the oscillation modes will change with increasing frequency. For very high frequencies, such that p and q are complex, the cavity rises higher into the chromosphere until the modes become the equivalent of those studied by Nye and Thomas (1976a). Their calculation was intended to model coronal oscillations and consists of the chromospheric part of the model used here but bounded below by a rigid reflecting boundary. The eigenmodes are similar to p-modes but the dispersion relations are quite different. For the model presented here, very high frequency modes are able to oscillate the thin chromosphere but the rapidly increasing density in the convection zone acts very much like a rigid wall thus creating the lower boundary. On the other hand, low frequency modes are able to move the dense photosphere and below but, since the low density fluid in the chromosphere responds very rapidly to disturbances, the upper atmosphere simply moves as a whole, i.e. waves are evanescent. A detailed observational investigation of cut-offs in p-modes and the effect that the chromosphere has may help to indicate atmospheric magnetic structure.

It is clear that for the uniform magnetic field model, *all modes show a frequency increase with the strengthening of the field.* For a given n and l, the frequency is higher in the presence of a constant magnetic field than in the absence of any field. The magnitude of this frequency shift increases with n and l; equations (3.55) and (3.74) giving the general trend. In certain cases the shift is quite large ($\approx 50\mu$Hz) so that the effect of strong magnetic fields should be clear on modes of high degree, provided sufficient observational resolution can be brought to bear.

This behaviour is to be compared with that of the constant Alfvén speed model of Campbell and Roberts (1989). In that case the overall frequency shifts are about an order of magnitude smaller, as would be expected from comparison of the asymptotic solutions. The f-mode behaves in a similar, though less extreme, way to the uniform field model. However, the other modes show quite different behaviour. The first p-mode increases in

frequency with small k, but at larger values decreases. This is difficult to see in the figures presented here due to the need to scale the results in comparison with the constant B model, but this behaviour is brought out clearly in Campbell and Roberts (1989). Finally, the modes with n≥2 show a frequency *decrease*.

3.4.4 The Effects of a Penumbral Magnetic Field

The parameters used for the above calculations (Table 3.1) represent conditions typical of those to be expected in an average solar region at solar minimum (B=10 G) and solar maximum (B=30 G). It is also of interest to investigate the effects that the penumbrae of active regions may have. For this purpose another set of calculations has been done for a field which lies lower in the atmosphere. The parameters relating to this situation are given in Table 3.2.

The results for this penumbral parameter set are presented in Figures 3.15 and 3.16, where the frequency difference between the magnetic and non-magnetic cases ($\Delta\nu=\nu(B)-\nu(0)$) has been plotted against the chromospheric field strength. Figure 3.15 shows the f-mode and the first two p-modes for l=100 and Figure 3.16 shows the same modes for l=500 (the solutions are all numerically calculated from the full dispersion relation). For comparison, Table 3.3 shows the frequency shifts for selected modes in each model atmosphere.

These results show that, contrary to what might at first be expected, for a given mode and chromospheric field strength the frequency shift is lower for the penumbral model than the quiet Sun. This does not necessarily mean that the influence of a penumbral field is less than that of the quiet Sun since the penumbral field will be proportionately stronger as well as being lower down. The important factor in determining the size of the frequency shift is the strength of the field in relation to the fluid pressure in the chromosphere. This is borne out by the fact that the asymptotic corrections (3.55) and (3.74) show a rough dependence of $1/\beta$. For the results of Table 3.3, β=19.4 for the quiet Sun and β=118.4 for the penumbra. Thus the ratio of $1/\beta$ for the two models is quite close to the corresponding ratio of frequency shifts.

T_p	4460 K
p_p	512.5 kg m^{-1} s^{-2}
γ_p, γ_c	5/3
m	3/2
R	6425.97 m^2 s^{-2} K^{-1}
g	274.0 m s^{-2}
R_{sun}	6.96×10^8 m
c_{sp}	6.9113 km s^{-1}
v_{Ac} (B_0=10 G)	0.2110 km s^{-1}
v_{Ac} (B_0=30 G)	0.6351 km s^{-1}
v_{Ac} (B_0=100 G)	2.1965 km s^{-1}

Table 3.2. Parameters used for the penumbral atmospheric model. The value of m is given by assuming marginally stable, adiabatic stratification i.e. $m=1/(\gamma_p-1)$. The Alfvén speeds are calculated assuming that $T_c=T_p$.

The actual effects of penumbral fields will be complicated by variations in field strength as well as canopy height. Penumbral magnetic fields are likely to be quite high (≈200 G). The numbers used in Table 3.3 are simply convenient for purposes of comparison between the quiet Sun and penumbral situations. These points will be discussed further in Chapter 4 where a generalised model atmosphere is used. This facilitates an investigation of more general canopy structures. Now, though, it is important to investigate the physical reasons for the results that have been shown here.

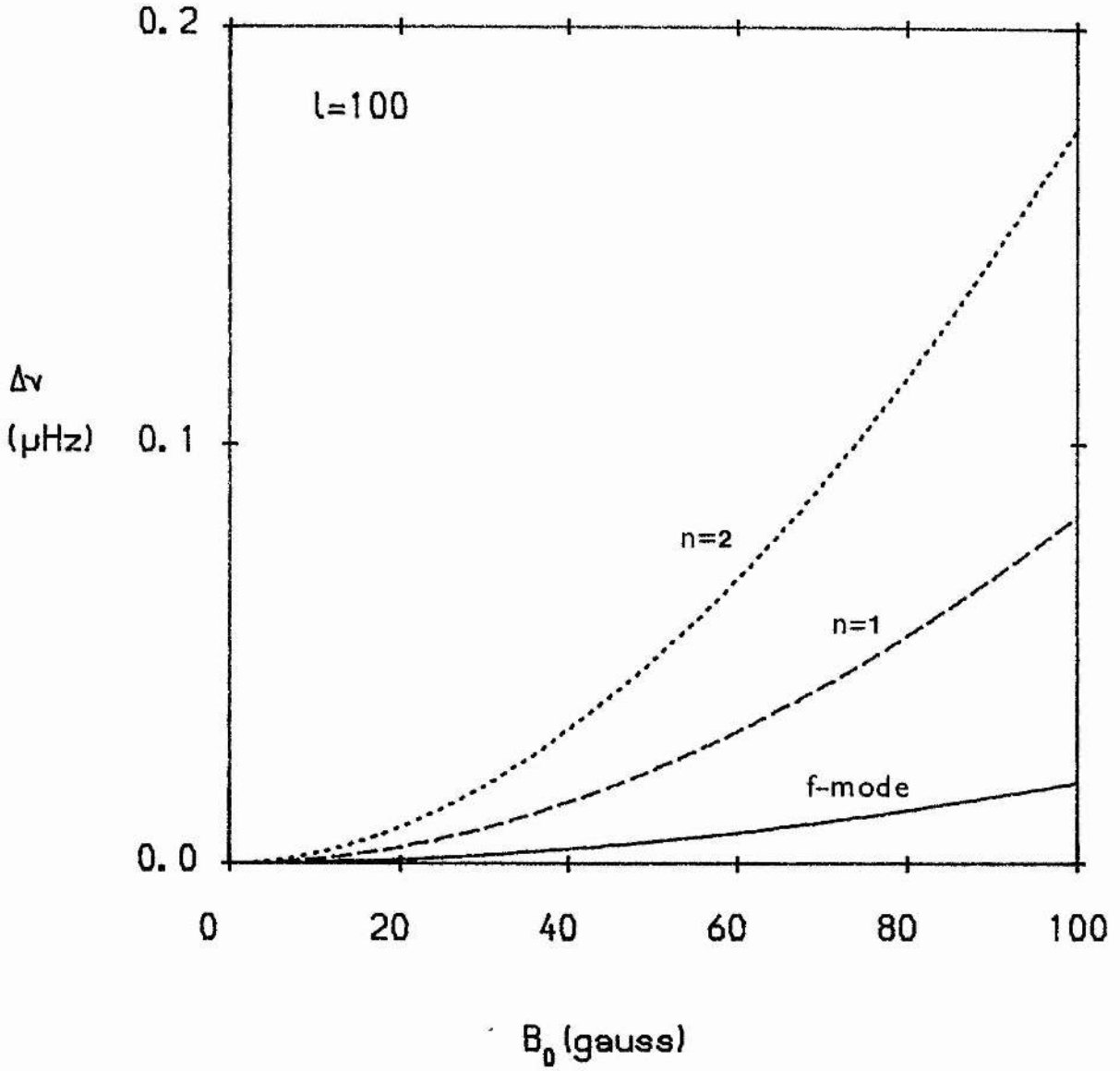

Figure 3.15 Variation of the frequency shift $\Delta\nu$ ($=\nu(B)-\nu(0)$) as a function of field strength for the penumbral model atmosphere (see Table 3.2). Here, the f-mode and the first two p-modes are shown for l=100. The solid line is the f-mode, dashed is n=1 and dotted is n=2.

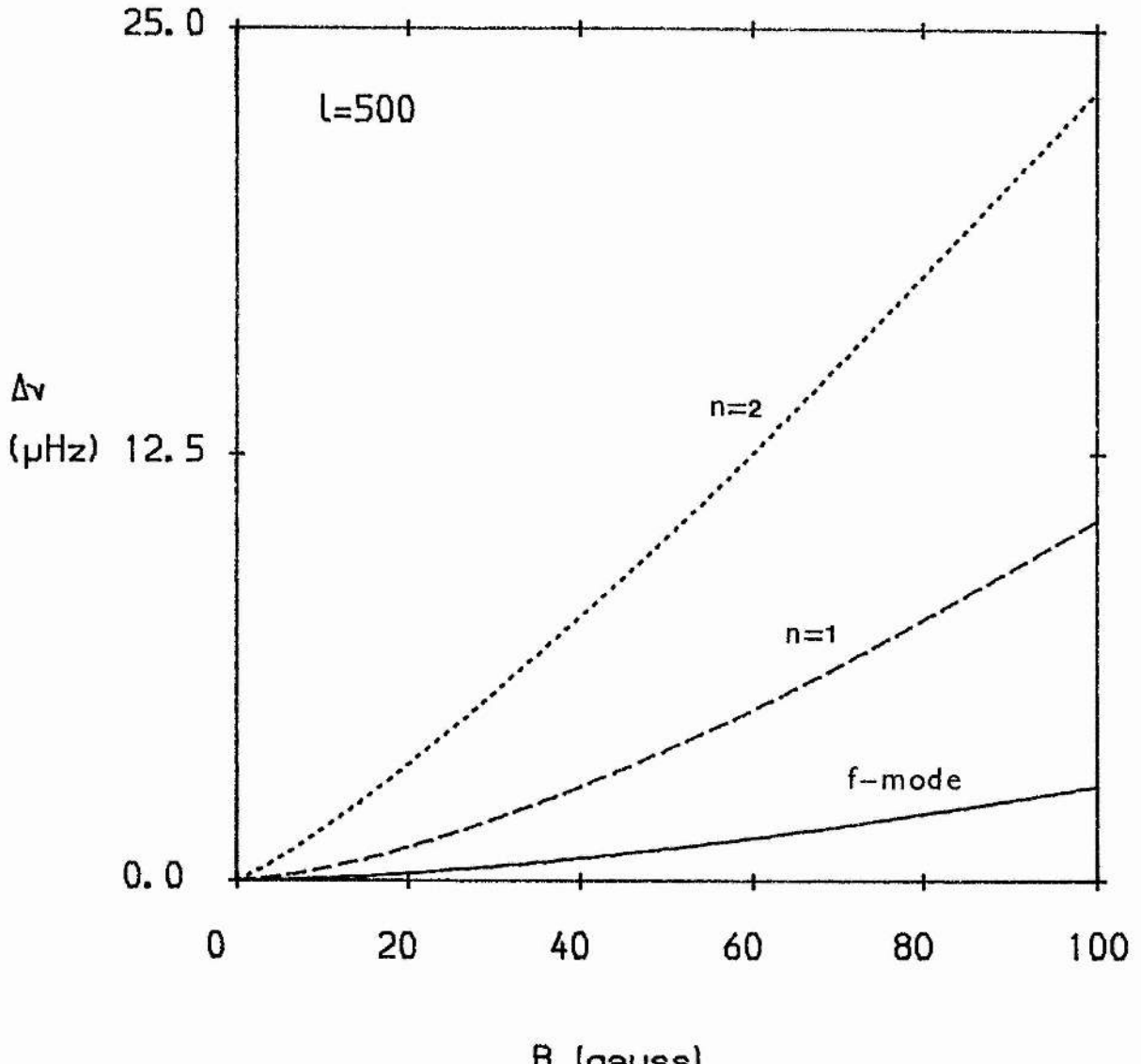

Figure 3.16 As for Figure 3.15 but here l=500.

Model	l=100 n=1	l=500 n=1
Quiet Sun	38.425×10^{-3}	5.5620
Penumbra	8.4686×10^{-3}	1.8048

Table 3.3 Frequency shifts $\Delta\nu$ ($=\nu(B)-\nu(0)$) for a representative pair of modes in the two cases of a quiet Sun type chromosphere (see Table 3.1) and a penumbral type chromosphere (see Table 3.2). The assumed magnetic field has a strength of 0.003 T (30 G).

3.5 Physical Interpretation

3.5.1 Effects of an Isothermal Atmosphere.

In order to explain the effects discussed in the previous section it is useful to look first at the much simplified case of a wave incident on a region in which oscillatory motions become evanescent. Suppose the wave is propagating for $z>0$ and evanescent for $z<0$ such that an incident wave is completely reflected with some phase change dependent on the degree of evanescence. If y is the quantity supporting the oscillation then the situation outlined can be described mathematically by:

$$y=\begin{cases} A\,e^{\kappa z}\,e^{i\omega t}, & z<0, \\ \left(e^{ikz}+B\,e^{-ikz}\right)e^{i\omega t}, & z>0, \end{cases} \tag{3.86}$$

where A and B are simply constants. Then, assuming that y and its spatial derivative are continuous at z=0, conditions that are analogous to those used in the derivation of dispersion relation (3.33), it can be shown that

$$B=e^{i\psi},\quad \sin\psi=\frac{2k\kappa}{k^2+\kappa^2},\quad \cos\psi=\frac{k^2-\kappa^2}{k^2+\kappa^2}. \tag{3.87}$$

The "displacement" y is then given by (taking the real part)

$$y = 2\cos(\omega t + \psi/2)\cos(kz - \psi/2), \qquad z > 0. \tag{3.88}$$

Thus the wave is reflected with a total phase shift between incident and reflected parts of ψ. If $\kappa=0$, then the line z=0 is effectively a free boundary so that y will have a maximum there, i.e. $\psi=0$. In this case, the first node occurs at $z=\pi/2k$. On the other hand, $\kappa \to \infty$ represents, in the limit, a completely rigid wall, and for this case there are nodes at z=0 and π/k correspondin to $\psi=\pi$. For positive κ between 0 and ∞, it can be seen from (3.87) that ψ lies between 0 and π so that the position of the first node is given by

$$z_{node} = \frac{\pi + \psi}{2k}. \tag{3.89}$$

The parameter κ is a measure of the rigidity of the region z<0 in the sense that a rigid medium damps out wave motion more rapidly than a flexible one. Making the reflecting region less (more) rigid, corresponding to decreasing (increasing) κ, is seen from equation (3.89) to make the first node (i.e., the node that is closest to z=0) approach (recede from) the boundary and vice-versa. This is illustrated in Figure 3.17.

Increasing the value of the chromospheric temperature T_c has the effect of decreasing the chromospheric density (and thus the inertia) of the upper region. In other words, with increasing T_c the upper region becomes a less "rigid" reflector to waves approaching from below. On this basis it would be expected that the highest node should rise with increasing chromospheric temperature.

Figure 3.18 is a comparison of the eigenmodes for u_z in the cases of high (T_c=50,000 K) and low (T_c=4170 K) chromospheric temperatures. The mode presented is n=1, l=100. Here, only the region around the highest, and in this case only, node has been shown. It is clear that there is a rise of approximately 10 km in the node when the chromospheric temperature is increased from 4170 K to 50,000 K. Thus it would seem that the nodes, and hence the whole eigenfunction, moves up with increasing chromospheric temperature.

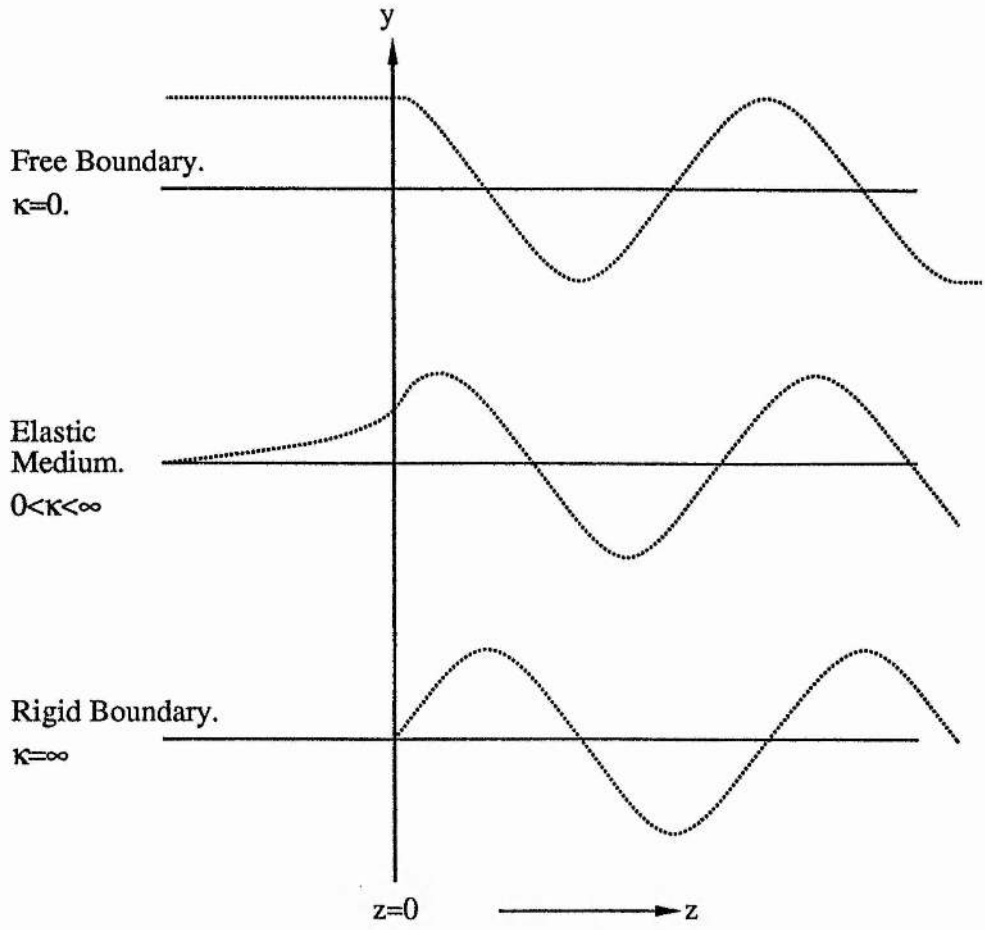

Figure 3.17. The behaviour of the standing wave pattern produced by the interference between an incident and a reflected wave for varying degrees of rigidity of the boundary. The rigidity is measured by the damping rate κ. It can be seen here that an increasing rigidity moves the node closest to the reflecting boundary further away.

For an acoustic wave in a polytropic medium it is possible to define a local vertical wavenumber k_z from the local dispersion relation:

$$k_z = \left(\frac{\omega^2}{c_s^2} - k_x^2 \right)^{\frac{1}{2}} = \left(\frac{\omega^2}{c^2 z / z_0} - k_x^2 \right)^{\frac{1}{2}}, \qquad (3.90)$$

where k_x and k_z are the wavenumbers in the x and z directions and c_s^2 is assumed to be equal to $c^2 z/z_0$, c being a constant and z_0 a characteristic vertical height dependent on the gradient of the sound speed: $(c_s^2)' = c^2/z_0$. Here, for simplicity, the sound speed has been taken to be

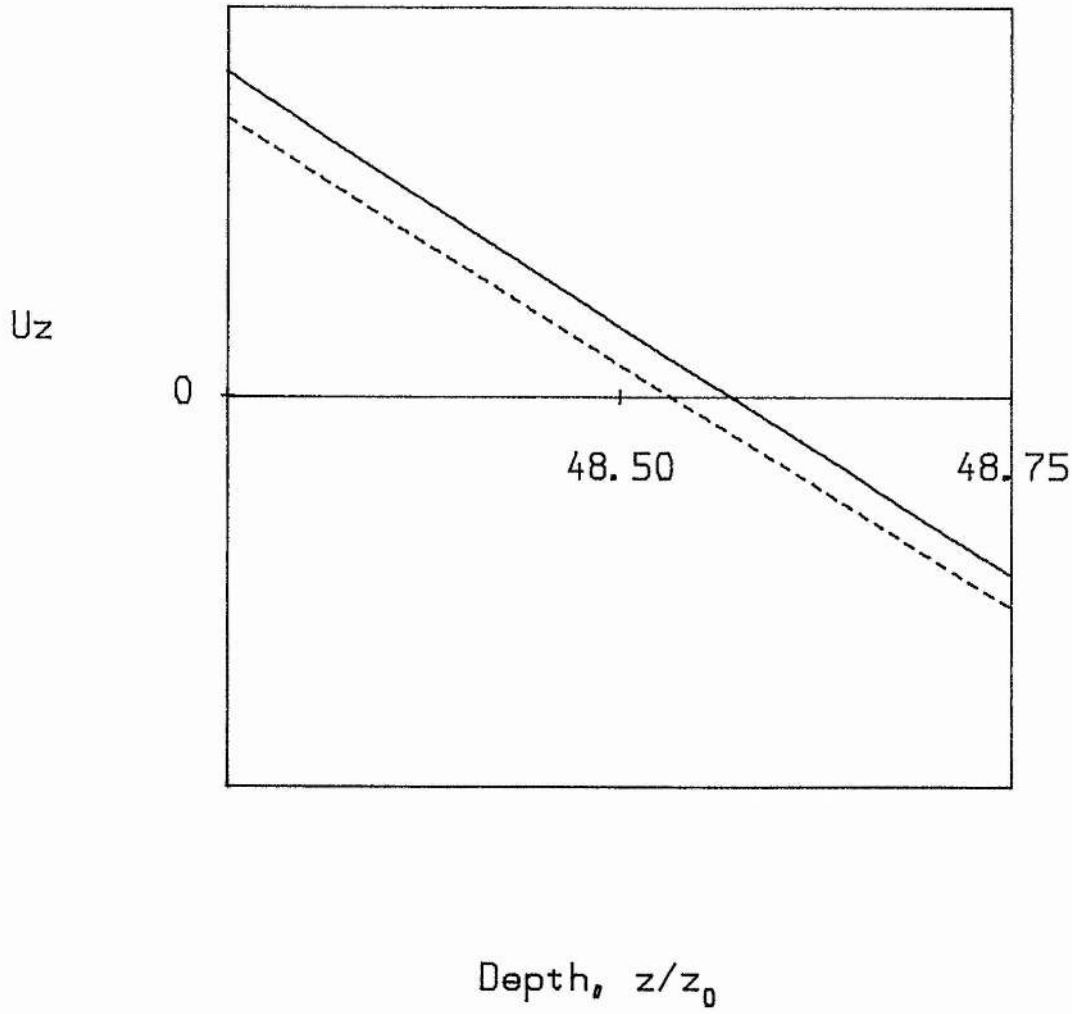

Figure 3.18. Vertical velocity component for the n=1, l=100 mode in the vicinity of the highest, and in this case only, node. The solid line has T_c=4170K while the dotted line is for T_c=50,000K. The value of z_0 is approximately 250 km, so we can see that this increase in temperature causes the first node to drop by about 10 km.

zero at z=0. The lower turning point of a trapped mode is the value of z where k_z vanishes. Denoting this by L, equation (3.90) shows that $L=z_0\omega^2/k_x^2c^2$. Now suppose that the upper turning point is at z=0 so that the wave is trapped between z=0 and z=L. Then the total phase α traversed by a wave crossing the cavity from z=0 to z=L is given by

$$\alpha = \int_0^L k_z \, dz = \frac{z_0\omega^2}{k_x c^2}\frac{\pi}{2} = k_x L \frac{\pi}{2} \quad . \tag{3.91}$$

It has been shown that increasing the chromospheric temperature T_c has the effect of raising the eigenfunction of the p-mode. This corresponds to a decrease, $-\delta L$, in the value of L and hence a corresponding decrease, $-\delta\alpha$, in α. From equation (3.91) it can be seen that this will cause a drop in frequency such that

$$\frac{\delta\alpha}{\alpha} = \frac{\delta L}{L} = 2\frac{\delta\omega}{\omega} = 2\frac{\delta\nu}{\nu} \quad . \tag{3.92}$$

In the case illustrated in Figure (3.18), the numerical solution of the dispersion relation (3.33) indicates that L≈20,000 km, δL≈10 km, ν =1.521 mHz and δν =3.5 μHz; thus, $\delta\nu/\nu=-2.3\times10^{-3}$. This is to be compared with the estimate provided by equation (3.92) which gives $\delta\nu/\nu=-2.5\times10^{-4}$. Thus (3.92) gives a frequency change that is of the correct sign but it underestimates the magnitude of the change. However, since the physics embodied in equation (3.91) takes no account of how non-vertical propagation and movement of the *upper* turning point affects matters, this seems a quite reasonable result.

The fact that the frequency decreases with a rise of the eigenfunction reflects the fact that the sound speed increases with depth. As the eigenfunction rises it no longer samples the lower regions where the waves propagation speed is highest. Both the frequency of p-modes for a given value of *l*, and the depth of the lower turning point increase as n increases. Consequently, the net effect of propagation through ever lower layers must be to increase the total transit time by a sufficiently small amount that causes the frequency to increase.

The f-mode is not a trapped mode in the normal sense, though it can be regarded as

being in a cavity of zero length (the upper and lower turning points coincide). However, it is more useful to look at it as a surface mode. For the model with no magnetic field, the f-mode, with frequency given by $\omega^2 = gk$, has vertical velocity of the form

$$u_z \propto e^{-kz} \quad , \qquad \text{provided } k < \frac{\gamma_c g}{2c_{sc}^2} \quad . \qquad (3.93)$$

The condition on k is required to ensure that the kinetic energy density vanishes as $z \to -\infty$. Equation (3.11) indicates that the f-mode is incompressible ($\Delta=0$). Thus the degree of compressibility of the gas, i.e. the value of the sound speed or the temperature, will not affect the f-mode in any way. Essentially, the f-mode is driven by buoyancy forces which are proportional to density. Any changes in density, such as may arise from a change in chromospheric temperature, will change the buoyancy forces acting on an element of fluid in exact proportion to the change in that element's inertia. Thus the fluid element will experience the same accelerations. It is for this reason that in the absence of a magnetic field the f-mode retains the same dispersion relation, $\omega^2=gk$, whatever the temperature of the chromosphere.

3.5.2 Effects of the Magnetic Field

There are three main effects which the presence of the magnetic field introduces. Since the total pressure balance at the interface between the upper and lower regions must be maintained when the magnetic field is present, the gas pressure in the chromosphere is correspondingly reduced in comparison with the field-free case at the same temperature. Consequently, there is a reduction in the chromospheric density and hence in the "rigidity" to waves approaching from below. This tends to decrease the mode frequency in much the same way that an increase in chromospheric temperature does.

The second effect of a *uniform* magnetic field is that it introduces greater rigidity into the interface. To see this, suppose a field-free gas at uniform pressure p, is trapped between two infinite, plane-parallel, horizontal plates. If the lower plate is raised by a small amount δz, then there is a consequent increase in gas pressure δp given by

$$\frac{\delta p}{p} = -\frac{\delta z}{z} \quad , \tag{3.94}$$

where z is the original distance between the plates.

Suppose now that most of the gas is replaced with a uniform magnetic field B aligned parallel to the plates and of strength such that the magnetic pressure precisely matches the gas pressure p of the non-magnetic case. Again, the lower plate is raised but this time the change will be of magnetic pressure $p_m \equiv B^2/2\mu$. Within the assumptions of ideal MHD the total magnetic flux through an area normal to the field will be conserved, implying that $\delta B/B = -\delta z/z$, and so

$$\frac{\delta p_m}{p_m} = -2\,\frac{\delta z}{z}\,. \tag{3.95}$$

Thus it is clear that the magnetic field in the present model is more rigid than the gas since a given pressure perturbation causes a displacement in a field-free region which is twice that for a region permeated by a uniform field. The effect of the uniform field on the mode frequencies will be opposite to that for the simple increase in chromospheric temperature discussed in the previous section. On the basis of this effect it would be expected that the frequency of a given mode will increase with the strength of magnetic field. Indeed, as Figures 3.4-3.7 indicate, it appears to be the dominant effect.

The final significant influence that a magnetic field exerts is that of magnetic tension. The standing wave pattern established by the p- and f-modes takes the form of fluid sloshing back and forth between the nodes. This has the effect of bending the interface between the convection zone and the chromosphere in a sinusoidal pattern. In the presence of chromospheric magnetism there will be significant field line bending so that magnetic tension will become important.

To illustrate the effect of magnetic tension forces, imagine that a standing wave pattern of the form $\xi = a \cos kz \sin \omega t$, ξ being the vertical displacement, has been established and examine the motion of an element of fluid about z=0. In the absence of the magnetic field there is a restoring force $-f_0\xi$, which has been assumed to be proportional to the displacement in the vertical direction. Then the fluid elements exhibit simple harmonic

motion such that $\omega^2 = f_0/\rho$, where ρ is the density of the fluid element under consideration. For the f- and p-modes, $\omega^2 \approx (1+2n/m)gk$ and so it is assumed that $f_0 = \rho\, gk\, (1+2n/m)$.

The tension force due to a magnetic field B, bent with a radius of curvature r, is simply $B^2/\mu r$. In the case of the standing wave pattern, with a vertical displacement ξ, the radius of curvature at z=0 is $r = 1/(\xi k^2)$. Thus the equation of motion of the fluid element becomes

$$\rho\, \ddot{\xi} = -f_0\, \xi - \frac{k^2 B^2}{\mu}\, \xi \ , \tag{3.96}$$

with associated dispersion relation

$$\omega^2 = \frac{f_0}{\rho} + \frac{k^2 B^2}{\mu\rho} = gk\left(1 + \frac{2n}{m} + \frac{k^2 B^2}{\mu f_0}\right). \tag{3.97}$$

As a representative density it may be assumed that

$$\rho = k \int_0^{1/k} \frac{p_p}{RT_p}\left(1 + \frac{z}{z_0}\right)^m dz, \tag{3.98}$$

this being the average density of the fluid over a characteristic depth dependent on the horizontal wavelength. This expression thus uses a smaller depth for modes with large k which is desirable because these are the modes trapped in a narrow band near the photosphere. For small kz_0, equation (3.98) reduces to

$$\rho \approx \frac{p_p}{g z_0}\frac{1}{(kz_0)^m} \ . \tag{3.99}$$

Hence, equation (3.97) becomes

$$\Omega^2 \approx 1 + \frac{2n}{m} + \left(\frac{1}{1+2n/m}\right)\left(\frac{2\gamma_c}{\gamma_c + 2\beta}\right)(kz_0)^{m+1}, \tag{3.100}$$

which is in qualitative agreement with the asymptotic results (equations (3.55) and (3.74)) derived earlier.

The results for the chromosphere with a uniform field show that the field tends to increase the frequency of oscillation of all modes. It is thus not possible that the dominant effect of the magnetic field is simply the evacuation of the chromosphere. This will have some influence, but compared to other effects it must be insignificant.

Magnetic tension seems to be very significant. Indeed, for the f-mode (corresponding to n=0 in the above), equation (3.100) gives the correct frequency correction, save for one factor, when compared to equation (3.74). It seems likely, then, that the effects of magnetic tension , as outlined above, are crucial for the frequency shift experienced by the f-mode. It would be expected that magnetic pressure would exhibit a similar effect and this may possibly account for the missing factor. However, equation (3.100) indicates that for the p-modes the contribution of magnetic tension and pressure diminishes quite rapidly with increasing n. By contrast, the numerical solutions to the dispersion relation (3.33) indicate that quite the opposite occurs. Thus, it must be other physical effects, not incorporated in equation (3.100), which explains the p-mode behaviour.

The natural conclusion, within the effects discussed above, is that the p-mode frequency shift is due to the rigidity of the chromosphere introduced by the uniform magnetic field. This will cause the eigenfunctions to drop and hence the frequency to increase as the waves sample regions of higher phase speed. This must be the dominant effect for the p-modes, while the f-mode submits to the influence of magnetic pressure and tension as illustrated by (3.100).

It is interesting at this point to consider the results of the model described in Campbell and Roberts (1989), pertaining to a chromosphere in which the Alfvén speed is constant. Their calculations have been illustrated for purposes of comparison in Figures 3.2-3.7. Due to necessary scalings in presenting these graphs, not all the features of their modes are clear. The p-modes with $n \geq 2$ all show a magnetically induced frequency decrease when compared to the zero field results. This decrease grows in magnitude with l, n and B. The f-mode, however, shows the same behaviour as for the chromosphere with a uniform field. The frequency of the f-mode is always increased by the presence of the magnetic field though, as seen in Figures 3.2 and 3.3, the magnitude of the effect is much smaller than for the case of a uniform field. Also, the n=1 p-mode shows a somewhat hybrid behaviour as can be clearly

seen in Figure 6 of Campbell and Roberts (1989). For small values of l it shows a frequency increase smaller than, but otherwise similar to, the f-mode. However, for larger wavenumbers this trend is reversed and there is a frequency decrease more like the other p-modes.

It seems unlikely that the effect of magnetic rigidity of the chromosphere plays much part in the explanation of the p-mode frequency decreases. This would be quite reasonable in view of the magnetic structure in the chromosphere. For, in order to maintain a constant Alfvén speed in a gravitationally stratified isothermal atmosphere, it is necessary for the magnetic field strength to decrease exponentially with height. There is thus only a small layer close to the bottom of the chromosphere in which the field strength is relevant. A disturbance from below will tend to push this thin layer up and down but, since there is little resistance from above, there need not be any significant compression. In this way, an exponentially decreasing magnetic field offers little contribution to chromospheric rigidity.

For the constant Alfvén speed model the only significant effects will be magnetic tension and pressure reacting to the bending of field lines, and magnetic evacuation of the chromosphere. The latter will affect the p-modes by reducing their frequencies with increasing field strength. The f-mode will not be affected by this since it is not a wave trapped in a cavity. Instead, the effects described by equation (3.100) will dominate to produce a frequency increase. The effect is presumably weaker in this model than in the uniform field model due to the reduced effectiveness of the magnetic pressure of an exponentially decreasing magnetic field. As pointed out earlier, the effects described by equation (3.100) reduce in magnitude for increasing values of n. Thus, p-modes with $n \geq 2$ will be dominated by the evacuation of the chromosphere. The first p-mode will be affected partly by both evacuation and field line bending and this is presumably the reason for its hybrid behaviour.

The mechanisms described here give a reasonably good qualitative description of how a chromospheric magnetic field can affect the frequencies of the p- and f-modes. Armed with these ideas it is possible to obtain a rough idea of what effects any particular magnetic structure may have. A realistic magnetic profile will almost certainly be such that the Alfvén speed lies between a constant Alfvén speed, as in the model of Campbell and Roberts (1989),

and an exponentially increasing Alfvén speed, as in the model presented here.

The frequency of the f-mode is only affected by the field bending and results in corrections of the form of (3.100). Thus it can be expected that the f-mode will always suffer a frequency increase whatever the horizontal magnetic field profile of the chromosphere. The magnitude of the effect will vary from model to model but will always have the same sense. Thus the f-mode is an important test of whether chromospheric magnetic fields are significant in helioseismology. The effect of chromospheric magnetism on the p-modes is more model dependent. If the field is roughly constant, then the frequencies will increase. On the other hand, if the field declines with height, so as to give an Alfvén speed that is roughly constant, then the frequencies will mostly decrease. More realistic models will presumably give results somewhere between the two cases that have been examined.

3.6. Discussion

Since the model presented here does not take account of the detailed temperature structure of the convection zone and chromosphere it is not possible to predict the precise frequencies likely to be observed on the solar surface. It is only possible to bring out the qualitative effects that would be expected if chromospheric magnetism were indeed to be of importance to solar seismology. These effects may be clear from the observations, even if the exact frequencies do not match up.

As described in the previous section, the two models discussed here represent possible extremes of the actual chromospheric magnetism. The real Alfvén speed profile will lie between that for the uniform Alfvén speed model (UA) of Campbell and Roberts (1989) and the uniform field model (UB) given here. The physical interpretation of the results can give some idea of the results that might be expected for an intermediate model. It seems likely that the f-mode will always suffer an increase in frequency over its field-free value while the p-mode frequencies are more dependent on the precise details of the chromospheric magnetism.

The effects of chromospheric magnetism and high chromospheric temperatures has thus

far been studied separately. In the solar chromosphere both are likely to occur at the same time. Thus it is important to examine the combined effect. Figures 3.19 and 3.20 show the frequency shift as a function of chromospheric temperature (as in Figure 3.1 but here the f-mode and the first two p-modes are shown) with a field of 30 G present. Figure 3.19 shows the results for the uniform field and Figure 3.20 for the constant Alfvén speed model. The frequency shift is calculated as $\delta\nu=\nu(T_c)-\nu(T_c=4170\ K)$. These two figures show quite clearly that the combined effects of high chromospheric temperatures and magnetic fields are roughly the sum of the individual effects. The effect of the temperature is more marked for the UA model but otherwise the trends are much the same. Thus a high chromospheric temperature tends to moderate the effects for the UB model but increases the effects for the UA model.

It is quite evident that by simply varying the parameters determining the atmospheric structure a wide variety of p-mode frequency shifts can be generated. Add to this different field profiles and it is likely that, within reasonable bounds, magnetic chromospheres would be able to reproduce any desired pattern of frequency shifts. The one exception to this is the f-mode which seems likely to suffer only frequency increases. The magnitude of the effect will vary according to the model but the sense is always the same. This makes it a very distinctive feature of these models since the f-mode is commonly not affected by non-magnetic changes, as was seen in the case of variations in temperature in an unmagnetised atmosphere. Furthermore, the f-mode dispersion relation is known exactly for the case of a field-free standard model, being simply $\omega^2=gk$. Thus, it is possible to determine the variation from standard solar models quite simply in this case.

On the basis of the results of Figure 3.8 it would be expected that for high l values there should be an increase in frequency, due to a field $B_0=30$ G, of up to 10–15 μHz for the UB model and 1–2 μHz for the UA model. Lower frequency shifts would result from a smaller field strength and higher shifts for the field strengths associated with active regions (say $B_0=100$G). Such frequency shifts are close to the accuracy of present observations. Libbrecht and Kaufmann (1988) find an increase in frequency for the f-mode of the order of 13μHz for high values of l. This fits in quite well with the predictions of the UB model. However, it should be noted that residual errors in their data are of the same order. It will be

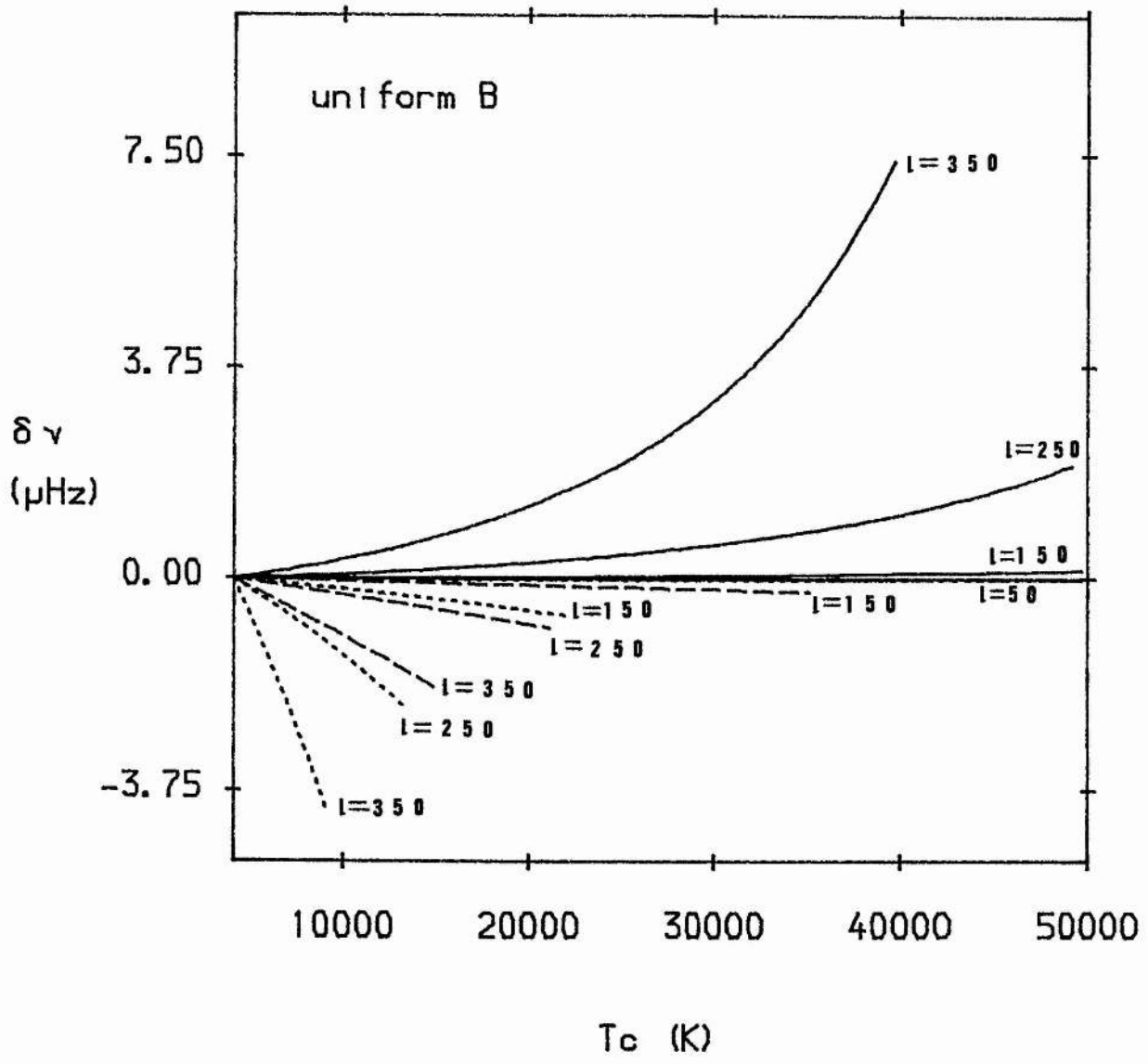

Figure 3.19. Variation of the frequency shift $\delta\nu=\nu(T_c)-\nu(T_c=4170\ K)$ as a function of the chromospheric temperature T_c, with a uniform magnetic field of $B_0=30$ G. Here the basic model parameters of Table 3.1 have been used. The f-mode and the first two p-modes are plotted for l=50, 150, 250, and 350. Solid lines denote the f-mode, dashed lines represent n=1 and dotted lines represent n=2. The magnitude of the effect increases monotonically with l for each radial order.

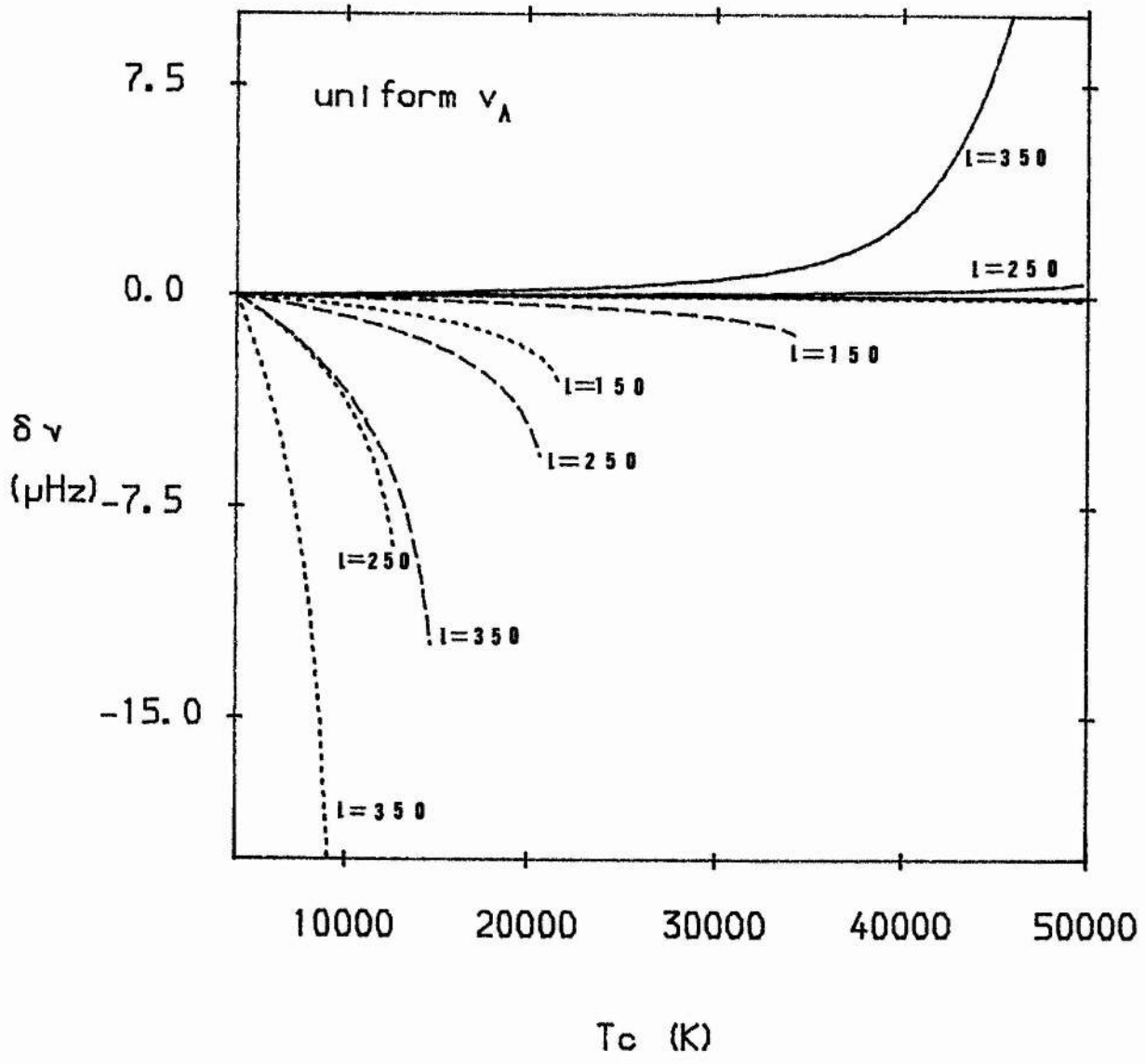

Figure 3.20. As for Figure 3.19 but here the uniform Alfvén speed model has been used instead.

interesting to see if this result remains after more sophisticated data reduction, currently being carried out. Nonetheless, the f-mode is a good indicator of the overall importance of chromospheric magnetic fields. In order to obtain more information on the field profile though, it is necessary to examine the p-modes in detail.

There are two ways in which the results calculated here could be tested against observations. Firstly, for modes with short horizontal wavelengths it may be possible to make measurements in two separate regions, one of the quiet Sun and the other in the vicinity of an active region. This would allow an examination of the differences in frequencies and eigenmodes which presumably reflect differences in magnetic field structure. The second possibility is to study variations in frequency over the solar cycle on the assumption that changes in activity levels lead to field strength changes in the chromosphere.

Over the surface of the Sun the chromospheric canopy field strength will vary according to the effective filling factor. In active regions it will be quite high (up to 100 G) while quiet regions will have fairly low field strengths (around 10 G or less). Thus, variations in field strength of an order of magnitude are not unexpected. Though most of this discussion has considered frequency shifts, it would be more accurate to refer to shifts in the dispersion relations of the p- and f-modes. This is important in considering how a p-mode may be affected by a field varying in strength from place to place.

For a spherically symmetric model of the Sun the acoustic waves that make up the p-modes propagate through the convection zone or below and reflect from the surface at intervals dependent on their horizontal wavelength. Clearly such a wave will at all times maintain the same frequency. The particular modes that are strongly detected are due to the constructive interference of these waves after travelling one circumference and returning to their point of origin.

Now suppose an acoustic wave is travelling along one of these typical ray paths (see Figure 3.21). At the first surface reflection it may experience an average magnetic chromosphere and be reflected back down to a lower turning point at $z=z_{av}$. At the next point of reflection at the surface it may experience a strong magnetic field, such as that surrounding an active region. This will cause the eigenfunction to shift downwards, as shown in Figure 3.18, and so the lower turning point $z=z_s$, following this reflection, will be

deeper than the turning point that occurred on reflection from a region of average field strength, i.e. $z_s > z_{av}$. Finally, the wave may encounter a region of weak field and will subsequently reach a depth $z=z_w$, such that $z_s > z_{av} > z_w$.

The effect of this will be to modulate the depth of penetration for the wave as it propagates around the Sun. Consequently, the distance between consecutive reflection points on the solar surface, and equivalently the horizontal wavelength, will be modulated around the Sun according to the strength of the chromospheric field. On average there can be no change in horizontal wavelength since for constructive interference the wave must have an exact integer number of reflections for each circuit of the Sun. However, if observations are restricted to a small region of the solar surface then the modulation of the horizontal wavenumber will become important. In particular, it would be interesting to compare k-ν power spectra for simultaneous observations in two neighbouring areas, one active and one quiet. If chromospheric magnetic fields are important then a difference in horizontal wavenumbers for a given mode should be detectable. The sense of the change would be as illustrated in Figure 3.21 for a UB type model but the opposite for a UA model.

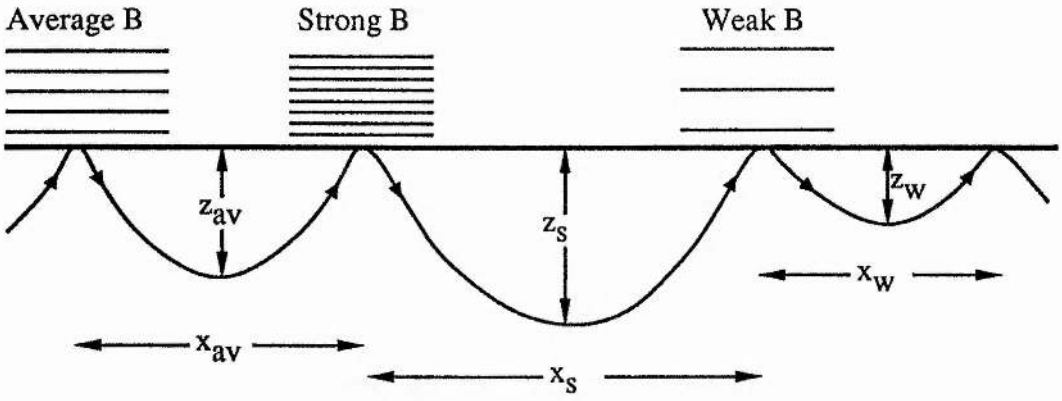

Figure 3.21 Progress of an acoustic wave through a region of the Sun in which the chromospheric magnetic field is inhomogeneous. The z values are the lower turning point depths and the x values are the distances between consecutive surface reflections. Here the case for a UB type model is shown and $z_w < z_{av} < z_s$, $x_w < x_{av} < x_s$.

Another interesting effect caused by the magnetic field in the chromosphere is the reduction in chromospheric amplitude of the eigenfunctions. In the absence of a

chromospheric field the vertical component of velocity increases exponentially with height in the chromosphere. In the presence of a magnetic field, however, much of the kinetic energy in the mode is sapped away in doing work against the magnetic field and so the amplitude of the motion is reduced. This is illustrated in Figure 3.22 which shows the n=1, l=100 mode in the field-free case and when fields of 10 G and 100 G are present. Such a reduction in amplitude has been observed around an active region (Tarbell et al, 1988) and in a plage region (Woods and Cram, 1981). Tarbell et al. (1988) find reductions in power of around 1/3-1/2 in the magnetic regions. Woods and Cram (1981) suggest that the magnetic field of the plage region they observed must be partly the cause of a 60% reduction in photospheric power there for oscillations with periods of about five minutes. Direct comparisons with the models used here is of little value due to their simplicity. Nevertheless the qualitative effect seems correct.

The second way in which chromospheric field strengths may vary is as part of the solar activity cycle. Since the report by Woodard and Noyes (1985) of a drop in the frequency of low degree p-modes, there has been considerable attention paid to the question of whether there are any significant variations over the solar cycle. Pallé et al (1986), Jefferies et al (1988) and Rhodes et al (1988) find no significant change in frequency between 1980/1 and 1984/5. Gelly et al (1986), Henning and Scherrer (1986), Fossat et al (1987), Woodard (1987) and Pallé, Régulo and Roca Cortes (1989) find decreases in the frequency of low degree modes between 0.3 and 0.4 μHz for the same period. Isaak et al (1986) supports the result of Woodard and Noyes (1985) but also finds an *increase* of 0.18 μHz/year in low degree modes taken over a wider range of frequencies. Finally, considering intermediate l values, Duvall et al (1988), find that between 1981 and 1984/5 there is a *decrease* in frequency of up to 0.5 μHz but Rhodes et al. (1988) find a frequency *increase* of comparable magnitude.

Clearly no consensus view has yet been reached. For this to emerge it may prove necessary to await systematic programmes of observations over an entire solar cycle. Nonetheless, from a theoretical viewpoint, the calculations presented here suggest that frequency changes may occur as the mean field strength in the chromospheric canopy changes over the solar cycle. It has been shown that frequency corrections due to canopy

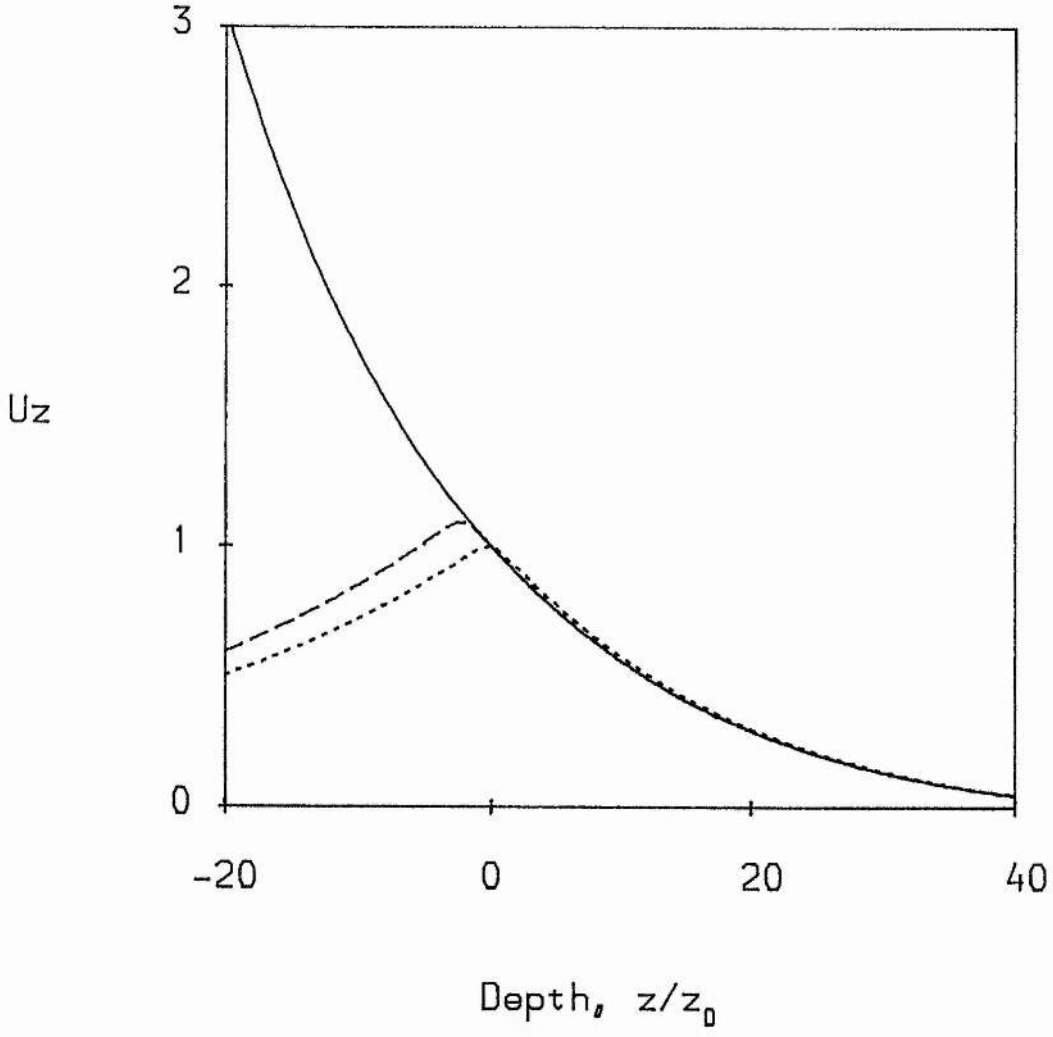

Figure 3.22 Plot of the vertical component of velocity, u_z, for the n=1, l=100 mode in the absence of any magnetic field (solid line), with a uniform chromospheric field of 10 G (dashed line) and a uniform chromospheric field of 100 G (dotted line). The units of u_z are such that $u_z(0)= 1$. The depth is given in units of z_0 (≈250km), z=0 being the temperature minimum. Atmospheric parameters are as in Table 3.1 with T_c=4170K.

fields for small values of l are virtually negligible, so it is not possible to draw conclusions from the presently reported observations (which are for low l and therefore likely to respond most to changes deep within the solar interior), with the exception of Duvall et al. (1988). For l =100 and n=20 the formula (3.55) predicts that a drop in a *uniform* canopy field from 10 G to 0 G causes a decrease in frequency of approximately 1 μHz, which agrees with Duvall et al. (1988) quite reasonably, suggesting that this model may be the more accurate. Alternatively, the results of Rhodes et al. (1988) would seem to indicate that the constant Alfvén speed model is more appropriate. It is impossible to decide at this stage but further study of intermediate and, more especially, high degree p-modes over the solar cycle may reflect the presence of canopy fields and possibly the form of field profile that exists in the chromosphere. Unfortunately these are the very modes for which frequencies are currently less accurately known, though developments in this area are about to take place (K. Libbrecht, 1989, private communication; J. W. Harvey, 1989, private communication).

Comparison between theoretically predicted and observed p-mode frequencies has indicated errors of 20 μHz or more, significantly larger than the observational accuracy (e.g. Christensen-Dalsgaard et al 1988; Ulrich and Rhodes 1983; Dziembowski et al 1988; Duvall and Harvey 1983). Since the effects of chromospheric fields are only significant for intermediate and high degree modes, the disparities for low values of l, which tend to be of a slightly different character, will here be ignored. It is probably true that such disparities are due to small errors in the description of the plasma of the convection zone. A sophisticated equation of state for such a plasma has been used by Christensen-Dalsgaard, Dappen and Lebreton (1988) to calculate theoretical p-mode frequencies. This has the effect of considerably reducing the discrepancies for low l modes.

Libbrecht (1988) compares observed frequencies from Duvall et al (1988) with the theoretical results of Christensen-Dalsgaard (1982). These theoretical results are obtained assuming magnetic effects are negligible. For l =100 it is found that the theoretical frequencies are too high for large n (n>8), whilst the opposite is true for small n. If this disparity is assumed to be due to chromospheric magnetic fields, then the reported difference suggests a field profile more like that of the UA model with the hybrid frequency shifts for low n, though there is not an exact match. This suggests that an Alfvén speed profile that

increased linearly with height, say, might provide a frequency shift of the appropriate form to explain the discrepancy. There are bound to be other effects at work too, making the overall picture somewhat confused.

Figure 3b of Christensen-Dalsgaard, Dappen and Lebreton (1988), reproduced overleaf, indicates the form of the normalised frequency error as a function of ν. Figures 3.11 and 3.12 show similar plots, though not normalised, for the uniform B model, while Figures 3.13 and 3.14 show the same for the constant Alfvén speed model. On this basis, it would seem that the sign of the frequency shift is consistent with that given by the constant Alfvén speed model, but the magnitude of the effect is better represented by the constant magnetic field model. Once again, then, it may be that an intermediate field profile, or possibly the addition of effects of high chromospheric temperatures, would give the desired result.

3.7. Summary

The dispersion relation describing p- and f-modes in a polytropic convection zone surmounted by an isothermal chromosphere, which is permeated by a uniform horizontal magnetic field, has been derived in some generality. This relation is complicated but it has proved possible to solve it asymptotically in the long wavelength limit and numerically for general wavenumbers.

The results of these calculations clearly show that the effect of the magnetic field is to increase the frequency of all modes. The amount of the increase grows with field strength B, horizontal wavenumber k and vertical order n. A model atmosphere representing a low, penumbral type chromosphere makes clear that it is the ratio of gas pressure to magnetic pressure, as measured by the plasma β, that is important rather than the absolute field strength. These results have been compared with an earlier model (Campbell and Roberts, 1989) in which the magnetic field was assumed to have a structure which gave a uniform Alfvén speed in the chromosphere. The results of this latter model show that the frequency shifts are less pronounced and, except for the f-mode and the first p-mode at small and intermediate l, are of opposite sense.

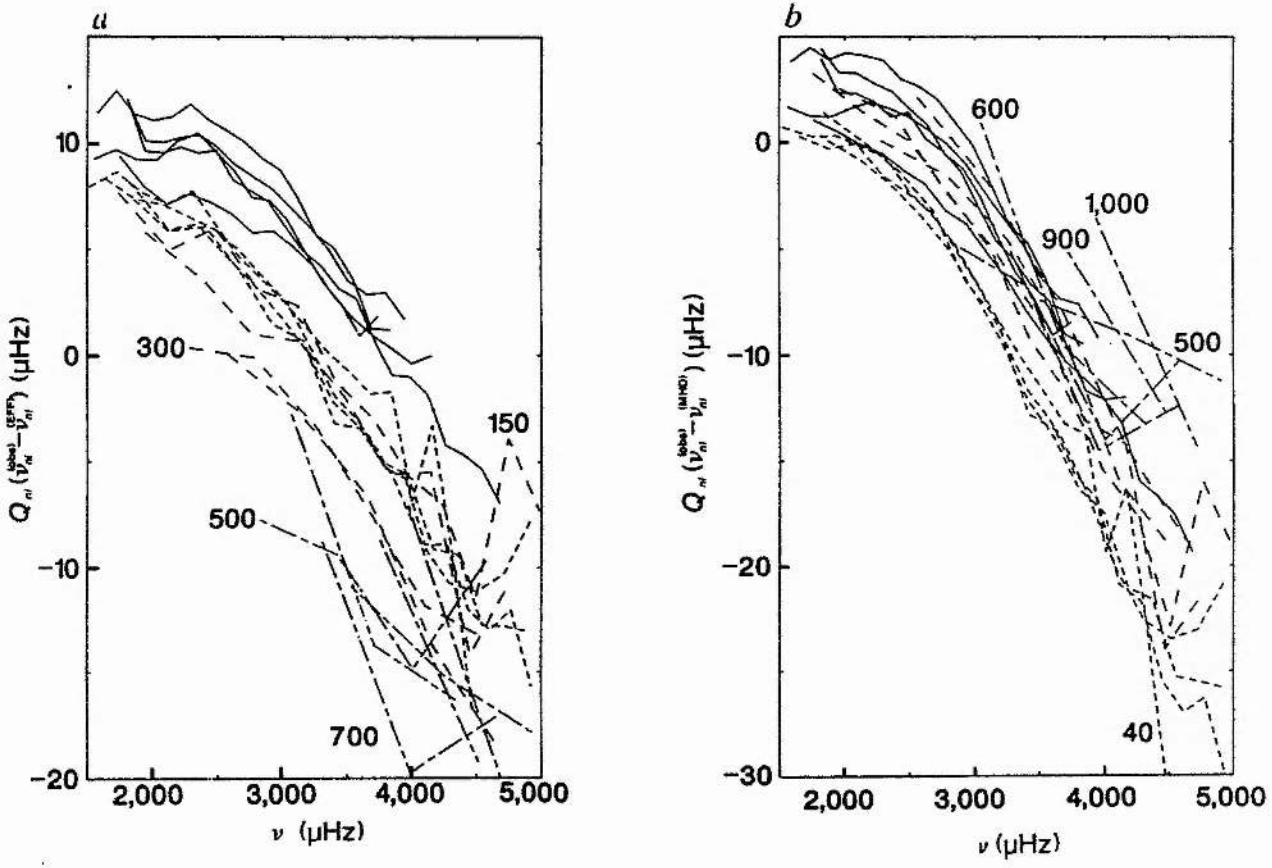

Fig.3 Scaled differences $Q_{nl}(\nu_{nl}^{(obs)} - \nu_{nl}^{(EFF)})$ between observed frequencies and frequencies computed for the EFF model (*a*), and the corresponding scaled differences $Q_{nl}(\nu_{nl}^{(obs)} - \nu_{nl}^{(MHD)})$ for the MHD model (*b*). The key is the same as that for Fig. 2.

A physical explanation of these effects has been put forward. The f-mode is primarily affected by the bending of magnetic field lines which introduces an extra restoring force causing the frequency of oscillation to increase. The p-modes, however, are trapped in a cavity not unlike an organ pipe. In this case frequency changes occur because of changes in the rigidity of the reflecting boundary at the chromosphere. Increasing the chromospheric temperature makes this region more flexible and this reduces the oscillation frequency. The presence of a magnetic field which falls off rapidly with height has a similar effect, while a uniform field causes the chromosphere to become more rigid and this increases frequencies.

The effects outlined here are of likely significance for solar observations; indeed it should be possible to observe frequency increases for the f-mode. Such an increase may already have been seen by Libbrecht and Kaufmann (1988), though problems of data reduction make this presently unclear. Also, a comparison of simultaneous observations of oscillations in quiet and active regions should show variations in horizontal wavenumber. The strength of the chromospheric field is likely to vary over the solar cycle. This should be apparent in variations over a cycle of p-mode frequencies for high and intermediate l modes. Observations of such effects have been made by Duvall et al. (1988) and Rhodes et al. (1988) but unfortunately they disagree as to the sense of the change in frequency. Finally, the discrepancies between the frequencies predicted by standard solar models and those observed on the Sun indicate that if the deficit is to be made up by the influence of a magnetic chromosphere then a model like that of Campbell and Roberts (1989) would be preferred though it is difficult to see how this could give the required magnitude of frequency change.

Appendix 3

The equilibrium atmosphere is given by equations (3.1)-(3.5). Linear analysis of the perturbations about this equilibrium, which are described by equations (3.6)-(3.9), and elimination of the pressure, density and magnetic field leaves two, coupled p.d.e.s for u_x and u_z. The Fourier analysis then reduces these to two coupled o.d.e.s:

$$(\omega^2 - k^2 c_s^2)\, u_x - i\,k\left(c_s^2 \frac{du_z}{dz} + g u_z\right) = 0, \qquad \text{(A3.1)}$$

$$(\omega^2 - k^2 v_A^2) u_z + (v_A^2 + c_s^2)\frac{\rho_0'}{\rho_0}\frac{du_z}{dz} + \frac{d}{dz}\left((v_A^2 + c_s^2)\frac{du_z}{dz}\right)$$

$$+ i\,k\left(g u_x + c_s^2 \frac{\rho_0'}{\rho_0} u_x + \frac{d}{dz}(c_s^2 u_x)\right) = 0, \qquad \text{(A3.2)}$$

where $'$ denotes d/dz. Elimination of u_x between these two equations then gives the governing equation (3.10).

When the magnetic field, B_0, is equal to 0, equation (A3.1) remains valid and (A3.2) reduces to

$$\omega^2 u_z + c_s^2 \frac{\rho_0'}{\rho_0}\frac{du_z}{dz} + \frac{d}{dz}\left(c_s^2 \frac{du_z}{dz}\right) + i\,k\left(g u_x + c_s^2 \frac{\rho_0'}{\rho_0} u_x + \frac{d}{dz}(c_s^2 u_x)\right) = 0. \qquad \text{(A3.3)}$$

Now introduce Δ=div **u**:

$$\Delta = \operatorname{div} \mathbf{u} = -i\,k u_x + \frac{du_z}{dz}, \qquad \text{(A3.4)}$$

or rearranging,

$$i\,k u_x = \frac{du_z}{dz} - \Delta. \qquad \text{(A3.5)}$$

Substitution of (A3.5) for u_x in (A3.1) then gives equation (3.11). Substitution of (A3.5) for u_x in (A3.3), using (3.11) to eliminate du_z/dz and using

$$c_s^{2\prime} = \gamma g - c_s^2 \frac{\rho_0'}{\rho_0}, \qquad \text{(A3.6)}$$

then gives equation (3.12).

The linearised form of the induction equation (3.8) is

$$\frac{\partial \mathbf{B}}{\partial t} = (\mathbf{B}_0.\nabla)\,\mathbf{u} - \mathbf{B}_0\,(\nabla.\mathbf{u}). \tag{A3.7}$$

Here $\mathbf{B}_0 = B_0\mathbf{e}_x$, $\mathbf{e}_x$ being the unit vector in the x-direction. Thus, the x-component of (A3.7) is

$$\frac{\partial B_x}{\partial t} = -\,B_0\,\frac{\partial u_z}{\partial z}, \tag{A3.8}$$

which, on Fourier decomposing, becomes

$$i\,\omega\,B_x = -\,B_0\,\frac{du_z}{dz}. \tag{A3.9}$$

Now, the magnetic energy density of the perturbation is

$$E_B = \mathbf{B}_0.\mathbf{B}/\mu = \frac{B_x\,B_0}{\mu}. \tag{A3.10}$$

Hence, (A3.9) immediately gives equation (3.24).

4. Chromospheric Effects on the Frequencies of p- and f-modes and their Sensitivity to Variations in Magnetic Canopy Heights.

4.1 Introduction

In the previous chapter it was shown that a magnetic field in the chromosphere could have a significant influence on fluid motions in the photosphere. This was made clear by the way in which a uniform magnetic field can influence the frequencies of p- and f-modes. The simplicity of the model employed in that discussion places a limitation on the atmospheric parameters used to describe the chromospheric structure. It would be interesting to examine the effects that varying the height of the magnetic canopy while keeping the same convection zone structure may have on p- and f-mode frequencies. In the model described in chapter 3 this would not be possible. The only way that the effective height of the canopy can be changed is by moving the level at which the temperature changes from varying linearly with height to being constant. Clearly, this changes the structure of the model convection zone and is of no use.

The primary motivation here is to assess how changes in magnetic canopy height can modulate the p- and f-mode frequency shifts associated with chromospheric magnetism. This is desirable because there is some uncertainty as to the level at which the canopy resides in the Sun. Detailed analysis of ultraviolet spectral data has yielded an empirical structure for the solar atmosphere. A spherically symmetric model based simply on considerations of global energy balance produces a temperature structure which significantly underestimates the temperature derived from the spectral analysis (e.g. Gabriel, 1976). It has been proposed that this dilemma could be resolved by employing an inhomogeneous atmosphere created by the presence of magnetic flux originating from the intense flux tubes in the lanes between supergranules. Energy balance is then applied in relative isolation to the individual regions demarcated by the flux tubes.

Gabriel (1976) made the first successful attempt to produce a model atmospheric configuration; see the illustration in Figure 1.1 of Chapter 1. This was a simple magnetohydrostatic calculation incorporating energy balance in each flux tube seperately from the surrounding atmosphere. Using a numerical solution to the relevant equations Gabriel was able to match the observed spectral emission measure for temperatures over 2×10^5 K. The canopy, or merging, height (the height at which the outer field lines from adjacent flux tubes meet) for these models was found to be around 1500 km above the photosphere. This is equivalent to around 1000 km above the the temperature minimum. The model used in the previous chapter placed the base of the canopy at the temperature minimum. This discrepancy is may be quite serious.

Observational measurement of canopy heights was first carried out by Giovanelli (1980) and later in more detail by Giovanelli and Jones (1982) and Jones and Giovanelli (1983). Their findings are that canopy heights are generally between 400 km and 800 km above the photosphere. Close to active regions it can be as low as 200 km and in the weak field regions as high as 1000 km. However, there is little doubt that, on average, there is a discrepancy of up to 1000 km between theory and observation. Jones and Giovanelli (1983) found magnetic field strengths in the canopy between 5 G and 25 G in various regions but indicate that there seems little variation in canopy height as a function of B.

Recently, Solanki and Steiner (1989) have proposed that the carbon monoxide molecule may play an important part in the structuring of the atmosphere outside of magnetic flux tubes. The formation of CO can cause a thermal instability which makes the field free atmosphere above the temperature minimum cooler than might otherwise be expected. This reduces the gas pressure and hence allows magnetic flux tubes to fan out very rapidly creating a lower canopy base. They also find that for small photospheric filling factors (the ratio of areas of strong magnetic flux to field free regions) the canopy height becomes fairly constant. This work may explain the difference between previous theoretical models and the observations outlined above.

Nevertheless, the uncertainty in canopy height is a major factor in assessing how strong

the influence of the magnetic chromosphere on p-mode frequencies might be. Because the characteristic density scale height is only about 100 km near the photosphere, a degree of uncertainty in the canopy height of the order of 1000 km, evident in the discussion above could be critical. It is for this reason that the effects of variations in the canopy height will be investigated here. Also, the more flexible model to be described here can more readily be used to investigate how strong magnetic canopy fields might affect p-modes. Such fields arise close to active regions and are likely to lie quite low down in the solar atmosphere.

4.2 Model and Dispersion Relations

The model of the previous chapter is generalised quite simply by adding an extra layer in the atmosphere between the top of the convection zone and the bottom of the chromosphere. This layer is taken to be isothermal and field free so that the atmospheric structure is as shown in Figure 4.1. This figure also shows a comparison with the H.S.R.A. model atmosphere (Gingerich et al., 1971). The three layer model to be used in the calculations has been calibrated to agree with H.S.R.A. at a point 200 km above the photosphere (τ_c=1) and at the temperature minimum. The lower point corresponds to the lowest canopy heights observed by Giovanelli and Jones (1982).

4.2.1 Uniform Magnetic Field

The three layers of this model are delineated by the temperature which is given by:

$$T_0(z) = \begin{cases} T_p(1 + z/z_0), & z>0, \\ T_m, & -z_c<z<0, \\ T_c, & z<-z_c. \end{cases} \qquad (4.1)$$

T_m is the constant temperature of the middle region and z_c is the height of the magnetic canopy. All other notation is as in Chapter 3. For the uniform field model the magnetic

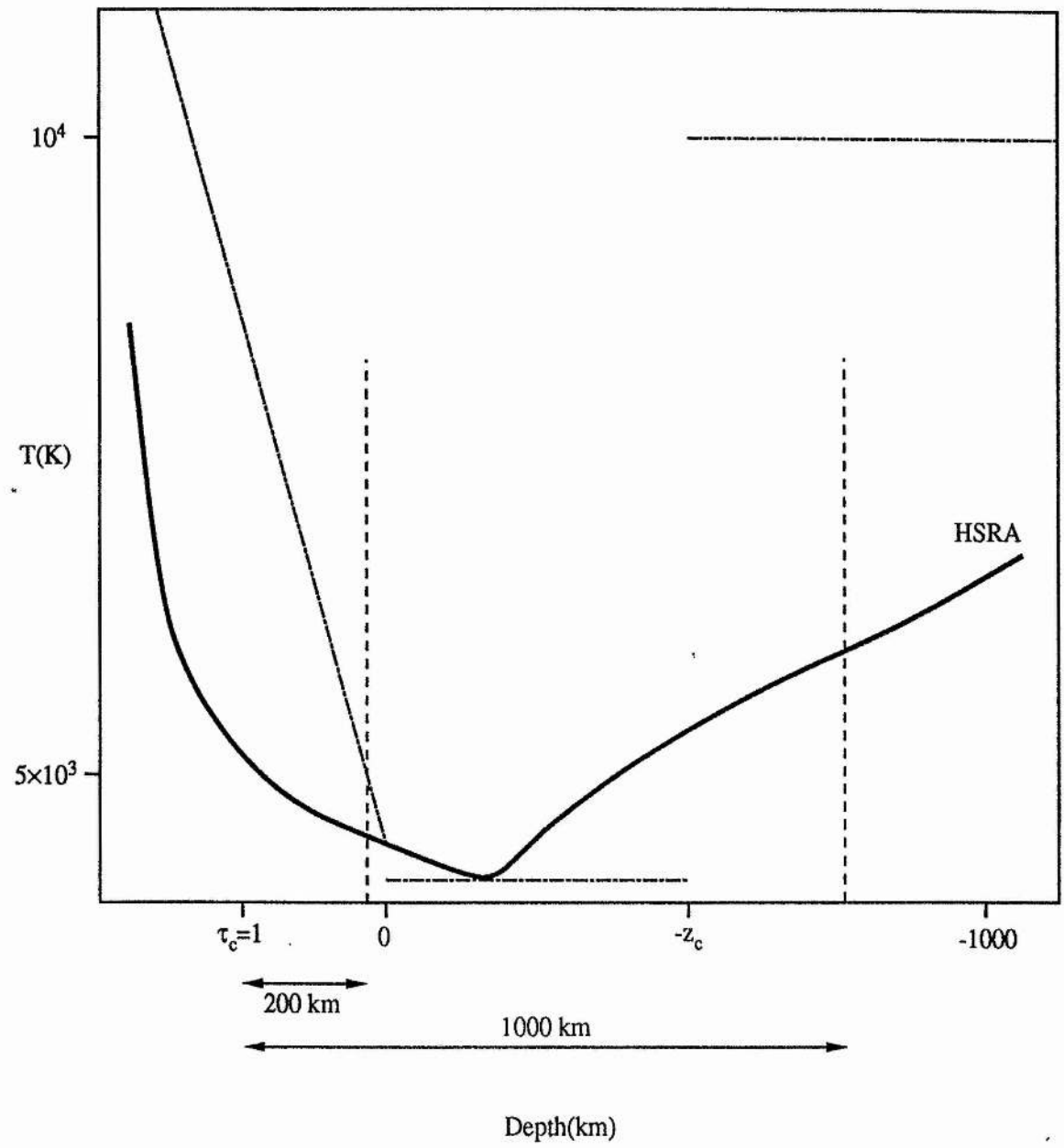

Figure 4.1. A comparison of the temperature structure of the simple model atmosphere (dashed-dotted line) employed in the calculations here, with H.S.R.A. (thick solid line). this shows how the parameter z_c, used here, relates to the canopy heights measured relative to the photosphere (τ_c=1). The vertical dashed lines indicate the range of chromospheric canopy heights observed by Giovanelli and Jones (1982). The magnetic field is zero except for $z<-z_c$.

field strength is given by

$$B(z) = \begin{cases} 0, & z>-z_c, \\ B_0, & z<-z_c, \end{cases} \tag{4.2}$$

B_0 being a constant.

Applying equations (3.2) and (3.3) for the equilibrium structure gives

$$p_0(z) = \begin{cases} p_p(1 + z/z_0)^{m+1}, & z>0, \\ p_p \exp(z/H_m), & -z_c<z<0, \\ p_c \exp([z + z_c]/H_c), & z<-z_c, \end{cases} \tag{4.3}$$

and

$$\rho_0 = \begin{cases} \dfrac{p_p}{RT_p}(1 + z/z_0)^m, & z>0, \\ \dfrac{p_p}{RT_m}\exp(z/H_m), & -z_c<z<0, \\ \dfrac{p_c}{RT_c}\exp([z + z_c]/H_c), & z<-z_c, \end{cases} \tag{4.4}$$

where

$$H_m = \frac{RT_m}{g}, \quad H_c = \frac{RT_c}{g}, \quad p_c = p_p e^{-z_c/H_m} - \frac{B_0^2}{2\mu}.$$

Balance of total pressure (gas plus magnetic) across the interface $z=z_c$ implies a maximum value for the magnetic field since p_c, the gas pressure at the base of the chromosphere ($z<-z_c$), must be positive. Hence $B_0<B_{max}$, where

$$B_{max} = \left(2\mu p_p \, e^{-z_c/H_m}\right)^{\frac{1}{2}}. \tag{4.5}$$

The analysis for the convection zone (z>0) is exactly as given in Chapter 3. Hence the solution in the region z>0 is given by

$$(\omega^4 - g^2k^2)\, e^{k(z+z_0)}\, u_z =$$

$$C_1 \left(\left[kc_s^2(\omega^2+gk) - \gamma_p g\omega^2 \right] U(-a, m+2, 2k[z+z_0]) \; - 2a\omega^2 c_s^2 k \; U(-a+1, m+3, 2k[z+z_0]) \right), \tag{4.6}$$

where C_1 is a constant. For the middle region ($-z_c<z<0$) the governing equation (3.10) is reduces to

$$\frac{d^2u_z}{dz^2} + \frac{1}{H_m}\frac{du_z}{dz} + A\,u_z = 0, \tag{4.7}$$

where

$$A = \frac{(\gamma_m - 1)g^2k^2 + \omega^2(\omega^2 - k^2c_{sm}^2)}{\omega^2 c_{sm}^2}, \quad c_{sm}^2 = \gamma_m R T_m;$$

γ_m is the adiabatic index for the middle region and c_{sm} is the local sound speed. All the coefficients in (4.7) are constants so that a solution is readily obtained:

$$u_z = e^{-z/H_m}\left(C_2 \exp\left[\frac{z\sqrt{1-4AH_m^2}}{2H_m} \right] + C_3 \exp\left[-\frac{z\sqrt{1-4AH_m^2}}{2H_m} \right] \right), \tag{4.8}$$

C_2 and C_3 being constants.

For a uniform magnetic field in the chromosphere ($z<-z_c$) the analysis of the previous chapter in this case gives the solution

$$u_z = C_4\, e^{kz}\, F\left(p,\, q,\, r,\, -\frac{A_1}{A_2} e^{(z+z_c)/H_c}\right), \tag{4.9}$$

with C_4 a constant and all other terms as previously defined (see equations (3.19)-(3.27) in Chapter 3). The only difference in this solution compared to the version in chapter 3 is that the extra layer of the present model has vertically translated z by z_c.

As before, the vertical velocity component u_z is required to be continuous everywhere. Hence, after integrating the ordinary differential equation it is also necessary that the expression (3.31), given in the last chapter, be continuous everywhere. These two conditions applied at $z=0$ and $z=-z_c$ yield four equations for C_1-C_4 and elimination between these leads to the dispersion relation which generalises equation (3.32).

Continuity of u_z at $z=-z_c$ implies

$$e^{z_c/H_m}\left(C_2 E^{-1} + C_3 E\right) = C_4\, e^{-kz_c}\, F(p,\, q,\, r,\, -\Xi), \tag{4.10}$$

where

$$E = \exp\left(\frac{z_c\sqrt{1-4AH_m^2}}{2H_m}\right), \quad \Xi = \frac{\omega^2 c_{sc}^2}{v_{Ac}^2(\omega^2 - k^2 c_{sc}^2)}.$$

Continuity of (3.31) at $z=-z_c$ requires that

$$\frac{\omega^2 - k^2 c_{sc}^2}{\omega^2 - k^2 c_{sm}^2}\frac{\rho_{mc}}{\rho_c}\frac{c_{sm}^2}{c_{sc}^2}\, e^{z_c/2H_m}\left(C_2\alpha_2 E^{-1} + C_3\alpha_3 E\right)e^{kz_c} =$$

$$C_4\left(k\left[1+\frac{1}{\beta}\right]\left[\omega^2 - k^2 c_{Tc}^2\right] + gk^2\right)F(p,\, q,\, r,\, -\Xi) - \tag{4.11}$$

$$\frac{pq}{r}\gamma_c g\omega^2 \frac{(1+1/\beta)(\omega^2 - k^2 c_{Tc}^2)}{v_{Ac}^2(\omega^2 - k^2 c_{sc}^2)} F(p+1, q+1, r+1, -\Xi)\, C_4,$$

where

$$\rho_c = \frac{p_c}{RT_c}, \quad \rho_{mc} = \frac{p_p}{RT_m} e^{-z_o/H_m}, \quad \beta = \frac{c_{sc}^2}{v_{Ac}^2},$$

$$\alpha_2 = gk^2 + \frac{\omega^2}{2H_m}\left(\left[1 - 4AH_m^2\right]^{\frac{1}{2}} - 1\right), \qquad \alpha_3 = gk^2 - \frac{\omega^2}{2H_m}\left(\left[1 - 4AH_m^2\right]^{\frac{1}{2}} + 1\right).$$

Then, dividing (4.11) by (4.10) gives

$$\frac{\alpha_2 C_2 E^{-1} + \alpha_3 C_3 E}{C_2 E^{-1} + C_3 E} = \frac{\gamma_o/\gamma_m}{\Re_B}, \tag{4.12}$$

where

$$\Re_B = \frac{\left[(2\beta + \gamma_c)/2\beta\right]\left[(\omega^2 - k^2 c_{sc}^2)/(\omega^2 - k^2 c_{sm}^2)\right]}{\left(k\left[1+1/\beta\right]\left[\omega^2 - k^2 c_{Tc}^2\right] + gk^2\right) - \frac{pq}{r}\gamma_c g\omega^2 \frac{(1+1/\beta)(\omega^2 - k^2 c_{Tc}^2)}{v_{Ac}^2(\omega^2 - k^2 c_{sc}^2)} \frac{F(p+1, r+1, q+1, -\Xi)}{F(p, q, r, -\Xi)}}.$$

Similarly, the continuity conditions applied at z=0 require that

$$C_1\left(\left[kc_{sp}^2(\omega^2 + gk) - \gamma_p g\omega^2\right] U(-a, m+2, 2kz_0) - 2a\omega^2 c_{sp}^2 k U(1-a, m+3, 2kz_0)\right) =$$

$$(\omega^4 - g^2k^2)\, e^{kz_0}\, (C_2 + C_3)\,, \tag{4.13}$$

and

$$(\omega^2 - k^2 c_{sm}^2)\frac{\rho_p}{\rho_{mp}}\frac{c_{sp}^2}{c_{sm}^2} C_1 e^{-kz_0} U(-a, m+2, 2kz_0) = \alpha_2 C_2 + \alpha_3 C_3, \qquad (4.14)$$

where

$$\rho_p = \frac{p_p}{RT_p}, \quad \rho_{mp} = \frac{p_p}{RT_m}.$$

Then (4.13) divided by (4.14) gives

$$\Im = \frac{\omega^2 - k^2 c_{sm}^2}{\omega^2 - k^2 c_{sc}^2}\frac{\gamma_p}{\gamma_m}\frac{C_2 + C_3}{\alpha_2 C_2 + \alpha_3 C_3}, \qquad (4.15)$$

where

$$\Im = \frac{2a\omega^2 c_{sp}^2 k \dfrac{U(1-a, m+3, 2kz_0)}{U(-a, m+2, 2kz_0)} + \gamma_p g\omega^2 - k\omega^2 c_{sp}^2 - gk^2 c_{sp}^2}{(\omega^2 - k^2 c_{sc}^2)(g^2 k^2 - \omega^4)}.$$

Finally, elimination of C_2 and C_3 between equations (4.12) and (4.15) yields the dispersion relation

$$\Im = \frac{\omega^2 - k^2 c_{sm}^2}{\omega^2 - k^2 c_{sc}^2}\frac{\dfrac{\gamma_p}{\gamma_c}(\alpha_2 E^{-1} - \alpha_3 E) + \dfrac{\gamma_p}{\gamma_m}(E - E^{-1})/\Re_B}{\dfrac{\gamma_m}{\gamma_c}\alpha_2\alpha_3 (E^{-1} - E) + (E\alpha_2 - E^{-1}\alpha_3)/\Re_B}. \qquad (4.16)$$

Rewritten in dimensionless form, the dispersion relation is

$$2aK\Omega^2 \frac{U(1-a, m+3, 2K)}{U(-a, m+2, 2K)} + (m+1)\Omega^2 - (1+\Omega^2)K =$$

$$\frac{\gamma_c T_c}{\gamma_p T_p}\frac{\Lambda\Omega^2 - K/\eta}{\Lambda\Omega^2 - K}\frac{\dfrac{\gamma_p}{\gamma_c}(\bar{\alpha}_2 E^{-1} - \bar{\alpha}_3 E) + \dfrac{\gamma_p}{\gamma_m}(E - E^{-1})/\bar{\Re}_B}{\dfrac{\gamma_m}{\gamma_c}\bar{\alpha}_2\bar{\alpha}_3 (E^{-1} - E) + (E\bar{\alpha}_2 - E^{-1}\bar{\alpha}_3)/\bar{\Re}_B}(1 - \Omega^4). \qquad (4.17)$$

The terms used here are as in chapter 3 (see equation (3.33))with the addition of

$$E = \exp\left(\zeta_c\left[\frac{\gamma_m^2}{4}\eta^2\Lambda^2 - K\left\{\eta\Lambda\frac{\gamma_m - 1}{\Omega^2} - K + \eta\Lambda\Omega^2\right\}\right]^{\frac{1}{2}}\right),$$

$$\zeta_c = z_c/z_0, \quad \eta = c_{sc}^2/c_{sm}^2 ,$$

$$\overline{\alpha}_2 = 1 + \Omega^2\frac{\gamma_m}{2}\frac{\eta\Lambda}{K}\left(\left[1 - 4AH_m^2\right]^{\frac{1}{2}} - 1\right), \quad \overline{\alpha}_3 = 1 - \Omega^2\frac{\gamma_m}{2}\frac{\eta\Lambda}{K}\left(\left[1 - 4AH_m^2\right]^{\frac{1}{2}} + 1\right),$$

$$\overline{\mathfrak{R}}_B = \frac{(\Omega^2 - K/\Lambda)\,(\Omega^2 - K/\eta\Lambda)}{\dfrac{2\beta}{\gamma_c + 2\beta}\left(1 + \left[1 + \dfrac{1}{\beta}\right]\left[\Omega^2 - \dfrac{1}{1+\beta}\dfrac{K}{\Lambda}\right]\varphi\right)}.$$

Equation (4.17) is the generalisation of (3.33) due to the additional isothermal layer in the model atmosphere. Taking the limit $z_c \to 0$ puts the chromosphere directly on top of the convection zone as in chapter 3 and recovers the original dispersion relation (3.33). Also, letting $z_c \to \infty$ with fixed β gives the simple model with a field free isothermal atmosphere. In this limit equation (4.17) gives the dispersion relation quoted earlier as equation (3.80).

4.2.2 Uniform Alfvén Speed

A relation equivalent to (4.17) may be derived for a chromosphere with a uniform Alfvén speed. The temperature is again as given by (4.1). Then, solving the equations (3.2) and (3.3) gives the same solutions as (4.3) and (4.4) for $z > -z_c$ but otherwise it is found that

$$p_0 = p_c \exp\left(\frac{g(z + z_0)}{RT_c + v_{Ac}^2/2}\right), \qquad z < -z_c , \qquad (4.18)$$

$$\rho_0 = \frac{p_c}{RT_c}\exp\left(\frac{g(z+z_c)}{RT_c + v_{Ac}^2/2}\right), \qquad z<-z_c\,, \tag{4.19}$$

$$B = B_0 \exp\left(\frac{g(z+z_0)}{2RT_c + v_{Ac}^2}\right), \qquad z<-z_c\,, \tag{4.20}$$

where

$$v_{Ac}^2 = RT_c B_0^2/\mu p_c\,,$$

B_0 here being the magnetic field strength at the *base* of the chromosphere. Similarly, the solutions for u_z in the region $z>-z_c$ are still given by (4.6) and (4.8).

In the chromosphere ($z<-z_c$) c_{sc}^2 and v_{Ac}^2 are constant and so the governing equation for u_z reduces to (Campbell and Roberts, 1989)

$$\frac{d^2u_z}{dz^2} + \frac{1}{H_{cA}}\frac{du_z}{dz} + A_c\,u_z = 0, \tag{4.21}$$

where

$$H_{cA} = \frac{c_{sc}^2}{\Gamma g}\,, \quad \Gamma = \frac{2\beta\gamma_c}{2\beta+\gamma_c}, \quad A_c = \frac{(\Gamma-1)g^2k^2 + (\omega^2 - k^2v_{Ac}^2)(\omega^2 - k^2c_{sc}^2)}{(c_{sc}^2 + v_{Ac}^2)(\omega^2 - k^2c_{Tc}^2)}\,.$$

Then the solution with total energy density decaying with height is simply (Campbell and Roberts, 1989)

$$u_z = C_4 \exp\left(\frac{z}{2H_{cA}}\left[-1 + \left\{1 - 4A_cH_{cA}^2\right\}^{\frac{1}{2}}\right]\right), \tag{4.22}$$

The continuity conditions applied at z=0 clearly remain valid so that (4.15) still holds. At $z=-z_c$, however, continuity of the vertical velocity component u_z implies that

$$e^{z_c/2H_m}\left(C_2E^{-1}+C_3E\right)=C_4\,e^{z_c/2H_c}\exp\left(-\left[1-4A_cH_c^2\right]^{\frac{1}{2}}z_c/2H_c\right). \tag{4.23}$$

Similarly, continuity of (3.31) requires that

$$\frac{\omega^2-k^2c_{sc}^2}{\omega^2-k^2c_{sm}^2}\frac{\rho_{mc}}{\rho_c}\frac{c_{sm}^2}{c_{sc}^2}e^{z_c/2H_m}\left(C_2\alpha_2E^{-1}+C_3\alpha_3E\right)=$$

$$C_4\exp\left(\frac{-z_c}{2H_c}\left[-1+\left\{1-4A_cH_c^2\right\}^{\frac{1}{2}}\right]\right)\left(gk^2+\frac{(1+1/\beta)(\omega^2-k^2c_{Tc}^2)}{2H_c}\left[-1+\left\{1-4A_cH_c^2\right\}^{\frac{1}{2}}\right]\right). \tag{4.24}$$

Finally, following a procedure similar to that in the uniform magnetic field case yields the dispersion relation

$$\Im=\frac{\omega^2-k^2c_{sm}^2}{\omega^2-k^2c_{sc}^2}\frac{\frac{\gamma_p}{\gamma_c}(\alpha_2E^{-1}-\alpha_3E)+\frac{\gamma_p}{\gamma_m}(E-E^{-1})/\Re_A}{\frac{\gamma_m}{\gamma_c}\alpha_2\alpha_3(E^{-1}-E)+(E\alpha_2-E^{-1}\alpha_3)/\Re_A}, \tag{4.25}$$

where

$$\Re_A=\frac{2\beta+\gamma_c}{2\beta}\frac{(\omega^2-k^2c_{sc}^2)/(\omega^2-k^2c_{sm}^2)}{gk^2+\frac{(1+1/\beta)(\omega^2-k^2c_{Tc}^2)}{2H_c}\left[-1+\left\{1-4A_cH_c^2\right\}^{\frac{1}{2}}\right]}.$$

In dimensionless form this gives the same expression as (4.17) but with $\overline{\Re}_B$ replaced by $\overline{\Re}_A$, where

$$\overline{\Re}_A = \frac{2\beta + \gamma_c}{2\beta} \frac{(\Omega^2 - K/\Lambda)/(\Omega^2 - K/\eta\Lambda)}{1 + \left(1 + \frac{1}{\beta}\right)\left(\Omega^2 - \frac{1}{1+\beta}\frac{K}{\Lambda}\right)\Phi},$$

with

$$\Phi = \frac{\Gamma\Lambda}{2K}\left(-1 + \left[1 - 4A_c H_c^2\right]^{\frac{1}{2}}\right), \quad A_c H_c^2 = \frac{K}{\Gamma^2\Lambda} \frac{(\Gamma - 1) + \left(\Omega^2 - \frac{1}{\beta}\frac{K}{\Lambda}\right)\left(\Omega^2 - \frac{K}{\Lambda}\right)}{\left(\Omega^2 - \frac{1}{1+\beta}\frac{K}{\Lambda}\right)\left(1 + \frac{1}{\beta}\right)}.$$

4.3 Solutions to the Dispersion Relations

4.3.1 Asymptotic Solution

It is possible to derive an asymptotic solution to equation (4.17), valid for $kz_0 \rightarrow 0$, in exactly the same way as in the previous chapter. This will be useful so that a comparison with the equivalent solutions of Chapter 3 will allow a determination of what the additional effect of the extra layer in the model atmosphere might be. This additional effect is likely to be the same for both uniform field and uniform Alfvén speed variants and so it is expedient just to look at the one case. Here, the uniform field model will be examined asymptotically.

Firstly the p-modes will be examined. It is assumed that as $K \rightarrow 0$, $\Omega^2 \rightarrow \Omega_*^2$, as before, with $\Omega_*^2 \neq 0, \pm 1$. Then it is easy to show that

$$E \rightarrow E_* = \exp\left(\zeta_c \frac{\gamma_m \eta \Lambda}{2}\right), \tag{4.26}$$

$$\overline{\alpha}_2 \rightarrow \frac{1}{\gamma_m}(1 - \Omega_*^4), \qquad \overline{\alpha}_3 \sim -\Omega_*^2 \frac{\gamma_m \eta \Lambda}{K}, \tag{4.27}$$

$$\varphi \rightarrow 1 - \frac{\beta}{1+\beta}\left(1 + \frac{\gamma_c - 1}{\gamma_c}\frac{1}{\Omega_*^2} + \frac{\Omega_*^2}{\gamma_c}\right), \tag{4.28}$$

$$\overline{\Re}_B \to \overline{\Re}_{B*} = \frac{\gamma_c(\gamma_c + 2\beta)/2}{\beta(1-\Omega_*^4) + \gamma_c\Omega_*^2}, \tag{4.29}$$

as K→0. Thus the right hand side of the dispersion relation (4.17) has a well behaved limit as K→0, namely

$$\frac{(m+1)\,E_*^2(\gamma_c+2\beta)\,\Omega_*^2(1-\Omega_*^4)}{\left(\gamma_c\left[E_*^2-1\right]+2\beta E_*^2\right)(1-\Omega_*^4)+2\gamma_c\Omega_*^2}. \tag{4.30}$$

In order to expand the left hand side of (4.17) it is convenient to assume that

$$\Gamma(-a) \sim \theta_n(2K)^{-s}, \quad K \to 0, \tag{4.31}$$

so that expansions for a and Ω^2 are given by equations (3.47) and (3.48) for n>1. For n=1 the expansions (3.51)-(3.53) must be used. Then

$$\Im \to \begin{cases} 0, & s<m+1, \\ \Im_*, & s=m+1, \\ (m+1)\Omega_*^2, & s>m+1, \end{cases} \tag{4.32}$$

where

$$\Im_* = \Omega_*^2 \frac{(-1)^{n-1}(m+1)\,\Gamma(1+m+n)\,\theta_n}{(m+1)\left[\Gamma(m+1)\right]^2 + (-1)^{n-1}\Gamma(1+m+n)\,\theta_n}.$$

In just the same way as before an examination of the consequences of each of these three cases shows that only if s=m+1 are any sensible results obtained. With s=m+1, equating the limits for both sides of the dispersion relation gives an equation for θ_n which can be rearranged to yield

$$\theta_n = (-1)^{n-1} \frac{E_*^2(\gamma_c + 2\beta)(1-\Omega_*^4)}{2\gamma_c\Omega_*^2 - \gamma_c(1-\Omega_*^4)} \frac{(m+1)[\Gamma(m+1)]^2}{\Gamma(1+m+n)}. \tag{4.33}$$

Then the asymptotic solution for Ω^2 is

$$\Omega^2 \sim \Omega_*^2 + \frac{2\Gamma(1+m+n)\,\gamma_c\,((1-\Omega_*^4) - 2\Omega_*^2)\,E_*^{-2}}{\left(\frac{m+1}{\gamma_p} - \left[m - \frac{m+1}{\gamma_p}\right]\frac{1}{\Omega_*^4}\right)(n-1)!\Gamma(m+2)\Gamma(m+1)(\gamma_c+2\beta)(1-\Omega^4)} (2K)^{m+1}, \tag{4.34}$$

valid for n=1, 2, 3,... This gives the asymptotic solution for the p-modes with the added effect of the variable canopy height. The expression for Ω_*^2, given in equation (3.55), is reproduced here for convenience:

$$\Omega^2 \sim \Omega_*^2 + \frac{2\Gamma(1+m+n)\,\gamma_c\,((1-\Omega_*^4) - 2\Omega_*^2)}{\left(\frac{m+1}{\gamma_p} - \left[m - \frac{m+1}{\gamma_p}\right]\frac{1}{\Omega_*^4}\right)(n-1)!\Gamma(m+2)\Gamma(m+1)(\gamma_c+2\beta)(1-\Omega^4)} (2K)^{m+1}.$$

Comparison of (4.34) with the equivalent result (3.55) for the model without the field free isothermal middle layer shows that the difference is simply the factor E_*^{-2}. Rewriting E_* in dimensional form gives

$$E_* = e^{z_c/2H_m}, \tag{4.35}$$

H_m being the density scale height in the middle region of the atmosphere. Thus it is clear that the frequency shift due to the magnetism in the atmosphere decreases exponentially with the height of the canopy. For parameters typical of the temperature minimum, $H_m \approx 100$ km and so the frequency shift will decrease by a factor of ten with a change of canopy height of approximately 250 km, everything else being kept equal.

The asymptotic solution for the f-mode can also be calculated for this model. With the assumption that

$$\Omega^2 \sim 1 + r\,(2K)^s, \tag{4.36}$$

the expansions for the left hand side of the dispersion relation give the same result as before, namely that the asymptotic expansion for $K \to 0$ is (see equation (3.70) in Chapter 3)

$$O(K^3) + o(K^s) - \frac{(2K)^{m+1}}{\Gamma(m+1)} + o(K^{m+1}). \tag{4.37}$$

Now, however, the right hand side of the dispersion relation has the following expansion:

$$-2(m+1)E_*^2\, r \left(\frac{\gamma_c + 2\beta}{2\gamma_c}\right)(2K)^s + o(K^s). \tag{4.38}$$

Comparing (4.76) and (4.38) again implies that s=m+1, and then r can be obtained. The result is that for the f-mode

$$\Omega^2 \sim 1 + \frac{\gamma_c\, E_*^{-2}}{(\gamma_c + 2\beta)\Gamma(m+2)}(2K)^{m+1}. \tag{4.39}$$

Again, the effect of the middle region is to simply introduce the extra E_*^{-2} factor as for the p-modes.

4.3.2 Numerical Solutions

The dispersion relations (4.17) and (4.25) can be solved numerically in the same way as for the the simpler models of the previous chapter. This time though the main concern is how the frequencies vary as a function of z_c. For the basic atmosphere the parameters given in Table 3.2, representing a low lying canopy, have been used with suitable modifications for

the generalisation of the model. These are summarised in Table 4.1.

T_p	4460 K
T_m	4170 K
T_c	10,000 K
p_p	512.5 kg m^{-1} s^{-2}
γ_p, γ_c, γ_m	5/3
m	3/2
R	6425.97 m^2 s^{-2} K^{-1}
g	274.0 m s^{-2}
R_{sun}	6.96×10^8 m

Table 4.1. Parameters for the atmospheric model used in the numerical solution of the dispersion relations (4.17) and (4.25).

Two sets of data have been illustrated here. Figures 4.2-4.4 show the variation of mode frequency as z_c is increased from 0 to 600 km, keeping the magnetic field strength at the base of the chromosphere constant at 20 G. The modes shown are l=300 for the f-mode and the first two p-modes. Higher n modes follow the same pattern. Throughout the numerical results the behaviour of the mode concerned is given for a magnetic field which is uniform in the chromosphere (solid line), one which has a uniform Alfvén speed in the chromosphere (dotted line) and one in which there is no magnetic field (dashed line). For B_0 constant, the maximum permissible field strength at the base of the chromosphere, given by equation (4.5), is a decreasing function of the canopy height. The curves for the uniform

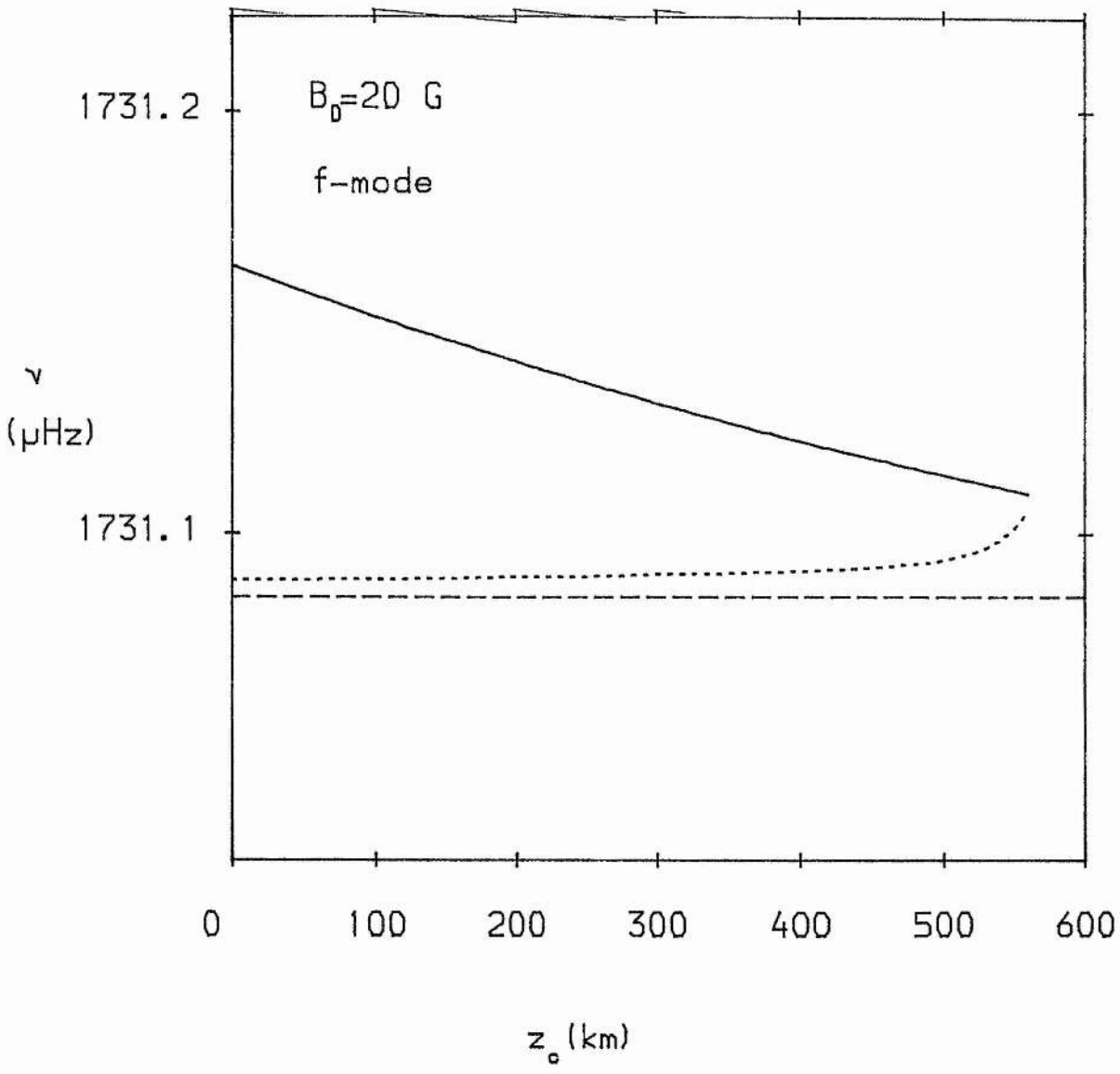

Figure 4.2. The variation of the f-mode frequency as a function of the canopy height z_c, for l=300. As z_c is varied the magnetic field at the base of the chromosphere is kept constant at 20 G. The solid line shows the case of a uniform field, the dotted line gives the variation for a chromosphere in which the Alfvén speed is constant and the dashed line is for a field free atmosphere. The curves stop where the maximum permissible magnetic field strength at the base of the chromosphere, as given by equation (4.5), falls below 20 G.

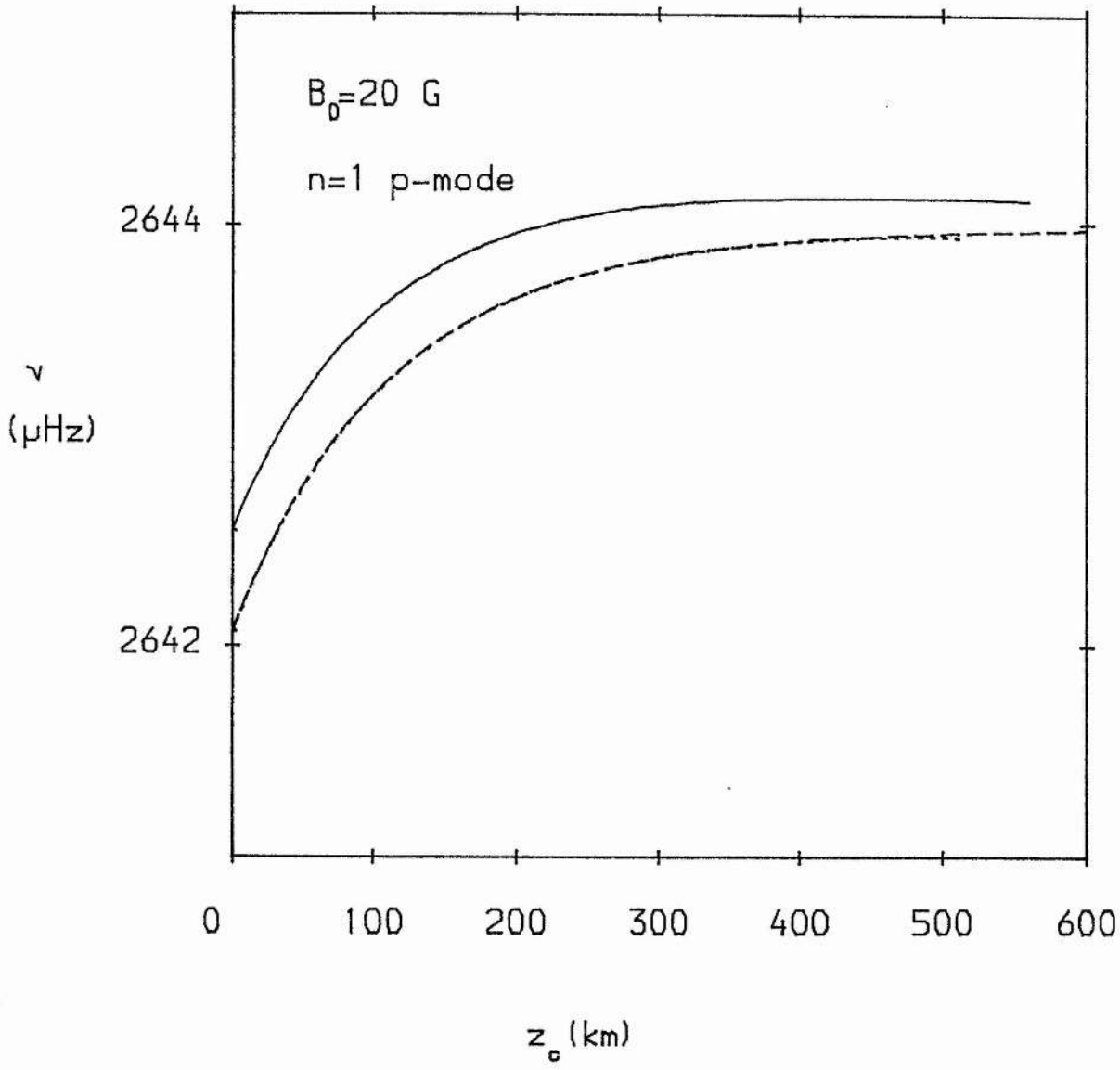

Figure 4.3. The variation of the frequency of the first p-mode as a function of the canopy height z_c, for l=300. As z_c is varied the magnetic field at the base of the chromosphere is kept constant at 20 G. The solid line shows the case of a uniform field, the dotted line gives the variation for a chromosphere in which the Alfvén speed is constant and the dashed line is for a field free atmosphere. The latter two are almost indistinguishable at this scale. The uniform field case stops where the maximum permissible field strength is less than 20 G but the uniform Alfvén speed case is affected by magnetoacoustic cut-off at a lower value of z_c.

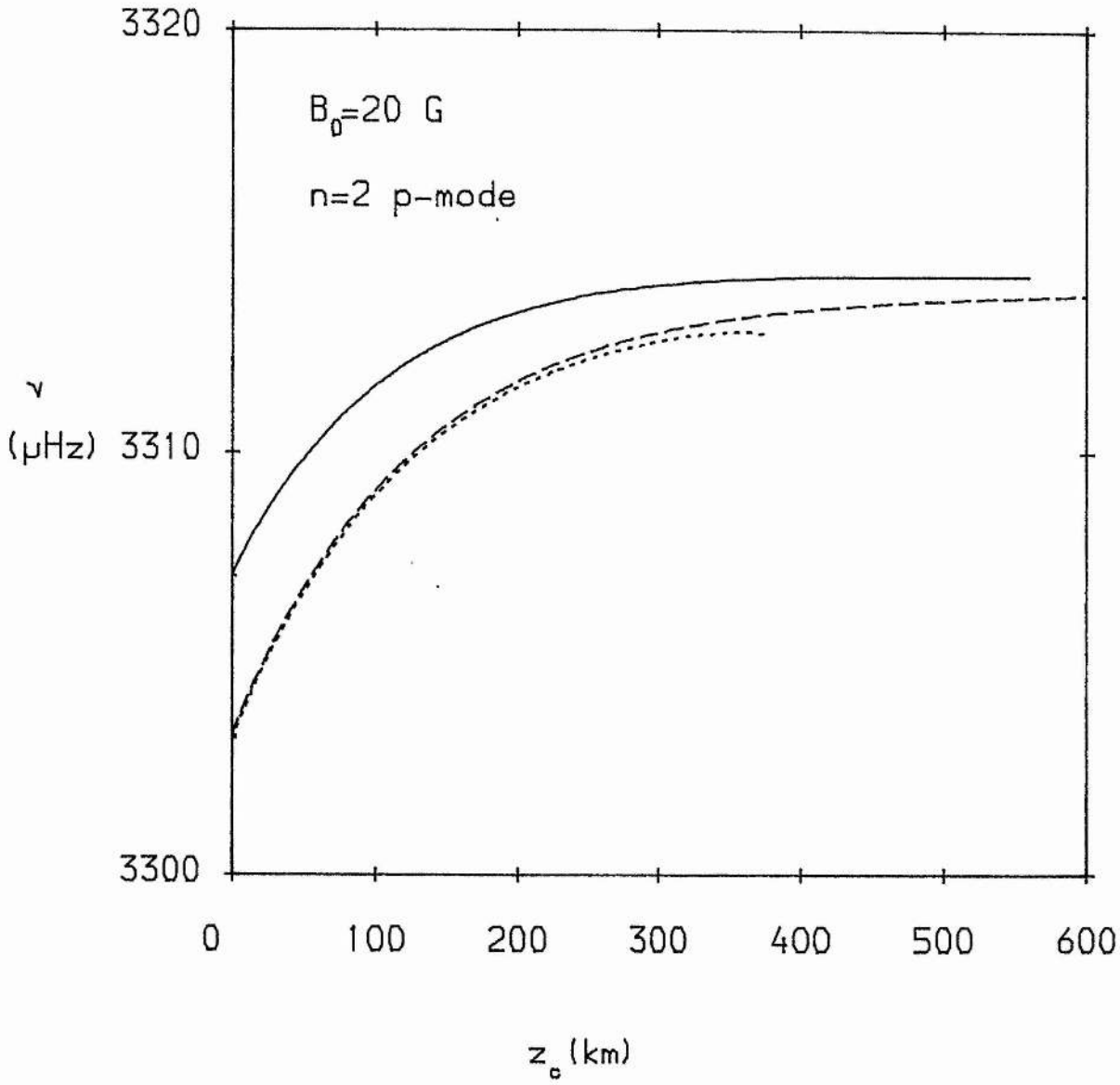

Figure 4.4. The variation of the frequency of the second p-mode as a function of the canopy height z_c, for l=300. As z_c is varied the magnetic field at the base of the chromosphere is kept constant at 20 G. The solid line shows the case of a uniform field, the dotted line gives the variation for a chromosphere in which the Alfvén speed is constant and the dashed line is for a field free atmosphere. The uniform field case stops where the maximum permissible field strength is less than 20 G but the uniform Alfvén speed case is affected by magnetoacoustic cut-off at a lower value of z_c.

field model stop when the canopy height z_c is such that this maximum permissible field strength is less than 20 G implying that the chromospheric pressure would have to be negative. The zero field curves are obviously unaffected by this. However, the uniform Alfvén speed models stop at a lower value of z_c due to the effects of the magnetoacoustic cut-off (see Campbell and Roberts, 1989).

The second set of results, Figures 4.5-4.7, show the way in which the frequency varies as a function of canopy height while the magnetic field strength is also varied such that β remains constant. The modes shown are the same as in Figures 4.2-4.4. The value at which β is fixed is chosen to correspond to the value of β when z_c =500 km and the magnetic field strength is 20 G. The effects of magnetoacoustic cut-off only appear in Figure 4.7 for the n=2 p-mode and has the consequence of disallowing this mode completely for the uniform Alfvén speed case.

4.4 Discussion

The basic effect introduced by the addition of the extra isothermal layer to the model atmosphere is illustrated quite clearly by the asymptotic formulae (4.34) and (4.39). The only difference between these expressions and their equivalents for the simpler two layer model is the factor E_*^{-2} multiplying the frequency correction due to the magnetic field. This simply represents an exponential decrease with canopy height. The constant β plots given in Figures 4.5-4.7 show a similar sort of behaviour with the frequencies in all three cases (uniform B, uniform v_A and zero B) converging on the same value as $z_c \to \infty$. Such a dependence is to be expected since the eigenfunctions for the p-modes are evanescent in the isothermal region. The rate of evanescence of the kinetic energy will be strongly dependent on the density scale height H_m. If the kinetic energy of the eigenmode has all but vanished by the time it reaches the chromosphere then there can only be a very small effect due to the magnetic field. In this way the magnitude of the magnetic effects will depend on the rate of evanescence and hence on the density scale height, as exhibited in the asymptotic formulae

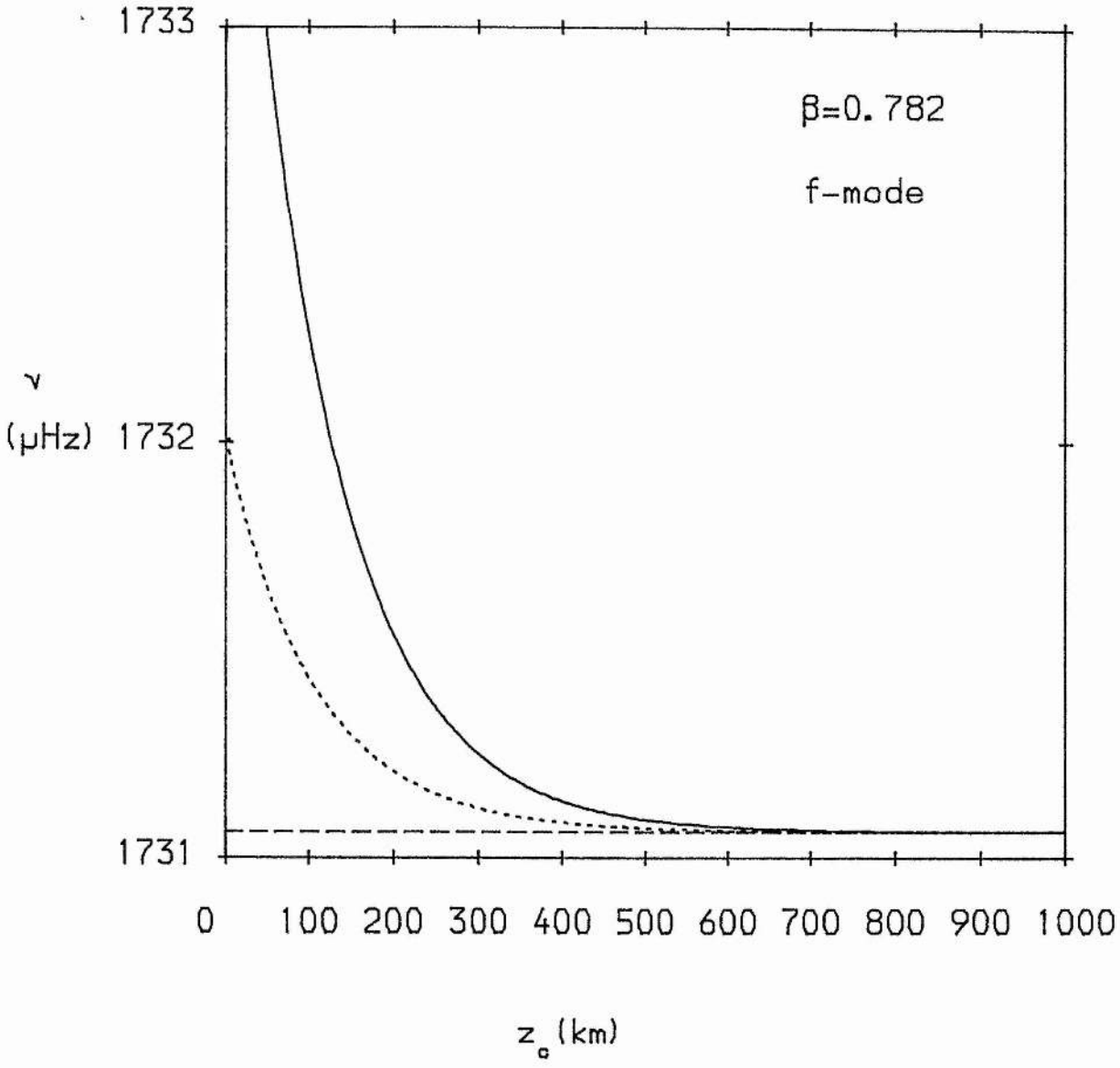

Figure 4.5. The variation of the frequency of the f-mode as a function of canopy height z_c, for l=300. Here β is kept constant at its value when the magnetic field strength is 20 G and z_c=500 km (β=0.782). The solid line shows the results for the uniform field model while the dotted line gives the uniform Alfvén speed, and the dashed line the zero field, models.

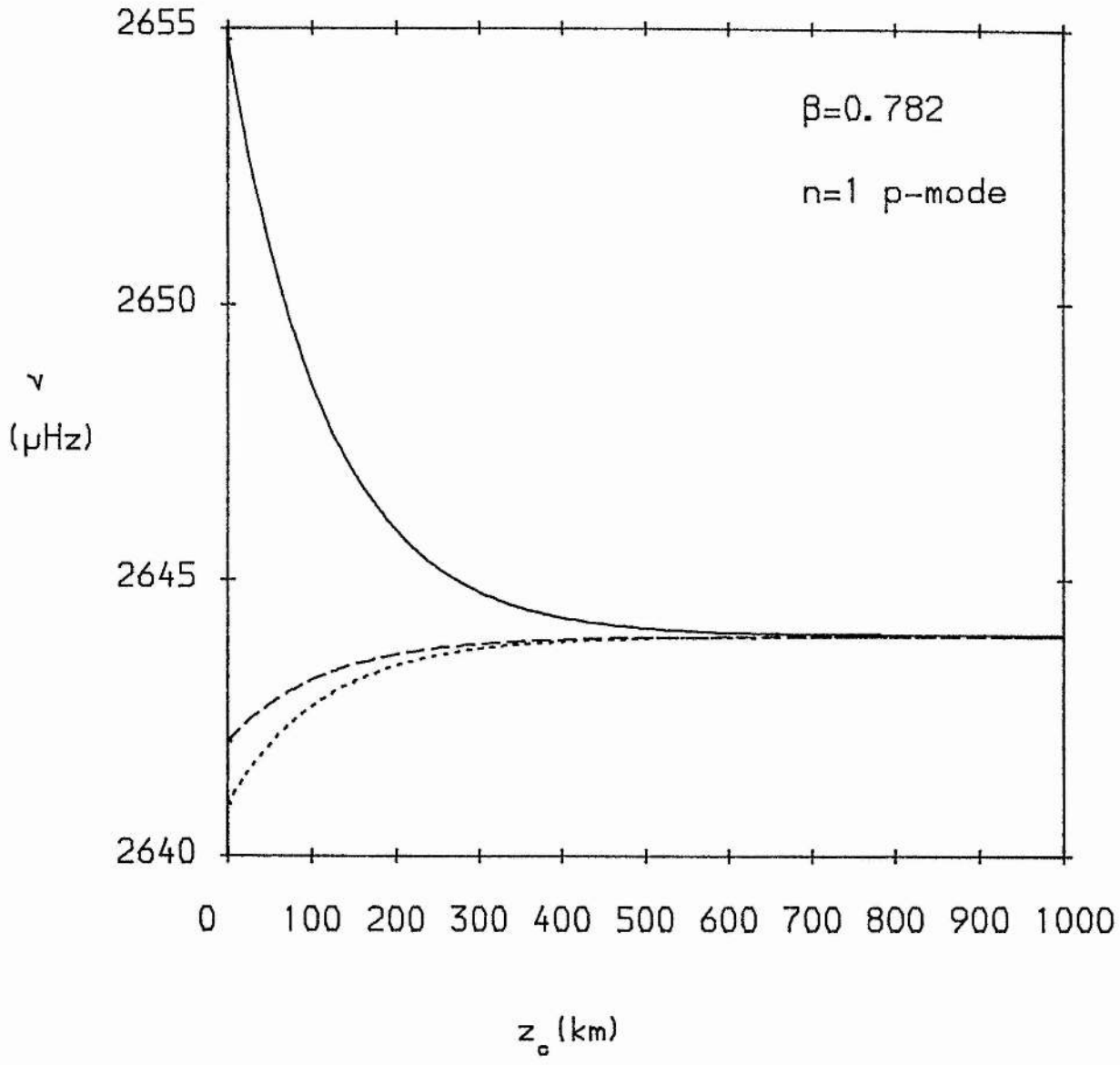

Figure 4.6. The variation of the frequency of the first p-mode as a function of canopy height z_c, for l=300. Here β is kept constant at its value when the magnetic field strength is 20 G and z_c=500 km (β=0.782). The solid line shows the results for the uniform field model while the dotted line gives the uniform Alfvén speed, and the dashed line the zero field, models.

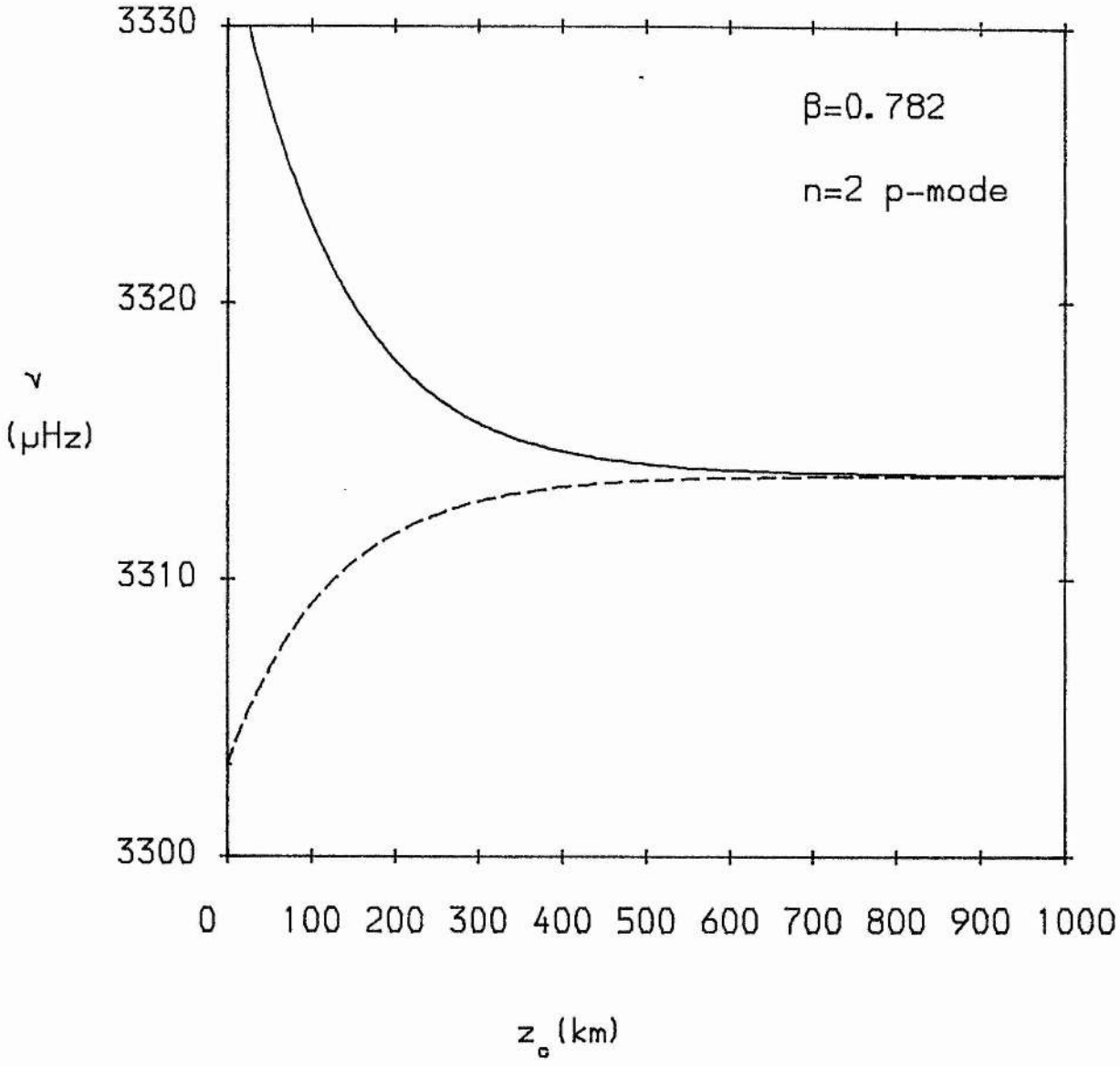

Figure 4.7. The variation of the frequency of the second p-mode as a function of canopy height z_c, for l=300. Here β is kept constant at its value when the magnetic field strength is 20 G and z_c=500 km (β=0.782). The solid line shows the results for the uniform field model while the dashed line gives the results for the zero field model. The uniform Alfvén speed case is absent due to the effects of magnetoacoustic cut-off.

(4.34) and (4.39).

It is also possible to see from these graphs what the effect of a penumbral type field is when compared to the more average canopy configurations. Assuming the two cases have a comparable value of β and taking the penumbra to be z_c=0 km and the average case to be z_c=500 km, the asymptotic results would predict a difference in frequency shifts of roughly 100-fold. The numerical results in Figures 4.5-4.7 point to the same conclusion. Thus a penumbral field is likely to have a very marked effect on the p- and f-mode dispersion curves. Overall though there will not be such a drastic effect on p-mode frequencies since such strong, low chromospheric fields are very localised to the vicinity of active regions. In the neighbourhood of active regions the p-mode dispersion curves may be significantly different from those in quiet regions due to modulation of the horizontal wavenumber by a varying magnetic field strength as discussed in section 3.6. The assumption of constant β may also prove erroneous and consequently also affect the results.

Figures 4.2-4.4, in which the magnetic field strength is kept constant while the value of z_c is increased, show that the exponential behaviour indicated by the asymptotic formulae need not be universal. Here the frequency shift due to the magnetic field does decrease with a rising canopy but only very slowly. The asymptotic corrections for this case actually remain constant. The only factors in (4.34) and (4.39) which change for a constant B, variable z_c scenario are $(\gamma_c+2\beta)$ and E_*^{-2}. In order that the field remain constant, β must decrease as a function of z_c:

$$\beta = \gamma_c \left(\frac{\mu p_p}{B_0^2} e^{-z_c/H_m} - \frac{1}{2} \right). \tag{4.40}$$

Then

$$(\gamma_c + 2\beta)\, E_*^2 = 2\gamma_c \frac{\mu p_p}{B_0^2}, \tag{4.41}$$

which is a constant in the case under discussion.

Although the basic effect of the isothermal layer is to introduce the exponential decrease in the frequency correction, the results of Figure 4.2-4.4 show that the actual effects will depend on how β and, to a lesser extent, the chromospheric temperature vary as a function of z_c. Unfortunately, the magnetic structure of the chromosphere is not as well known as might be desired. The detailed structure of the magnetic canopy must ultimately depend on the physics of magnetic flux tubes. This will involve magnetic and thermal effects. Broadly though, it would be expected, and is observed to occur, that in magnetically active regions the canopy is lower than in magnetically quiet regions (e.g. Giovanelli and Jones, 1982; Jones and Giovanelli, 1983). Thus it is unlikely that the magnetic field is constant for varying canopy height. For a given set of thermal parameters the magnetic canopy is likely to form at a height which keeps β roughly constant. In other words, strong fields can "push" their way lower in the atmosphere until the gas pressure is sufficient to oppose them, while weak fields are forced to reside higher up. It is unlikely that β will take the same value at the base of all magnetic chromospheres but of the two simple possibilities presented here it seems likely to be closer to the truth.

As shown in Figure 4.1 the simple model used here is chosen to agree with H.S.R.A. at z=0, the top of the polytropic region, where the temperature is 4460 K. This corresponds to a height of roughly 200 km above the photosphere (τ_c=1). The vertical dashed lines in Figure 4.1 indicate the range of height above the photosphere of the magnetic canopy as measured by Giovanelli and Jones (1982), this being roughly 200 km-1000 km. From this it can be seen that z_c would be expected to take a value roughly between 0 and 800 km.

Assuming the canopies at various heights have roughly equal values of β and that this value is given by a typical field strength of around 20 G at a canopy height of z_c=500 km, then Figures 4.5-4.7 indicate the likely effects. Low canopies will give strong frequency shifts but if z_c is greater than 600-700 km then there will be a negligible effect. This would correspond to a canopy height of around 800 km above the photosphere. According to Giovanelli and Jones (1982) and Jones and Giovanelli (1983), approximately 50% of canopy fields in quiet network regions and 80% of canopy fields in the vicinity of active regions have

heights below 800 km. Thus, a significant proportion of the solar surface is likely to create frequency shifts of a detectable amount. However, if these observations were found to be in error by around 250 km then this conclusion would have to be reconsidered. If canopy heights are higher by this amount then there are likely to be only very small effects, quite probably below the level of detectability. Thus, the conclusion that magnetically induced p-mode frequency shifts should be reasonably detectable is quite sensitive to the reported canopy heights. Fortunately the results seem to indicate that such errors are unlikely and will probably be less than 150 km (Giovanelli, 1980). Thus, it seems safe to say that the effects of magnetic canopy fields on high l, p- and f-modes should be detectable.

5. Conclusions.

Because the magnetic field in the solar atmosphere is concentrated into small areas of large flux density, the effects it has on the dynamics of the convection zone, photosphere and chromosphere are not obvious. Such effects in two particular cases, sunspots and chromospheric canopies, have been studied here.

A sunspot is an extremely complex phenomenon in terms of its detailed dynamics. All three significant forces on the Sun (gravity, magnetism and internal fluid stresses) act simultaneously. Much detailed study has been done on the gravitational effects in the presence of vertical magnetic fields though firm conclusions have still not been reached. The fact that the magnetic field is strong within the upper layers of the sunspot but negligible outside must have some significance. In order to study the effects of this magnetic structuring it was felt that a simple flux tube model would suffice. This describes the lateral structure effectively but is a poor model for the vertical structure owing to the neglect of gravity.

An examination of the rough vertical structure of a sunspot indicates that the temperature within is lower than outside but that both temperatures increase with depth. The external temperature exceeds the internal temperature though this deficit declines with depth. Furthermore, the significance of the magnetic field diminishes with depth. This means that the ordering of the various characteristic speeds which describe the behaviour of the sunspot and its environment changes with depth. To accommodate this effect, it is necessary to look at the different cases and how they might change the pattern of oscillations present in a flux tube. There are two significantly different regions. These are determined by the ordering of the internal Alfvén speed v_A and the external sound speed c_{se}. In the deeper levels of a sunspot $v_A<c_{se}$, whereas close to the photospheric layers this ordering is reversed.

The modes of oscillation of an isolated flux tube (that is its patterns of oscillation which are radially evanescent outside the tube) are described by their characteristic speed and the

form of the eigenmode. Modes can be horizontally propagating within the tube; such oscillations are called *body* modes. Alternatively, modes may be evanescent within the tube, and are then called *surface* modes (since the amplitude of the motion is at a maximum along the tube's edge). These modes are further classified, by analogy with magnetoacoustic waves in a uniform medium, as fast or slow according to whether their vertical propagation speed is greater than or less than $\inf\{v_A, c_{se}\}$ respectively. For the deeper levels of the sunspot it is found that slow and fast body modes can arise but only slow surface waves are allowed. However, above the level where $v_A=c_{se}$ the fast body modes give way to fast surface modes.

Observations indicate the existence of oscillations in sunspots which can be grouped into three broad categories. The umbra supports oscillations with periods around three minutes and five minutes. The three minute oscillations are observed over a large range of heights while the five minute oscillations are restricted to the photosphere and below. Three minute oscillations tend to exhibit motion channelled by the magnetic field and are sometimes absent in young or unstable spots. The third category of oscillations is penumbral waves. These have a range of periods roughly from 3 minutes to over 5 minutes. Some of these, called running penumbral waves, show coherent oscillation fronts emanating from the umbral-penumbral boundary and propagating out across the penumbra, while others have more of the appearance of standing waves.

In terms of the simple flux tube model the slow body modes seem to match the three minute oscillation best. The oscillation is observed with, if anything, the most vigorous activity near the centre. Thus, these oscillations cannot be surface waves. The fact that the motion tends to be channelled along the field lines higher up in the sunspot indicates that slow modes are more appropriate than fast. The effect of the lateral structure of the sunspot is to produce discrete modes which may explain the existence of several peaks in the observed power spectrum. Of several possible driving mechanisms, a simple analysis indicates that overstable convection in the superadiabatic layer below the photosphere is most likely. Finally, the observation that the oscillation spectrum across the umbra exhibits some

spatial variation seems to indicate that sunspot umbrae are fragmented into separate flux tubes rather than being a single cohesive whole.

Umbral five minute oscillations are similar to three minute oscillations in that they must be body modes. However, they are detected only in photospheric spectral lines so that they appear to vanish at higher levels. This matches the behaviour of fast body modes in a tube which cannot propagate above the level where v_A approaches c_{se}. This level is roughly at the photosphere. It is widely believed that the five minute oscillations are caused by the interaction of the sunspot with the p-modes of the surrounding solar atmosphere. Because body modes are evanescent outside the flux tube, it is not possible for external acoustic waves to directly drive fast body modes.

In order to discuss the interaction of p-modes with a sunspot it was found to be convenient to look at the way acoustic waves are reflected and transmitted at a magnetic interface. These properties depend on the characteristic speeds of the media and so they may vary with height in the case of a sunspot. In particular, for the deeper layers where the effects of the magnetic field are less important, it is found that waves which are transmitted into the magnetic region with a significant upward component of propagation vector at one level, can be trapped within the magnetic region at a higher level. In other words, waves can enter a sunspot low down, propagate up the flux tube and become trapped fast body modes at a higher level. Such a mechanism may help to explain how a sunspot can absorb p-mode energy as observed by Braun, Duvall and Labonte (1988).

It has been suggested that running penumbral waves are surface waves propagating along the magnetic interface which forms the penumbra. This implies that these surface waves originate from the sunspot at a lower level where it is more like a flux tube. At this level both fast and slow surface waves may propagate and recent evidence given by Lites (1988) may indicate that both are present, the slow surface wave being more tightly bound to the magnetic interface than the fast. Slow surface waves may be driven low down in the sunspot either by overstable oscillations, like the three minute umbral oscillations, or by buffeting from nearby granules. The fast surface modes are more difficult to drive since

they only exist around the photosphere and above. It may be possible for a fundamental fast body mode to be transformed into a fast surface mode as it propagates upwards through the layer where $v_A=c_{se}$.

Other oscillations in the outer penumbra, with periods around five minutes, seem to be simply p-modes that have been affected by the low lying, roughly horizontal magnetic field present there. Such modes have been discussed in some depth here, though mostly from the standpoint of what frequency changes the magnetic field is likely to produce. From these models it is expected that the magnetic field can also reduce the amplitude of the p-modes. Reduced amplitudes in the vicinity of sunspots have been observed (Lites, 1988; Tarbell, et al., 1988).

The model employed here is clearly a great simplification of reality. Nevertheless, it serves well to illustrate the effects of the lateral structure on the oscillation modes. Previous work, discussed in the Introduction (Chapter 1), has looked at the effects of gravity without taking much account of magnetic structuring. This seems to lead to a complicated set of vertical wave cavities with some argument over their true nature. It seems that for some of the effects that may occur in sunspots, both the effects of vertical stratification and lateral magnetic structuring will be necessary for them to be fully described. An example of this is the mechanism, postulated in Chapter 2, for driving the fast body modes. This requires the sound speeds to vary with height in a certain manner and the existence of a roughly vertical magnetic interface. A theoretical examination of a model incorporating these conditions with gravity as well would be extremely complicated. One possible way to proceed would be to perform a numerical simulation of p-modes interacting with a simple sunspot model. This may indicate whether the ideas put forward here are at all feasible. The complexity of this calculation reflects what is intrinsically a very complex problem.

The frequencies of solar p-modes are among the best measured quantities of the Sun. They are also among the most accurately, theoretically predicted solar quantities. Observations can obtain frequency data to an accuracy of up to 1 in 10,000 in the case of low

l modes. Though the theoretical understanding of p- and f-modes is very thorough, it is still not possible to consistently predict frequencies of all modes to this level of accuracy. The oscillations appear to be quite sensitive, at this level, to several subtle effects, such as the detailed nature of the equation of state for the solar plasma or the rate of change of rotation speed with depth, etc. One possibility which has not received much attention is the influence of a chromospheric canopy formed by the fanning out of the slender photospheric flux tubes.

Early theoretical predictions of the chromospheric canopy structure put its height at around 1500 km above the photosphere (Gabriel, 1976). At such a height it is quite difficult for the magnetic field to have any influence on the dynamics of the photosphere. Since the observed p-modes are evanescent in this region it is understandable that such effects should be ignored. More recently, however, direct observations by Giovanelli (1980), Giovanelli and Jones (1982) and Jones and Giovanelli (1983) have shown that the magnetic canopy is likely to be much lower, in extreme cases, such as around active regions, down to 200 km above the photosphere. This means that, as pointed out by Giovanelli (1980), the magnetic chromosphere may indeed have a significant effect on photospheric dynamics.

Campbell and Roberts (1989) have investigated the effects of a *weak* chromosphere in which the magnetic field declines exponentially with height. This is likely to underestimate the strength of a realistic model. Nevertheless, they found that, except for the f-mode and the first p-mode, all modes show a decrease in frequency due to the field. The f-mode shows an increase in frequency while the first p-mode exhibits a hybrid behaviour. The amount of frequency shift is of the order of a few μHz, rarely getting above 10 μHz.

The model presented here uses a constant magnetic field in the chromosphere and is *strong* in the sense that this is likely to overestimate the influence of the field on p- and f-modes. Also, this model is generalised to allow for discontinuous temperatures so that it is possible to investigate the effects of a hot chromosphere. The two models (that of Campbell and Roberts, 1989 and that presented here) thus represent extreme cases with reality probably lying somewhere in between.

It was found that in the absence of a magnetic field an increase in chromospheric

temperature causes the p-mode frequencies to be affected in much the same way as for the weak field model with no temperature discontinuity, save for the f-mode which is never affected by simple changes in temperature structure. All the p-modes, including the first, show a decrease in frequency of a few μHz for an increase in chromospheric temperature of approximately 50,000 K. The similarity in behaviour between the high temperature and weak field models occurs because both models introduce a reduction in the inertia of the chromosphere. With the exception of the f-mode and the first p-mode, the weak magnetic field has little other effect. This reduction in inertia affects the way in which waves propagating upwards reflect at the upper turning point of the cavity. Consequently the cavity structure is changed which in turn leads to frequency changes. A decrease in chromospheric inertia leads to a decrease in frequency and vice versa. In the case of the weak magnetic field, the f-mode is affected by the additional restoring force introduced by magnetic field line bending. This has the effect of increasing the oscillation frequency. The magnitude of this effect decreases rapidly with increasing radial order for the p-modes. The first p-mode is partially affected, hence its hybrid behaviour, while for all other modes the effect is negligible.

For the strong field model the effects on frequencies are quite different. The frequencies of *all* modes are increased by the presence of a uniform field. The magnitude of the frequency shift increases with field strength, horizontal wavenumber and radial order and is roughly five times the effect for the comparable weak field model. The f-mode is affected by the magnetic field in much the same way as in the weak field model, though the effect is stronger because now the field does not decrease with height. The p-modes, however, show a new effect. Though the magnetic field contributes to a reduction in chromospheric inertia, because it is uniform with height a much more significant factor is the extra rigidity which the field imposes on the plasma. This has the same effect as a substantial increase in chromospheric inertia and hence causes the frequency of the p-modes to increase.

Because the effects of chromospheric fields are restricted to the surface of the Sun the frequencies of high l modes, which are trapped in the upper part of the convection zone, are

likely to be most affected. Unfortunately, the frequencies of these modes are not so well known. However, recent evidence (Libbrecht and Kaufmann, 1988) may indicate that the f-mode frequency is higher, by a few μHz than it should otherwise be. If confirmed, this would indicate that the effects of magnetic chromospheres are indeed of some importance.

Another way in which the effects discussed here may be observed is through variations in the solar cycle. It is quite probable that the mean magnetic canopy strength may change by up to 20 G between solar maximum and minimum. This being the case, there should be some detectable change in high l mode frequencies over the same period. It is too early to form any definite conclusions yet but Duvall et al. (1988) and Rhodes et al. (1988) both indicate that there may be such a frequency change for modes with $l \approx 100$ though they disagree as to the direction of the change.

Since high l modes have a small horizontal wavelength, it may be possible to detect local effects due to small regions of strong magnetic field. Globally, the horizontal wavelength is fixed by the need for an integral number of wavelengths to fit into one circumference of the Sun. Locally, however, variations in the magnetic field strength may cause variations in horizontal wavelength. These ought to be detectable in simultaneous observations of p-modes in quiet and active regions. Also, the strong field model indicates that there should be a reduction in p-mode amplitude in the presence of a strong field. Such effects have been observed by Tarbell et al. (1988) and Woods and Cram (1981).

An extension of the previous models has been calculated in order to determine the effect of variations in the canopy height since there remains some uncertainty over the exact value. These calculations show that for a canopy with constant plasma beta, the magnitude of the frequency shift decreases exponentially with canopy height, reducing by a factor of ten in about 250 km. Thus the frequency changes are quite sensitive to the canopy height. The calculations indicate that if the average canopy height is around 500 km above the photosphere, as indicated by the work of Giovanelli (1980), Giovanelli and Jones (1982) and Jones and Giovanelli (1983) then the effects should still be detectable. However, if tthe canopy is much higher (say at 750 km) then the effects may well be negligible.

An assumption of all the models presented here is that the horizontal wavenumber is parallel to the magnetic field. It is important that this assumption be relaxed. If the physical interpretation given here is correct then the effect on the p-modes is likely to be mostly unchanged. However, since the f-mode is affected by the bending of field lines, perpendicular propagation may severely reduce the effects of magnetic canopies.

The physical interpretation described here is based solely on the two models thus far calculated. To test whether these hypotheses do hold it is necessary to investigate more general and realistic models. In the absence of exact solutions for realistic models there are two possible ways to progress. One would be to find solutions as a perturbation expansion for large β. This would be best done for the variable $\rho_0^{1/2}u_z$, since the solutions for u_z are highly singular as the magnetic field strength diminishes, i.e. $\beta \to \infty$. The second possibility, not restricted by the need for a large β, would be to solve the equations numerically as a boundary value problem. Such a calculation would allow a comprehensive set of models to be examined and this would hopefully determine the significance of the chromospheric magnetic field for p-mode frequencies. Following this it will simply be a case of waiting for the observational results to pour in!

References

Abdelatif, T E: 1988, *Ap. J.*, **333**, 395.

Abdelatif, T E, Lites, B W and Thomas, J H. : 1986, *Ap. J.*, **311**, 1015.

Abdelatif, T E and Thomas J H. : 1987, *Ap. J.*, **320**, 884

Abramowitz, M and Stegun, I A. : 1965, *Handbook of Mathematical Functions*, (New York: Dover).

Adam, J A. : 1975, PhD. Thesis, University of London.

Adam, J A. : 1977, *Solar Phys.*, **52**, 293.

Antia, H M and Chitre, S M. : 1979, *Solar Phys.*, **63**, 67.

Balthasar, H, Kuveler, G and Wiehr, E. : 1987, *Solar Phys.*, **112**, 37.

Beckers, J M and Schultz, R B. : 1972, *Solar Phys.*, **27**, 61.

Beckers, J M and Tallant, P E. : 1969, *Solar Phys.*, **7**, 351.

Belvedere, G. : 1986, in *Advances in Helio- and Asteroseismology*, ed. J Christensen-Dalsgaard and S Frandsen, IAU Symp. **123**, 167.

Bender, C M and Orszag, S A. : 1978, *Advanced Mathematical Methods for Scientists and Engineers*, (McGraw Hill).

Bogdan, T J. : 1987, *Ap. J.*, **318**, 889.

Bogdan, T J. : 1989, in *Workshop on Flux Tubes in the Solar Atmosphere*, Univ. of Oslo, June 19-21.

Bogdan, T J. : 1989, *Ap. J.*, in press.

Bogdan, T J and Cattaneo, F. : 1989, *Ap. J.*, **342**, 545.

Bogdan, T J and Zweibel, E G. : 1985, *Ap. J.*, **298**, 867.

Bogdan, T J and Zweibel, E G. : 1987, *Ap. J.*, **312**, 444.

Braun, D C, Duvall, T L and Labonte, B J. : 1987, *Ap. J.*, **319**, L27.

Braun, D C, Duvall, T L and Labonte, B J. : 1988, *Ap. J.*, **335**, 1015.

Cally, P S. : 1986, *Solar Phys.*, **103**, 27.

Campbell, W R and Roberts, B. : 1986, in *Advances in Helio- and Asteroseismology*, ed. J Christensen-Dalsgaard and S Frandsen, IAU Symp. **123**, 161.

Campbell, W R and Roberts, B. : 1989, *Ap.J.*, **338**, 538.

Christensen-Dalsgaard, J. : 1982, *Mon. Not. R. Astr. Soc.*, **199**, 735.

Christensen-Dalsgaard, J. : 1986, in *Advances in Helio- and Asteroseismology*, ed. J Christensen-Dalsgaard and S Frandsen, IAU Symp. **123**, 3.

Christensen-Dalsgaard, J, Däppen, W and Lebreton, Y. : 1988, *Nature*, **336**, 634.

Christensen-Dalsgaard, J, Duvall, T L, Gough, D O, Harvey, J W and Rhodes, E J. : 1985, *Nature*, **315**, 378.

Danielson, R E and Savage, B D. : 1968, in *Structure and development of Solar active regions*, ed. K O Kiepenheuer (Reidel: Dordrecht, Holland), IAU Symp., **35**, 112.

Davis, R Jr, Evans, J C and Cleveland, B T. : 1978, *Proc. Conf. Neutrinos*, Lafayette, **53**.

Deubner, F-L. : 1975, *Astron. Ap.*, **44**, 371.

Deubner, F-L and Gough, D. : 1984, *Ann. Rev. Astron. Astrophys.*, **22**, 593.

Duvall, T L and Harvey, J W. : 1983, *Nature*, **302**, 24.

Duvall, T L, Harvey, J W, Libbrecht, K G, Popp, B D and Pomerantz, M A. : 1988, *Ap. J.*, **324**, 1158.

Duvall, T L, Harvey, J W and Pomerantz, M A. : 1986, *Nature*, **321**, 500.

Dziembowski, W and Goode P R. : 1986, in *Advances in Helio- and Asteroseismology*, ed. J Christensen-Dalsgaard and S Frandsen, IAU Symp. **123**, 171.

Dziembowski, W A, Paterno, L and Ventura, R. : 1988, *Astron. Ap.*, **200**, 213.

Edwin, P M and Roberts, B. : 1983, *Solar Phys.*, **88**, 179.

Evans, D J and Roberts, B. : 1990a, *Ap. J.*, in press (January 1 issue).

Evans, D J and Roberts, B. : 1990b, *Ap. J.*, in press (June 21 issue).

Evans, J W and Michard, R. : 1962, *Ap. J.*, **136**, 493.

Fossat, E, Gelly, B, Grec, G and Pomerantz, M. : 1987, *Astron. Ap.*, **177**, L47.

Gabriel, A H. : 1976, *Phil. Trans. R. Soc. Lond. A*, **281**, 339.

Galloway, D J and Weiss, N O. : 1981, *Ap.J.*, **243**, 945.

Garcia de la Rosa, J I. : 1987, *Solar Phys.*, **112**, 49.

Gelly, B, Fossat, E, Grec, G and Pomerantz, M. : 1986, in *Advances in Helio- and Asteroseismology*, ed. J Christensen-Dalsgaard and S Frandsen, IAU Symp. **123**, 21.

Gingerich, O, Noyes, R W, Kalkofen, W and Cuny, Y. : 1971, *Solar Phys.*, **18**, 347.

Giovanelli, R G. : 1972, *Solar Phys.*, **27**, 71.

Giovanelli, R G. : 1974, in "*Chromospheric Fine Structure*", IAU Symp. **56**, 137.

Giovanelli, R G. : 1980, *Solar Phys.*, **68**, 49.

Giovanelli, R, Harvey, J W and Livingston, W C. : 1978, *Solar Phys.*, **58**, 347.

Giovanelli, R G and Jones, H P. : 1982, *Solar Phys.*, **79**, 267.

Goedblood, J P. : 1971, *Physica*, **53**, 412.

Gough, D O and Thompson, M J. : 1986a, in *Advances in Helio- and Asteroseismology*, ed. J Christensen-Dalsgaard and S Frandsen, IAU Symp. **123**, 155.

Gough, D O and Thompson, M J. : 1986b, in *Advances in Helio- and Asteroseismology*, ed. J Christensen-Dalsgaard and S Frandsen, IAU Symp. **123**, 175.

Gurman, J B. : 1987, *Solar Phys.*, **108**, 61.

Gurman, J B and Leibacher, J W. : 1984, *Ap. J.*, **283**, 859.

Henning, H M and Scherrer, P H. : 1986, in *Advances in Helio- and Asteroseismology*, ed. J Christensen-Dalsgaard and S Frandsen, IAU Sump. **123**, 29.

Hollweg, J V. : 1988, *Ap. J.*, **335**, 1005.

Hollweg, J V and Roberts, B. : 1981, *Ap. J.*, **250**, 398.

Hurlburt, N E, Proctor, M R E, Weiss, N O and Brownjohn, D P. : 1989, *J. Fluid Mech.*, **207**, 587.

Isaak, G R, Jefferies, S M, McLeod, C P, New, R, van der Raay, H B, Pallé, P L, Régulo, C and Roca Cortés, T. : 1986, in *Advances in Helio- and Asteroseismology*, ed. J Christensen-Dalsgaard and S Frandsen, IAU Sump. **123**, 201.

Jefferies, S M, Pallé, P L, van der Raay, H B, Régulo, C and Roca Cortés, T. : 1988, *Nature*, **333**, 646.

Jones, H P and Giovanelli, R G. : 1983, *Solar Phys.*, **87**, 37.

Lamb, H. : 1908, *Proc. London Math. Soc. Series 2*, **7**, 122.

Lamb, H. : 1932, *Hydrodynamics*, (Cambridge: Cambridge University Press).

Leibacher, J W and Stein, R F. : 1971, *Ap. Lett.*, **7**, 191.

Leibacher, J W and Stein, R F. : 1981, in *The Sun as a Star*, Chapter 10, ed. S D Jordan, NASA SP-450.

Leighton, R B. : 1960, Proceedings of IAU Symp., **12**, 321.

Leighton, R B, Noyes, R W and Simon, G W. : 1962, *Ap. J.*, **135**, 474.

Libbrecht, K G. : 1988a, *Space Sci. Rev.*, **47**, 275.

Libbrecht, K G. : 1988b, *Ap. J.*, **334**, 510.

Libbrecht, K G and Kaufmann, J M. : 1988, *Ap. J.*, **324**, 1172.

Libbrecht, K G and Zirin, H. : 1985, *Ap. J.*, **308**, 413.

Lites, B W. : 1984, *Ap. J.*, **277**, 874.

Lites, B W. : 1986a, *Ap. J.*, **301**,. 992.

Lites, B W. : 1986b, *Ap. J.*, **301**, 1005.

Lites, B W. : 1988, *Ap. J.*, **334**, 1054.

Lites, B W and Thomas J H. : 1985, *Ap. J.*, **294**, 682.

Lites, B W, White, O R, and Packman, D. : 1982, *Ap. J.*, **253**, 286.

Meyer, F, Schmidt, H U and Weiss, N O. : 1977, *Mon. Not. R. Astr. Soc.*, **179**, 741.

Miles, A J and Roberts, B. : 1989a, *Solar Phys.*, **119**, 257.

Miles, A J and Roberts, B. : 1989b, in *Plasma Phenomena in the Solar Atmosphere*, Cargese, 10-15 July 1989, ed. M A Dubois.

Moore, R L. : 1973, *Solar Phys.*, **30**, 403.

Moore, R L and Rabin, D. : 1985, *Ann. Rev. Astron. Ap.*, **23**, 239.

Mullan D J and Yun H S. : 1973, *Solar Phys.* **30**, 83.

Musman, S, Nye, A H and Thomas, J H. : 1976, *Ap. J. Letters*, **206**, L175.

Nye, A H and Thomas, J H. : 1974, *Solar Phys.*, **38**, 399.

Nye, A H and Thomas, J H. : 1976a, *Ap. J.*, **204**, 573.

Nye, A H and Thomas, J H. : 1976b, *Ap. J.*, **204**, 582.

Pallé, P L, Peréz, J C, Régulo, C, Roca Cortés, T, Isaak, G R, Mcleod, C P and van der Raay, H B. : 1986, *Astron. Ap.*, **170**, 114.

Pallé, P L, Régulo, C and Roca Cortés, T. : 1989, preprint submitted to *Astron. Astrophys.*

Parker, E N. : 1974, *Solar Phys.*, **37**, 127.

Parker, E N. : 1979a, *Ap. J.*, **230**, 905.

Parker, E N. : 1979b, *"Cosmical Magnetic Fields"*, Clarendon Press, Oxford.

Pizzo, V J. : 1986, *Ap. J.*, **302**, 785.

Phillis, G L. : 1975, *Solar Phys.*, **41**, 71.

Priest, E R. : 1982, *Solar Magnetohydrodynamics*, (Reidel; Dordrecht, Holland).

Rae, I C and Roberts, B. : 1983, *Astron. Ap.*, **119**, 28.

Rhodes, E J, Woodard, M F, Cacciani, A, Tomczyk, S, Korzennik, S G and Ulrich, R K. : 1988, *Ap. J.*, **326**, 479.

Rice, J B and Gaizauskas, V. : 1973, *Solar Phys.*, **32**, 421.

Roberts, B. : 1976, *Ap. J.*, **204**, 268.

Roberts, B. : 1981a, *Solar Phys.*, **69**, 27.

Roberts, B. : 1981b, *Solar Phys.*, **69**, 39.

Roberts, B. : 1981c, in *The Physics of Sunspots*, ed. L E Cram and J H Thomas (Sunspot, NM: Sacramento Peak Observatory), p. 369.

Roberts, B. : 1985 in *Solar System Magnetic Fields*, ed. E R Priest (Dordrecht: Reidel), chap. 3.

Roberts, B. : 1986, in '*Small Scale Magnetic Flux Concentrations in the Solar Photosphere*', ed. W Deinzer, M Knolker and H H Voigt, p.169.

Roberts, B and Campbell, W R. : 1986, *Nature*, **323**, 603.

Roberts, B and Webb, A R. : 1978, *Solar Phys.*, **56**, 5.

Roberts, B and Webb, A R. : 1979, *Solar Phys.*, **64**, 77.

Savage, B D. : 1969, *Ap. J.*, **156**, 707.

Scheuer, M A and Thomas, J H. : 1981, *Solar Phys.*, **71**, 21.

Small, L M and Roberts, B. : 1984, in proceedings of the Fourth European Solar Physics Meeting, *The Hydromagnetics of the Sun*, Noordwijkerhout, The Netherlands, 1-3 Oct 1984 (ESA SP-220, Nov. 1984).

Solanki, S K and Steiner, O. : 1989, preprint, submitted to *Astron. Ap.*

Soltau, D, Schroter, E H, Wohl, H. : 1976, *Astron. Ap.*, **50**, 367.

Spruit, H C. : 1981, *Space Sci. Rev.*, **28**, 435.

Spruit, H C. : 1982, *Solar Phys.*, **75**, 3.

Spruit, H C and Roberts, B. : 1983,*Nature*, **304**, 401.

Tarbell, T, Peri, M, Frank, Z, Shine, R and Title, A. : 1988, proceedings of *Seismology of the Sun and Sun-like Stars*, Tenerife, Spain, 26-30 Sept 1988, ESA SP-286, p. 315.

Thomas, J H. : 1981, in *'The Physics of Sunspots'* edited by L E Cram and J H Thomas (Sunspot N M: Sacramento Peak Observatory), p.345.

Thomas, J H. : 1984, *Astron. Ap.*, **135**, 188.

Thomas, J H, Cram, L E and Nye, A H. : 1982, *Nature*, **297**, 485.

Thomas, J H, Cram, L E and Nye, A H. : 1984, *Ap. J.*, **285**, 368.

Thomas, J H, Lites, B W, Gurman, J B and Ladd, E F. : 1987, *Ap. J.*, **312**, 457.

Thomas, J H and Scheuer, M A. : 1982, *Solar Phys.*, **79**, 19.

Thompson, M J. : 1988, proceedings of *Seismology of the Sun and Sun-like Stars*, Tenerife, Spain, 26-30 Sept 1988, ESA SP-286, p. 321.

Uchida, Y and Sakurai,T. : 1975, *Publ. Astr. Soc. Japan*, **27**, 259.

Uexküll, M V, Kneer, F and Mattig, W. : 1983, *Astron. Ap.*, **123**, 263.

Ulrich, R K. : 1970, *Ap. J.*, **162**, 993.

Ulrich, R K and Rhodes, E J. : 1983, *Ap. J.*, **265**, 551.

Vorontsov, S V. : 1986, in *Advances in Helio- and Asteroseismology*, ed. J Christensen-Dalsgaard and S Frandsen, IAU Symp. **123**, 151.

Webb, A R and Roberts, B. : 1978, *Solar Phys.*, **59**, 249.

Weiss, N O, Brownjohn, D P, Hurlburt, N E and Proctor, M R E. : 1989, preprint, submitted to *Mon. Not. R. Astr. Soc.*

Wentzel, D G. : 1979, *Ap. J.*, **227**, 319.

Wilson, P R. : 1980, *Astron. Ap.*, **76**, 20.

Wood, D T and Cram, L E. : 1981, *Solar Phys.*, **69**, 233.

Woodard, M F. : 1987, *Solar Phys.*, **114**, 21.

Woodard, M F and Noyes, R W. : 1985, *Nature*, **318**, 449.

Zhugzhda, Y D. : 1984, *Mon. Not. R. Astr. Soc.*, **207**, 731.

Zhugzhda, Y D and Dzhalilov, N S. : 1982, *Astron. Ap.*, **112**, 16.

Zhugzhda, Y D and Dzhalilov, N S. : 1984a, *Astron. Ap.*, **132**, 45.

Zhugzhda, Y D and Dzhalilov, N S. : 1984b, *Astron. Ap.*, **132**, 52.

Zhugzdha, Y D and Locans, V. : 1981, *Pis'ma v Astron. Zh.*, **7**, 44.

Zhugzdha, Y D, Locans, V and Staude, J. : 1983, *Solar Phys.*, **82**, 369.

Zhugzdha, Y D, Locans, V and Staude, J. : 1985, *Astron. Ap.*, **143**, 201.

Zhugzdha, Y D, Locans, V and Staude, J. : 1987, *Astron. Nachr.*, **308**, 257.

Zhugzdha, Y D, Staude, J and Locans, V. : 1984, *Solar Phys.*, **91**, 219.

Zirin, H and Stein, A. : 1972, *Ap. J. Lett.*, **178**, L85.

Zweibel, E G and Bogdan, T J. : 1986, *Ap. J.*, **308**, 401.

Zweibel,E G and Däppen W. : 1989, *Ap. J.*, **343**, 994.